

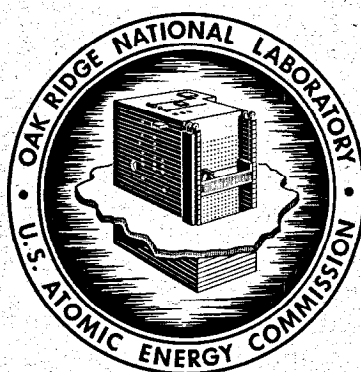
226
3-16

2076

ORNL-4658
UC-80 – Reactor Technology

CHEMICAL ASPECTS OF MSRE OPERATIONS

Roy E. Thoma



OAK RIDGE NATIONAL LABORATORY
operated by
UNION CARBIDE CORPORATION
for the
U.S. ATOMIC ENERGY COMMISSION

DISTRIBUTION OF THIS DOCUMENT IS UNLIMITED

Printed in the United States of America. Available from
National Technical Information Service
U.S. Department of Commerce
5285 Port Royal Road, Springfield, Virginia 22151
Price: Printed Copy \$3.00; Microfiche \$0.95

This report was prepared as an account of work sponsored by the United States Government. Neither the United States nor the United States Atomic Energy Commission, nor any of their employees, nor any of their contractors, subcontractors, or their employees, makes any warranty, express or implied, or assumes any legal liability or responsibility for the accuracy, completeness or usefulness of any information, apparatus, product or process disclosed, or represents that its use would not infringe privately owned rights.

Contract No. W-7405-eng-26

MOLTEN-SALT REACTOR PROGRAM

CHEMICAL ASPECTS OF MSRE OPERATIONS

Roy E. Thoma

REACTOR CHEMISTRY DIVISION

NOTICE

This report was prepared as an account of work sponsored by the United States Government. Neither the United States nor the United States Atomic Energy Commission, nor any of their employees, nor any of their contractors, subcontractors, or their employees, makes any warranty, express or implied, or assumes any legal liability or responsibility for the accuracy, completeness or usefulness of any information, apparatus, product or process disclosed, or represents that its use would not infringe privately owned rights.

DECEMBER 1971

OAK RIDGE NATIONAL LABORATORY
Oak Ridge, Tennessee 37830
operated by
UNION CARBIDE CORPORATION
for the
U.S. ATOMIC ENERGY COMMISSION

DISTRIBUTION OF THIS DOCUMENT IS UNLIMITED

Frey

ج

ج

CONTENTS

ABSTRACT	1
EXECUTIVE SUMMARY	1
ACKNOWLEDGMENTS	2
KEY-WORD INDEX	3
1. INTRODUCTION	3
2. CHEMICAL BEHAVIOR IN THE FUEL AND COOLANT SALT SYSTEMS DURING PRENUCLEAR OPERATIONS	9
2.1 Preoperational Procedures	9
2.2 Flush Salt	10
2.3 Coolant Salt	14
2.4 Fuel Salt	15
2.4.1 On-Site Preparation	15
2.4.2 Uranium Assay	16
2.4.3 Structural Metal Impurities	19
2.4.4 Oxide Contaminants	26
2.4.5 Analysis of Helium Cover Gas	30
2.4.6 Lithium Analysis	31
2.4.7 Examination of Salts after Zero-Power Experiment	31
2.4.8 Appraisal of Chemical Surveillance in Prepower Tests	33
3. CHEMICAL COMPOSITION OF THE FUEL SALT DURING NUCLEAR OPERATIONS	36
3.1 Introduction	36
3.2 Component Analysis	50
3.3 Oxide Analysis	50
3.4 Uranium Concentration	52
3.5 Structural Metal Impurities	53
3.6 Chemical Effects of Reprocessing	55
3.7 Material Balances for ^{235}U and ^{233}U Operations	57
3.7.1 Recovery of ^{235}U and ^{238}U	57
3.7.2 Inventories for Stored Salts	58
3.7.3 Salt Loss from Leakage	59

4. CHEMICAL COMPOSITION OF THE FLUSH SALT DURING NUCLEAR OPERATIONS	61
4.1 Role of Flush Salt Analysis in the Determination of Salt Residue Masses	61
4.2 Transfer of Uranium and Plutonium to Flush Salt in ^{233}U Operations	64
4.3 Flush Salt Loss to Off-Gas Holdup Tank	64
5. CHEMICAL BEHAVIOR OF THE COOLANT SALT	65
5.1 Composition Analysis	66
5.2 Corrosion Behavior	69
6. CORROSION IN THE FUEL CIRCUIT	71
6.1 Modes of Corrosion	71
6.2 Corrosion in Prenuclear Operations	74
6.3 Corrosion in Power Operations	74
6.4 Additions of Reductants and Oxidants to the Fuel Salt	79
6.5 Effect of Uranium Trifluoride on the ^{95}Nb Concentration of the Fuel Salt	94
7. DETERMINATION OF REACTOR POWER	99
7.1 Power Estimates with ^{235}U Fuel from Heat Balance and Other Methods	99
7.2 Power Output of the MSBR Based on the Isotopic Composition of Plutonium	101
7.3 Isotopic Composition of Uranium during ^{233}U Operations	108
7.4 Isotopic Composition of Uranium during ^{235}U Operations	110
8. PHYSICAL PROPERTIES	112
8.1 General Properties	112
8.2 Density of Fuel and Coolant Salts	112
8.3 Crystallization of the MSRE Fuel	116
9. INTERACTIONS OF FUEL SALT WITH MODERATOR GRAPHITE AND SURVEILLANCE SAMPLE MATERIALS	118
10. CHEMICAL SURVEILLANCE OF AUXILIARY FLUID SYSTEMS	121
10.1 Water Systems	121
10.1.1 Cooling Tower Water	122
10.1.2 Treated Water Supply	122
10.1.3 Vapor Condensing System	123
10.2 Helium Cover Gas	127
10.3 Reactor Cell Air	128
10.4 Oil Lubrication Systems	128
11. TRANSPORT OF MATERIALS FROM SALT TO COVER GAS SYSTEMS	131
11.1 Fission Products	131
11.2 Restrictions in the Off-Gas System	132
11.3 Tritium Transport in the MSRE	138
12. IMPLICATIONS OF THE MSRE CHEMISTRY FOR FUTURE MOLTEN SALT REACTORS	139

CHEMICAL ASPECTS OF MSRE OPERATIONS

R. E. Thoma

ABSTRACT

In this report are tabulated all results of laboratory analyses performed in surveillance of MSRE salt, water, cover gas, and oil systems. Excepted are analytical data pertaining to fission product and tritium distribution and transport. The report recapitulates conclusions derived from chemical analyses performed from the 1964 preoperational test period until termination of power operations in 1969, modified by the results of postoperational examination of the reactor components. Surveillance results were evaluated with respect to their significance as indicators of the performance of the MSRE and as indicators of the need and potential for development of specific in-line methods of analysis for molten-salt power reactors.

As judged from chemical data, the MSRE was highly successful as a materials demonstration. The flowing salts did not wet their containment systems; fuel salt neither wetted nor penetrated the graphite moderator surface. The cumulative generalized corrosion within the fuel circuit resulted in the removal of chromium from the alloy to an average depth of 0.4 mil, while that in the coolant system was undetectably low. The results of postoperational examinations, although corroborative of predicted corrosion, also indicated finite but slight intergranular attack. In operations which successively employed ^{235}U , ^{233}U , and ^{239}Pu as sources of power in the reactor, the circulated fluids remained chemically stable, free of radiation damage, and free of contamination. The average full-power output of the reactor, as computed from experimental results of isotopic dilution mass spectrometric analysis of fissile species and subsequently confirmed by capture-to-absorption ratio measurements, was shown to be 7.4 MW(t).

EXECUTIVE SUMMARY

The Molten-Salt Reactor Experiment (MSRE) was conducted during the period from 1965 to 1969 as the first extensive demonstration of the operability of molten-salt reactors. During this period, continuous surveillance of the chemical behavior in the circulating fluid salt, water, cover gas, and oil systems was maintained through a program of laboratory analysis. The principal function of the program was to ensure that the Experiment would proceed with the freedom

from chemical problems that was anticipated from the results of prior supporting research and development programs. The results of chemical analyses were also used for assistance in developing operational plans for nuclear engineering experiments with the reactor. In these experiments, the reactor was employed to a limited extent as an experimental chemical facility to obtain chemical data that were not otherwise available.

All of the results of laboratory analyses (except the mass of data on fission product and tritium distribution and transport) performed in surveillance of the MSRE salt, water, cover gas, and oil systems are summarized in the current report. In this archive record are recapitulated various conclusions derived from the laboratory analyses performed from 1965 to 1969 as modified by the results of postoperational examination of the reactor components.

Surveillance results were evaluated with respect to their significance as indicators of the need and potential for development of specific in-line methods of analyses for molten-salt power reactors. Examination of metal-graphite assemblages removed periodically from a flow channel in the graphite moderator confirmed inferences from chemical data that materials compatibility was excellent.

This report is divided into chapters that pertain to the chemical behavior of flush, coolant, carrier, and fuel salts in the prenuclear operational period, the chemical composition of the fuel and flush salts during nuclear operations, the results of corrosion surveillance, power estimates from chemical and isotopic dilution data, and the results obtained from analysis of samples from auxiliary fluid systems.

Experience with the MSRE throughout the shake-down periods preceding power operations confirmed that the molten fluoride salt mixtures were intrinsically noncorrosive to Hastelloy N and that effective procedures were employed to prevent serious contamination of the salt circuits during this period.

Upon initiation of power operations, orifices in the fuel off-gas system became restricted. Investigation showed that the cause was organic material: oil that seeped into the fuel pump. Improved filters successfully alleviated the plugging problem, but the continued passage of hydrocarbons through the pump constituted a chemical factor that introduced a degree of uncertainty to some interpretations of chemical behavior in the MSRE.

In operations which successively employed ^{235}U , ^{233}U , and ^{239}Pu as sources of power in the reactor, the circulated fuel salt remained chemically stable, free of radiation damage, and essentially free of contamination.

While chemical data alone were useful as statistical indicators of trends in the concentration of fissile species in the fuel salt over extended periods of power operation, they were of secondary importance in day-to-day operations because on-site reactivity balance measurements proved to be some ten times more sensitive to changes in the concentration of fissile material than the individual chemical results. The combined results of chemical and mass spectrometric analysis, however, furnished information that was uniquely suited to use in establishing numerous absolute values and were applicable for determination of trends in performance, in computation of inventory, and in establishing the distribution of uranium between the fuel- and flush-salt systems.

After three years of operations with $^{235},^{238}\text{U}$ fuel salt, uranium was removed from the carrier salt in preparation for tests of ^{233}U as a fuel for molten-salt reactors. Uranium was removed from the carrier salt by fluorination; the uranium hexafluoride product was absorbed on NaF beds. Recovery of the uranium from the NaF absorber beds yielded less uranium than expected. A painstaking investigation was made which led to a refinement in the material balances of fissionable species in the reactor from the outset of operations. From these it was deduced that the disparity was caused by retention of 0.8 kg of ^{235}U (2.48 kg ΣU) in the chemical reprocessing facility at the MSRE.

Fuel salt was prevented from becoming increasingly oxidizing as burnup of fissionable material proceeded by the addition of small amounts of beryllium metal to the salt flowing through the pump bowl. The results of these experiments showed that the disposition of ^{95}Nb between the containment materials and the salt could be used as an indicator of the freedom from our development of a potentially oxidizing condition in the fuel salt.

Disposal of gaseous tritium emanating from the MSRE posed no radiological hazard; consequently, no program for completely defining its distribution was instituted at the outset of operations. After recognition of the importance of tritium control in large molten-salt reactors, studies of tritium in the MSRE were actively pursued. Results of these studies are described in other MSRP reports and are not treated extensively here.

As judged from chemical data, the MSRE was highly successful as a materials demonstration. The flowing salts did not wet their containment systems; fuel salt neither wetted nor penetrated the graphite moderator surface. Chemical analyses showed corrosion with the $2\text{LiF}\cdot\text{BeF}_2$ coolant system to be negligible. This has been borne out by subsequent examination of the salt side of the tubes from the air-cooled radiator and of the coolant side of the primary heat exchanger. Similar but more numerous analyses suggested that corrosion within the fuel system was slight (but observable). The cumulative generalized corrosion within the fuel circuit resulted in the removal of chromium (the most chemically active constituent of the alloy) from an average depth of 0.4 mil, some ten times less than was anticipated from the preoperational laboratory measurements of self-diffusion coefficients of chromium in Hastelloy N. It is inferred that the major fraction of this corrosion resulted from interactions of atmospheric oxygen retained in the graphite moderator after periods of reactor maintenance.

Postoperational examination by metallographic techniques confirmed the low generalized corrosion but disclosed a grain-boundary effect near surfaces exposed to the fuel which resulted in cracks to a depth of one grain in strained specimens. This hitherto unobserved phenomenon is currently being investigated.

A salient conclusion from the chemical studies described in the current report is that development of automated in-line methods for determination of redox potential ($[\text{U}^{3+}]/[\Sigma\text{U}]$) of fuel salts, for dynamic assessment of corrosion rates, and for measurement of the presence of oxides at low (<50 ppm) concentrations in flowing salt will be required for operation of larger reactors.

Operation of the MSRE served to demonstrate the practicality of the molten-salt reactor concept, its safety, reliability, and tractability to simple maintenance methods. These operations confirmed that the molten fluoride salts are immune to radiation damage, equally serviceable with various fissile species as energy sources, and tolerant of the buildup of fission and corrosion products. The MSRE thus fulfilled its role and demonstrated chemical compatibility of materials, simple refueling and reprocessing of salts, and the potential need for automated in-line analysis as part of the operational controls system in molten-salt reactors.

ACKNOWLEDGMENTS

The data recorded in this document were obtained through the efforts of a large number of people in

several Divisions of the Oak Ridge National Laboratory: Analytical Chemistry, Chemistry, Chemical Technology, Metals and Ceramics, Operations, Reactor, and the Solid State Divisions. We are especially indebted to the staff of the Analytical Chemistry Division, for only through the enthusiastic commitments of these chemists to the needs of the Molten-Salt Reactor Program was it possible to obtain the excellent quality of chemical information pertaining to MSRE operations that we now have. The efforts of this group were led by R. F. Apple, R. E. Eby, J. M. Dale, C. E. Lamb, A. S. Meyer, Jr., and W. F. Vaughan, with the administrative support of L. T. Corbin, J. C. White, and M. T. Kelley. We were assisted as well by E. M. King and his associates in hot-cell examinations of specimens from the MSRE.

Counsel and advice was provided throughout the period of reactor operations by members of the MSR program staff, M. W. Rosenthal, R. B. Briggs, P. N. Haubenreich, J. R. Engel, R. H. Guymon, and B. E. Prince, and by the chemists who have been my associates in the program. Of this group W. R. Grimes, E. G. Bohlmann, F. F. Blankenship, and H. F. McDuffie supplied special assistance and provided significant contributions to the conclusions offered here.

KEY-WORD INDEX

- *analytical chemistry + *burnup + *chemical properties
- + *chemistry + *corrosion products + *fluorides +
- *fuels + *fused salts + *MSRE + *power measurement
- + *primary salt + *reactors + *sampling + *secondary salts + *single-fluid reactors + *surveillance + *uranium fluorides + *uranium-233 + *uranium-235 + beryllium fluoride + coolants + cover gas + fuel preparation + graphite + Hastelloy N + inventories + lithium fluoride + MSRP + nickel alloys + oxides + oxidation + oxygen + phase equilibria + plutonium fluorides + primary system + reactor vessel + zirconium fluoride

1. INTRODUCTION

During the last two decades a great number of reactor concepts have been proposed to fill the foreseeable need for electric power toward the end of the century and to conserve supplies of fissionable materials. Of these concepts, only a few remain of potential significance to the nuclear economy. Foremost among this group are the Liquid-Metal Fast Breeder (LMFBR), the Gas-Cooled Fast Breeder (GCFBR), the Light Water Breeder (LWBR), and the Molten-Salt Breeder (MSBR).

The initial efforts to develop the molten-salt system began more than 20 years ago at the Oak Ridge National Laboratory. A detailed examination of the program which followed is described in a series of papers published early in 1970.¹ By 1964 development of MSR's had culminated in the construction and operation of the Molten-Salt Reactor Experiment (MSRE) as a demonstration of the practicality of these reactors. It was designed to employ, as nearly as was feasible, the same materials that were proposed for use in molten-salt breeder reactors. Thus the MSRE was constructed to circulate uranium fuel as UF_4 dissolved in a molten fluoride mixture within a Hastelloy N circuit. The fuel mixture was pumped at a rate of 1200 gpm through a graphite core matrix contained in a cylindrical core vessel (Fig. 1.1). Dry, deoxygenated helium was supplied at 5 psig to the pump bowl. A flow of this gas carried xenon and krypton out of the pump bowl to charcoal beds.

When the reactor was operated at full power, fuel entered the graphite core at 632°C (1170°F) and was heated to 654°C (1210°F). The salt was then discharged through the shell side of a tube and shell heat exchanger, returning through a fuel inlet to the reactor vessel. A coolant salt circulated through the heat exchanger, through the air-cooled radiator to the coolant pump, and back to the heat exchanger to complete the circuit. At full power, the temperature of the coolant salt varied from 546°C (1015°F) to 579°C (1075°F) in this circuit. Design parameters of the MSRE are summarized in comparison with those for larger molten-salt reactors in Table 1.1. Here it is noted that two fuel salt compositions were employed in the MSRE. The reactor was operated initially with a ^{235}U fuel charge; the uranium from this charge was recovered and replaced with ^{233}U for the latter period of reactor operations. Nuclear characteristics of the MSRE with its ^{235}U fuel charge are listed in Table 1.2.

From the inception of operations with the MSRE in 1965, the performance of the MSRE was positive indication of the technical feasibility of molten-salt reactors. The MSRE has shown that a molten-fluoride reactor can be operated at temperatures above 1200°F without attack on either the metal or graphite parts of the system; that reactor equipment in the radioactive parts of the plant can be repaired or replaced; and that xenon can be stripped continuously from the fuel.

Operations with the MSRE were terminated as planned late in 1969. The reactor was operated for a cumulative period of 13,172 equivalent full power hours during the period of nuclear operations from June 1, 1965, to December 12, 1969. A chronological

ORNL-LR-DWG 61097RIA

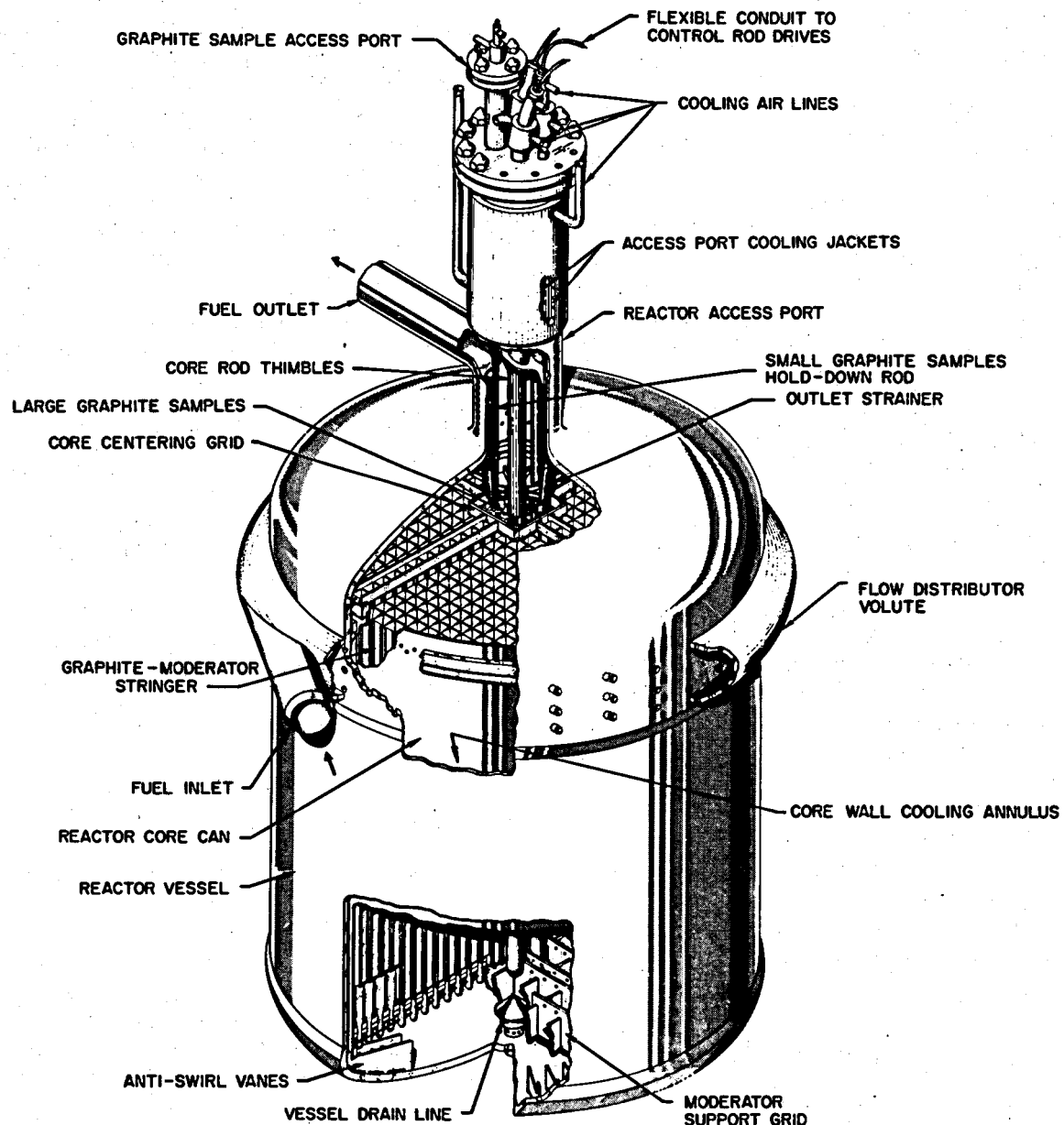


Fig. 1.1. MSRE reactor vessel.

Table 1.1. Comparison of MSRE, MSBE, and MSBR design data^a

	MSRE	MSBE	MSBR
Reactor power, MW(t)	7.3	150	2250
Peak graphite damage flux ($E_n > 50$ keV), neutrons cm^{-2} sec $^{-1}$	3×10^{13}	5×10^{14}	3×10^{14}
Peak power density, W/cc			
Primary salt	30	760	500
Core including graphite	6.6	114	65
Peak neutron heating in graphite, W/cc	0.2	2.6	1.7
Peak gamma heating in graphite, W/cc	0.7	6.3	4.7
Primary salt			
Volume fraction in core	0.225	0.15	0.13
Composition, mole %			
^7LiF	65 (64.5) ^b		
BeF_2	29.2 (30.2)	71.5	71.7
ThF_4	0 (0)	16	16
$^{235,238}\text{UF}_4$	0.83 (0)	12	12
$^{233}\text{UF}_4$	0 (0.14)	0.5	0.3
ZrF_4	5 (5.2)	None	None
Liquidus, °C	434	500	500
Liquidus, °F	813	932	932
Density, lb/ft ³ at 1100°F	141	211 ^c	210
Viscosity, lb ft ⁻¹ hr ⁻¹ at 1100°F	19	29 ^d	29
Heat capacity, Btu/lb°F	0.47	0.32	0.32
Thermal conductivity, Btu hr ⁻¹ ft ⁻¹ °F ⁻¹	0.83	0.75	0.75
Volumetric heat capacity, Btu ft ⁻³ °F ⁻¹	66	66	66
Temperature, °F			
Inlet reactor vessel	1170	1050	1050
Outlet reactor vessel	1210	1300	1300
Circulating primary salt volume, ft ³	70	266	1720
Inventory fissile, kg	76 (32) ^b	396 ^e	1470
Power density primary salt circulating average, W/cc	4	20	46

^aFrom J. R. McWherter, *Molten-Salt Breeder Experiment Design Bases*, ORNL-TM-3177, p. 3 (November 1970).

^bFigures in parentheses refer to the second fuel loading, containing $^{233}\text{UF}_4$.

^c206 at 1300°F; 212 at 1050°F.

^d16.4 at 1300°F; 34.2 at 1050°F.

^e ^{233}U initial.

Table 1.2. Nuclear characteristics of MSRE with ^{235}U fuel

Thermal neutron fluxes, ^a neutrons cm^{-2} sec ⁻¹	
Maximum	3.79×10^{13}
Average in graphite-moderated regions	1.48×10^{13}
Average in circulating fuel	4.74×10^{12}
Reactivity coefficients ^b	
Temperature, ($^{\circ}\text{F}$) ⁻¹	-7.7×10^{-5}
^{235}U concentration	0.253
Fuel salt density	0.23
Graphite density	0.53
Prompt neutron lifetime, sec	2.8×10^{-4}

^aAt operating fuel concentration, 7.4 MW.

^bAt initial critical concentration. Where units are shown, coefficients for variable x are of the form $(1/k)/(\partial k/\partial x)$; other coefficients are of the form $(x/k)/(\partial k/\partial x)$.

history of reactor operations is summarized in Fig. 1.2. Detailed accounts of these operations are described in the Molten-Salt Reactor Program semiannual progress reports.

In operation, the MSRE employed three salt mixtures: fuel, coolant, and flush salt (that was used to scavenge impurities from the fuel circuit and from surfaces of the graphite moderator before and after the fuel containment system was opened).

Fuel and coolant salts for use in the MSRE were selected on the basis of considerations which are discussed in detail in an earlier report.² The fuel salt consisted essentially of a carrier mixture into which suitable amounts of fissile material could be dissolved to produce fuel salt. The carrier was selected to be a mixture of ^7LiF - BeF_2 - ZrF_4 such as to provide the optimum physical and chemical properties of the fuel salt. Some of the criteria included in optimizing the carrier composition were liquidus temperature, viscosity, and zirconium (included to ensure that UO_2 could not be precipitated from the molten fluoride solution) concentration. The phase diagram of the LiF - BeF_2 - ZrF_4 system^{3,4} shown in Fig. 1.3 illustrates the options available for choice of carrier salt. The salt composition selected on the basis of the considerations mentioned was ^7LiF - BeF_2 - ZrF_4 (65-30-5 mole %).

An additional measure was adopted in the selection of salt composition of the fuel to minimize the possibility that troublesome deposits containing fissionable material might segregate from the molten-fluoride fuel solution. This was the choice to constitute the uranium fuel charge of about two-thirds ^{238}U and one-third ^{235}U ; it was based on chemical considerations, and arose from uncertainty as to the probable value of the oxidation-reduction potential that would prevail in the

fuel salt in normal operations. From Long and Blankenship's⁴ results, it was concluded that the disproportionation of UF_4 would not proceed to the extent that the amount of metallic uranium produced would precipitate or cause problems by alloying with the fuel salt containment system. If, for some reason, however, the $[\text{U}^{3+}]/[\Sigma\text{U}]$ concentration ratio were to rise above 50%, formation of uranium alloys and carbides was foreseen as possible. This difficulty was recognized in the inexactness of our information concerning the value of the average total cation-anion balance that would result from one fission event in the reactor environment. If the tendency was toward a slight excess of cations, the potential for reduction of $\text{U}^{4+} \rightarrow \text{U}^{3+}$ and disproportionation was increased. Increasing the total inventory of uranium would reduce proportionately the rate of development of unfavorable $[\text{U}^{3+}]/[\Sigma\text{U}]$ concentration ratios. For these reasons, the choice was made to specify that the concentration of uranium in the fuel salt would be 0.9 mole %, even though <0.3 mole % of highly enriched uranium would have been sufficient to make the MSRE critical. Such measures, it was shown, were overly conservative in affording protection which it is recognized now was not essential. Notwithstanding, they, like the meticulous operational methods which were employed, comprise the margins of safety which were appropriate to the experiment. Under similar considerations, the coolant salt was chosen as a mixture corresponding to the fuel composition but containing neither fissile material nor zirconium. Salt of the composition ^7LiF - BeF_2 (66-34 mole %) was used both as the coolant and as the flush salt.

Samples of the MSRE fuel mixture and (less frequently) the coolant mixture were analyzed routinely during all periods when salts were circulated in the reactor. On each occasion of its use, the flush salt also was analyzed. The concentrations of the salt constituents, oxide contaminants, and fission product species were monitored on a continuing basis. Chemical analyses were performed regularly with samples removed from the circulating salts in order to evaluate the utility of a continuous surveillance program as well as to fix goals for in-line analytical controls for future molten-salt reactors. The MSRE provided the initial experience in these respects; although a molten-salt reactor, the Aircraft Reactor Experiment,⁵ previously demonstrated the operability of molten-salt reactors, the scheduled period of its operation was brief and did not include a program of chemical analysis. For the MSRE, however, we sought to demonstrate through a long period of operation the stability of such reactors,

ORNL-DWG 69-7293R2

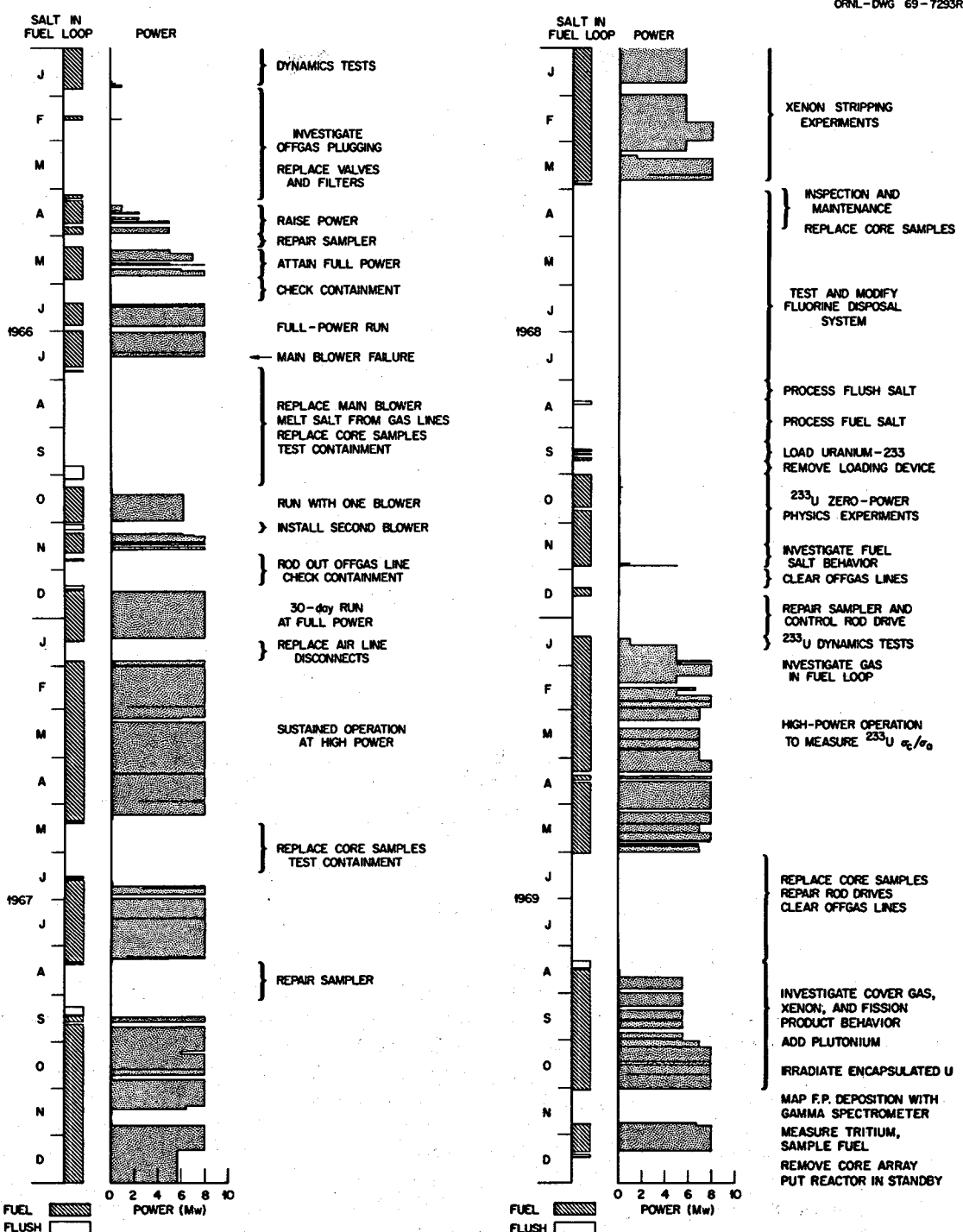
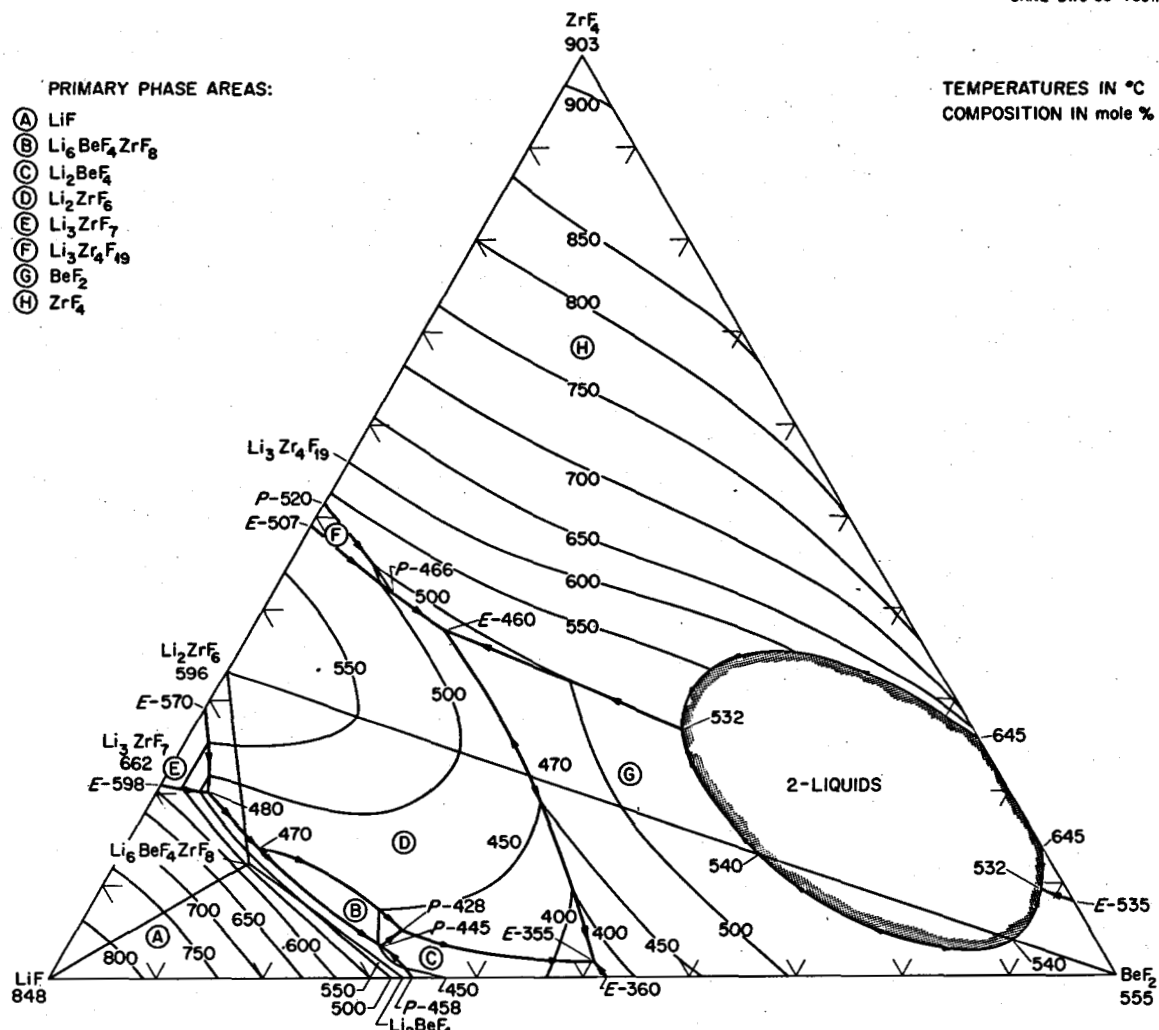


Fig. 1.2. Chronological outline of MSRE operations.

Fig. 1.3. The system $\text{LiF-BeF}_2\text{-ZrF}_4$.

and their capability to operate free from corrosion problems for long periods of time at high temperatures. It was also our purpose to examine the possibility of adapting those analytical chemical methods which proved to be most successful with the MSRE to the development of in-line methods for MSBR analysis and control. Accordingly, our primary goals were to determine continually whether the concentration of uranium in the fuel salt coincided with that expected from reactor physics calculations and on-site neutronic measurements, whether chemical evidence would indicate that the salts remained free of oxide as a contaminant, and to establish rates of corrosion. The frequency of sampling was set at the beginning of operations essentially to coincide with estimates of

reasonable maximum capability of the analytical laboratory, and was at first about one sample per shift, decreasing in frequency as it became evident that no serious problems were developing in relation to corrosion and reactivity anomalies to one per day, three per week, and in the final stages of MSRE operations to once a week.

The results of chemical analyses have served as a good measurement of the generalized corrosion and have provided a convincing demonstration of the compatibility of molten-fluoride fuels and coolants with Hastelloy N. Analyses of the changes in isotopic composition of the plutonium and uranium in the fuel salt samples established with good precision the average power output of the reactor. Studies of the relation of ^{95}Nb

disposition within the fuel system of the MSRE showed that the distribution of the isotope within the system reflects the oxidation-reduction potential of the salt in such a manner that behavior of ^{95}Nb in molten-salt breeder reactors may be exploited as an in-line indicator of potential corrosion.

Results of the chemical analyses performed in support of MSRE operations comprise the basic data from which various inferences can be made pertaining to the performance of the MSRE. For example, those relating to corrosion phenomena, power output, fuel stability, fission product chemistry, and distribution of tritium within the system have been judged on the basis of results obtained in a program of chemical monitoring of specimens removed from the MSRE. They comprise a body of information which forms the basis for ranking priorities in future research and development programs. For these reasons, this report has been prepared to include all of the available results of chemical analysis which were obtained in connection with the operation of the MSRE. Except for the correlations of the disposition of ^{95}Nb in the fuel salt in relation to the oxidation-reduction potential of the salt, fission product chemistry is omitted. Studies of the behavior of fission products in the MSRE have been carried out by F. F. Blankenship, S. S. Kirslis, E. G. Bohlmann, and E. L. Compere. The results of their studies are described in a report⁶ which summarizes this aspect of the operational experience with the MSRE.

References

1. *Nucl. Appl.* 8(2) (February 1970).
2. W. R. Grimes, *Nucl. Appl.* 8, 137 (1970).
3. R. E. Thoma et al., *J. Nucl. Mater.* 27, 166 (1968).
4. G. Long and F. F. Blankenship, *Reactor Chem. Div. Ann. Progr. Rep.* Jan. 31, 1965, ORNL-3789, p. 65.
5. E. S. Bettis and W. K. Ergen, "Aircraft Reactor Experiment," chap. 16 in *Fluid Fuel Reactors*, ed. by J. A. Lane, H. G. MacPherson, and F. Maslan, Addison-Wesley, Reading, Pa., 1958.
6. F. F. Blankenship, E. G. Bohlmann, S. S. Kirslis, and E. L. Compere, *Fission Product Behavior in the MSRE*, ORNL-4684 (in preparation).

2. CHEMICAL BEHAVIOR IN THE FUEL AND COOLANT SALT SYSTEMS DURING PRENUCLEAR OPERATIONS

2.1 Preoperational Procedures

Three types of fluoride mixtures were prepared for use in the MSRE: (1) a salt mixture of the approximate composition $^7\text{LiF-BeF}_2-\text{ZrF}_4$ (65.30.5 mole %), for use as the fuel carrier; (2) another of the composition $^7\text{LiF-BeF}_2$ (66.34 mole %), for use as the coolant and flush salts; and (3) $^7\text{LiF-}^{238}\text{UF}_4$ and $^7\text{LiF-}^{235}\text{UF}_4$ (73.27 mole %) mixtures, for use in constituting the initial fuel charge as well as for subsequent enrichment of the fuel as required. A detailed description of the methods employed is reported elsewhere.¹

Late in 1964, the MSRE fuel and coolant salt systems were heated to $\sim 650^\circ\text{C}$ and purged of moisture; the fuel and coolant drain tanks were then charged with salt of the composition $^7\text{LiF-BeF}_2$ (66.34 mole %), 2611 kg in the coolant system and 4187 kg in the fuel system. The coolant loop was filled on January 9, 1965, and on January 12, 1965, flush salt was circulated in the fuel loop for the first time.

After the operability of the equipment and the cleanliness of the system had been demonstrated, fuel carrier salt (lacking enriched uranium) was charged into fuel drain tank No. 2 (FD-2) beginning on April 21, 1965. The contents of 35 shipping containers (4560 kg of salt) were melted and transferred to the drain tank. To this was added 236 kg of $^7\text{LiF-UF}_4$ eutectic containing 147 kg of ^{238}U (depleted in ^{235}U). Batch containers were heated above the liquidus temperature of the salt mixture in auxiliary furnaces and connected by a small-diameter Inconel tube to the drain tank. The connecting tube extended to the bottom of the batch container so that the salt mixture could be transferred as a liquid by controlling the differential gas pressure in the two containers. All fill operations were accomplished in a routine manner without causing detectable beryllium contamination of the reactor facilities.

The initial fuel loading of the MSRE required approximately 75 ft³ of fused fluorides having the composition $^7\text{LiF-BeF}_2-\text{ZrF}_4-\text{UF}_4$ (65.0-29.2-5.0-0.83 mole %); fissionable ^{235}U comprised about one-third of the uranium inventory. To provide for an orderly approach to critical operation of the reactor and to facilitate fuel preparation, the fuel was produced from

the three salt mixtures described above. The enriched fuel concentrate mixture, in which all ^{235}U was combined with ^7LiF as UF_4 93% enriched in ^{235}U , to form the binary eutectic mixture (27 mole % UF_4), was prepared in six small batches (15 kg of ^{235}U each) for nuclear safety and for planned incremental additions to the reactor fuel system. The balance of the uranium required for the fuel was provided as a chemically identical mixture with UF_4 depleted of ^{235}U . The third component mixture, the barren fuel solvent, consisted of the remaining constituents of the reactor fuel and had the chemical composition $^7\text{LiF-BeF}_2-\text{ZrF}_4$ (64.7-30.1-5.2 mole %). The reactor fuel for the zero-power experiments was produced subsequently by adding small increments of $^7\text{LiF-}^{235}\text{UF}_4$ into this carrier salt in the drain tanks and finally into the pump bowl. The composition of the salt was fixed at this point by the amount of $^{235}\text{UF}_4$ required for criticality to be sustained with one control rod completely inserted.

The addition of the enriched fuel concentrate mixture to the MSRE to within 1 kg of ^{235}U of criticality was accomplished during the latter part of May 1965. The first major addition of enriched fuel concentrate consisted of the transfer of about 44.17 kg of ^{235}U from three containers directly into the fuel drain tank. Three subsequent additions of ^{235}U to the reactor drain tank increased its ^{235}U inventory to 59.35, 64.42, and finally 68.76 kg. The transfer of less than batch-size quantities of ^{235}U was made by inserting the salt transfer line to a predetermined depth in the batch container.

It was anticipated that the composition of the fuel at this point would be $^7\text{LiF-BeF}_2-\text{ZrF}_4-\text{UF}_4$ (65.0-29.17-5.0-0.83 mole %); the composition calculated from the weights of the carrier and enriching salts added to the reactor was changed steadily throughout the zero-power experiments as capsules of the enriching salt were added to the pump bowl.

Complete results of all analyses performed with MSRE salts during the precritical and zero-power experiments are summarized in the following sections of this chapter.

2.2 Flush Salt

Part of the LiF-BeF_2 mixture which was furnished for use in the MSRE was employed to flush the fuel system initially and later, on occasions before and after maintenance periods if it were likely that atmospheric contaminants could have entered the system. Samples of each of the batches of $^7\text{LiF-BeF}_2$ mixtures for use as

flush and coolant salts were analyzed in the facilities of the ORNL Analytical Chemistry Division prior to use in the MSRE. Analytical results for the 61 batches of salt used as flush salt and primary coolant are listed in Table 2.1. Although the nominal composition was $^7\text{LiF-BeF}_2$ (63.34 mole %), the average composition as determined by chemical analysis was $^7\text{LiF-BeF}_2$ (63.56 ± 0.005 - 36.44 ± 0.005 mole %). Examinations of the material balance of the production operations indicate that the disparity in composition was due to an analytical bias. Efforts to determine whether such a bias actually existed were made by the analytical chemists, but were unfruitful.

Before salt was charged into the reactor, the drain tanks and salt loop systems were carefully dried by evacuating and purging with dry helium. A detailed description of the procedures employed is given elsewhere.² Thereafter, late in 1964, approximately 4187 kg of flush salt was charged into the fuel drain tank; it was then transferred among the tanks in the drain tank cell. These operations served to calibrate the weighing devices, to check elevations and volumes, and to establish the operating requirements of the freeze valves. Throughout the prenuclear test period, specimens of the circulating flush salt were obtained for chemical and spectrochemical analysis. The results of spectrochemical analysis are listed in Table 2.2; chemical analyses are listed in Table 2.3. Spectrochemical data were of principal value to ensure that during the early stages of operation the salt charge was free from any unexpected cationic contaminants in the containment system. These analyses were very useful in that they provided the assurance required, but with extended experience with the reactor they became of less significance and were discontinued.

The data shown in Table 2.3 suggest that the operations connected with transfers of the flush salt among the storage tanks in the drain tank cells in November and December of 1964 did not introduce appreciable amounts of structural metal contaminants into the salt; the analytical results for iron suggest, rather, that since its apparent concentration in the salt samples removed from the drain tank was lower by about one standard deviation than the average concentration in the salt before use and in use, it was present in the flush salt initially as metallic particulates which were precipitated from the salt during this period. Little or no change is evident in the chromium concentration before circulation of the flush salt; the data in Table 2.3 can be interpreted, however, to indicate that after completion of the flushing operations in January-March 1965, the chromium analyses represent an

**Table 2.1. Chemical analyses of LiF-BeF₂ (66-34 mole %) produced
for use as MSRE flush and coolant salts**

Batch No.	Net wt. of salt (kg)	⁷ Li Assay	Analyses					
			Li	Be (wt %)	F	Cr	Ni (ppm)	Fe
116	117.3	99.992	13.76	9.61	77.3	18	14	204
117	119.3	99.992	13.77	9.75	77.5	32	14	171
121	119.8	99.992	13.29	9.51	77.2	62	6	125
125	117.8	99.991	13.20	9.59	77.3	16	5	55
126	119.8	99.992	13.27	9.69	76.9	15	32	103
127	119.6	99.992	12.98	9.86	76.8	7	12	123
128	119.6	99.992	13.06	9.81	76.9	9	45	112
129	117.1	99.992	13.20	9.53	77.2	<5	<5	97
131*	117.2	99.991	13.30	9.67	77.0	14	31	104
132	117.7	99.992	13.00	9.78	77.1	<5	18	76
133	124.8	99.992	12.41	9.30	76.3	8	79	161
134	126.1	99.991	12.80	9.84	77.3	6	72	151
135	120.4	99.991	12.90	9.82	77.5	7	21	123
136	120.0	99.991	12.20	9.97	77.2	8	11	180
137	119.4	99.991	12.76	9.49	77.8	6	10	72
138	119.2	99.991	12.70	9.90	77.0	15	23	85
139	105.5	99.991	12.91	9.78	76.2	6	66	119
140	125.3	99.991	12.70	9.81	77.1	21	91	130
141	117.7	99.991	12.70	9.86	77.4	37	36	138
142	111.0	99.991	12.90	10.00	77.2	23	5	130
143	124.4	99.993	12.70	9.97	77.3	19	34	79
144*	118.1	99.994	12.90	9.98	77.2	14	56	110
145	119.8	99.994	12.80	9.96	77.0	15	<5	142
146	119.8	99.994	13.00	10.00	77.4	23	134	135
147	118.8	99.994	12.90	10.00	77.1	18	107	117
148	119.1	99.993	12.90	10.10	77.3	24	12	119
149	117.5	99.993	12.80	9.89	77.4	13	105	166
150	118.7	99.993	13.20	9.70	76.7	18	34	86
151	124.6	99.993	12.90	9.82	77.4	13	12	143
152	112.3	99.994	12.50	9.62	77.4	9	27	172
153	125.6	99.994	13.00	9.84	76.7	17	31	132
154	95.9	99.994	11.10	9.55	77.2	26	47	106
155	128.1	99.994	13.90	8.92	76.2	27	91	117
156	119.1	99.993	12.70	9.55	77.3	17	28	92
157	118.8	99.993	13.20	9.80	77.0	11	29	93
158	119.4	99.993	13.20	9.80	77.1	17	29	124
159	119.2	99.993	13.10	9.74	76.9	13	108	163
160*	119.6	99.994	13.20	9.77	77.0	13	11	99
161	118.9	99.994	13.20	9.80	77.2	8	18	75

* Production Excess.

Table 2.2. Spectrochemical analysis of MSRE flush salt during initial use

Sample No.	Impurity concentration ^a											
	Al	B	Bi	Ca	Cu	Mg	Mn	Na	Pb	Si	Sn	Zr
FD-2-2 ^b	B		A	C	C	C						
FD-2-3	B		A	C	C	C						
FD-2-4	A	C	A	C	C	C						
FD-2-5	A		A	C	C	C	B					
FP-1 ^c	A		A	C	C	C		B	B			
FP-2	A		A	C	C	C			B			
FP-3	A		A	C	C	C		B	B			
FP-4	A		A	C	C	C		A	B			
FP-5	A	B	A	C	C	C		B	B			
FP-6	A		A	C	C	C						
FP-7	A		A	B	C	C						
FP-8	A	C	A	B	C	C						
FP-9	A	A	A	B	C	C	C	B				
FP-10	A	C	A	B	C	C	C					
FP-11	A	A	A	B	C	C						
FP-12	A	A	A	B	C	C	B					
FST-1 ^d	B		A		B	C		B				
FST-2	B		A	<C	B	C						
FST-3	B		A		B	C						
FD2-7	B		A					>A				
FD2-8	B		A					>A				
FD2-9	B		A					>A				

^aLi and Be omitted. A = 100 to 1500 ppm, B = 10 to 100 ppm, C = 1 to 10 ppm.

^bFD designates samples removed from the fuel drain tank.

^cFP designates samples removed from the fuel pump bowl.

^dFST designates samples removed from the fuel storage tank.

average final value of 60 ppm. If it is assumed that the increase resulted from scavenging of moisture or oxides from the system, one would anticipate a corresponding increase of 12 ppm of oxygen in the salt (see Sect. 6.1).

Results of oxygen analyses of the flush salt exhibited perplexing variance. The larger values are believed to reflect adsorption of moisture inadvertently introduced through the handling procedures after samples were removed from the reactor. If the oxygen concentrations were representative of either contamination of the salt by water or oxidation of the container alloy by atmospheric oxygen, the occurrence of chemical attack on the Hastelloy N walls of the circuit should have been reflected in increased concentrations of chromium in the salt. For example, if an increase of oxide concentration in the order of 200 ppm were to have been caused by such reactions, an equivalent increase in chromium concentration of 60 ppm should have been observed.

To test whether a large bias might have been involved in the fluorination assay of oxygen concentration (the KBrF₄ method), large (50 g) samples of the salt were obtained and analyzed by a newly developed method which, like the purification procedures, depends on the removal of water by sparging the molten salt with an H₂-HF stream. For the three samples that were analyzed in this manner, the average concentration found was 75 ppm.

After the flush salt was drained from the reactor on completion of the tests in which it was used, the flush

Table 2.3. Composition of MSRE flush salt in prenuclear operations

Date	Sample	Weight percent						Parts per million					
		Li	Be	Zr	U Book	U Analytical	F	Σ	Fe	Cr	Ni	Pu	O ^a
11/30/64	Charge salt ^b	12.68	9.62				76.51	99.01	137	17	34		
	DC-1	13.12	9.68				77.08	99.94	45	45	7	432	
12/8/64	DT-1								59	16	24	419	
12/11/64	DT-2								48	18	<3	390	
12/15/64	FD-2-3								44	22	49	555	
1/12/65	FD-2-5								140	24	10		
1/12/65	FP-1											35	
1/13/65	FP-2	13.65	9.83				80.52	104.02	110	<10	33	56	
1/14/65	FP-3											46 ^c	
1/16/65	FP-4	13.55	9.35				79.34	102.27	212	62	30	74	
1/18/65	FP-5											72 ^c	
1/20/65	FP-6	13.50	9.96				80.07	103.56	125	<10	<20	180	
1/23/65	FP-7	13.65	9.46				77.85	101.00	180	54	<20	150	
2/3/65	FP-8											106 ^c	
2/3/65	FP-9	13.35	9.98				75.80	99.17	210	57	<20	142	
2/11/65	FP-10		9.49				75.05		128	60	<20	1560 ^d	
2/23/65	FP-11												
3/4/65	FP-12							No analyses performed					144
	Av	13.47	9.68				77.96	101.66	118	38	22		

^aKBrF₄ method unless otherwise noted.

^bAverage for 61 batches.

^cHF purge method.

^dSample stored 48 hr in capped plastic container before analysis.

salt was reprocessed.³ The salt was transferred by gas pressure to the fuel storage tank in the fuel reprocessing system and sparged with a mixture of H₂ and HF. It was concluded from measurements of the HF concentration in the off-gas stream that the reprocessing operations were effective in removing 115 ppm of oxide from the salt.³ The oxide concentration should have been reduced by this process to the same concentration which resulted from preparation and purification of the salt, ~55 ppm.⁴ The results of chemical analysis indicated that the chromium concentration of the flush salt increased by 43 ppm in use, corresponding to an increase of 180 g of chromium, and equivalent to 55.5 g of oxide, or to an increase of 13 ppm in oxide concentration. The H₂-HF analytical data indicated that the average concentration of oxide in the flush salt during its use was 75 ppm, or that the oxide concentration of the salt increased by 20 ppm in use. This increase, while slightly greater than would have been anticipated from the above discussion, may be rationalized by the following considerations. An indeterminate fraction of the oxide removed in reprocessing was introduced from the oxide scales present on the surfaces of the chemical reprocessing facility containers, the fuel storage tank, and the walls of the fuel circuit. Prior purge of the system with dry inert gas was performed before the facility was used for reprocessing the flush salt, but the system was not previously flushed with a scavenger salt. It might therefore have been anticipated that the oxide concentration of the salt in the reprocessing system, after its initial use, would yield a higher concentration of oxide than that removed from the salt in the fuel circulation system. Thus, if it is assumed that in the reprocessing experiment ~0.4 kg of oxide scale was removed from the system, good agreement exists among the analytical data, except for measurement of oxide concentration by the KBrF₄ method.

One potential use of the flush salt that had been anticipated was to remove any oxides that might deposit in the heat exchanger if the fuel salt were to become seriously contaminated. Concurrent with the beginning of MSRE operations, chemical data appeared⁵ which showed that the solubility of the least soluble oxide in the LiF-BeF₂-ZrF₄ carrier salt was some three times that in LiF-BeF₂ mixtures. It was thus necessary to regard the flush salt as an agent which might have limited capacity to scavenge oxide impurities from the fuel circuit unless, if saturated, it were reprocessed. Its principal function after initial use was to remove residues containing uranium fluoride from the fuel circuit after it was drained. Concurrently, the

capacity of the flush salt to contain dissolved oxides increased with each use in the reactor, because the fuel residues carried into the flush salt added about 2.5 kg of zirconium to the salt each time it was used. It would probably have questionable value if it were expedient to dissolve precipitated oxide deposits from the heat exchanger. This did not preclude the use of LiF-BeF₂ flush salt for such application, because at 650°C the solubility of the saturating oxide phase, BeO, in the salt was known to be ~200 ppm, corresponding to a capacity of the flush salt to dissolve and retain 1.135 kg of ZrO₂ in solution at this temperature. Successive repurification and removal of oxides that were picked up in the salt would permit it to be used to clear the heat exchanger of an oxide plug if necessary. No such requirement developed. A preferable alternative was also available if needed. The increased solubility which small amounts of zirconium fluoride provide, increasing the oxide solubility to 800 ppm for a few mole percent of ZrF₄, showed that if it were expedient to do so, the composition of the flush salt could have been changed simply by the addition of ⁷LiF-ZrF₄ so as to enhance its solvent capacity for precipitated oxides.

Operation with the flush salt also shed light on another aspect of the use of molten fluorides in a circulating system, namely, the appearance of salt (or salt constituents) in the cover gas. Analysis of the helium cover gas by Million and Pappas (see Sect. 2.4.5) indicated the presence of fluorides in the fuel off-gas, but this probably represented salt droplets rather than any decomposition product.

The principal difference in the design of the fuel and coolant pumps is that the fuel pump contains a spray ring which functions to remove fission product gases from the fuel. The major salt flow into the pump tank is through a bypass that is taken from the volute discharge line into a toroidal spray ring in the upper part of the pump bowl. From there the salt sprays out through two rows of holes and impinges on the salt surface in the tank to provide gas-liquid contact for gas stripping.⁶ This difference in design of the two pumps seems to account for the fact that it was occasionally necessary to remove solids from filters, valves, and lines in the fuel system, but rarely necessary with the coolant system. Material recovered from the coolant off-gas system showed only traces of salt constituents, but the fuel off-gas solids generally contained minute beads of frozen salt.

One experiment conducted during the precritical operation period consisted of krypton stripping tests. For these tests, a special insert was installed into the side of the off-gas flange nearest to the fuel pump bowl.

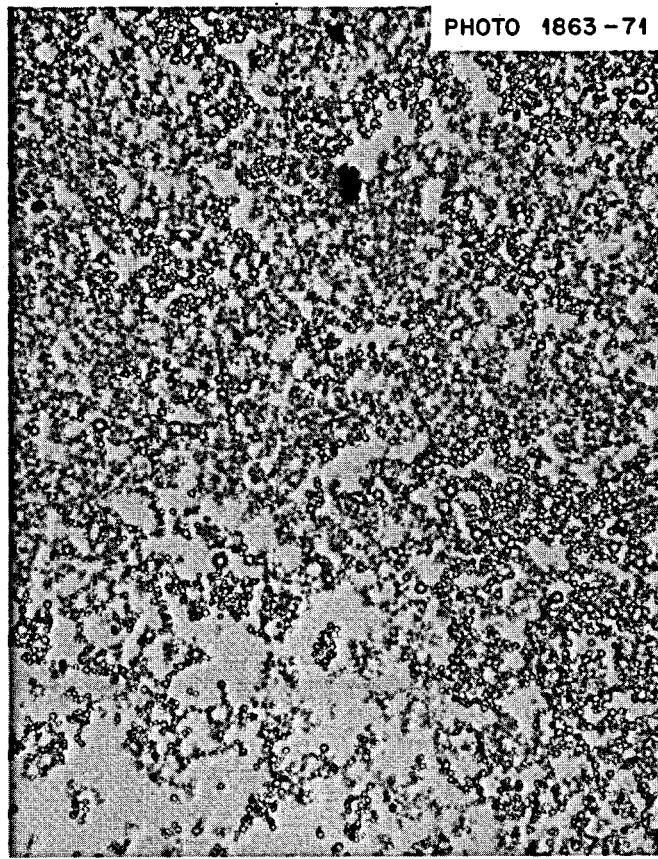


Fig. 2.1. Fluoride glass beads removed from MSRE off-gas line after precritical experiment PC-1.

Later, the flange was opened to remove the insert; inspection showed that small amounts of small glassy beads were deposited between the flange faces.

Toward the end of the first set of experiments with flush salt, fuel pressure control became erratic (see Chap. 11). After the salt was drained from the circuit in March 1965, the gas pressure control valve far downstream at the vent house was found to be partially plugged. The valve body was rinsed with acetone, which was found to contain beads (1 to 5 μ in diameter) of a glassy material.

After a week of carrier salt circulation in May 1965, the small control valve again began to plug. This time, it was removed and cut open for examination. A deposit on the stem was found to be about 20% amorphous carbon, and the remainder was 1- to 5- μ beads having the composition of the flush salt. A photograph of these beads, obtained with the petrographic microscope, is shown in Fig. 2.1. The glass beads were found to have a refractive index of 1.315. As computed by interpolation of the refractive indices of the crystalline components LiF and BeF₂, its composition would be

LiF-BeF₂ (54-45 mole %). Chemical analysis showed, however, that its actual composition was LiF-BeF₂ (66-34 mole %). The anomalous refractive index of the glass results from its glassy character; that is, the liquid phase at LiF-BeF₂ (66-34 mole %) is of significantly lower density than the crystalline solids of this composition. The beads were glass rather than crystalline, implying rapid cooling of the molten-salt mist. The carbon was presumably soot from oil that had been thermally decomposed in the pump bowl.

2.3 Coolant Salt

The coolant salt mixtures for use in the MSRE were prepared as described elsewhere.¹ Twenty-four batches of the salt mixture were allocated for use as the coolant. The composition and purity of these mixtures are listed in Table 2.4. A charge of 2610 kg of ⁷LiF-BeF₂ (66-34 mole %) was delivered in molten form to the coolant drain tank in October 1964. The coolant system was preheated and purged of moisture in a similar manner to the fuel system, but was not

Table 2.4. Fluoride production for MSRE coolant salt mixture
 LiF-BeF_2 (66-34 mole %)

Batch No.	Net weight of salt (kg)	^{7}Li assay	Chemical analyses					
			Weight percent			Parts per million		
			Li	Be	F	Cr	Ni	Fe
101	118.1	99.991	13.68	9.43	76.9	8	32	133
102	116.2	99.991	14.23	9.14	77.2	5	8	175
103	121.2	99.991	13.81	9.32	76.7	10	58	182
104	119.5	99.990	13.68	9.82	77.2	17	11	208
105	113.2	99.990	12.83	9.57	77.1	27	45	216
106	119.0	99.990	13.43	9.66	77.2	11	68	309
107	115.0	99.990	13.12	9.58	76.9	10	18	94
108	114.5	99.990	12.81	9.65	77.3	7	13	246
109	119.9	99.990	13.73	9.27	77.0	8	5	62
110	127.9	99.990	13.15	9.57	76.6	19	12	94
111	121.2	99.990	13.99	9.21	76.5	13	8	142
112	120.0	99.991	13.81	9.47	77.0	11	48	218
113	117.6	99.991	13.80	9.53	77.0	<5	25	212
114	120.9	99.991	13.14	9.79	77.0	9	22	196
115	120.8	99.991	13.74	9.54	77.4	14	5	131
118	125.0	99.991	13.06	9.91	77.3	9	20	134
119	114.5	99.991	12.41	10.16	76.9	10	18	182
120	125.5	99.991	13.65	9.52	77.1	8	35	127
122	117.8	99.991	13.26	9.48	77.3	39	70	126
123	117.9	99.991	13.37	9.48	76.9	48	10	113
124	118.5	99.991	13.35	9.45	77.1	86	14	154
130	119.9	99.990	13.10	9.55	77.4	40	13	188

preflashed with molten salt. The system was filled and drained 18 times during the time the MSRE was operated. The chemical behavior of the coolant salt was not noticeably different during prenuclear operations from those that followed, and will be described in detail later in this report.

2.4 Fuel Salt

2.4.1 On-site preparation. After circulation in the reactor in March 1965, the flush salt was drained to fuel drain tank FD-1. The fuel salt was then constituted within the reactor. The $^{7}\text{LiF-BeF}_2\text{-ZrF}_4$ fuel carrier mixture was charged into fuel drain tank FD-2, starting April 21, 1965. On-site records show that 4558.1 kg (the contents of 35 shipping containers) of this carrier salt was melted and transferred to the drain tank; to this was added 236.2 kg of $^{7}\text{LiF-}^{238}\text{UF}_4$, containing 147.6 kg of ^{238}U (depleted in ^{235}U). In our current review of the significance of the results of chemical and mass spectrochemical analyses, it becomes evident that these values are in minor error. The $^{7}\text{LiF-BeF}_2\text{-ZrF}_4\text{-}^{238}\text{UF}_4$ as described above was circulated through the fuel circuit for some 250 hr during precritical test PC-2.

Each of the two fuel drain tanks on the MSRE incorporates two pneumatic weigh cells for estimating the inventory of the salt in these tanks. Calibrations of the weigh cells in the drain tanks were made carefully during the initial stages of operations. The precision of these measurements was found to be about $\pm 0.8\%$ (± 28 kg).⁷ Continued experience with this equipment indicated long-term drifts in the readings. It was necessary, therefore, to determine inventories on the basis of analytical chemical data, and on computations involving salt densities and volumes at certain reference points (the circulating loops filled to the pump bowls or the tanks filled to the level probe points) to eliminate the effects of extraneous forces on the indicated weight.⁸

During the initial fill operations, $^{7}\text{LiF-BeF}_2$ flush salt was admitted to all parts of the fuel circuit system. On draining the reactor, flush salt remained on the pump rotor and in the freeze valves, as well as residue in the heat exchanger. At this point, some 35 kg of salt was unaccounted for by the weigh cell data and was presumed to have remained in these locations. The $^{7}\text{LiF-BeF}_2\text{-ZrF}_4\text{-}^{238}\text{UF}_4$ salt mixture was introduced into the same circuitry at the beginning of the PC-2 test and was, therefore, diluted slightly by flush salt. Later in this report, it is shown that the increased concentration of uranium in the flush salt after use indicates that the salt residue left in the fuel circuit system after it is drained is about 20 kg. Estimation of the nominal concentration of uranium in the fuel during precritical test PC-2 thus requires the assumption that ~20 kg of flush salt was added initially to the fuel. As noted in Sect. 2.4.2, however, the best agreement between expected and observed concentration is found when it is assumed that a negligible amount of flush salt residue remained in the system at completion of PC-2. This assumption is untenable. An alternate assumption, that less carrier salt was delivered to the reactor than was credited in the loading operation, is more credible as an explanation of the apparent anomaly.

Chemical analyses were conducted during the precritical experiments for the purpose of establishing analytical base lines for use in the full-power operating period. Prior to the zero-power experiment, analyses of all salt samples were conducted with conventional equipment in the facilities of the ORNL Analytical Chemistry Division. Thereafter, the fission product activity made it necessary to perform all analyses in the ORNL High-Radiation-Level Analytical Laboratory (HRLAL). The facilities of this laboratory have been described elsewhere.⁹ In order to provide continuity which would relate the results of prenuclear operations with those that followed, specimens of the fuel salt obtained

during the precritical test period were analyzed concurrently in both facilities.

Mass spectrometric analyses were performed routinely throughout $^{235},^{238}\text{U}$ operations. Samples of the fuel salt were analyzed before, during, and at the completion of the ^{235}U loading operation. The results reflected the isotopic dilution of ^{238}U precisely and were used in tests for corroboration of the agreement between estimated and analytical values of the concentration of uranium in the fuel salt and to refine estimates of the amount of depleted uranium that was charged into the fuel system.

The composition of the fuel salt was changed steadily throughout the zero-power experiments (run No. 3) as capsules of the enriching salt were added to the pump bowl. Compositional analysis during this period served, therefore, to permit evaluation of the fuel composition dynamically rather than as a statistical base for reference during the power run.

Most of the uranium required for enrichment was loaded in four charging operations to one of the fuel drain tanks, FD-2. After each addition the salt was transferred to the second drain tank and back again to ensure thorough mixing. The mixed salt was loaded into the reactor system after each charging operation, and count rate data were taken at several salt levels in the core and with the reactor vessel full. These data were compared with the barren-salt data to monitor the neutron multiplication and to establish the size of the next addition.¹⁰ Extrapolation of inverse-count-rate plots with the reactor vessel full showed that the loading after the fourth addition was within 0.8 kg of ^{235}U of the critical loading when the salt was not circulating and the control rods were withdrawn to their upper limits. The remainder of the ^{235}U was added directly to the circulating loop with enriching capsules. These were inserted into the fuel-pump bowl via the sampler-enricher to increase the loading by 85 g of uranium at a time. Count rates were measured after each capsule with the fuel pump off and the control rods withdrawn. The reactor became critical after the eighth capsule with the pump off, two rods fully withdrawn, and one rod poisoning 0.03 of its available worth.

These zero-power experiments (run 3) were completed on July 4, 1965, after 764 hr of circulation of the salt. The fuel was then drained and mixed with the salt remaining in the drain tanks. After the fuel loop was drained, it was filled with flush salt, which was circulated 1.3 hr, sampled, and drained. Analysis of the flush salt led to the conclusion that 0.77 kg of uranium remained in the fuel circuit on completion of run No. 3.

Final preparations were made for operation of the reactor at power. In December 1965, low-power experiments were begun. As soon as containment testing was finished, the instruments, controls, and equipment were given the check-outs required prior to startup. The fuel system was then heated, and flush salt was circulated for three days. Samples of the flush salt were taken. Then fuel was charged to the loop for tests in the reactor at various low power levels, 100 and 500 kW and finally 1 MW. The experiments that were conducted during this time extended over a one-month period, providing the single period of operation when the composition of the fuel salt remained nominally constant.

Samples of the fuel salt were obtained regularly during this period in a continuing effort to appraise the utility of the chemical surveillance program and in order to verify that the reactor system was in suitable condition for the initiation of power operations. Good agreement between anticipated and observed results was found. The results of chemical analyses indicated that the system had remained free of corrosion during all preliminary operations, and it seemed that the analyses would serve as a reliable measure of fuel stability and corrosion.

2.4.2 Uranium assay. Chemical analyses and on-site nuclear measurements were accumulated regularly when fuel salt was circulated in the reactor in order to evaluate as many aspects of the behavior of the molten radioactive fuel salt as feasible in contact with the Hastelloy N containment system and with the graphite moderator. A number of important characteristics of the reactor soon became evident. For example, by the time that statistically significant populations of analytical chemical data were produced from the HRLAL it had become apparent that on-site neutronic measurements of the reactivity balance were sufficiently sensitive to detect changes of as little as 0.1% in the concentration of fissile material circulating in the fuel system.¹¹ This represented at least a factor of 10 greater sensitivity than was indicated by the statistically significant results of chemical analysis. In addition, reactivity balance measurements were made dynamically and, essentially, on a continuous basis. While chemical data alone were useful as statistical indicators of trends in the concentration of uranium over extended periods, the combined results of chemical and mass spectrometric analyses furnished information that was uniquely suited for use in establishing numerous fundamental values for use in subsequent evaluations of MSRE performance, and in accounting for the changes in the distribution of uranium between the fuel and flush salt systems.

In order to compare the concentration of uranium in the fuel salt as measured analytically with expected values, we have evaluated the results of chemical analysis, mass spectrometric analysis, the weights of the fluorides as measured in the production facility, and on-site measurements of the weights of the salt containers delivered to the MSRE. From the weights of the enriching salts credited to the reactor and from the isotopic composition a uranium material balance was computed. Progress reports for this period of MSRE operations indicate that satisfactory agreement between nominal and analytical values was found. As the results of mass spectrometric analyses were accumulated, however, comparisons of the nominal isotopic composition of uranium during initial loading operations at the MSRE with the results of mass spectrometric analyses disclosed that closest agreement is reached when the assumption is made that the initial ^7LiF - $^{238}\text{UF}_4$ charge contained 145.6 kg of uranium rather than 147.6 kg as credited (see below). This lesser amount of uranium, carried by 234.5 kg of ^7LiF - $^{238}\text{UF}_4$ enriching salt and

added to the amount of ^7LiF - BeF_2 - ZrF_4 carrier salt credited to the MSRE (4558.1 kg), would produce a salt mixture in which the concentration of uranium is 3.038 wt %.

The average concentration observed was 3.044 wt %. In the early stages of analysis, a bias of -0.8% was discovered in the amperometric data¹² which, when used to correct the analytical results, causes the average observed concentration in precritical run No. 2 to be 3.068 wt %. Thus the nominal concentration of uranium in the fuel salt is inexplicably lower than the averages of the observed values if the amount of carrier salt credited to the MSRE (4558.1 kg) is assumed to be accurate. A computation of the material balance for the MSRE fuel salt in prepower tests, using this value, is summarized in Table 2.5, which shows that the analytical values tend to indicate slightly greater average concentrations than nominal. If, however, we assume that ~40 kg of the carrier salt was not charged into the fuel circuit, and the fuel charge during the precritical experiment was constituted from 145.60 kg of uranium

Table 2.5. Material balance for MSRE fuel salt in prepower tests

	Inventory (kg)			Uranium concentration (wt %)	
	U	^7LiF - UF_4	Total	Nominal	Analytical
Run PC-2 (av)	145.60	234.5	4792.6	3.038	3.068
Run 3, FP-3-1,2					
Added	+47.49	76.5			
Total	193.09	311.0	4869.1	3.965	3.998
Run 3, FP-3-3					
Added	+21.43	34.53			
Total	214.52	345.53	4903.6	4.375	4.390
Run 3, FP-3-4					
Added	+4.67	+7.52			
Total	219.19	353.05	4911.1	4.463	4.446
Loop charge	195.23		4374.3	4.463	
Left in drain tank	23.96		536.8	4.463	
Run 3-F					
Added	+7.83	+12.74			
Σ charge	227.02		4923.7	4.611	
Loop charge	203.06		4386.9	4.629	
Loop residue	-0.77		-16.5		
To drain tank	202.29		4370.4	4.629	
Already in drain tank	+23.96		+536.8	4.462	
FD-10-3	226.25		4907.2	4.611	4.648
Run 4-I, loop charge	208.15		4514.6	4.611	
Flush residue		+18.0			
Loop charge	208.15		4532.6	4.592	4.642 ± 0.028
Run 5-I, drain tank	226.25		4925.2	4.593	
Runs 5-7 (av of 14 samples)					4.629 ± 0.026
Run 4 (av of 22 samples)					4.642 ± 0.028
Runs 4-7 (av of 36 samples)					4.638 ± 0.025

and 4754.5 kg of salt, the nominal concentration of uranium should be 3.062 wt %, as compared with an analytical value of 3.068 wt %. Comparably improved agreement is found between the nominal and observed concentrations of uranium for all other prepower measurements when the assumption is made that the above quantities of uranium and salt were charged to the MSRE fuel system. A uranium material balance for the prepower period was computed on the basis of these values, and is given in Table 2.6. We deduce, therefore, that the salt charge which was used for the precritical test, PC-2, consisted of 145.6 kg ^{238}U in a total salt charge of 4754.5 kg. The results of the chemical analyses performed with samples of the fuel salt during this test are listed in Table 2.7. Most of the uranium required for enrichment was loaded in four charging operations to one of the fuel drain tanks, FD-2. Samples of the fuel salt were obtained frequently during this period in a continuing attempt to appraise the utility of the chemical surveillance program, and to

verify that the reactor system was in suitable condition for the initiation of power operation.

As the concentration of uranium in the fuel salt was increased in preparation for operating the reactor at full power, fuel-salt samples were obtained for isotopic and compositional analysis after groups of three or four capsules of enriching salt were added. Changes in the isotopic composition of uranium in the fuel salt during initial loading operations are summarized in Table 2.8. Compositional analyses were obtained over a period when the incremental change in the concentration of uranium in the fuel salt was large in comparison to that in the normal operating mode of the reactor. They serve, therefore, to permit evaluation of the fuel composition dynamically rather than as a statistical base for reference during the power run. The results of these analyses are listed in Tables 2.9 and 2.10.

As noted previously, the salt mixture used in the precritical test, PC-2, was formed from purified salt mixtures of the nominal compositions ^7LiF - BeF_2 - ZrF_4

Table 2.6. Material balance for MSRE fuel salt in prepower tests

	Inventory (kg)			Uranium concentration (wt %)	
	U	^7LiF - UF_4	Total	Nominal	Analytical
Run PC-2 (av)	145.60	234.5	4752.6	3.064	3.068
Run 3, FP-3-1,2					
Added	+47.49	76.5			
Total	193.09	311.0	4829.1	3.998	3.998
Run 3, FP-3-3					
Added	+21.43	34.53			
Total	214.52	345.5	4863.6	4.410	4.390
Run 3, FP-3-4					
Added	+4.67	+7.52			
Total	219.19	353.05	4871.1	4.500	4.446
Loop charge	195.23		4338.6	4.500	
Left in drain tank	23.96		532.5	4.500	
Run 3-F					
Added	+7.83	+12.74			
Σ charge	227.02		4883.8	4.648	
Loop charge	203.06		4351.3	4.667	4.665
Loop residue	-0.77		-16.5		
To drain tank	202.29		4334.8	4.667	
Already in drain tank	+23.96		+532.5	4.500	
FD-10-3	226.25		4867.3	4.648	4.648
Run 4-I, loop charge	208.15		4477.9	4.648	
Flush residue		+18.0			
Loop charge	208.15		4495.9	4.630	4.642 ± 0.028
Run 5-I, drain tank	226.25		4885.3	4.631	
Runs 5-7 (av of 14 samples)					4.629 ± 0.026
Run 4 (av of 22 samples)					4.642 ± 0.028
Runs 4-7 (av of 36 samples)					4.638 ± 0.025

Table 2.7. Summary of MSRE salt analyses, experiment No. 2, fuel salt
Nominal composition of salt: ^7LiF - BeF_2 - ZrF_4 - $^{238}\text{UF}_4$ (64.86-29.54-5.07-0.53 mole %)

Date	Sample	Weight percent						Parts per million				
		Li	Be	Zr	U		F	Σ	Fe	Cr	Ni	O
					Nominal	Analytical						
5/11/65	FP-2-13 ^a	10.30	6.99	11.32	3.062	3.043	67.50	98.66	74	26	34	2045 ^b
5/12/65	FP-2-14 ^c	10.20	6.55	11.49	3.062	3.041	71.90	103.18	149	<50	36	
5/12/65	FP-2-15	10.14	7.09	11.42	3.062	3.023			95	19	18	4715
5/13/65	FP-2-16	10.50	6.60	12.09	3.062	3.044	71.60	103.84	271	<50	33	
5/13/65	FP-2-17	10.30	6.54	11.08	3.062	3.053	67.40	98.38	75	21	21	155
5/13/65	FP-2-18	10.50	6.54	11.81	3.062	3.053	73.40	105.31	152	<50	43	
5/14/65	FP-2-19	10.20	6.16	11.41	3.062	3.061	71.40	102.22	130	26	47	
5/15/65	FP-2-20	10.53	6.64	11.36	3.062	3.023	68.20	99.76	120	23	21	660
5/16/65	FP-2-21	10.30	6.38	11.08	3.062	3.039	71.00	101.81	133	25	49	
5/17/65	FP-2-22	10.20	6.21	11.17	3.062	3.052	71.10	101.74	221	28	55	
5/18/65	FP-2-23	10.30	6.16	11.23	3.062	3.033	70.50	101.23	159	28	42	
5/18/65	FP-2-24	10.78	6.84	11.18	3.062	3.014	68.60	100.42	76	23	<5	215
5/19/65	FP-2-25	10.52	6.50	11.36	3.062	3.014	67.00	98.40	110	24	17	
5/19/65	FP-2-26	10.60	6.67	11.27	3.062	3.038	71.40	102.98	113	24	<20	
5/20/65	FP-2-27	10.46	6.44	11.28	3.062	3.063	67.10	98.35	27	23	14	70
5/20/65	FP-2-28	10.55	6.57	11.05	3.062	2.998	72.30	103.47	123	34	<20	
5/21/65	FP-2-29	10.51	7.30	11.11	3.062	3.053	67.70	99.68	203	28	20	405
5/21/65	FP-2-30	10.61	6.59	11.66	3.062	3.025	71.9	103.70	175	27	<20	
									95	23	16.5	
									±21	±2	±4	

^aAnalyses performed under supervision of W. F. Vaughan.

^bAnalyzed by KBF_4 method.

^cAnalysis performed under supervision of C. E. Lamb.

(64.7-30.1-5.2 mole %) and ^7LiF - UF_4 (73.27 mole %). The results of chemical analyses of the individual batches of these salts are listed in Tables 2.11 and 2.12. Results of the analyses of the carrier salt indicate that its composition was ^7LiF - BeF_2 - ZrF_4 (62.25-32.47-5.28 mole %), or that the Li/Be ratio is skewed as noted previously in connection with the coolant and flush salt. While the results from chemical analyses show similar bias in determination of lithium and beryllium when compared with nominal values, they are in good agreement when the analyses of the salts are compared with those for the starting materials. Reexamination of the material balance in the preparation of these salts indicated that deviations from the nominal compositions are much less than is indicated by the analytical data.¹³ In order to estimate how closely the composition of the fuel-salt mixture matched the design composition, it is necessary to compare the analytical results with a nominal composition computed from the analyses of production plant samples. The composition of the salt mixture used in the precritical run compares as shown in Table 2.13 with the nominal composition which would result from (1) combining the carrier salt and LiF - $^{238}\text{UF}_4$ of the design compositions and (2)

combining compositions as indicated from chemical analysis.

In the foregoing discussion, we have estimated the quantities of carrier salt and LiF - UF_4 mixtures used to constitute the MSRE fuel for power tests. The chemical composition of the salt circulated in the fuel circuit at various stages during the zero power and in all prenuclear operations is compared with the results of chemical analyses in Tables 2.14 and 2.15. The values listed in these tables coincide within the precision limits of the analytical chemical results, the mass spectrometric methods, and the estimates of the physical properties of these fluids. We have therefore adopted the nominal compositions listed in Table 2.15 as reference compositions for appraisal of results throughout the remainder of MSRE operations.

2.4.3 Structural metal impurities. One of the features which originally suggested the potential feasibility of molten-salt reactors was the recognition that if the physical and mechanical properties of any one of several nickel-based alloys, such as those composed principally of Ni-Mo-Cr-Fe, were suitable for reactor construction, the alloys would almost certainly be

Table 2.8. Isotopic composition of uranium in the MSRE fuel salt
during initial loading operations

	Σ U Inv. (kg)	Loop Inv. (kg)	^{234}U	^{235}U (kg)	^{236}U	^{238}U	^{234}U	^{235}U	^{236}U (wt %)	^{238}U
LiF- $^{238}\text{UF}_4$ Loading	145.60		-	0.323	-	145.277				
LiF- $^{235}\text{UF}_4$ to 5/25/65	47.49		0.452	44.143	0.187	2.708				
Sample No. FP3-2	193.090		0.452	44.466	0.187	147.985	0.234	23.029	0.097	76.640 ^a
							0.234	22.501	0.099	77.086 ^b
LiF- $^{235}\text{UF}_4$ to 5/30/65	+26.100		0.249	+24.261	+0.102	+1.488				
	219.190		0.701	68.727	0.289	149.473	0.320	31.355	0.132	68.193
		195.240	0.625	61.218	0.257	133.140				
Sample No. FP3-7		+0.820	+0.008	+0.762	+0.003	+0.047				
		196.060	0.633	61.980	0.260	133.187	0.323	31.613	0.133	67.932
							0.247	23.133	0.103	76.437 ^c
Sample No. FP3-12		+1.094	+0.010	+1.017	+0.004	+0.063				
		197.154	0.643	62.997	0.264	133.250	0.326	31.953	0.134	67.587
							0.335	31.784	0.138	67.743
Sample No. FP3-17		+1.789	+0.017	+1.663	+0.007	+0.102				
		198.943	0.660	64.660	0.271	133.352	0.332	32.502	0.136	67.030
							0.340	32.606	0.136	66.918
Sample No. FP3-22		+1.787	+0.017	+1.661	+0.007	+0.102				
		200.730	0.677	66.321	0.278	133.454	0.337	33.041	0.138	66.484
							0.352	33.122	0.141	66.386
Sample No. FP3-27		+1.030	+0.010	+0.957	+0.004	+0.059				
		201.760	0.687	67.278	0.282	133.513	0.340	33.346	0.140	66.174
							0.355	33.340	0.141	66.165
Sample No. FP3-32		+1.274	+0.012	+1.184	+0.005	+0.073				
		203.034	0.699	68.462	0.287	133.586	0.344	33.720	0.141	65.795
							0.355	33.719	0.139	65.787
Run 3-Residue		-0.77	-0.003	-0.241	-0.001	-0.525				
		202.264	0.696	68.221	0.286	133.061				
			0.077	7.510	0.032	16.332				
Run 4-I	23.950									
	226.214		0.773	75.730	0.318	149.393	0.342	33.477	0.141	66.041
							0.354	33.553	0.145	65.948 ^d
							0.350	33.250	0.140	66.260 ^e

^aBold face type indicates nominal values.

^dAverage of 3 analyses.

^bResults of mass spectrometric analyses.

^eAverage of 4 analyses.

^cAnomalous results; possible misidentification of sample.

Table 2.9. Summary of MSRE salt analyses, experiment No. 3, fuel salt

Date	Sample	Weight percent						Parts per million				^{235}U in fuel circuit (kg)	
		Li	Be	Zr	Nominal	Analytical ^a	F	Σ	Fe	Cr	Ni	O	
5/27/65	FP-3-1	10.45	6.49	10.90	4.01	3.984	66.8	98.62	115	28	38	335	39.3
5/27/65	FP-3-2	10.7	6.14	11.19	4.01	3.822	68.63	100.49	161	30	44	3350	39.3
5/30/65	FP-3-3	10.7	6.51	11.08	4.42	4.355	69.23	101.88	323	24	53	3915	56.9
5/31/65	FP-3-4	10.8	6.57	11.10	4.51	4.411	68.4	101.33	371	36	48		60.93
5/31/65	FP-3-5 ^b	10.35	6.71	11.04	4.51	4.450	67.6	100.15	162	28	30	490	60.93
6/2/65	FP-3-6	10.75	6.16	11.60	4.52	4.457	69.69	102.66	112	31	39	330	61.46
6/3/65	FP-3-7	10.6	6.62	11.18	4.52	4.416	70.9	103.72	121	31	44		61.46
6/4/65	FP-3-8	10.65	6.39	11.57	4.53	4.448	70.10	103.16	130	28	49	520	61.62
6/6/65	FP-3-9	10.6	6.29	11.43	4.53	4.448	69.35	102.13	113	34	61	320	61.87
6/7/65	FP-3-10	10.75	6.75	11.39	4.54	4.464	70.12	103.45	122	34	25	875	62.05
6/8/65	FP-3-11	10.65	6.46	11.11	4.54	4.444	70.90	103.56	123	35	62	3715	62.22
6/9/65	FP-3-12	10.55	6.70	11.69	4.55	4.461	68.21	101.61	238	42	68	1745	62.47
6/10/65	FP-3-13	10.70	6.56	11.06	4.56	4.494	70.08	102.89	150	33	53	2465	62.89
6/11/65	FP-3-14	10.50	6.38	11.32	4.57	4.439	69.72	102.36	141	38	60	1760	63.23
6/12/65	FP-3-15	10.70	6.55	11.27	4.57	4.454	69.25	102.22	116	38	39	1115	63.31
6/13/65	FP-3-16	10.30	6.36	11.23	4.58	4.462	68.15	100.90	185	48	34	555	63.81
6/15/65	FP-3-17	10.50	6.28	11.11	4.59	4.523	68.94	101.56	151	44	44	855	64.14
6/16/65	FP-3-18	10.80	6.46	11.62	4.59	4.463	69.48	102.82	143	42	68		64.30
6/17/65	FP-3-19	10.00	6.53	11.13	4.60	4.566	67.12	99.54	139	36	71	605	64.71
6/18/65	FP-3-20	10.50	6.68	10.75	4.60	4.499	68.57	101.03	105	49	61	425	65.12
6/19/65	FP-3-21	10.45	6.31	10.69	4.61	4.504	68.30	100.32	97	31	74	705	65.46
6/20/65	FP-3-22	10.50	6.54	11.24	4.62	4.535	68.90	101.82	134	35	73	820	65.80
6/21/65	FP-3-23	9.90	6.67	10.99	4.63	4.568	68.09	100.47	122	35	84	1570	66.13
6/22/65	FP-3-24	10.30	6.50	11.17	4.63	4.582	68.99	101.54	77	37	47	840	66.13
6/23/65	FP-3-25	10.60	6.80	11.12	4.63	4.587	67.99	101.10	135	38	52	580	66.21
6/24/65	FP-3-26	10.45	6.51	11.48	4.63	4.557	68.20	101.21	135	34	90	440	66.37
6/25/65	FP-3-27	10.40	6.44	10.27	4.64	4.633	68.68	100.42	167	53	28	310	66.80
6/26/65	FP-3-28	10.65	6.26	10.85	4.65	4.610	67.43	99.80	105	38	34	475	67.05
6/27/65	FP-3-29	10.40	6.52	10.18	4.66	4.640	68.54	100.28	110	36	44	520	67.56
6/28/65	FP-3-30	10.35	6.55	10.54	4.66	4.651	68.25	100.34	121	37	40	935	67.90
6/29/65	FP-3-31	10.10	6.56	10.84	4.67	4.642	67.83	99.97	128	39	49	326	67.98
6/30/65	FP-3-32	10.10	6.97	11.20	4.67	4.605	71.66	104.55	149	42	93	1235	67.98
7/2/65	FP-3-33	10.40	6.47	11.24	4.67	4.563	68.20	100.87	170	40	88	965	67.98
7/3/65	FP-3-34 ^c				4.67								67.98
7/4/65	FP-3-35	10.40	6.85	11.15	4.67	4.597	67.79	100.79	158	48	74	1070	67.98
							Av (34)		148	37	55		

^aCorrected for ^{235}U enrichment.^bCriticality.^c50-g sample obtained for A. S. Meyer.

compatible with molten-fluoride mixtures. This recognition developed from the fact that numerous metal fluorides were more stable than the fluorides of these alloy constituents and could be used for fuel and coolant mixtures. By the time conceptual plans for the MSRE were formulated, an alloy of this type was developed at ORNL specifically for application in molten-salt reactor systems, and is now designated as Hastelloy N. Its average composition is 70Ni-16Mo-7Cr-7Fe-0.05C wt %. The selection of salt constituents with respect to their compatibility with such alloys has

been reviewed by Grimes¹⁴ and does not require further elaboration here.

Values for the standard free energies of formation of the structural metal fluorides, CrF_2 , FeF_2 , and NiF_2 , signify that, as impurities in the reactor salts, iron and nickel should be present in metallic form.

In the molten-salt reactor fuel salt, the fluid contains small amounts of UF_3 generated in the equilibrium reaction $\text{Cr}^0 + 2\text{UF}_4 \rightleftharpoons 2\text{UF}_3 + \text{CrF}_2$. In power operations with the MSRE the concentration of UF_3 was adjusted occasionally by in-situ generation of U^{3+}

**Table 2.10. Comparison of nominal and analytical values of uranium concentration
in the MSRE fuel circuit - zero-power experiment**

Sample No.	Reactor Inventory		Loop Inventory		Additions		Concentration U	
	U	Salt	U	Salt	U	Salt	Nominal	Observed ^a
			(kg)				(wt %)	
Run 3-I	145.60	4754.5			145.60	234.5	3.044	3.068 ^b
FP 3-1	193.09	4831.0			47.49	76.5	3.997	4.016
FP 3-2							3.822	3.853
FP 3-3	214.52	4865.5			21.43	34.53	4.409	4.390
FP 3-4	219.19	4873.0			4.67	7.52	4.498	
FP 3-5	195.24	4340.4					4.498	4.446
FP 3-6	195.24	4340.4					4.498	4.486
FP 3-7	195.70	4341.1			0.4581	0.7394	4.508	4.493
FP 3-8	196.06	4341.7			0.3622	0.5847	4.516	4.452
FP 3-9	196.24	4342.0			0.1813	0.2926	4.520	4.484
FP 3-10	196.51	4342.5			0.2687	0.4337	4.525	4.484
FP 3-11	196.70	4342.7			0.1853	0.2989	4.529	4.500
FP 3-12	196.88	4343.0			0.1847	0.2981	4.533	4.480
FP 3-13	197.15	4343.5			0.2742	0.4426	4.539	4.497
FP 3-14	197.60	4344.2			0.4527	0.7306	4.549	4.530
FP 3-15	197.97	4344.8			0.3632	0.5862	4.557	4.475
FP 3-16	198.06	4345.0			0.0893	0.1441	4.558	4.490
FP 3-17	198.59	4345.8			0.5323	0.8589	4.570	4.498
FP 3-18	198.94	4346.4			0.3516	0.5674	4.577	4.559
FP 3-19	199.12	4346.7			0.1723	0.2782	4.581	4.499
FP 3-20	199.56	4347.4			0.4421	0.7136	4.590	4.602
FP 3-21	200.01	4348.1			0.4494	0.7253	4.600	4.535
FP 3-22	200.37	4348.7			0.3648	0.5887	4.608	4.540
FP 3-23	200.73	4349.3			0.3581	0.5779	4.615	4.571
FP 3-24	201.09	4349.8			0.3558	0.5742	4.623	4.604
FP 3-25	201.09	4349.8					4.623	4.618
FP 3-26	201.17	4350.0			0.0883	0.1426	4.625	4.623
FP 3-27	201.35	4350.3			0.1756	0.2833	4.628	4.593
FP 3-28	201.80	4351.0			0.4494	0.7252	4.638	4.669
FP 3-29	202.16	4351.6			0.3599	0.5760	4.646	4.646
FP 3-30	202.61	4352.3			0.4538	0.7324	4.655	4.676
FP 3-31	202.98	4352.9			0.3675	0.5932	4.663	4.688
FP 3-32	203.07	4353.0			0.0918	0.1482	4.665	4.679
FP 3-33	203.07	4353.0					4.665	4.642
FP 3-34	203.07	4353.0					4.665	4.599
FP 3-35	203.07	4353.0					4.665	4.634
Run 3-F	203.07	4353.0					4.665	
Run 3-F circuit residue	-0.77				-0.77	16.50	4.665	
Drain tank charge	202.30	4353.0 ^c						
Run 4-1	23.95	532.6					4.631	
	226.25	4885.6						

^aCorrected for -0.8% bias.

^bAverage for Precritical Experiment, PC-2.

^cNeglects probability that mass of fuel and flush residues are not identical.

Table 2.11. Chemical analyses for MSRE fuel carrier salt
 ${}^7\text{LiF-BeF}_2\text{-ZrF}_4$ (64.7-30.1-5.2 mole %)

Batch	Net wt. of salt (kg)	${}^7\text{Li}$ Assay	Analyses					
			Li	Be	Zr (wt %)	F	Cr	Ni (ppm)
F-162	130.8	99.994	10.6	7.43	11.5	70.0	23	17
F-163	131.6	99.994	10.6	7.36	12.0	69.9	21	21
F-164	133.8	99.996	11.0	7.43	11.6	69.9	14	24
F-165	132.0	99.996	10.8	7.30	12.1	70.1	29	24
F-166	137.0	99.996	11.3	6.98	11.5	70.0	23	8
F-167	125.2	99.996	10.9	7.23	12.1	70.1	19	<3
F-168	133.1	99.996	10.8	7.30	12.0	70.0	13	3
F-169	132.6	99.995	11.1	7.38	12.0	69.6	15	16
F-170	134.5	99.995	10.5	7.37	11.8	70.3	20	7
F-171	132.9	99.995	10.69	6.98	11.90	70.3	17	17
F-172	134.2	99.995	10.61	7.33	11.72	70.3	26	16
F-173	133.1	99.995	10.50	7.29	12.12	70.0	18	24
F-174	133.8	99.995	10.66	7.57	11.99	70.0	31	17
F-175	133.6	99.995	11.17	7.05	11.97	70.37	19	<5
F-176	133.8	99.995	11.65	7.27	11.84	69.65	13	<5
F-177	133.8	99.995	10.58	6.95	11.92	69.77	29	26
F-178	131.1	99.995	11.03	7.37	12.09	69.91	28	7
F-179	131.1	99.995	10.79	7.47	12.24	69.75	33	11
F-180	133.4	99.995	11.19	7.49	11.72	70.45	29	40
F-181	134.8	99.995	10.84	6.90	12.48	69.1	25	29
F-182	134.2	99.995	10.73	6.89	12.44	69.3	27	29
F-183	133.0	99.994	10.99	7.21	12.35	69.80	22	8
F-184	132.8	99.995	10.90	7.16	12.28	69.27	23	<5
F-185	133.2	99.995	10.92	7.30	11.99	70.24	22	<5
F-186	133.5	99.995	10.99	6.86	12.10	69.59	19	<5
F-187	133.4	99.995	10.87	7.13	12.25	69.71	27	9
F-188	133.8	99.995	10.86	7.14	11.84	69.86	24	19
F-189	134.2	99.995	10.87	7.32	11.93	70.74	22	6
F-190	134.1	99.995	10.89	7.26	11.78	70.62	22	8
F-191	132.0	99.995	10.35	7.23	12.0	71.2	17	13
F-192	134.3	99.995	10.31	7.19	11.5	72.0	28	28
F-193	133.4	99.995	9.75	7.40	11.4	71.4	13	10
F-194	137.3	99.995	10.82	7.33	12.1	70.3	21	12
F-195	134.1	99.994	10.56	7.34	12.2	70.5	19	16
F-196	131.1	99.994	10.48	7.34	11.4	71.5	24	11
F-197	132.6	99.994	10.88	7.39	11.18	70.6	21	10
F-198A	146.4	99.994	4.68.		U-62.26	33.60	8	29
F-198B	136.6	99.994	4.67		U-62.82	33.82	10	<5

in the salt or by addition of FeF_2 as an oxidant. Generally, an effort was made to limit the $[\text{U}^{3+}] / [\Sigma \text{U}]$ ratio to ~ 0.01 as a means of retarding the corrosion reaction.

The reaction $\text{Cr}^0 + 2\text{UF}_4 \rightleftharpoons 2\text{UF}_3 + \text{CrF}_2$ has an equilibrium constant with a small degree of temperature dependence. Since the equilibrium constant increases with temperature, operation of a loop with a significant temperature gradient causes the chromium concentration of the alloy surface that is at high temperature to decrease, transferring metal to the cooler regions. Since chromium comprises a small fraction of Hastelloy N and its availability to the salt is diffusion limited, attainment of equilibrium by this reaction is very slow.

In prenuclear operations with nonuraniferous salts, the salt loops were operated in essentially isothermal conditions. Under these conditions, corrosion of the circuit walls could arise only from contaminants.

In all the activities associated with the startup of the MSRE, stringent measures were taken to remove all traces of moisture from the newly constructed system and to prevent subsequent introduction of impurities.

Table 2.12. Chemical analyses for ${}^7\text{LiF}-{}^{235}\text{UF}_4$ (73-27 mole %) fuel concentrate for the MSRE

Batch No.	Chemical analysis					
	Weight percent		Parts per million			
Li	U	F	Cr	Ni	Fe	
E 201	4.79	61.53	33.0	17	<5	26
E 202	4.80	62.02	33.2	27	89	74
E 203	4.92	62.26	33.4	29	47	11
E 204	4.81	61.21	33.3	24	9	69
E 205	4.68	61.59	33.0	21	14	22
E 206	4.70	61.51	32.7	<5	21	<5

During October and November 1964, the fuel system was readied for use; it was purged of moisture, heated to 650°C , and tested for leak tightness. The purge gas was high-purity helium. To ensure that it was free of oxygen and moisture in use, the gas flowed through a series of dryers and preheaters and through hot titanium sponge before it entered the reactor.

From the results of analyses of the individual salt batches produced for use in the MSRE (see Tables 2.11 and 2.12) the average concentrations of Cr, Fe, and Ni in the blended salt charge (${}^7\text{LiF}-\text{BeF}_2-\text{ZrF}_4-{}^{238}\text{UF}_4$) at the beginning of the precritical experiment PC-2 should have been 21, 99, and 14 ppm respectively. The salt samples removed from the fuel pump during this test were supplied to the ORNL General Analytical Laboratory (GAL) as well as to the HRLAL so the overlapping results would show whether slight biases might result as new equipment and necessary modifications in methods were employed. As determined by the GAL, the average concentrations of structural metal impurities in the PC-2 fuel circuit salt were Cr: 19, Fe: 99, Ni: 23 ppm, while from the HRLAL, the average concentrations were found to be Cr: 37, Fe: 163, Ni: 34 ppm (Table 2.7). Following run PC-2, ${}^7\text{LiF}-{}^{235}\text{UF}_4$ enriching salt was added to the carrier salt to constitute the final ${}^{235}\text{U}$ fuel mixture. The average concentrations of the impurities on completion of this experiment as determined by the HRLAL were Cr: 37, Fe: 148, Ni: 55 ppm (Table 2.7).

With extended experience, we learned that one standard deviation for Cr analysis was ~ 7 ppm; therefore, the difference in chromium concentration as measured in the two laboratories can be regarded as a bias correction — that is, HRLAL results could be expected to average about 18 ppm higher than those from the GAL.

Table 2.13. Composition of the MSRE fuel salt in the precritical examination

	${}^7\text{Li}$	Be	Zr	${}^{237,934}\text{U}$	Total
Carrier (nominal composition), kg	516.91	309.62	541.36		4520.0
${}^7\text{LiF}-{}^{238}\text{UF}_4$ (nominal composition), kg	11.55			145.60	234.5
Total fuel salt (nominal), kg	528.46	309.62	541.36	145.60	4754.5
Weight percent	11.12	6.51	11.39	3.062	
Weight percent analytical (18 samples)	10.42	6.60	11.35	3.068	
Carrier (analytical composition), kg	487.75	327.61	539.06		
${}^7\text{LiF}-{}^{238}\text{UF}_4$ (analytical composition), kg	10.96			146.34	234.5
Total fuel salt (analytical), kg	498.71	327.61	539.06	146.34	
Weight percent	10.49	6.89	11.34	3.077	
Weight percent analytical (18 samples)	10.42	6.60	11.35	3.068	

Table 2.14. Summary of MSRE salt analyses, experiment No. 4, fuel salt

Date	Sample	Weight percent						Parts per million			
		Li	B ¹⁰	Zr	U ^a Nominal	U ^a Analytical	F	Σ	Fe	Cr	Ni
12/21/65	FP-4-15										80 ^b
12/21/65	FP-4-16 ^c										65 ^b
12/22/65	FP-4-17										85 ^d
12/24/65	FP-4-18	10.25	6.68	11.24		4.651	67.44	100.26	144	43	44
12/22/65	FP-4-19 ^e										
12/23/65	FP-4-20 ^e										
12/24/65	FP-4-21	10.47	6.40	10.82		4.671	66.79	99.15	121	60	52
12/25/65	FP-4-22	10.54	6.54	10.95		4.664	64.68	97.37	116	44	84
12/26/65	FP-4-23	10.27	6.74	10.86		4.642	65.06	97.57	99	46	35
12/27/65	FP-4-24	10.65	6.65	10.96		4.655	67.66	100.58	116	48	45
12/31/65	FP-4-25	10.60	6.37	11.41		4.646	65.44	98.47	26	35	42
1/1/66	FP-4-26	10.60	6.63	11.20		4.642	66.90	99.97	89	48	47
1/2/66	FP-4-27	10.55	6.53	11.07		4.618	67.68	100.45	222	50	41
1/3/66	FP-4-28	10.60	6.42	11.10		4.663	66.19	98.97	211	49	34
1/5/66	FP-4-29	10.70	6.71	11.54		4.654	69.75	103.35	111	39	31
1/7/66	FP-4-30	10.63	6.81	11.19		4.661	67.32	100.58	83	49	27
1/10/66	FP-4-31	10.30	6.63	11.26		4.632	68.51	101.33	190	37	41
1/12/66	FP-4-32	10.55	6.71	11.80		4.625	67.66	101.34	173	43	33
1/14/66	FP-4-33	11.20 ^f	6.75	11.07		4.596	66.25	99.97	55	50	39
1/17/66	FP-4-34	11.35 ^f	6.49	11.13		4.601	68.20	101.82	164	58	16
1/19/66	FP-4-35	11.36 ^f	6.68	10.86		4.721	69.35	103.01	74	54	<5
1/21/66	FP-4-36	11.25 ^f	6.32	11.20		4.632	66.76	100.16	125	47	<5
1/22/66	FP-4-37	11.30 ^f	6.33	11.08		4.622	69.35	102.68	189	53	80
1/24/66	FP-4-38	10.70	6.54	11.46		4.608	67.25	100.56	311	51	25
1/26/66	FP-4-39										

^aValues corrected to 33.696 at. % ²³⁵U.^bHF-purge method.^cNo sample obtained.^dKBrF₄ method.^eFor amperometric analysis.^fErroneously high because of weak batteries in automatic pipet.

On completion of the fueling operation in July 1965, the reactor was drained and flushed. Radiation levels were low enough to permit maintenance and installation work to begin immediately in all areas, in preparation for high-power operation. In August 1965, the assembly of graphite and Hastelloy N surveillance specimens, which had been in the core from the beginning of salt operation, was removed. While the reactor vessel was open, inspection revealed that pieces were broken from the horizontal graphite bar that supported the sample array. The pieces were recovered for examination, and a new sample assembly, designed for exposure at high power and suspended from above, was installed. The fuel-pump rotary element was removed in a final rehearsal of remote maintenance and to permit inspection of the pump internals. It was reinstalled after inspection showed the pump to be in very good condition.

Tests had shown that the heats of Hastelloy N used in the reactor vessel had poor high-temperature rupture life and ductility in the as-welded condition. Since the vessel closure weld had not been heat treated, the entire vessel was heated to 760°C (1400°F) for 100 hr, using the installed heaters, to improve these properties.

The experience which was developed with the MSRE throughout the shakedown period preceding power operations confirmed that the molten-fluoride salt mixtures were intrinsically noncorrosive to Hastelloy N and that effective procedures were employed to prevent serious contamination of the salt circuits during this period.

By December, maintenance and modifications were completed, and flush salt was circulated through the fuel system for a period of three days. On December 20, 1965, the fuel salt was loaded into the system, and the zero-power experiment began. On completion of

Table 2.15. Chemical composition of the MSRE fuel salt in prenuclear operations

	⁷ Li	Be	Zr	U	Σ
Carrier salt, kg	516.91	309.62	541.36		4520.0
⁷ LiF- ²³⁸ UF ₄ , kg	11.55			145.60	234.5
⁷ LiF- ²³⁵ UF ₄ (bulk charge), kg	5.84			73.59	118.55
Total fuel salt, kg	534.30	309.62	541.36	219.19	4873.05
Loop charge (89.07%), kg					
Carrier salt	460.41	275.78	482.19		
LiF- ²³⁸ UF ₄	10.29			129.69	
LiF- ²³⁵ UF ₄	5.20			65.55	
Additions to loop	6.32			7.83	12.736
Total					4353.0
Loop charge, wt %	11.08	6.34	11.08	4.665	
FP 3-32-35 (3), wt %	10.30	6.76	11.20	4.624	
Fuel salt residue in loop, kg	1.83	1.05	1.83	0.77	16.5
Salt to drain tank, kg	480.39	274.73	480.36	202.30	4336.5
Drain tank charge, kg	58.40	33.84	59.08	23.95	532.6
	538.79	308.57	539.44	226.25	4869.1
Drain tank charge, wt %	11.07	6.34	11.08	4.647	
Charge to loop for run 4 (92%), kg	495.69	283.88	496.29	208.15	4479.6
Flush salt residue in loop, kg	2.51	1.66			18.0
Total fuel salt, kg	498.20	285.54	496.29	208.15	4497.6
Total fuel salt, wt %	11.08	6.35	11.04	4.628	
Analytical (69 samples), wt %	10.785 ± 0.064	6.571 ± 0.076	11.197 ± 0.260	4.641 ± 0.026	

this period the concentrations of the structural metal impurities had average values of Cr: 48 ± 7, Fe: 131 ± 65, Ni: 40 ± 20 ppm. Here, for the first time, there was evidence that an increase in the concentration of chromium in the fuel-salt mixture had taken place. As will be noted later, such increases followed a regular pattern, occurring almost exclusively after periods of maintenance when the reactor was opened to the ambient atmosphere for some period of time. It now seems that circulation of the flush salt for periods of only a few days was insufficient to negate the effect of the exposure completely.

2.4.4 Oxide contaminants. Among the summary reports on various aspects of MSRE operations, no separate review of analytical chemical developments is included. Except for a few analyses, for example, for oxide and for lithium, the methods in the ORNL Master Analytical Manual were employed routinely and found to be satisfactory. In response to the need for improved methods for determination of the concentration of oxides in the MSRE salts, a reliable and accurate method was devised and applied concurrent with early MSRE operations. This development was an important aspect of MSRE chemical development and is therefore described in detail here.

Long before operations with the MSRE were started it was demonstrated in laboratory tests that precipitation of oxide as the saturating phase in the molten fuel, flush, or coolant salt was very unlikely. However, assurance that the concentration of oxide as a contaminant of these salts was not increasing could not be obtained from initial measurements using conventional methods.¹⁵ Many of the results of early analyses of MSRE flush and carrier salts were anomalous, as shown in Tables 2.2, 2.7, and 2.9. At face value, the analytical data shown in these tables might suggest that the concentration of oxide in the samples examined ranged sporadically from 100 to 4000 ppm. If real, the higher values would represent the presence of more than 0.5% ZrO₂ in the specimens. Each of the 52 specimens obtained for analysis during precritical run No. 2 and during the zero-power experiment was subjected to petrographic examination. With the carrier and LiF-BeF₂ salt, the sensitivity for detection of well-formed crystals of ZrO₂ by the petrographic methods is well below 100 ppm; neither crystalline ZrO₂ nor oxyfluorides were found to be present in any of the specimens examined.

The sampling procedures employed at the MSRE effectively protected salt specimens from contact with

moisture up to the point where they were transferred into a transport container; subsequent handling procedures, however, were not so stringent and are presumed to have allowed moisture to contact the surfaces of the fluoride specimens on occasion. Beryllium fluoride and LiF-BeF₂ glassy phases are hygroscopic. Crystallization of each of the MSRE salt mixtures can produce minute quantities of these phases; typical sampling conditions effect rapid cooling of the samples and are therefore even more conducive toward the production of the hygroscopic phases than equilibrium crystallization of the salt mixtures. These hygroscopic phases, once moistened, cannot be redried completely by ordinary desiccants at room temperature. The anomalously high values for oxide analyses during the early stages of MSRE operations are thus indicative of exposure of the salt samples to moisture-laden atmospheres.

An effort was initiated to develop improved methods for oxide analysis that would be adaptable for use in the HRLAL. After a study of several methods which might have application under conditions such as those which prevailed in the HRLAL and where no provision for atmospheric control in the hot cells was made, the analytical chemists¹⁶ concluded that a hydrofluorination-transpiration method based on the reaction O²⁻ + 2HF(g) ⇌ H₂O(g) + 2F⁻ was potentially the most useful. Their development of the new method is described in the following paragraphs.

In principle, the amount of water evolved from purging a molten-salt sample with an H₂-HF gas mixture would serve as a measure of the quantity of oxide in the molten-salt sample. Since the water evolved and the HF consumed are both proportional to the amount of oxide present, either compound would serve as an indicator species. Water monitoring methods were selected because of their greater convenience and reliability than those for HF.

The application of this method to the analysis of radioactive samples required the development of (1) a sampling technique which minimized atmospheric contamination, (2) the incorporation of a water-measurement technique which was convenient for hot-cell operations, and (3) the fabrication of a compact apparatus for conserving the limited space available in the hot cells. It was necessary to adapt the sampling techniques from methods already developed to obtain samples for wet analysis. By using a copper ladle of nearly the same dimensions as the enriching capsules, approximately 50-g samples were obtained which could be transported in the existing transport container. Exposure to the atmosphere was minimized by remelting and hydrofluorinating the entire sample in the

sample ladle. The ladle was sealed in a nickel-Monel hydrofluorinator, with a delivery tube spring-loaded against the surface of the frozen salt. Before the salt was melted, the apparatus was purged with a hydrofluorinating gas mixture to remove water from the inner surface of the hydrofluorinator and from the exposed surface of the salt. As the sample was melted, the delivery tube was driven to the bottom of the ladle by spring action for efficient purging of the salt.

In all preliminary tests the water in the effluent purge gas was measured by Karl Fischer titration. While the Karl Fischer reagent was shown to be remarkably stable to radiation, the titration would have been excessively difficult to perform routinely in the hot cell. As an alternative, an electrolytic moisture monitor was adapted for these measurements. Since such equipment is subject to interference and damage from HF,¹⁷ it was practical to include a sodium fluoride column in the effluent gas train. In operation at about 90°C it removed HF from the effluent gas without significant holdup of water.

A schematic flow diagram of the apparatus installed in the HRLAL is shown in Fig. 2.2. The apparatus is pictured in Fig. 2.3. A modular design was selected to facilitate any changes found necessary during component testing and to permit necessary repairs in the hot cell. Except for the hydrofluorination furnace, all hot-cell components were contained within a cubical compartment, 16 in. on a side.

Samples of the flush and fuel salt taken during the December startup of the reactor were analyzed for oxide. Table 2.16 summarizes the results. Figure 2.4 is a recording of the data output from analysis of the first fuel-salt sample taken after the fuel was loaded into the reactor. The results of the analyses by the hydrofluorination method were in good agreement with those by the KBrF₄ procedure. The KBrF₄ values paralleled the trends shown by the hydrofluorination method but

Table 2.16. Oxide concentrations of flush and fuel salt from the MSRE

Sample	Time of salt circulation (hr)	Oxide concentration (ppm)
Flush salt	24.7	46
	29.1	72
	47.6	106
Fuel salt	3.4	120
	23.8	105
	32.2	80
	52.5	65

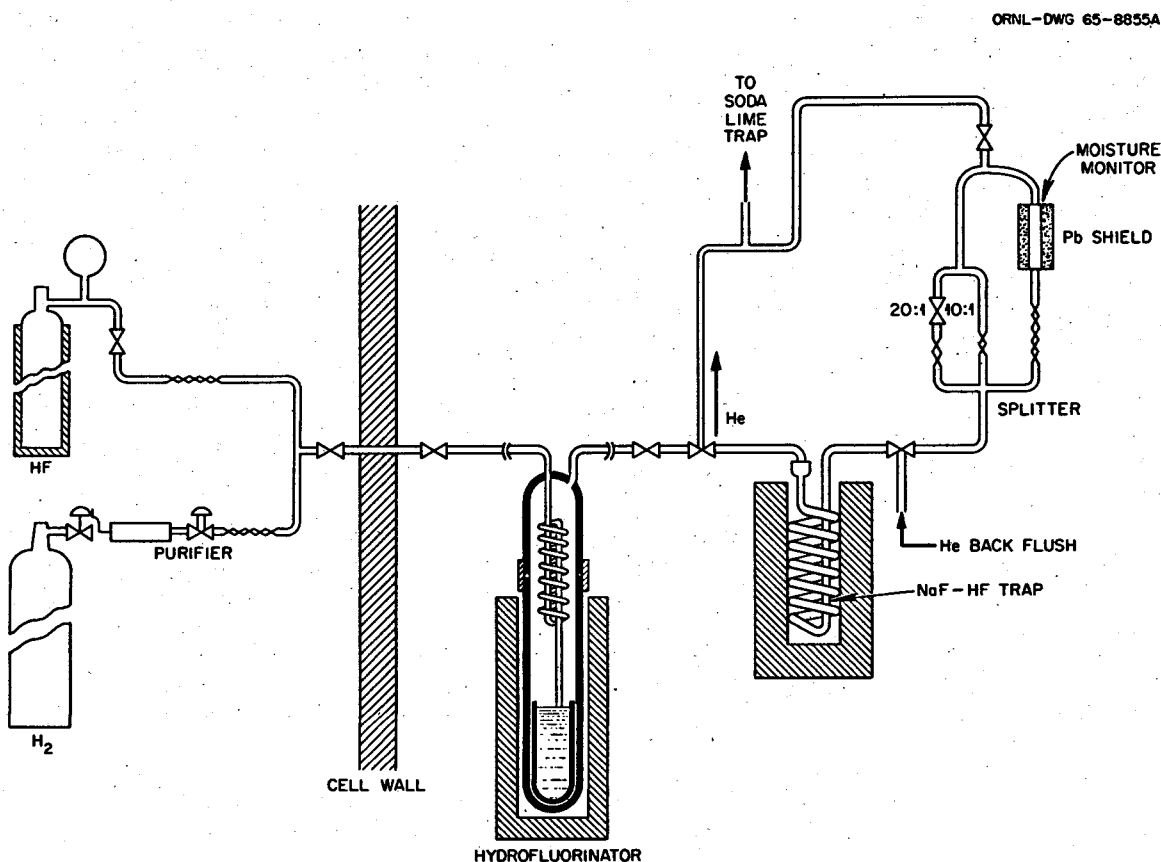


Fig. 2.2. Schematic flow diagram of the apparatus for the determination of oxide in MSRE fuel by hydrofluorination.

averaged slightly higher. This bias was not unexpected, since the pulverized samples required for the KBrF₄ method were easily contaminated by atmospheric moisture. Subsequently, 50-g fuel-salt samples were taken at various power levels from zero to full power. With an in-cell radiation monitor, the initial sample read 30 R at 1 ft. This activity increased to 1000 R at 1 ft at the full-power level. Results of the oxide analyses are given in Table 2.17.

The oxide in the coolant salt sample, 25 ppm, is, for practical considerations, identical with a value of 38 ppm obtained for a coolant salt sample taken on January 25, 1966, and analyzed in the laboratory after three weeks' storage. The fuel-salt analyses are in reasonable agreement with the samples analyzed in the development laboratory before the reactor was operated at power. The oxide concentration in these nonradioactive samples seemed to decrease gradually from 106 to 65 ppm. Between the FP-6 and FP-7 series the sampler-enricher station was opened for maintenance, and thus the apparent increase in oxide concentration (ca. 15 ppm) may represent contamination of

Table 2.17. Oxide concentrations of coolant and fuel salt from the MSRE

Sample	Code	Oxide concentration (ppm)
Coolant salt	CP-4-4	25
Fuel salt	FP-6-1	49
	FP-6-4	53
	FP-6-12	50
	FP-6-18	47
	FP-7-5	66
	FP-7-9	59
	FP-7-13	66
	FP-7-16	56

the samples by residual moisture in the sampling system; however, the number of determinations was not at the time sufficient to establish the precision of the method at these low concentration levels.

In an attempt to determine whether radiolytic fluorine removes oxide from the fuel samples, sample FP-7-9 was removed from the transport container and

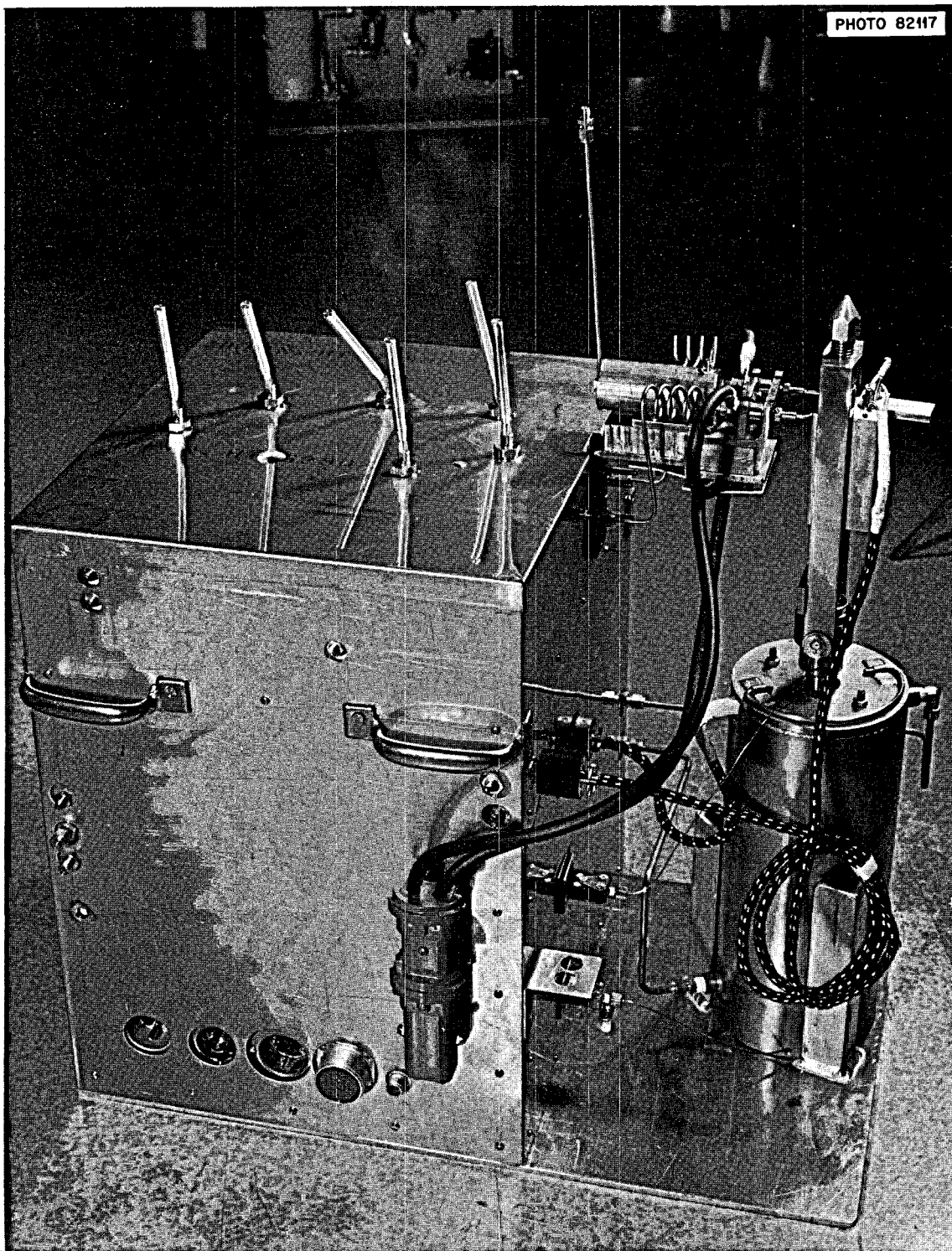


Fig. 2.3. Hot-cell apparatus.

ORNL-DWG 66-402BA

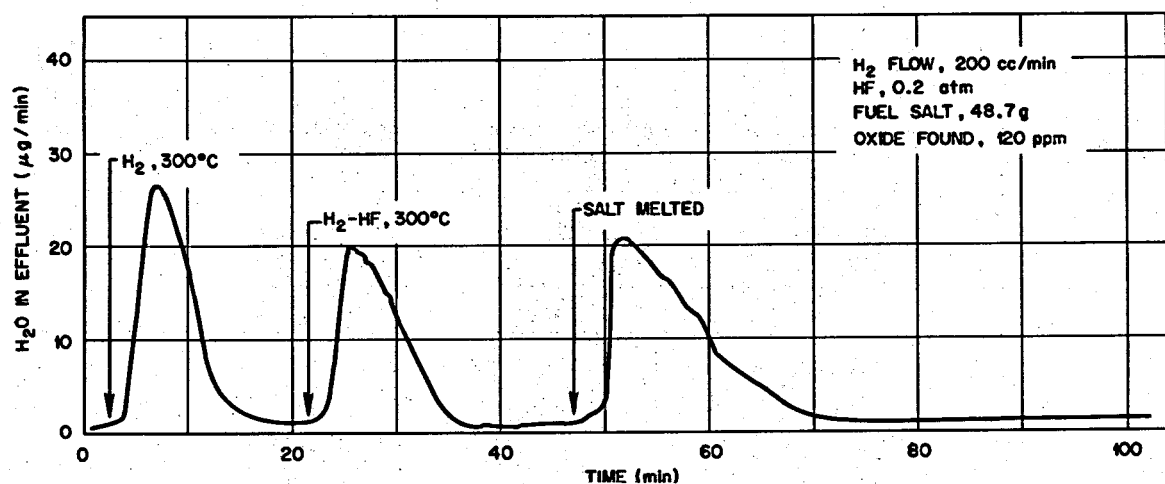


Fig. 2.4. Determination of oxide in MSR fuel sample FP4-11 by hydrofluorination.

stored in a desiccator for 24 hr prior to analysis. Since the oxide content, 59 ppm, is comparable with that of the remaining samples for which analyses were started 6 to 10 hr after sampling, no significant loss of oxygen is indicated. A more direct method of establishing the validity of these results by measuring the recovery of a standard addition of oxide was used in subsequent operations. A tin capsule containing a known amount of SnO₂ was heated to 550°C in the hydrofluorinator as hydrogen passed through the system. The SnO₂ was reduced to the metal, and the water that was formed passed on to the electrolysis cell. Two standard samples of SnO₂ were analyzed after a four-month interim, and oxide recoveries of 96.1 and 95.6% were obtained.

The slight negative bias was attributed to momentary interruptions in the flow of the hydrofluorinator effluent gas through the water electrolysis cell. Difficulty with cell plugging was encountered throughout the period of development of the oxide method. As an attempt to eliminate the negative bias and also to provide a replacement cell for the remote oxide apparatus, it was deemed necessary to find a method of regenerating the electrolysis cell that would permit a steady gas flow at relatively low flow rates.

The water electrolysis cell contains partially hydrated P₂O₅ in the form of a thin viscous film in contact with two spirally wound 5-mil rhodium electrode wires. The wires are retained on the inside of an inert plastic tube forming a 20-mil capillary through which the sample passes. The 2-ft-long tubing element is coiled in a helix inside of a $\frac{5}{8}$ -in.-diam pipe and potted in plastic for permanence.

During the course of the investigation of the cell, it was found that a wet gas stream in itself did not cause

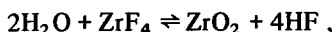
the electrolysis cell to plug. It was also necessary for current to be flowing through the cell for flow interruptions to occur. This indicated that the hydrogen and oxygen evolving from the electrodes create bubbles in the partially hydrated P₂O₅ film, which then grow in size sufficiently to bridge the capillary and form an obstructing film.

After many unsuccessful approaches, an acceptable solution to the problem was obtained by means of a special regenerating technique which employed dilute acetone solutions of H₃PO₄ as the regenerating solutions. This provided a desiccant coating sufficient to absorb the water in the gas stream and gave a minimal amount of flow interruptions during electrolysis. The cells were thereafter successfully regenerated in this manner and yielded oxide recoveries of 99.6 ± 1.3% from standard SnO₂ samples.

2.4.5 Analysis of helium cover gas. As noted in Sect. 2.4.4, a reliable means for the determination of oxide in the fuel salt did not exist when the initial experiments with the MSRE began. The results of the oxide analyses were perplexing, and they were almost certainly invalid as indicators of contamination by moisture, since the concentrations of structural metal contaminants in the salt remained essentially constant. In order to obtain some direct assurance that negligible inleakage of moisture was occurring in the fuel system, temporary measures were devised and applied. The method consisted in bleeding off a small flow of the helium gas in the pump bowl and passing it through a monitoring system in the high-bay area.

Mean values for the concentration of HF in the helium cover gas were obtained during the PC-2 and

zero-power experiments by adaptation of a continuous internal electrolysis analyzer for gaseous fluorides. Through the cooperation of ORGDP personnel, data were obtained regularly throughout prenuclear operations. The results showed that HF was evolved from the salt at a maximum mean value of 150 to 200 $\mu\text{g/liter}$.¹⁸ The validity of this value is somewhat questionable because of the probable positive bias that particulate fluorides would contribute. The results are, therefore, conservative to an indeterminate degree, but correspond to the introduction of no more than 1 ppm of oxide into the salt per day through the reaction



an amount which would escape detection by other methods.

2.4.6 Lithium analysis. In Sect. 2.4.2 we noted that chemical analyses of the fuel salt routinely indicated that Be/Li ratios were significantly greater than for the nominal composition of the salt. A careful examination of the results for all the salt mixtures prepared for use in the MSRE shows that if it is assumed that the analytical results are correct for beryllium in the coolant and flush salts, for beryllium and zirconium in the carrier salt, and for uranium in the LiF-UF₄ salt mixtures, and if a correction factor of 5 to 6% is added to each of the results of lithium analyses, the average results of composition analyses nearly coincide with nominal values.

When this disparity was first noted, a reexamination of the production records was made but did not disclose any disparity in the material balances that would account for the anomaly in Be/Li results. Evidence from the purification-plant inventory data indicated that the composition of the salt delivered into the reactor system was of the design composition, 66.0 ± 0.25 mole % LiF, 34.0 ± 0.25 mole % BeF₂. A sample of the MSRE coolant, taken from one of the batches loaded into the reactor, showed a liquid-solid phase transition temperature of 457.6°C ; this is within 0.1°C of the temperature of the equilibrium liquid-solid reactions which can occur in LiF-BeF₂ mixtures richer than ~ 33 mole % LiF. Chemical analyses of this material indicated its composition to be LiF-BeF₂ (63.63-36.37 mole %). The thermal data indicated, however, that the material contained at least 65.5 mole % LiF, and thus confirmed the composition indicated by the weights of the materials used in its preparation.

Application of the same correction factor to the results of lithium analyses for either LiF-UF₄ or LiF-BeF₂ mixtures effects equal improvement of the

match of analytical results with nominal values; we must conclude therefore that a negative bias of 5 to 6% existed in the lithium results. Lithium was determined in the MSRE salt samples by flame spectrophotometric methods. The results are compared with calibrated standards, and regarded by the analytical chemists to match satisfactorily with these standards. However, in view of the coincidence of values which results when a correction of $\sim 5\%$ is applied to the results, we must infer that a negative bias of that magnitude affected the MSRE results.

The lithium used to produce the salt charges for the MSRE was selected from stockpiled LiOH in which the ^6Li had been depleted to 0.01% or less. Assays were available on each batch of LiOH; these analyses served as criteria for selection of the material used.^{19,20} The assays of the batches of LiOH which were to be used for the MSRE ranged from 0.0072 to 0.0085% ^6Li , with the average of the batches which were to be used for the flush salt and the fuel carrier salt as 0.0074%. After each conversion of hydroxide to the fluoride,¹ the lithium in each product batch was again assayed before the LiF was used to make up the coolant, flush, or carrier salt. The assays of the batches of LiF used to make up the fuel salt ranged from 0.004 to 0.006% and averaged 0.0049%.²¹

In view of the relation of tritium production in the MSRE to the isotopic composition of lithium, Haubenreich²² recently completed a full review of the possible sources of tritium and of the analyses on which production estimates were based. In connection with that review, S. Cantor obtained new analyses for ^6Li in unused LiF-BeF₂-ZrF₄ carrier salt. The results coincided with those obtained initially for LiOH, but were, for reasons still unknown, substantially higher than the ~ 50 ppm which was previously used as the basis for estimation of production rates.²³

2.4.7 Examination of salts after zero-power experiment. At termination of the zero-power experiment, the fuel salt was drained for temporary storage in fuel drain tank FD-2. Flush salt was circulated through the fuel system for a 24-hr period and drained for storage. Four specimens of fuel salt were obtained from the fuel drain tank at intervals during the first 300-hr period of storage. This practice was not continued after power generation began because of the hazards which would be incurred by attempts to provide temporary access for sampling radioactive salt. One purpose of the effort to sample salt from the drain tank was to confirm that the composition of the salt in the tank conformed to that expected from mixing the newly constituted salt in the fuel circuit with that of lower uranium concen-

tration in the drain tank. Any mismatch noted at this time would serve as a base-line correction to data obtained later during power operations. A second purpose was to investigate the effectiveness of quiescent storage of the salt in reducing the amounts of suspended particles of the structural metals iron and nickel. In retrospect, this period afforded the opportunity for securing a wide variety of base-line data, an opportunity that was exploited only to a modest extent, in that only four salt samples were removed for analysis. Their compositions, as determined from chemical analysis, are listed in Table 2.18.

The data shown in Table 2.18 indicate that approximately the same bias noted previously in the analysis of carrier constituents continued to be evident and that the disparity between the analytical data and the nominal concentration of uranium was $\approx 0.3\%$, which is within the precision normally found for uranium analyses.

A comparison of the values for iron and nickel in the samples drawn from the drain tank and those previously

obtained from the pump bowl shows no significant difference. Evidence confirming this expectation was provided later by analysis of two samples removed from the pump bowl before the reactor was operated at power. Samples were withdrawn from the reactor in enricher ladles and were transferred under an inert atmosphere to the graphite crucible of an electrochemical cell assembly for electrochemical studies by D. L. Manning. The cell assembly and electrodes developed for these electrochemical studies are described elsewhere.²⁴ Average total concentrations of iron and nickel in the melt, as determined by conventional methods, were about 125 and 45 ppm respectively. Iron and nickel, as cationic species in the molten fuel, are electroreducible in the melt and can thus give voltammetric reduction waves. By voltammetry and by standard addition techniques, Manning found²⁴ that the salt contained ~ 10 ppm of iron as Fe^{2+} and that if nickel were present as a cationic species, its concentration was below the limit of detection by voltammetry (<1 ppm).

Table 2.18. Composition of MSRE fuel-salt samples obtained from fuel drain tank FD-2

Sample No.	Composition (wt %)				Composition (mole %)			
	Li	Be	Zr	U	LiF	BeF_2	ZrF_4	UF_4
FD-2-10	10.13	6.54	11.10	4.580				
FD-2-11	10.18	6.54	11.27	4.638				
FD-2-12	10.55	6.68	11.95	4.614				
FD-2-13	10.55	6.22	10.95	4.613				
Average Nominal	10.35	6.41	11.32	4.611	63.38 65.19	30.46 29.00	5.32 5.01	0.836 0.808
Sample No.	Parts per million							
	Cr	Fe	Ni					
FD-2-10								
A ^a	37	141	83					
B ^b	<30	53	<30					
FD-2-11								
A	37	97	72					
B	<30	63	<30					
FD-2-12								
A	26	91	31					
B	<70	50	7					
FD-2-13								
A	38	147	132					
B	<70	50	6					
Average								
A(4)	35	119	80					
A(3)	33	110	62					
Run 3								
A	37 ± 8	154 ± 55	48 ± 19					

^aAnalysis by wet-chemical methods.

^bAnalysis by spectrochemical methods.

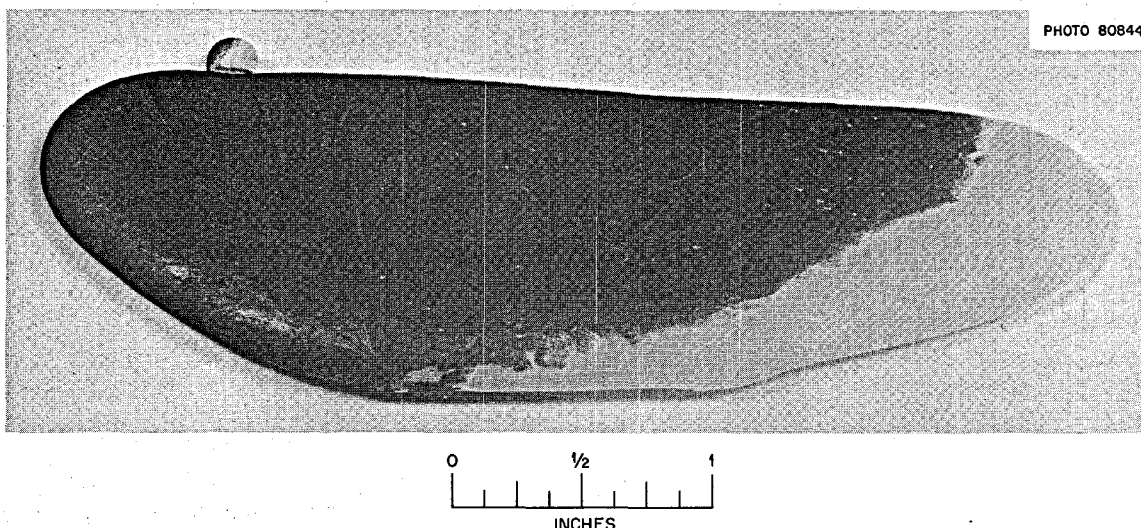


Fig. 2.5. Flush salt residue from volute of the pump bowl.

Since all previous transits of the salt were conducive to retaining suspended metal in the salt, we felt that possibly the finely divided metal (some threefold more dense than the fluoride mixtures) would gradually settle in drain tanks on conclusion of the zero-power experiment. In an attempt to test this possibility, samples of the static fuel salt were obtained from the fuel storage tanks throughout a two-week period following the zero-power experiment. The concentrations of the structural metal impurities were not found to change during this storage period. We concluded, therefore, that thermal convection in the storage tank was sufficient to prevent settling of fine metallic particles in this tank and that the concentrations of these metals in the salt might be expected to remain essentially constant throughout the remainder of MSRE operations.

On removal of the fuel pump rotor for examination,²⁵ approximately 1 kg of flush salt was found to have been retained in the rotor flange area (Fig. 2.6) and in the volute of the pump bowl (Fig. 2.5). Additional small fragments of salt were found in various adjacent locations: in the grooves of the shield-block O-ring and in line 903, through which pump-bowl gas was vented to an HF analyzer that was installed temporarily in the prenuclear operational period to analyze the composition of the off-gas. All salt specimens were submitted for microscopic and/or chemical analysis and were found to be entirely free of oxides or oxyfluorides. Results of the chemical analyses performed with these samples are listed in Table 2.19. A minor oil leak allowed oil to enter the shield-block

Table 2.19. Chemical analysis of fuel pump salt samples

Sample location	Chemical composition (wt %)				
	Li	Be	Zr	U	F
Labyrinth flange	13.36	9.81	0.15	0.0177	78.05
Pump volute	13.70	9.71	0.021	0.0195	77.68
Upper O-ring groove	9.81	6.9	10.87	4.294	62.57
Lower O-ring groove	12.1		0.910	0.295	72.76
Pump suction	No chemical analysis run. Contained dispersion of fine nongraphitic carbon.				
Fuel salt	10.25	6.71	11.11	4.602	68.87
Flush salt	13.12	9.68	0	0	77.08

section of the pump. Thermal decomposition products of the pump oil were in contact with the salt specimens in these areas and were found as partial films on some of the salt (Fig. 2.5) or dispersed through fragments of other specimens. In all locations where crystallized salt deposits were found, it was evident that the molten salt had not adhered to the metal surfaces. This was particularly evident in the volute deposit, where the molten specimen cooled rapidly and maintained the surface angle tangency characteristic of sessile drops which are free of contaminant oxides.

2.4.8 Appraisal of chemical surveillance in prepower tests. From a chemical standpoint, operations of the MSRE during the precritical and zero-power experiments were performed in a manner that maintained the purity of the salt charges during all transfer, fill, and circulation operations. The results of the chemical analyses obtained with samples from the fuel and

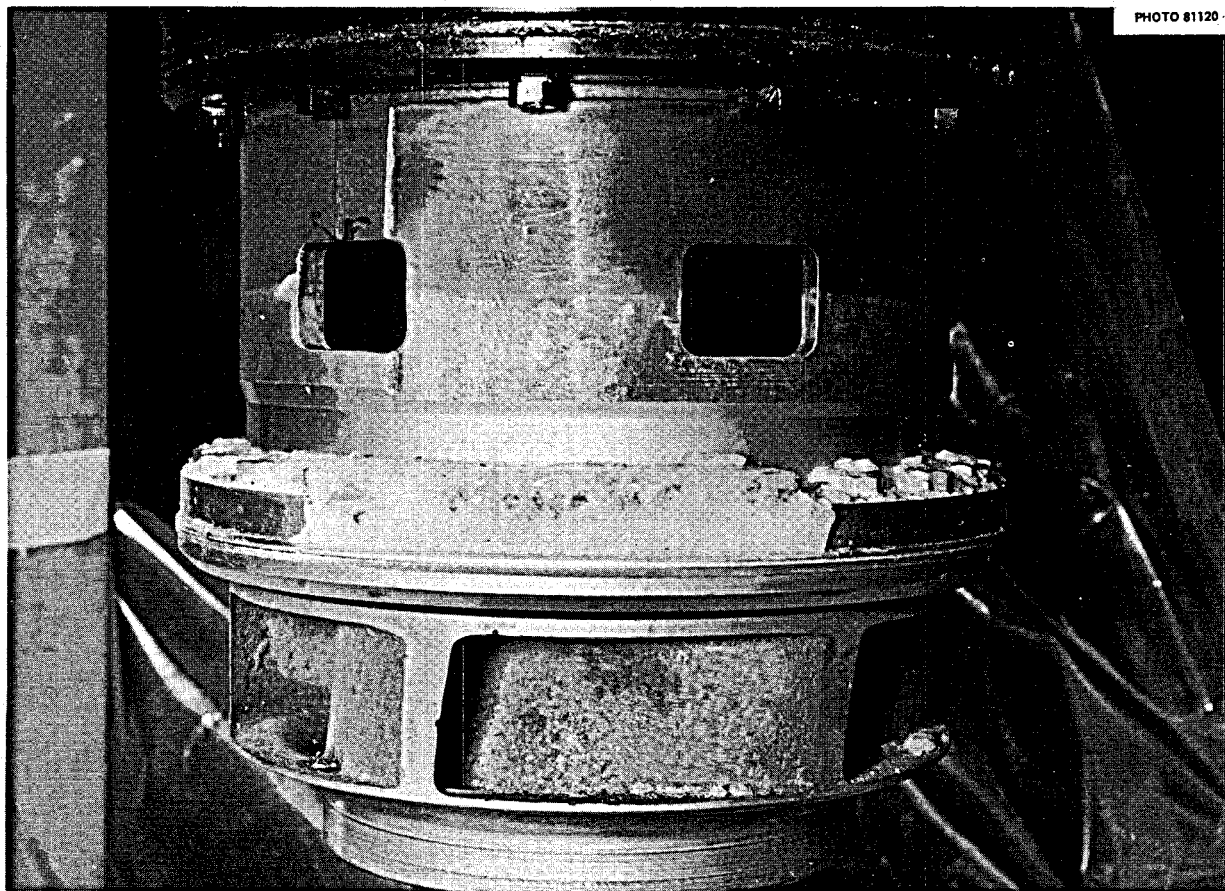


PHOTO 81120

Fig. 2.6. Flush salt in rotor flange area.

coolant systems reinforced the longstanding conclusion, drawn in laboratory and engineering-scale experiments, that pure molten-fluoride mixtures are completely compatible with nickel-based alloys.

The utility of routine analysis of salt samples removed from the circulating systems came to be realized as of questionable value with respect to several of the constituents after brief experience with the MSRE. It became quite clear, for example, that only easily recognized operational perturbations were likely to cause the average concentrations of carrier or coolant salt constituents to vary beyond standard deviations in the analyses and that without major refinement in the analytical methods for determining the concentration of uranium in fluoride mixtures these analyses would not provide operational control. Nonetheless, the potential value for applications of statistically significant results justified, in our judgment, a continued and active program of chemical analysis. Furthermore, by the time the zero-power experiment was completed, the value of chromium analysis as the single quantitative indicator of corrosion or of corrosion-free performance

was solidly established. Analysis of salt samples for this impurity involves wet chemical dissolution techniques, which account for some 90% of the cost of a complete analysis. Because of this factor, there was little reason to omit analysis of more than one component, for such omission would preclude determination of overall composition.

Several aspects of the relation of analysis to MSRE operations proved to be discomfiting by the completion of the zero-power experiment. Annoyingly, chemical analysis of the flush-salt samples removed from the system indicated that the amounts of salt residues remaining in the system after drain operations were somewhat more than could be accounted for by the on-site estimates of the volumes of probable void space where it was deduced that salt could reside. Ultimately, the application of neutron activation and mass spectrometric analysis to this problem confirmed that estimates made from chemical data were the most nearly correct. Until this problem was resolved, continued exchange of fuel and flush salt by drain-fill operations suggested a negative bias in the analysis of

uranium. Methods were developed for slight refinements in the uranium analysis, but not surprisingly, these did little to resolve the fundamental problem. Weigh cell data, in which some reliance was placed originally, proved to be of little value with continued experience, and accordingly, increasing reliance on chemical analyses was developed.

For a lengthy period, there was no absolute method for establishing the level of contamination of the salts by small amounts of oxide ion. This assay was performed in a partly satisfactory manner during the precritical and zero-power experiments, but the method was not adapted for application to highly radioactive materials until well into the power period.

The lack of dynamic methods for obtaining various analyses of the gas and vapor above the surface of the fuel salt proved to be a severe limitation in the interpretation of the chemical behavior which occurred in the fuel system. In the absence of on-site gas analysis, either by mass spectrometry or gamma-ray spectrometry (which was developed later for postoperational examinations), interpretation of several aspects of molten-salt reactor behavior remained less than completely resolved — in particular, of greater significance in power operations, the experimental investigation of factors controlling the transport of noble metal fission products.

In general, the surveillance program was, to this stage, a success principally because of the careful procedures which were employed to ensure its trouble-free operation and because of the intrinsic stability and compatibility of the materials used in its construction.

References

1. J. H. Shaffer, *Preparation and Handling of Salt Mixtures for the Molten-Salt Reactor Experiment*, ORNL-4614 (January 1971).
2. *MSR Program Semiannu. Progr. Rep. Feb. 28, 1965*, ORNL-3812, p. 5.
3. R. B. Lindauer, *Processing of the MSRE Flush and Fuel Salts*, ORNL-TM-2578 (August 1969); G. Long and F. F. Blankenship, *The Stability of Uranium Trifluoride*, ORNL-TM-2065 (November 1969).
4. R. B. Lindauer, private communication.
5. C. F. Baes, "The Chemistry and Thermodynamics of Molten-Salt Reactor Fluoride Solutions," IAEA Symposium on Thermodynamics with Emphasis on Nuclear Materials and Atomic Transport in Solids, Vienna, Austria, 1965.
6. A more detailed description of the hydraulics in the system is given in the report by J. R. Engel, P. N. Haubenreich, and A. Houtzeel, *Spray, Mist, Bubbles and Foam in the Molten-Salt Reactor Experiment*, ORNL-TM-3027 (June 1970).
7. *MSR Program Semiannu. Progr. Rep. Feb. 28, 1965*, ORNL-3812, p. 10.
8. *MSR Program Semiannu. Progr. Rep. Feb. 28, 1965*, ORNL-3812, p. 10.
9. L. T. Corbin, W. R. Winsbro, C. E. Lamb, and M. T. Kelley, "Design and Construction of ORNL High-Radiation-Level Analytical Laboratory," *11th Hot Lab Conf. Proceedings, ANS, November 1963*; "High-Radiation-Level Analytical Laboratories," *Anal. Chem.* 37(13), 83A (1965).
10. B. E. Prince et al., *Zero-Power Physics Experiments on the MSRE*, ORNL-4233 (February 1968).
11. J. R. Engel and B. E. Prince, *The Reactivity Balance in the MSRE*, ORNL-TM-1796 (March 1967).
12. *MSR Program Semiannu. Progr. Rep. Feb. 28, 1966*, ORNL-3936, p. 122.
13. J. H. Shaffer, internal correspondence, Oct. 9, 1964.
14. W. R. Grimes, *Nucl. Appl. Technol.* 8, 137 (1970).
15. G. Goldberg, A. S. Meyer, Jr., and J. C. White, *Anal. Chem.* 32, 314 (1960).
16. A. S. Meyer, R. F. Apple, and J. M. Dale, ORNL Analytical Chemistry Division.
17. W. S. Pappas, *Anal. Chem.* 38, 615 (1966).
18. Results summarized in a memorandum from J. G. Million (ORGDP) to R. E. Thoma, July 14, 1965.
19. P. N. Haubenreich, "Selection of Lithium for MSRE Fuel, Flush and Coolant Salt," internal correspondence, Apr. 10, 1962.
20. H. F. McDuffie, "Selection of ⁷Li Batches for MSRE Fuel, Flush and Coolant Salt," internal correspondence, May 22, 1962.
21. J. H. Shaffer, personal communication.
22. P. N. Haubenreich, *A Review of Production and Observed Distribution of Tritium in MSRE in Light of Recent Findings*, ORNL-CF-71-8-34 (in press).
23. P. N. Haubenreich, *Tritium in the MSRE: Calculated Production Rates and Observed Amounts*, ORNL-CF-70-2-7 (Feb. 4, 1970).
24. D. L. Manning, internal correspondence, Jan. 19, 1966.
25. C. H. Gabbard, *Inspection of Molten-Salt Reactor Experiment (MSRE) Fuel Pump after Zero Power Experiments (Run 3)*, ORNL-CF-66-8-5 (Aug. 4, 1966).

3. CHEMICAL COMPOSITION OF THE FUEL SALT DURING NUCLEAR OPERATIONS

3.1 Introduction

The MSRE was not the first reactor to use a molten-fluoride fuel mixture. The ARE (Aircraft Reactor Experiment) was operated as the initial demonstration of a molten-salt reactor in November 1954, using a fuel solution of $\text{NaF-ZrF}_4\text{-}^{235}\text{UF}_4$ (53-41-6 mole %).¹ The time during which the molten-fluoride fuel was circulated was brief, ~1000 hr, and did not include a program of chemical surveillance. In contrast, the MSRE was intended to provide the experience and operational data on which design and plans for molten-salt reactors of 30-year operating lifetimes could be based. Plans for its operation, therefore, included a chemical surveillance program that was comprehensive in scope. Moreover, chemical information and quantitative data pertaining to a number of phenomena that could only be obtained from operating reactors were lacking, even though a thorough program of laboratory, engineering-scale, and in-pile tests had established the principal parameters required to design and operate the MSRE. Among the most important of these are the chemical factors which control the distribution of fission products within the fuel and off-gas systems, and the redox chemistry typical of dynamic fuel systems in which fuel burnup and replenishment proceed concurrently. It was also important to establish the corrosion resistance of Hastelloy N under realistic and typical operating conditions, to examine the capability of a molten-salt reactor to operate under circumstances where contaminants might enter the salt occasionally or chronically, and to study the possible effects that operation of numerous chemical components of the reactor might have on fuel and coolant chemistry. It was the intent of these efforts to evaluate, on a continuing basis, the adequacy of the surveillance program to assess the performance and safety of the MSRE as the prototype of a molten-salt breeder reactor.

Initial activities of the program of chemical surveillance served to establish that the behavior of the fuel and coolant salts would conform with that expected from laboratory and engineering tests. We sought information that would indicate whether the fuel and coolant salts remained chemically stable and noncorrosive, to what extent the consumption of fissile material deviated from that expected from nuclear considerations, and whether or not uranium losses could be detected by chemical examination of salt samples. In

the beginning stages of MSRE operation, samples were taken on one-day intervals to assess the chemical stability of the fuel, to establish whether or not the concentration of oxide contaminants remained below the saturation limits (~700 ppm for the average operating temperature of 650°C), and to correlate concomitant corrosion, if it occurred, with possible introduction of contaminants into the system. Finally, we anticipated that through measurement of isotopic changes in the uranium composition of the fuel it might be possible to obtain accurate comparisons of the amounts of uranium burned with those expected from nuclear considerations.

After a significant amount of uranium had undergone fission, procedures were initiated to monitor the relative concentration of trivalent uranium in the fuel salt. Studies of the chemical effects of uranium fission in molten-fluoride mixtures had led to an early estimate that the fission reaction would be mildly oxidative and would produce ~0.8 equivalent of oxidation per gram atomic weight of uranium consumed. This estimate was based on an appraisal of the yield and chemical stability of the state of the fission products. Since it was possible to evaluate only the equilibrium states of all the various fission product species — for example, the rare earths, iodine, tellurium, and the “noble” metals, including Mo, Nb, Ru, Ta, Re, and Tc — nonequilibrium behavior in highly radioactive environments of the MSRE would not have been surprising and would conceivably introduce uncertainties into interpretation of fission product behavior in the MSRE. Previous experience with fission product behavior had been explored almost exclusively through in-pile capsule tests, although some appraisal of the ARE fission product distribution was made.² A vigorous investigation of the fate of fission products in the MSRE was therefore initiated and pursued throughout the entire period of reactor operations. The results of those studies are summarized elsewhere.³ Concurrently, laboratory studies were developed in support of the on-site efforts to establish the relationships of fission product distributions in the MSRE with chemical parameters. During the course of MSRE operations it became increasingly evident that minor variations in the oxidation-reduction potential of the fuel salt almost certainly had a real effect on some of the fission product distributions within the system and that accurate means for the determination of the concentration of trivalent uranium in MSR's would be needed. Active work was devoted thereafter to the development of means for analysis of $\text{U}^{3+}/\Sigma\text{U}$.

Based on the considerations discussed above, a program of chemical surveillance was formulated and

Table 3.1. Composition of the MSRE fuel salt

Date	Sample	Equiv. Full Power Hr.	(Weight %)				(ppm)				Σ U in Circula- tion	Δ U (kg)	Σ Eq. Oxida- tion	Σ Eq. Reduc- tion	$[\text{U}^{3+}/\Sigma \text{U}]$ % Nom.	
			Li	Be	Zr	U Nom.	U Obs.	F	Σ	Fe						
2/13/66	Run 5-I					4.631										
2/14/66	FP 5-1	4	10.65	6.53	11.45	4.631	4.625	68.18	101.44	68	51	15	209.950	0	0	3.633 0.41
2/16/66	Run 5-F													0	0	3.633 0.41
4/5/66	Run 6-I															
4/6/66	FP 6-1															
4/8/66	-															
4/9/66	FP 6-2															
4/13/66	FP 6-3															
4/14/66	FP 6-4															
4/15/66	FP 6-5	15	10.45	6.37	11.12	4.630	4.605	69.85	102.40	234	65	35	209.944	-0.006	-0.005	3.628 0.41
4/16/66	FP 6-6	15	10.55	6.46	11.32	4.630	4.625	68.56	101.52	101	46	49				
4/17/66	FP 6-7		10.32	6.41	11.42	4.630	4.647	69.67	102.47	71	46	58				
4/19/66	FP 6-8	30	10.43	6.49	11.29	4.630	4.655	68.90	101.77	89	45	58	209.938	-0.012	0.039	3.594 0.41
4/20/66	FP 6-9	39	10.48	6.66	11.52	4.630	4.684	68.92	102.26	168	58	55	209.934	-0.016	0.050	3.583 0.40
4/25/66	FP 6-10	55	10.30	6.76	11.54	4.630	4.595	68.81	102.00	129	42	36	209.928	-0.022	0.070	3.563 0.40
5/9/66	FP 6-11	115	10.30	6.42	11.28	4.630	4.612	70.09	102.70	95	59	125	209.904	-0.046	0.147	3.486 0.40
5/10/66	FP 6-12	138														
5/11/66	FP 6-13	147	10.50	6.41	11.06	4.629	4.628	66.79	99.38	101	52	54	209.891	-0.059	0.188	3.445 0.39
5/13/66	FP 6-14	166	10.50	6.45	11.33	4.629	4.617	68.18	101.08	107	48	74	209.884	-0.066	0.212	3.421 0.39
5/14/66	FP 6-15	190	10.55	6.86	11.35	4.629	4.601	68.18	101.54	94	45	52	209.874	-0.076	0.243	3.390 0.38
5/18/66	FP 6-16	254	10.50	6.58	11.31	4.628	4.629	67.88	100.90	84	45	36	209.848	-0.102	0.326	3.307 0.37
5/23/66	FP 6-17	322	11.44	6.64	11.05	4.628	4.652	68.26	102.04	122	49	54	209.822	-0.128	0.411	3.222 0.36
5/25/66	FP 6-18															
5/26/66	FP 6-19	400	10.40	6.88	11.72	4.627	4.667	69.10	102.77	99	39	39	209.790	-0.160	0.512	3.121 0.35
5/28/66	Run 6-F	400											209.790			
6/12/66	Run 7-I	400											209.806			
6/12/66	FP 7-1	400	10.60	6.78	11.16	4.627	4.647	69.26	102.45	108	51	70	209.806			
6/15/66	FP 7-2															
6/17/66	FP 7-3	487	10.55	6.56	11.44	4.626	4.656	68.24	101.45	148	50	51	209.756	-0.194	0.623	3.010 0.34
6/20/66	FP 7-4	526	10.50	6.40	11.61	4.626	4.640	67.82	100.97	110	52	38	209.740	-0.210	0.673	2.960 0.34
6/22/66	FP 7-5															
6/24/66	FP 7-6	658	10.60	6.63	11.35	4.625	4.614	69.22	102.41	115	61	66	209.687	-0.263	0.843	2.790 0.32
6/26/66	FP 7-7	706	10.55	6.65	11.13	4.624	4.641	69.60	102.57	78	46	54	209.668	-0.282	0.904	2.729 0.31
7/1/66	FP 7-8	725	10.60	6.59	11.67	4.624	4.663	67.87	101.39	94	49	52	209.661	-0.289	0.927	2.716 0.31
7/4/66	FP 7-9															
7/6/66	FP 7-10	846	10.63	6.91	11.21	4.623	4.609	68.20	101.56	36	49	<20	209.612	-0.338	1.084	2.549 0.29
7/10/66	FP 7-11	944	10.45	7.00	11.22	4.622	4.630	69.48	102.78	58	39	36	209.573	-0.377	1.210	2.423 0.27
7/13/66	FP 7-12	1012	10.50	6.65	11.04	4.622	4.640	68.44	101.27	84	46	45	209.546	-0.404	1.300	2.333 0.26
7/15/66	FP 7-13															
7/18/66	FP 7-14	1032	10.55	6.50	11.26	4.622	4.660	68.79	101.76	53	44	63	209.538	-0.412	1.321	2.312 0.26
7/20/66	FP 7-15	1047	10.55	6.71	11.60	4.621	4.638	67.59	101.08	83	44	28	209.532	-0.418	1.341	2.292 0.26
7/22/66	FP 7-16															
7/25/66	Run 7-F	1047											209.532	-0.418	1.341	2.292 0.26
9/25/66	Run 8-I	1047											208.711			
10/8/66	FP 8-5	1047	11.10	6.23	11.21	4.603	4.643	71.21	104.39	139			208.711	-0.434	1.341	2.292 0.26
10/11/66	FP 8-6	1100	10.95	6.37	10.97	4.603	4.624	70.24	103.15	133	61	72	208.706	-0.439	1.408	2.225 0.25

Table 3.1 (continued)

Date	Sample	Equiv. Full Power Hr	(Weight %)				(ppm)				ΣU in Circula- tion	ΔU (kg)	Σ Eq. Oxida- tion	Σ Eq. Reduc- tion	$[\text{U}^{3+}/\Sigma \text{U}]$ %		
			Li	Be	Zr	U	F	Σ	Fe	Cr							
10/13/66	FP 8-7					Concentration of oxide: 44 ppm ^a											
10/17/66	FP 8-8	1166	10.95	6.88	11.23	4.603	4.638	69.94	103.64	219	65	35	208.680	-0.465	1.491	2.142	0.24
10/19/66	FP 8-9	1200	11.00	6.60	10.79	4.602	4.626	72.27	105.29	124	66	42	208.666	-0.479	1.536	2.097	0.24
10/21/66	FP 8-10	1228	11.00	6.43	11.41	4.602	4.630	67.55	101.02	89	73	119	208.655	-0.490	1.572	2.061	0.23
10/24/66	FP 8-11					Sample for oxide analysis: analysis unsuccessful											
10/26/66	FP 8-12	1357	11.15	6.62	11.20	4.601	4.650	69.01	102.63	106	51	26	208.603	-0.542	1.738	1.895	0.22
10/28/66	FP 8-13	1380	14.25	6.49	11.29	4.601	4.623	68.82	105.47	84	63	60	208.594	-0.551	1.767	1.866	0.21
10/31/66	FP 8-14	1401	13.85	6.65	11.17	4.601	4.620	69.08	105.37	82	63	25	208.586	-0.559	1.793	1.840	0.21
10/31/66	Run 8-F	1401				4.601							208.586				
11/7/66	Run 9-I					4.582							207.754				
11/7/66	FP 9-1	1401	10.93	6.55	11.70	4.582	4.618	68.39	102.19	140	66	50	207.754	-0.559	1.793	1.840	0.21
11/9/66	FP 9-2	1449				Concentration of oxide: 44 ppm ^a											
11/11/66	FP 9-3	1480	10.95	6.60	10.97	4.582	4.621	69.06	102.20	140	65	58	207.723	-0.591	1.895	1.738	0.20
11/14/66	FP 9-4	1528				[$\text{U}^{3+}/\Sigma \text{U}$] = 0.10%							207.703	-0.610	1.956	1.677	0.19
11/16/66	FP 9-5	1544	10.95	6.64	10.96	4.581	4.618	67.96	101.13	145	56	26	207.697	-0.616	1.976	1.657	0.19
11/17/66	FP 9-6					Concentration of oxide:											
11/19/66	FP 9-7	1662	-	6.71	10.95	4.580	4.557	68.79		176	57	74	207.650	-0.663	2.126	1.507	0.17
11/20/66	Run 9-F	1662				4.580							207.650	-0.663	2.126	1.507	0.17
12/12/66	Run 10-I	1662				4.561							206.815				
12/12/66	FP 10-3	1662				Sample for determination of organics in offgas; sample faulty											
12/12/66	FP 10-4					Sample for determination of organics in offgas by CuO; 600 ppm HF											
12/14/66	FP 10-5	1662	11.10	6.47	11.00	4.561	4.608	66.65	99.83	181	58	93	206.815	-0.663	2.126	1.507	0.17
12/16/66	FP 10-6	1662	11.05	6.25	11.13	4.561	4.612	67.57	100.61	168	62	55	206.815	-0.663	2.126	1.507	0.17
12/19/66	FP 10-7	1677	11.20	6.82	11.27	4.561	4.605	66.98	100.88	174	53	65	206.809	-0.669	2.146	1.487	0.17
12/22/66	FP 10-8	1746	11.20	6.69	11.13	4.561	4.604	67.21	100.83	149	56	62	206.781	-0.697	2.235	1.398	0.16
12/24/66	FP 10-9	1794	11.05	6.51	10.89	4.560	4.575	70.20	103.22	167	62	49	206.762	-0.716	2.296	1.337	0.15
12/27/66	FP 10-10					50 g sample for oxide analysis; no results available											
12/27/66	FV 10-11G					Freeze valve capsule-gas sample											
12/28/66	FP 10-12	1813	11.10	6.66	11.24	4.560	4.577	67.72	101.29	91	63	48	206.754	-0.724	2.322	1.311	0.15
12/30/66	FP 10-13	1846	11.30	6.84	11.09	4.560	4.628	65.82	99.68	162	61	82	206.741	-0.737	2.364	1.269	0.15
1/1/67	FP 10-14	1870				Be addition: 3 g as powder							206.732	-0.746	2.393	1.906	0.22
1/2/67	FP 10-15					Special sample (50 g); not subjected to chemical analysis											
1/3/67	FP 10-16	1920				Be addition; 1 g as powder							206.712	-0.766	2.457	2.064	0.24
1/3/67	FP 10-17	1920	11.15	6.47	10.88	4.559	4.633	69.03	102.16	102	64	166	206.712	-0.766	2.457	2.064	0.24
1/4/67	FP 10-18	1948				Be addition; 1.63 g as rod							206.701	-0.777	2.492	2.391	0.27
1/6/67	FP 10-19	1968	11.15	6.64	11.03	4.559	4.621	67.75	101.19	145	62	62	206.693	-0.785	2.518	2.365	0.27
1/9/67	FP 10-20	2161	11.08	6.40	10.82	4.557	4.622	69.30	102.22	164	57	57	206.615	-0.863	2.768	2.115	0.24
1/11/67	FP 10-21					50 g sample for oxide determination											
1/11/67	FV 10-22G					Freeze valve capsule-gas sample											
1/13/67	FP 10-23	2247				Be addition: 10.65 g as rod							206.581	-0.897	2.877	4.369	0.50
1/13/67	FP 10-24	2247	11.23	6.55	11.21	4.556	4.606	68.73	102.36	151	56	87	206.581	-0.897	2.877	4.369	0.50
1/15/67	FP 10-25	2288				50 g sample for $[\text{U}^{3+}/\Sigma \text{U}]$ analysis; $[\text{U}^{3+}/\Sigma \text{U}] = 0.66\%$ ^c							206.565	-0.913	2.928	4.318	0.50
1/16/67	Run 10-F	2288				4.556							206.565	-0.913	2.928	4.318	0.50
1/28/67	Run 11-I	2288				4.556							206.585	-0.913	2.928	4.318	0.50
1/28/67	FP 11-1	2288	11.18	6.28	10.90	4.556	4.603	67.46	100.42	131	66	54	206.585	-0.913	2.928	4.318	0.50
1/30/67	FP 11-2	2308	11.10	6.27	10.65	4.556	4.599	69.16	101.78	112	75	63	206.577	-0.921	2.954	4.292	0.49
2/1/67	FP 11-3	2331	10.42	6.41	11.08	4.556	4.606	66.72	99.03	150	61	64	206.568	-0.930	2.983	4.263	0.49

Table 3.1 (continued)

Date	Sample	Equiv. Full Power hr	(Weight %)				(ppm)				Σ in Circula- tion	ΔU (kg)	Σ Eq. Oxida- tion	Σ Eq. Reduc- tion	$[\text{U}^{3+}/\Sigma \text{U}]$ %		
			Li	Be	Zr	U	Nom.	Obs.	F	Σ	Fe	Cr	Ni				
2/3/67	FP 11-4	2372	11.10	6.33	11.10	4.556	4.592	67.87	100.99	145	62	22	206.551	-0.947	3.037	4.209	0.48
2/6/67	FP 11-5	2468	50 g sample for $\text{U}^{3+}/\Sigma \text{U}$ analysis; $\text{U}^{3+}/\Sigma \text{U} = 0.60\%$ ^c										206.513	-0.985	3.159	4.037	0.47
2/8/67	FP 11-6	2516	11.25	6.31	10.97	4.554	4.555	67.44	100.52	131	67	33	206.494	-1.004	3.220	4.026	0.46
2/10/67	FL 11-7	2541	11.38	6.70	11.27	4.554	4.558	69.92	103.83	172	62	50	206.484	-1.014	3.252	3.994	0.46
2/13/67	FP 11-8	2614	11.50	6.62	10.81	4.553	4.569	68.89	102.39	312	54	107	206.455	-1.043	3.345	3.901	0.45
	FV 11-9G		Freeze valve capsule-gas sample														
2/15/67	FP 11-10	2663	Be metal addition; 11.66 g as rod										206.435	-1.063	3.409	6.424	0.74
2/17/67	FP 11-11	2779	10.67	6.57	10.87	4.552	4.551	69.94	102.60	165	73	43	206.389	-1.109	3.557	6.276	0.72
2/21/67	FP 11-12	2811	10.93	6.27	10.88	4.552	4.567	69.96	102.60	76	75	34	206.376	-1.122	3.598	6.235	0.72
2/22/67	FP 11-13	2835	50 g sample for $\text{U}^{3+}/\Sigma \text{U}$ analysis; $\text{U}^{3+}/\Sigma \text{U} = 0.69\%$ ^c										206.366	-1.132	3.631	6.202	0.71
2/24/67	FP 11-14	2884	10.98	6.35	11.26	4.551	4.525	67.83	100.95	98	78	75	206.347	-1.151	3.691	6.142	0.71
2/28/67	FP 11-15	2950	11.11	6.49	10.74	4.551	4.552	68.89	101.78	71	62	37	206.321	-1.177	3.775	6.055	0.70
2/28/67	FV 11-16G		Freeze valve capsule-gas sample														
3/1/67	FP 11-17	2994	11.33	6.47	11.21	4.550	4.553	70.25	103.81	67	58	47	206.303	-1.195	3.833	6.000	0.69
3/2/67	FP 11-19	3014	10.73	6.67	11.17	4.550	4.576	68.68	101.83	120	56	43	206.295	-1.203	3.858	5.975	0.69
3/3/67	FP 11-19	3038	10.47	6.57	11.11	4.550	4.589	67.12	99.86	117	68	42	206.285	-1.213	3.890	5.943	0.68
3/6/67	FP 11-20	3109	10.51	6.72	10.98	4.549	4.561	67.60	100.37	122	59	49	206.257	-1.241	3.980	5.853	0.67
3/8/67	FP 11-21	3126	10.50	6.36	10.89	4.549	4.576	66.83	99.16	168	63	46	206.250	-1.248	4.003	5.830	0.67
3/9/67	FP 11-22	3126	10.55	6.57	10.92	4.549	4.572	66.05	98.66	104	62	63	206.250	-1.248	4.003	5.830	0.67
3/10/67	FP 11-23	3126	10.53	6.49	10.95	4.549	4.583	69.70	102.25	136	63	55	206.250	-1.248	4.003	5.830	0.67
3/13/67	FP 11-24	3169	10.55	6.51	10.90	4.549	4.547	68.50	101.01	173	67	63	206.233	-1.265	4.057	5.776	0.66
3/16/67	FP 11-25		50 g sample for oxide analysis; analysis unsuccessful														
3/20/67	FP 11-26	3359	10.43	6.49	10.91	4.547	4.570	67.17	99.57	118	52	53	206.157	-1.341	4.301	5.532	0.64
3/21/67	FP 11-27	3380	10.52	6.85	10.85	4.547	4.577	66.04	98.84	72	63	80	206.149	-1.349	4.327	5.506	0.63
3/21/67	FP 11-28		Concentration of oxide: 58 ppm														
3/22/67	FP 11-29	3407	10.48	6.46	10.92	4.546	4.584	64.62	97.06	126	64	56	206.138	-1.360	4.362	5.471	0.63
3/23/67	FP 11-30	3460	10.48	6.39	11.02	4.546	4.597	64.51	96.99	115	66	71	206.117	-1.381	4.429	5.404	0.62
3/27/67	FP 11-31	3524	10.53	6.58	11.06	4.546	4.559	67.06	99.79	80	64	50	206.092	-1.406	4.509	5.324	0.61
3/28/67	FP 11-32	3548	50 g sample for $\text{U}^{3+}/\Sigma \text{U}$ analysis; $\text{U}^{3+}/\Sigma \text{U} = 0.045\%$ ^c										206.082	-1.416	4.541	5.292	0.61
3/29/67	FP 11-33	3571	10.53	6.43	11.14	4.545	4.567	66.38	99.04	142	72	72	206.073	-1.425	4.570	5.263	0.61
3/31/67	FP 11-34	3619	10.55	6.33	11.37	4.545	4.582	68.99	101.82	146	64	64	206.054	-1.444	4.631	5.202	0.60
4/3/67	FP 11-35	3690	10.53	6.35	11.12	4.544	4.566	67.24	99.81	194	73	64	206.025	-1.473	4.724	5.109	0.59
4/4/67	FV 11-36G		Freeze valve sample; capsule penetrated by leaching solution														
4/5/67	FP 11-37	3739	10.55	6.33	10.75	4.544	4.541	65.93	96.10	79	80	49	206.006	-1.492	4.785	5.048	0.58
4/6/67	FP 11-38	3763	50 g sample for $\text{U}^{3+}/\Sigma \text{U}$ analysis; $\text{U}^{3+}/\Sigma \text{U} =$ μ										205.996	-1.502	4.817	5.016	0.58
4/7/67	FP 11-39	3856	11.57	6.44	10.92	4.543	4.536	66.55	100.02	182	69	52	205.959	-1.539	4.936	4.897	0.56
4/10/67	FP 11-40	3856	Be addition: 8.40 g as rod										205.959	-1.539	4.936	6.761	0.78
4/10/67	FP 11-41	3856	10.42	6.37	10.77	4.543	4.579	68.58	100.72	135	56	58	205.959	-1.539	4.936	6.761	0.78
4/11/67	FV 11-42G		Freeze valve sample - wt gain: 0 g Pump off 40 min. Sampler port 2" above salt surface														
4/12/67	FP 11-43	3904	50 g sample for $\text{U}^{3+}/\Sigma \text{U}$ analysis; sampler machined improperly; no results obtained														
4/14/67	FP 11-44	3937	10.50	6.60	11.01	4.542	4.561	69.88	102.55	140	59	44	205.927	-1.571	5.038	6.659	0.77
4/17/67	FP 11-45 ^d	4007	10.58	6.50	10.65	4.541	4.548	67.13	99.41	88	54	41	205.899	-1.599	5.128	6.569	0.77
4/18/67	FV 11-46G		Freeze valve sample. Pump on. Sampler port above salt surface														
4/21/67	FP 11-47	4107	10.95	6.48	10.96	4.558	4.604	66.65	99.64	169	71	75	206.678	-1.639	5.257	6.440	0.74
4/24/67	FP 11-48	4172	10.45	6.52	10.85	4.558	4.578	67.23	99.63	210	49	58	206.652	-1.665	5.340	6.357	0.73
4/25/67	FP 11-49	4196	50 g sample for $\text{U}^{3+}/\Sigma \text{U}$ analysis; >2000 μ moles HF										206.642	-1.675	5.372	6.325	0.73

Table 3.1 (continued)

Date	Sample	Equiv. Full Power hr	(Weight %)			(ppm)					Σ U in Circula- tion	Δ U (kg)	Σ Eq. Oxida- tion	Σ Eq. Reduc- tion	$[\text{U}^{3+}/\Sigma \text{U}]$ %				
			Li	Be	Zr	U	F	Σ	Fe	Cr									
4/26/67	FP 11-50		Tandem graphite specimens - wire showed 30 X activity at salt-gas interface																
4/28/67	FP 11-51	4274	11.20	6.45	10.97	4.557	4.571	69.61	102.80	114	61	61	206.611	-1.706	5.471	6.226	0.71		
5/1/67	FP 11-52	4341	11.33	6.45	10.79	4.556	4.566	69.27	102.41	80	60	25	206.584	-1.733	5.558	6.139	0.70		
5/3/67	FV 11-53G	4388	Freeze valve sample. Pump on, level low (51%)												206.566	-1.751	5.616	6.081	0.70
5/5/67	FP 11-54	4436	10.93	6.63	10.95	4.556	4.551	69.91		158	61	63	206.547	-1.770	5.677	6.020	0.69		
5/8/67	FP 11-55	4507	50 g sample for use in hot cell experiments												206.518	-1.799	3.770	5.927	0.68
5/9/67	FP 11-56		50 g sample for oxide analysis - poor results obtained; estimate: 50-150 ppm																
5/10/67	FP 11-57		Sampler was found to be empty																
5/10/67	FP 11-58	4513	10.48	6.66	11.27	4.556	4.607	70.85	103.97	131	81	42	206.516	-1.801	5.777	5.920	0.68		
5/10/67	Run 11-F	4513				4.556							206.516	-1.801	5.777	5.920	0.68		
6/19/67	Run 12-I	4513				4.536							205.679						
6/19/67	FP 12-5	4513	11.2	6.74	10.94	4.536	4.550	66.32	99.75	123	52	60	205.679	-1.801	5.777	5.920	0.68		
6/21/67	FP 12-6	4513	50 g sample for $\text{U}^{3+}/\Sigma \text{U}$ analysis $\text{U}^{3+}/\Sigma \text{U} = 0.71\%$ ^c												205.679	-1.801	5.777	5.920	0.68
6/21/67	FV 12-7G		Freeze valve sample for Run 12 baseline data																
6/21/67	FP 12-8		Be addition: 7.933 g as rod												205.679	-1.801	5.777	7.676	0.89
6/23/67	FP 12-9	4558	Be addition: 9.840 g as rod												205.661	-1.819	5.834	9.807	1.13
6/26/67	FP 12-10	4602	11.6	6.91	10.57	4.536	4.525	67.27	110.87	134	71	72	205.643	-1.837	5.892	9.749	1.12		
6/29/67	FP 12-11	4674	50 g sample for $\text{U}^{3+}/\Sigma \text{U}$ analysis $\text{U}^{3+}/\Sigma \text{U} = 1.3\%$ ^c												205.615	-1.865	5.981	9.660	1.10
6/30/67	FP 12-12	4706	11.6	6.54	10.91	4.535	4.545	66.66	100.76	113	64	62	205.602	-1.878	6.023	9.618	1.11		
7/3/67	FP 12-13	4739	Be addition: 8330 g as rod												205.589	-1.891	6.065	11.424	1.32
7/5/67	FP 12-14	4787	11.5	6.50	11.22	4.534	4.557	67.95	101.73	145	82	47	205.569	-1.911	6.129	11.360	1.31		
7/6/67	FP 12-15	4811	Be addition: 11.677 g as rod												205.560	-1.920	6.158	13.922	1.61
7/7/67	FP 12-16	4836	11.4	6.40	10.62	4.534	4.567	68.27	101.26	269	110	68	205.550	-1.930	6.190	13.890	1.60		
7/10/67	FP 12-17	4885	11.3	6.40	10.66	4.533	4.532	66.92	99.81	216	144	53	205.530	-1.950	6.254	13.826	1.60		
7/11/67	FP 12-18	4909	Concentration of oxide 57 ppm																
7/11/67	FP 12-19	4917	11.5	6.19	11.00	4.533	4.522	65.05	98.26	100	102	62	205.518	-1.962	6.292	13.788	1.59		
7/12/67	FP 12-20	4933	10.6	6.36	10.76	4.533	4.557	65.76	98.04	81	64	44	205.511	-1.969	6.315	13.765	1.58		
7/13/67	FP 12-21	4981	50 g sample for $\text{U}^{3+}/\Sigma \text{U}$ analysis: $\text{U}^{3+}/\Sigma \text{U} = 1.07\%$ ^c												205.492	-1.988	6.376	13.704	1.58
7/13/67	FP 12-22	4981	10.5	6.52	10.43	4.532	4.566	66.18	98.19	247	90	50	205.492	-1.988	6.376	13.704	1.58		
7/14/67	FP 12-23	4998	10.6	6.68	10.58	4.532	4.526	65.26	97.64	154	78	76	205.485	-1.995	6.398	13.682	1.58		
7/15/67	FP 12-24	5022	11.38	6.36	10.67	4.532	4.567	66.46	99.44	176	67	56	205.476	-2.004	6.427	13.653	1.58		
7/16/67	FP 12-25	5046	10.7	6.46	10.53	4.532	4.496	66.10	98.29	208	68	62	205.466	-2.014	6.459	13.621	1.57		
7/17/67	FV 12-26G		Freeze valve capsule-gas sample																
7/17/67	FP 12-27	5070	10.7	6.61	10.78	4.532	4.550	67.50	100.14	195	75	72	205.457	-2.023	6.488	13.592	1.57		
7/18/67	FP 12-28	5097	10.7	6.44	10.66	4.531	4.569	69.00	101.37	150	68	52	205.446	-2.034	6.523	13.557	1.56		
7/19/67	FP 12-29	5121	10.7	6.41	10.87	4.531	4.529	67.11	99.62	177	84	78	205.436	-2.044	6.555	13.525	1.56		
7/19/67	FP 12-30		U Addn. caps. no. 99																
7/19/67	FP 12-31		U addn. caps. No. 100																
7/20/67	FP 12-32		U addn. caps. no. 101																
7/20/67	FP 12-33		U addn. caps. no. 102																
7/20/67	FP 12-34		U addn. caps. no. 103																
7/21/67	FP 12-35		U addn. caps. no. 104 4.543												205.983	-2.044	6.555	13.525	1.56
7/21/67	FP 12-36	5169	10.5	6.68	10.96	4.543	4.554	66.40	99.09	156	84	129	205.964	-2.063	6.616	13.464	1.55		
7/21/67	FP 12-37		U addn. caps. no. 105																
7/22/67	FP 12-38		U addn. caps. no. 106																
7/22/67	FP 12-39		U addn. caps. no. 107																
7/22/67	FP 12-40		U addn. caps. no. 108 4.551												206.328	-2.063	6.616	13.464	1.55

Table 3.1 (continued)

Date	Sample	Equiv. Full Power N _r	(Weight %)				(ppm)					Σ U in Circula- tion	Δ U (kg)	Σ Eq. Oxida- tion	Σ Eq. Reduc- tion	$[\text{U}^{3+}/\Sigma \text{U}]$ % Nom.			
			Li	Be	Zr	U	Nom.	Obs.	F	Σ	Fe	Cr							
7/23/67	FP 12-41	5229	10.6	6.52	10.68	4.550	4.562		68.00	100.36	110	64	192	206.304	-2.087	6.693	13.387	1.54	
7/23/67	FP 12-42		U	6.52	capsule No. 109														
7/23/67	FP 12-43		U addn.	caps.	no. 110														
	FP 12-44		U addn.	caps.	no. 111														
	FP 12-45		U addn.	caps.	no. 112														
	FP 12-46		U addn.	caps.	no. 113	4.560													
7/25/67	FP 12-47	5266	10.6	6.50	10.50	4.560	4.586		66.34	98.53	120	72	70	206.760	-2.087	6.693	13.387	1.54	
	FP 12-48		U addn.	caps.	no. 114														
	FP 12-49		U addn.	caps.	no. 115														
	FP 12-50		U addn.	caps.	no. 116	4.566													
7/26/67	FP 12-51	5296	11.22	6.60	10.32	4.566	4.588		66.32	99.05	94	72	39	207.020	-2.102	6.741	13.339	1.53	
7/28/67	FP 12-52	5366	10.7	6.47	10.71	4.565	4.594		65.98	98.45	119	72	92	206.980	-2.142	6.870	13.210	1.51	
7/31/67	FP 12-53	5433	10.5	6.39	10.66	4.565	4.503		65.48	97.53	182	72	60	206.954	-2.168	6.953	13.127	1.50	
8/1/67	FP 12-54	5433	50 g sample for isotopic analysis																
8/2/67	FP 12-55	5463				4.564													
			10.75	6.44	11.12	4.564	4.577		65.72	98.61	156	72	300	206.942					
			10.80	6.42	10.95	4.564	4.575		64.57	97.32	136	58	720	206.942					
8/3/67	FP 12-56	5492	Be addition: 9.71 g as rod												206.930	-2.192	7.030	15.205	1.74
8/3/67	FP 12-57	5496				4.564									206.928	-2.194	7.036	15.199	1.74
8/4/67	FP 12-58	5500	11.33	6.59	11.08	4.564	4.587		65.14	98.73	156	54	170	206.927	-2.195	7.040	15.195	1.74	
			11.30	6.74	11.28	4.564	4.549		66.53	100.40	160	64	424	206.927					
8/4/67	FP 12-59	5500	11.00	6.58	10.77	4.564	4.600		66.62	99.57	138	74	66	206.927	-2.195	7.040	15.195	1.74	
8/5/67	Run 12-F	5500	Sampler cable severed																
9/15/67	Run 13-I	5500				4.543									205.984	-2.195	7.040	15.195	1.74
9/15/67	FP 13-4	5568	10.98	6.90	11.21	4.543	4.552		65.88	99.55	141	82	82	205.957	-2.222	7.126	15.109	1.74	
9/15/67	FP 13-5	5568	50 g sample for $\text{U}^{3+}/\Sigma \text{U}$; $\text{U}^{3+}/\Sigma \text{U} = 1.60\%$ ^c												205.957	-2.222	7.126	15.109	1.74
9/18/67	FP 13-6	5666	10.95	6.42	10.78	4.542	4.587		67.01	99.77	118	66	76	205.918	-2.261	7.251	14.984	1.72	
9/18/67	Run 13-F					4.542								205.918					
9/20/67	Run 14-I					4.542								205.924	-2.261	7.251	14.984	1.72	
9/20/67	FP 14-1		Sample capsule suspended in empty pump bowl for 10 minutes																
9/21/67	FP 14-2		No sample obtained; sampler found to have no sample port.																
9/22/67	FP 14-3		50 g sample for isotopic analyses																
9/25/67	FP 14-4	5757	10.70	6.32	11.52	4.541	4.577		66.16	99.30	104	76	46	205.887	-2.298	7.370	14.865	1.71	
9/26/67	FP 14-5		50 g sample for isotopic analyses																
9/27/67	FP 14-6		50 g sample for isotopic analyses																
9/28/67	FP 14-7	5828	10.70	6.24	10.98	4.540	4.572		66.19	98.71	102	79	63	205.859	-2.326	7.460	14.775	1.70	
10/2/67	FP 14-8	5923	10.80	6.13	10.98	4.540	4.584		66.54	99.12	98	74	68	205.821	-2.364	7.582	14.653	1.69	
10/3/67	FP 14-9	5933	Sample for oxide analyses; no results obtained																
10/5/67	FP 14-10	5995	10.90	6.74	11.40	4.539	4.587		65.48	99.13	150	80	76	205.792	-2.393	7.675	14.560	1.68	
10/9/67	FP 14-11	6086	10.80	6.20	11.06	4.538	4.579		65.18	97.78	128	88	66	205.756	-2.429	7.790	14.445	1.66	
10/12/67	FP 14-12	6155	10.90	6.88	11.01	4.538	4.579		66.82	100.22	176	60	60	205.728	-2.457	7.880	14.355	1.65	
10/16/67	FP 14-13	6249	10.50	6.36	11.08	4.537	4.575		65.73	98.27	146	65	57	205.691	-2.494	8.000	14.235	1.64	
10/20/67	FP 14-14	6344	10.65	6.52	11.25	4.536	4.480		66.88	99.81	110	80	112	205.653	-2.532	8.120	14.115	1.63	
10/23/67	FP 14-15		50 g sample for hot cell experiments																
10/24/67	FP 14-16	6440	10.80	6.30	11.28	4.535	4.556		65.75	98.72	158	76	105	205.615	-2.570	8.242	13.993	1.61	
10/26/67	FP 14-17	6440	10.80	6.26	10.81	4.535	4.557		66.14	98.59	124	80	55	205.615	-2.570	8.242	13.993	1.61	
10/30/67	FP 14-18	6506	10.53	6.00	11.00	4.535	4.553		65.24	97.35	112	70	62	205.594	-2.591	8.310	13.925	1.61	

Table 3.1 (continued)

Date	Sample	Equiv. Full Power Hr	(Weight %)				(ppm)				Σ U in Circula-tion	Δ U (kg)	Σ Eq. Oxida-tion	Σ Eq. Reduc-tion %	$[\text{U}^{3+}/\Sigma \text{U}]$						
			Li	Be	Zr	U	Nom.	Obs.	F	Σ	Fe	Cr	Ni								
11/3/67	FP 14-19	6604	10.73	5.92	11.25	4.534	4.553		66.68	99.13	108	70	51	205.549	-2.636	8.454	13.781	1.59			
11/3/67	FV 14-20S		Freeze valve capsule - salt sample				10.60	5.94	10.69	4.533	4.557	65.88	97.69	128	76	61	205.520	-2.665	8.547	13.688	1.58
11/6/67	FP 14-21	6678	10.60	5.96	11.32	4.533	4.529		66.74	99.07	106	72	74	205.510	-2.675	8.580	13.655	1.58			
11/7/67	FP 14-22	6702	10.60	5.86	11.29	4.532	4.534		66.89	99.21	94	68	56	205.501	-2.684	8.608	13.627	1.57			
11/8/67	FP 14-23	6726	10.43	6.04	11.29	4.532	4.534		66.42	99.17	169	72	72	205.491	-2.694	8.640	13.595	1.57			
11/9/67	FP 14-24	6751	10.63	6.18	11.34	4.532	4.567		66.42	99.17	169	72	72	205.491	-2.733	8.765	13.470	1.55			
11/13/67	FP 14-25	6848	10.40	6.12	10.92	4.531	4.548		66.19	98.20	124	72	62	205.452	-2.743	8.797	13.438	1.55			
11/14/67	FP 14-26	6872	10.63	6.10	11.00	4.531	4.572		66.34	98.66	103	66	60	205.442	-2.759	8.848	13.387	1.54			
11/27/67	FP 14-27	6913	10.20	6.19	11.12	4.531	4.553		66.53	98.62	126	72	69	205.426	-2.802	8.986	13.249	1.53			
11/30/67	FP 14-28	7020	10.53	6.19	11.18	4.530	4.589		66.79	99.31	135	72	60	205.383	-2.850	9.140	13.095	1.51			
12/4/67	FP 14-29	7142	10.40	6.34	10.88	4.529	4.564		66.42	98.63	121	70	72	205.335	-2.919	9.362	12.873	1.49			
12/5/67	FV 14-30S		Freeze valve capsule - salt sample				50 g sample for use in hot cell experiments				10.40 6.45 10.94 4.527 4.550 66.52 98.88 120 70 58				205.266	205.266	9.554	12.681	1.47		
12/6/67	FP 14-31		10 g sample exposed to atmosphere in Line 928, 1.5 ft. above pump bowl				10 g sample exposed to atmosphere in Area 1C for 10 min.				10 g sample for isotopic analysis				10 g sample for isotopic analysis				12/19/67		
12/11/67	FP 14-32	7313	10.40	6.45	10.94	4.527	4.550		66.52	98.88	120	70	58	205.266	-2.919	9.362	12.873	1.49			
12/12/67	FP 14-33		10 g sample exposed to atmosphere in Line 928, 1.5 ft. above pump bowl				10 g sample exposed to atmosphere in Area 1C for 10 min.				10 g sample for isotopic analysis				10 g sample for isotopic analysis				12/19/67		
12/13/67	FP 14-34		Concentration of oxide: 46 ppm				10.80 6.38 10.56 4.526 4.561 66.06 98.39 174 82 96				205.206				-2.979	9.554	12.681	1.47	12/20/67		
12/20/67	FP 14-39		Concentration of oxide: 46 ppm				10.30 6.28 10.87 4.524 4.531 66.31 98.32 113 79 69				205.103				-3.032	9.724	12.511	1.45	12/26/67		
12/26/67	FP 14-20	7597	10.30	6.28	10.87	4.524	4.531		66.23	98.55	134	84	59	205.099	-3.086	9.897	12.338	1.43			
1/2/68	FP 14-41	7732	10.30	6.34	11.12	4.524	4.536		66.41	98.73	148	87	73	205.072	-3.113	9.984	12.251	1.42			
1/8/68	FP 14-42	7799	10.50	6.10	11.16	4.523	4.531		66.36	98.33	118	74	70	205.052	-3.133	9.984	12.251	1.42			
1/11/68	FP 14-43	7849	10.10	6.46	10.96	4.523	4.524		66.51	97.67	120	90	68	205.025	-3.160	10.13	12.105	1.40			
1/15/68	FP 14-44	7917	9.80	6.42	10.45	4.522	4.466		66.51	97.67	120	90	68	205.016	-3.169	10.16	12.075	1.40			
1/16/68	FP 14-45	7939	50 g sample for $\text{U}^{3+}/\Sigma \text{U}$ analysis;				10.20 6.50 11.16 4.522 4.516 67.06 99.47 152 84 72				205.011				-3.174	10.18	12.055	1.39	1/17/68		
1/17/68	FP 14-46	7953	10.20	6.50	11.16	4.522	4.516		66.78	99.25	136	81	53	205.005	-3.180	10.20	12.035	1.39			
1/18/68	FP 14-47	7970	10.50	6.40	11.01	4.522	4.536		66.96	99.13	111	90	51	204.977	-3.208	10.29	11.945	1.38			
1/22/68	FP 14-48	8038	10.25	6.42	10.92	4.521	4.557		66.92	99.17	108	74	56	204.976	-3.209	10.29	11.945	1.38			
1/25/68	FP 14-49	8040	10.28	6.56	10.85	4.521	4.538		66.24	98.76	121	79	70	204.976	-3.209	10.29	11.945	1.38			
1/29/68	FP 14-50	8040	10.20	6.38	11.38	4.521	4.541		66.57	98.74	110	68	48	204.969	-3.216	10.31	11.925	1.38			
2/1/68	FP 14-51	8057	10.3	6.70	10.96	4.521	4.541		66.43	98.96	132	81	73	204.941	-3.244	10.40	11.835	1.37			
2/5/68	FP 14-52	8129	10.15	6.56	10.90	4.520	4.541		66.57	98.74	110	68	48	204.918	-3.267	10.48	11.755	1.36			
2/6/68	FP 14-53		Concentration of oxide: 58 ppm				9.88 6.03 10.38 4.520 4.446 66.58 97.35 105 80 50				204.918				-3.267	10.82	11.415	1.32	2/9/68		
2/9/68	FP 14-55	8186	Ni rod suspended in Ni basket - 2 hours				10.28 6.36 11.08 4.519 4.533 66.53 98.84 117 90 68				204.898				-3.287	10.54	11.695	1.35	2/12/68		
2/12/68	FP 14-56	8236	50 g sample for $\text{U}^{3+}/\Sigma \text{U}$ analysis; $\text{U}^{3+}/\Sigma \text{U} = \sim 0.35\%$				10.30 6.40 10.93 4.515 4.529 66.70 98.89 94 82 58				204.870				-3.315	10.63	11.605	1.34	2/13/68		
2/13/68	FP 14-57		50 g sample for $\text{U}^{3+}/\Sigma \text{U}$ analysis; $\text{U}^{3+}/\Sigma \text{U} = \sim 0.35\%$				10.23 6.58 10.79 4.518 4.527 65.93 98.09 101 82 42				204.832				-3.353	10.75	11.485	1.33	2/15/68		
2/20/68	FP 14-60		50 g sample for F. P. experiments - S. S. Kirslis; 10 g obtained				- 6.21 10.96 4.517 - 66.63 - 74				204.810				-3.375	10.82	11.415	1.32	2/22/68		
2/22/68	FP 14-61	8456	50 g sample for use in hot cell experiments				- 6.21 10.96 4.517 - 66.63 - 74				204.810				-3.375	10.82	11.415	1.32	2/26/68		
2/26/68	FP 14-62		Freeze valve capsule - salt sample				80				204.752				-3.433	11.01	11.225	1.30	2/27/68		
2/27/68	FV 14-63S		Freeze valve capsule - salt sample				80				204.714				-3.471	11.13	11.105	1.29	2/28/68		
3/4/68	FP 14-64	8602	10.30	6.24	10.80	4.516	4.552		66.04	97.94	144	80	56	204.752	-3.433	11.01	11.225	1.30			
3/4/68	FP 14-65	8697	10.20	6.40	11.08	4.515	4.510		66.58	98.80	63	83	36	204.714	-3.471	11.13	11.105	1.29			

Table 3.1 (continued)

Table 3.1 (continued)

Date	Sample	Equiv. Full Power Hr	(Weight %)						(ppm)			ΣU in Circula- tion	ΔU (kg)	Σ Eq. Oxida- tion	Σ Eq. Reduc- tion	$[U^{3+}] / \Sigma U$ %	
			Li	Be	Zr	U	F	Σ	Fe	Cr	Ni	Pu					
10/ /68	FP 15-25																
10/10/68	FP 15-26		10 g sample for analysis of total concentration of reductants: $\Sigma = 0.6\%$, $[U^{3+}] / [U]$ equivalent: 0.09%														
10/12/68	FP 15-27		11.60 6.72 10.95 0.794 0.804			71.36 102.24 140		50 51			34.009		+0.579				
10/12/68	FV 15-28S		Capsule No. 22 Enrichment No. 13									34.009					
10/12/68	FV 15-29G		Freeze valve capsule - salt sample; no sample obtained														
10/13/68	FP 15-30		Freeze valve capsule - gas sample														
			Be addition; 8.34 g as rod													0	
			Scale from Be rod								36.5%	50.3%	13.2%				
			Scale from Ni cage								78.6%	4.0%	17.4%				
10/15/68	FP 15-31S		Capsule No. 35 Enrichment No. 14									34.189		+0.090			
10/15/68	FV 15-32S		11.75 6.44 11.17 0.795 0.785			- -		134	59	-		34.189		-			
10/17/68	FP 15-33		11.55 6.36 11.16 0.795 0.797			68.36 98.23		158	56	61	133	34.189		-			
10/18/68	FP 15-34		Capsule No. 42 Enrichment No. 15														
10/19/68	FP 15-35		Capsule No. 18 Enrichment No. 16														
10/19/68	FP 15-36		Capsule No. 17 Enrichment No. 17														
10/20/68	FP 15-37		Capsule No. 36 Enrichment No. 18														
10/20/68			Fuel circuit drained														
10/23/68			Fuel circuit filled														
10/23/68	FP 15-38		11.45 6.76 11.45 0.804 0.797			66.72 97.21		154	68	43	146	34.443		+0.571	-	-	0
10/26/68	FP 15-39a		0.804 0.795														
10/28/68	FP 15-40		12.37 - - 0.804 0.820			- -		676	139	74							
10/28/68	FP 15-41		Capsule No. 41 Enrichment No. 19									34.533		+0.090	-	-	0
10/29/68	FV 15-42S		- 6.13 11.09 0.804 0.779			- -		132	60	143	135	34.533		-	-	-	0
10/29/68	FP 15-43C		Freeze valve capsule - gas sample														
10/30/68	FP 15-44		Capsule No. 38 Enrichment No. 20														
10/30/68	FP 15-45		Capsule No. 34 Enrichment No. 21														
10/31/68	FP 15-46		Capsule No. 45 Enrichment No. 22														
10/31/68	FP 15-47		Capsule No. 39 Enrichment No. 23														
11/4/68	FP 15-48		Capsule No. 32 Enrichment No. 24														
11/4/68	FP 15-49		Capsule No. 31 Enrichment No. 25														
11/5/68	FP 15-50		Capsule No. 37 Enrichment No. 26														
11/6/68	FP 15-51S		- - 11.18 0.821 0.798									35.144		-			
11/6/68	FV 15-52G		Freeze valve capsule - gas sample														
11/6/68	FP 15-53		Cu capsule containing a magnet; exposed to salt 5 min.														
11/9/68	FP 15-54		Capsule No. 44 Enrichment No. 27									35.234		+0.090	-	-	0
11/11/68	FP 15-55		11.30 6.53 10.99 0.823 0.813			68.00 97.68		181	80	140		35.234		+0.070	-	-	0
11/11/68	FP 15-56		Capsule No. 32, from PF 15-48, for laboratory tests														
11/12/68	FV 15-57S		Freeze valve capsule - salt sample														
			0.823 0.736						2510	1290	340						
			0.823 0.794						183	76	76						
			Freeze valve capsule - gas sample														
11/12/68	FP 15-58G		Segmented magnets - suspended in salt 1 hr; pump off														
11/13/68	FP 15-59		11.25 6.64 11.15 0.823 0.828			68.50 98.41		176	62	31	148						
11/15/68	FP 15-60		Segmented magnets - suspended in salt 1 hr; pump on														
11/15/68	FP 15-61		Be addition: 9.38 g as rod									4.72%	3.26%	4.71%			
11/15/68	FP 15-62		Scale from Ni cage cap									2.74%	4.53%	0.10%			
11/16/68	FP 15-63		Scale from Ni cage body														
			11.50 6.50 11.04 0.823 0.818			69.52 99.42		143	62	46	153						

Table 3.1 (continued)

Date	Sample	Equiv. Full Power hr	(Weight %)				(ppm)				ΣU in Circula- tion	ΔU (kg)	Σ Eq. Oxida- tion	Σ Eq. Reduc- tion	$[U^{3+}/\Sigma U]$ %
			Li	Be	Zr	U	F	Σ	Fe	Cr					
11/19/68	FP 15-64					Magnet No. 4 (segmented) immersed 4 times									
11/20/68	FP 15-65		11.80	6.99	11.23	0.823	0.843	66.91	97.90	98	63	52	171		
11/20/68	FP 15-66					Segmented magnets, separated by Be metal spacers. Be addition: 1.0 g.									
11/21/68	FP 15-67					Magnet No. 6; immersed 5 min.									
11/22/68	FP 15-68		11.68	6.73	11.02	0.823	0.816	68.70	98.99	148	62	26	168		
11/25/68	FV 15-69G					Freeze valve capsule - gas sample									
11/26/68	FP 15-70					50 g sample for oxide analysis; specimen not usable									
11/27/68	FV 15-71S					Freeze valve capsule - salt sample									
11/28/68	Run 15-F ^f														
12/11/68	Run 16-I														
12/12/68	FP 16-1														
12/13/68	FP 16-2					Magnet capsule									
12/13/68	FV 16-3S					Magnet capsule 12/13/68									
12/16/68	FV 16-4S		-	6.85	10.90	0.823	0.807	67.88	-	152	84	30			
12/16/68	Run 16-F														
1/12/69	Run 17-1	0													
1/12/69	FP 17-1	0	11.35	6.39	10.94	0.823	0.780	70.63	100.09	116	52	57	140	35.234	0
1/14/69	FV 17-2S	2		-	7.02	11.08	0.823	0.812	66.18	-	122	68	53	35.233	-0.0005
1/16/69	FP 17-3	84				50 g sample for oxide determination - overheated - not usable								35.207	
1/21/69	FP 17-4		11.58	6.82	11.32	0.822	0.812	67.89	98.46	112	62	56	144	35.207	-0.0266
1/21/69	FP 17-5					50 g sample for oxide determination: 61 ppm									
1/22/69	FV 17-6S					Freeze valve capsule - salt sample									
1/22/69	FV 17-7S	124				Freeze valve capsule - salt sample								35.195	-0.039
1/22/69	FV 17-8	124				Be addition: 8.57 g as rod								0.13	-0.09
1/27/69	FP 17-9	148	11.35	6.88	11.08	0.822	0.823	66.64	96.97	149	58	64	158	35.187	0.15
1/28/69	FP 17-10S	172	6.68	10.39	0.822	0.598 ^c			162	128	270			35.180	-0.053
1/30/69	FP 17-11	220				Cr ^o rod exposed to fuel for 6.5 hr, 4.73 g dissolved (0.18 eq.)								35.165	-0.070
2/6/69	FP 17-12	374	11.50	6.58	10.71	0.820	0.815	70.09	99.74	148	78	60	145	35.116	-0.118
2/8/69	FP 17-13-16					50 g samples for mass spectrometric analysis								0.38	1.70
2/10/69	FV 17-17G					Freeze valve capsule - gas sample									
2/12/69	FP 17-18	467	11.60	6.90	11.14	0.819	0.820	67.63	98.13	163	70	54	156	35.087	-0.148
2/19/69	FP 17-19	543	11.40	7.00	11.12	0.819	0.817	68.50	98.88	125	70	56	156	35.063	-0.172
2/26/69	FP 17-20	698	11.30	6.92	10.86	0.818	0.817	69.03	98.97	143	63	54	145	35.014	-0.221
2/26/69	FP 17-21					Dumbbell shaped Ni rod exposed to fuel salt for 30 seconds								0.72	1.36
2/31/69	FV 17-22S	818				Freeze valve capsule - salt sample								34.976	-0.258
3/5/69	FP 17-23	839	11.60	6.75	10.60	0.817	0.814		132	70	58	132	34.969	-0.265	
3/13/69	FP 17-24	921	11.50	6.64	10.62	0.816	0.816		136	76	40	144	34.943	-0.291	
3/17/69	FV 17-25G					Freeze valve capsule - gas sample								0.95	1.13
3/17/69	FP 17-26	1006				50 g sample for determination of $U^{3+}/\Sigma U$ concentration								1.04	0.69
3/19/69	FP 17-27	1048	11.50	6.72	11.03	0.815	0.806		98	70	77	141	34.903	-0.331	
3/26/69	FP 17-28	1147	11.93	6.82	11.56	0.814	0.805		147	71	33	159	34.872	-0.362	
3/26/69	FV 17-29S	1171				Freeze valve capsule-salt sample								34.864	-0.370
4/1/69	FP 17-30	1292	11.40	7.01	11.09	0.813	0.817	68.60	98.96	148	69	34	148	34.826	-0.408
4/2/69	FV 17-31S		10.40	7.24	7.69	0.813	0.972							1.33	0.75
4/3/69	FV 17-32S	1340				Freeze valve capsule - salt sample								34.811	-0.423
4/4/69	FV 17-33G					Freeze valve capsule - gas sample								1.38	0.70
4/7-8/69	FP 17-34-40					50 g samples for mass spectrometric analysis								0.50	0.47
4/9/69	Run 17-F	1538												34.748	-0.486
4/14/69	Run 18-I	1538												1.58	0.50

Table 3.1 (continued)

Date	Sample	Equiv. Full Power Hr	(Weight %)				(ppm)				Σ U in Circula- tion	Δ U (kg)	Σ Eq. Oxida- tion	Σ Eq. Reduc- tion	$[\text{U}^{3+}/\Sigma \text{U}]$ % Nom.			
			Li	Be	Zr	U Nom.	U Obs.	F	Σ	Fe	Cr	Ni	Pu					
4/14/69	FP 18-1	1538	11.30	6.50	10.65	0.812	0.800	66.50	95.78	151	86	53	157	34.787	-0.486	1.58	0.50	0.34
4/14/69	FV 18-2S	1538	11.36	6.70	14.16	0.812	0.897			Nb: 42%				34.787	-0.486	1.58	0.50	0.34
4/18/69	FP 18-3	1564	Zr rod exposed to fuel for hr; 20.24 g dissolved (0.89 eq.)											34.779	-0.494	2.61	1.36	0.91
4/19/69	FV 18-4S	1565	10.50	6.62	13.82	0.812	0.861							34.779	-0.494	2.61	1.36	0.91
4/18/69	FDE-A																	
4/22/69	FDE-B		9.50	5.14	17.68									0.179%	2.73%	0.037%		
4/23/69	FDE-C		5.49	5.67	13.39									0.510%	1.61%	0.227%		
4/23/69	FP 18-5	1718	11.35	6.53	11.41	0.811	0.805	69.10	99.23	100	77	50	156	34.730	-0.543	2.77	1.20	0.81
4/23/69	FV 18-6S		6.28	6.19	9.34	0.811	0.755											
4/25/69	FP 18-7	1766	Zr Rods exposed to fuel: 24.04 g dissolved (1.05 eq.)											34.715	-0.558	2.25	1.77	1.18
4/26/69	FP 18-8		50 g sample for isotopic analyses															
4/29/69	FP 18-9		50 g sample for isotopic analyses															
4/29/69	FP 18-10	1855	11.50	6.38	11.18	0.810	0.826	69.40	99.32	119	79	44	139	34.687	-0.586	1.91	2.11	1.41
4/30/69	FP 18-11		Empty Ni cage, exposed to salt for 10 hours															
5/2/69	FP 18-12S		9.61															
5/5/69	FP 18-13	1979	10.50	6.21	10.95	0.809	0.781	69.80	98.28	119	65	50	147	34.648	-0.625	2.04	1.98	1.33
5/6/69	FV 18-14G		Freeze valve capsule - gas sample															
5/6/69	FV 18-15G		Freeze valve capsule - gas sample															
5/8/69	FP 18-16	2044	50 g sample for $\text{U}^{3+}/\Sigma \text{U}$ analysis. $\text{U}^{3+}/\Sigma \text{U} = 0.4\%$											34.627	-0.646	2.10	1.92	1.28
5/8/69	FP 18-17		30 g FeF_2 added to pump bowl. (0.64 oxidation equiv.).															
5/9/69	FP 18-18		Interfacial tension measurement												2.74	1.28	0.86	
5/9/69	FP 18-19S		7.16	10.61	0.672													
5/12/69	FP 18-20		Cu cage exposed to fuel salt for 10 hr.															
5/13/60	FV 18-21G		Freeze valve capsule - gas sample															
5/14/69	FP 18-22	2224	11.23	6.89	11.32	0.807	0.804	70.10	100.38	107	65	33	154	34.570	-0.703	2.93	1.09	0.73
5/15/69	FP 18-23	2248	Be addition: 5.68 g as rod (1.26 eq)											34.563	-0.710	2.95	2.33	1.57
5/17/69	FP 18-24		Interfacial tension measurement															
5/17/69	FV 18-25G		Freeze valve capsule - gas sample															
5/17/69	FV 18-26G		Freeze valve capsule - gas sample															
5/19/69	FP 18-26		Fission product deposition sampler (liquid phase test), 1 hr. exposure															
5/20/69	FP 18-27	2344	10.50	7.10	10.82	0.807	0.799	68.20	97.46	149	79	33	133	34.436	-0.740	3.05	2.23	1.51
5/20/69	FP 18-28	2344	Interfacial tension measurement - Be^0 present in sampler (3.17 g; 0.704 eq)											34.532	-0.740	3.05		
5/21/69	FV 18-29G		Freeze valve capsule - gas sample															
5/21/69	FP 18-30		50 g sample for isotopic analyses (48.1 g obtained)															
5/22/69	FP 18-31		50 g sample for isotopic analyses (41.7 g obtained)															
5/22/69	FP 18-32		50 g sample for isotopic analyses (36.5 g obtained)															
5/23/69	FP 18-33		50 g sample for isotopic analyses (44.1 g obtained)															
5/23/69	FP 18-34		50 g sample for isotopic analyses (40.4 g obtained)															
5/23/69	FP 18-35		50 g sample for isotopic analyses (37.4 g obtained)															
5/26/69	FP 18-36		50 g sample for isotopic analyses (42.6 g obtained)															
5/26/69	FP 18-37		50 g sample for isotopic analyses (42.0 g obtained)															
5/27/69	FP 18-38		50 g sample for isotopic analyses (41.0 g obtained)															
5/27/69	FP 18-39		50 g sample for isotopic analyses (39.7 g obtained)															
5/27/69	FP 18-40		50 g sample for isotopic analyses (44.5 g obtained)															
5/27/69	FP 18-41		50 g sample for isotopic analyses (41.3 g obtained)															
5/28/69	FV 18-42G		Freeze valve capsule - gas sample															
5/28/69	FP 18-43	2464	10.40	5.92	10.40	0.806	0.791	70.60	98.16	199	72	38	153	34.495	-0.778	3.17		

Table 3.1 (continued)

Date	Sample	Equiv. Full Power hr	(Weight %)				(ppm)				Σ U in Circula-tion	Δ U (kg)	Σ Eq. Oxida-tion	Σ Eq. Reduc-tion	$[U^{3+}/\Sigma U]$ % Nom.	
			Li	Be	Zr	U	F	Σ	Fe	Cr	Ni	Pu				
			Nom.	Obs.												
5/29/69	FV 18-44G															
6/1/69	FV 18-45G															
6/1/69	FV 18-46G															
6/6/69	Run 18-F	2547				0.805										
8/11/69	Run 19-I	2547				0.802										
8/16/69	FP 19-8	2547	10.50	6.12	10.90	0.802	0.850	78.5	106.82	186	78	92	181a 126n	34.360	-0.805	
8/18/69	FV 19-9S										66	Nb:	34%			
8/19/69	FP 19-10															
8/19/69	FP 19-11															
8/21/69	FV 19-12	2547														
8/21/69	FP 19-13G															
8/21/69	FP 19-14G															
8/21/69	FP 19-15G															
8/21/69	FP 19-16G															
8/27/69	FP 19-17	2629	11.0	5.69	10.94	0.809	0.811	72.2	100.68	221	83	48	117a 98n	34.626	-0.830	
8/28/69	FP 19-18	2646	11.4	5.85	11.01	0.809	0.797	68.0	97.09	197	75	42	124	34.621	-0.836	
9/4/69	FV 19-19G															
9/4/69	FV 19-20G															
9/5/69	FP 19-21	2727	10.90	7.20	11.20	0.808	0.795	69.80	99.92	177	89	15	98	34.595	-0.861	
9/9/69	FP 19-22	2793	10.95	6.92	11.30	0.807	0.799	68.50	98.50	147	87	20	104	34.575	-0.882	
9/10/69	FV 19-23G															
9/10/69	FV 19-24S															
9/12/69	FP 19-25															
9/19/69	FP 19-26															
9/19/69	FP 19-27	2793	10.70	7.12	10.80	0.807	0.792	70.10	99.55	183	96	50	144	34.575	-0.882	
9/23/69	FV 19-28G															
9/23/69	FV 19-29G															
9/24/69	FP 19-30		10.70	7.38	10.90	0.807	0.781	66.30	96.10	227	97	48	142			
9/24/69	FP 19-31															
9/25/69	FP 19-32															
9/25/69	FP 19-33															
9/26/69	FP 19-34															
9/29/69	FP 19-35	2968	10.75	7.07	11.10	0.806	0.775	69.00	98.73	214	97	52	165a 161n	34.519	-0.938	
9/29/69	FV 19-36S										97	Nb:		(0.18) ^g	0.71	0.48
9/30/69	FV 19-37G	2992												34.512	-0.945	(0.21) 0.68 0.46
9/30/69	FV 19-38G	2992														
10/1/69	FP 19-39															
10/2/69	FP 19-40	3040														
10/2/69	FP 19-40															
10/3/69	FP 19-41G															
10/3/69	FP 19-42S															
10/5/69	FP 19-43	3106	10.60	6.61	11.40	0.805	0.767	71.70		183	96	45	165	34.476	-0.981	(0.32) 1.21 0.82
10/6/69	FP 19-44S															
10/6/69	FP 19-45	3130	50 g for $U^{3+}/\Sigma U$											34.468	-0.989	(0.35) 1.18 0.79
10/7/69	FV 19-46G															
10/7/69	FV 19-47S	3154														

developed by correction

Table 3.1 (continued)

Date	Sample	Equiv. Full Power Hr	(Weight %)				(ppm)				EU in Circula- tion	ΔU (kg)	Σ Eq. Oxida- tion	Σ Eq. Reduc- tion	[U ³⁺ /EU] %					
			Li	Be	Zr	U	F	Σ	Fe	Cr	Ni	Pu								
			Nom.	Obs.																
10/8/69	FP 19-48	3178	Be addition: 4.91 g as rod (1.09 eq.)				8.58 6.95 14.7 0.804 0.849 (65.11)				0.21%	3.53%	0.07%	161	34.461	-0.996	(0.37)	2.25	1.52	
10/9/69	FP 19-49		Graphite assembly exposed to pump bowl vapor												34.453	-1.004	(0.40)	2.22	1.50	
10/9/69	FP 19-50		Graphite assembly exposed to pump bowl salt																	
10/9/69	FP 19-51		Graphite assembly exposed to pump bowl salt																	
10/13/69	FP 19-52		Copper rod exposed to pump bowl salt																	
10/13/69	FP 19-53	3321	11.48	6.79	11.60	0.804	0.786	68.50	235	102	40	164	34.411	-1.049	(0.54)	2.08	1.41			
10/14/69	FV 19-54G		Freeze valve capsule - gas sample																	
10/14/69	FV 19-55S		Freeze valve capsule - salt sample																	
10/15/69	FV 19-56G		Freeze valve capsule - gas sample																	
10/17/69	FV 19-57S		Freeze valve capsule - salt sample																	
10/17/69	FV 19-58S		Gas sample taken 1 hr after reduction of power to 10 kw																	
10/18/69	FV 19-59S		Gas sample taken 4 hr after reduction of power to 10 kw																	
10/20/69	FP 19-60	3458	50 g sample for U ³⁺ /EU analysis; U ³⁺ /EU = 0.07%											34.365	-1.092	(0.68)	1.94	1.31		
10/21/69	FP 19-61		Nb foil exposed to fuel salt 45 min																	
10/22/69	FV 19-62G		Gas sample with intake port at bottom																	
10/22/69	FP 19-63	3506	11.25	6.78	10.90	0.802	0.802	70.0	99.78	136	95	33	173	34.350	-1.107	(0.73)	1.89	1.29		
10/22/69	FV 19-64G		Freeze valve capsule - gas sample																	
10/23/69	FV 19-65G		Capsule for FP plating experiment - 10 hr exposure																	
10/24/69	FP 19-66		Capsule for FP plating experiment - 3 hr exposure																	
10/24/69	FP 19-67		Capsule for FP plating experiment - 10 min exposure																	
10/27/69	FP 19-68		50 g sample for oxide analysis; sample not removable from transport container.				34.311								-1.146	(0.86)	1.76	1.20		
10/28/69	FP 19-69	3627	50 g sample for oxide analysis; sample not removable from transport container.				34.311													
10/28/69	FV 19-70G		Gas sample with intake port at top																	
10/28/69	FP 19-71		50 g sample for hot cell tests																	
10/29/69	FP 19-72		50 g sample for hot cell tests																	
10/29/69	FV 19-73G																			
10/30/69	FP 19-74	3698	11.20	7.31	10.70	0.801	0.796	69.30	99.35	124	101	20	168	34.289	-1.168	(0.93)	1.69	1.15		
10/30/69	FP 19-75		50 g sample for U ³⁺ /EU analysis; U ³⁺ /EU = 0.02%																	
10/31/69	FV 19-76S		Freeze valve capsule - salt sample																	
10/31/69	FV 19-77S		Freeze valve capsule - salt sample																	
11/2/69	FP 19-78G		Gas sample obtained 1 hr after drain																	
	Run 19-F	3777													34.267	-1.193	(1.01)	1.61	1.10	
11/26/69	FV 20-1S		0.800 0.784												34.274	-1.193	-	-	0	
11/26/69	FP 20-2	3777	Surface tension experiment - control sample, 2 hr exposure				7LiF-233UF ₄ addition U = 97.2 g													
11/27/69	FP 20-3		50 g sample for oxide determination: 58 ppm												34.371	-1.201				
11/27/69	FP 20-4		Sample for U ³⁺ /EU analysis by spectrophotometric method																	
11/28/69	FP 20-5																			
11/28/69	FP 20-6	3825	10.00	7.19	10.90	0.802	0.783	72.80	101.71	199	98	72	117	34.356	-1.208		0.15	0.1		
11/29/69	FP 20-7	3849	Be addition: 6.974 as rod (1.55 eq.)				9.92	7.42	11.95	0.803	0.799	--	0.17%	1.88%	0.04%					
	White Salt														0.10%	6.44%	0.047%			
	Dark Crust																			
11/30/69	FP 20-8		CuO-Ni assembly exposed to fuel pump vapor 8 hr				Freeze valve capsule - gas sample													
12/1/69	FP 20-9G		Ni powder in Ni capsule, exposed to fuel pump vapor 8 hr				Electron microscope screen assembly, exposed to fuel pump vapor 2 hr				Freeze valve capsule - gas sample									
12/1/69	FP 20-10																			
12/2/69	FP 20-11																			
12/2/69	FP 20-12G																			
12/3/69	FP 20-13		Ni rod, exposed to fuel pump vapor 8 hr																	

Table 3.1 (continued)

Date	Sample	Equiv. Full power Hr	(Weight %)			(ppm)					Σ U in Circula- tion	Δ U (kg)	Σ Eq. Oxida- tion	Σ Eq. Reduc- tion	$[\text{U}^{3+}/\text{EU}]$ % Nom.		
			Li	Be	Zr	U	F	Σ	Fe	Cr							
			Nom.	Obs.													
12/3/69	FP 20-14					50 g sample for U^{3+}/EU analysis: 0.11%											
12/3/69	FP 20-15					Sample for U^{3+}/EU analysis by spectrophotometric method											
12/4/69	FP 20-16					CuO-Ni assembly exposed to fuel pump vapor 8 hr											
12/4/69	FP 20-17					CuO-Ni assembly exposed to fuel pump vapor 8 hr											
12/4/69	FP 20-18					$^7\text{LiF}-^{233}\text{UF}_4$ addition, U: 92 g											
12/5/69	FP 20-19S					Freeze valve capsule - salt sample											
12/5/69	FP 20-20					Ni bar exposed to fuel pump 8 hr											
12/8/69	FP 20-21					CuO-Ni assembly exposed to fuel pump salt 8 hr											
12/9/69	FP 20-22	4093				Be addition; 9.874 g as rod (2.19 eq.)						34.271	-1.293	(0.25)	3.54	2.41	
12/9/69	FP 20-23					Surface tension experiment, with Be^0 , 4 hr exposure											
12/9/69	FP 20-24					Sample for U^{3+}/EU analysis by spectrophotometric method. ^h											
12/10/69	FP 20-25					Ni bar exposed to fuel pump vapor 8 hr											
12/10/69	FP 20-26					50 g sample for U^{3+}/EU analysis; $\text{U}^{3+}/\text{EU} = 0.20\%$											
12/10/69	FP 20-27G					Freeze valve capsule - gas sample											
12/10/69	FP 20-28					CuO-Ni assembly exposed to fuel pump salt 8 hr											
12/11/69	FP 20-29					CuO-Ni assembly with Pd windows exposed to pump bowl vapor 8 hr											
12/11/69	FP 20-30	4140				Sample for U^{3+}/EU analysis by spectrophotometric method						34.256	-1.308	(0.30)	3.49	2.37	
12/12/69	FP 20-31	4165				10.80 6.80 10.90 0.800 0.801 71.60 101.03 265 92						160	34.249	-1.316	(0.33)	3.46	2.35
12/12/69	FP 20-32G					Obtained 1 hr after fuel drain											
12/12/69	Run 20-F	4167				0.800							34.249	-1.316	(0.33)	3.46	2.35

*Analyzed after storage for 30 hr at room temperature.

a MSRP Semiann. Prog. Rept. for P/E Feb. 28, 1967, ORNL-4119, p 156.

b MSRP Semiann. Prog. Rept. for P/E Aug. 31, 1967, ORNL-4191, p. 168.

c R. E. Thoma and J. M. Dale, ORNL-4396, Feb. 28, 1969, p. 134.

d 0.819 kg U added; sample addition capsules not designated by FP-numbers

e Samples removed from the fuel storage tank

f 50 g sample for determination of uranium concentration by fluorination.

g Increase in oxidation equivalents after FP 19-26. ORNL-4548, p 180

h Sample was not usable for U^{3+}/EU analysis. Oxide concentration determined to be 71 ppm.

maintained throughout the entire period of reactor operations with the MSRE. All salt, metal, and gas specimens removed from or introduced into the fuel system were assigned sample designation numbers. Analytical data obtained with these specimens are summarized in Table 3.1, which will serve as the basis for the discussion in the remainder of this section.

3.2 Component Analysis

As soon as a statistically significant number of fuel-salt samples were obtained it became evident that the average variation in the analytical values for the components Li, Be, Zr, and F within one standard unit of deviation (1σ) would preclude the use of the results of chemical analyses for these components for operational control of the reactor. Of special interest in this connection is the component zirconium. It might seem that if reduction in the concentration of zirconium in the salt were detectable analytically, such reduction would signal that the oxide saturation limit was exceeded. However, assuming that the salt was originally completely free of oxide and that the solubility limit is ~700 ppm at 650°C, the fuel salt could accommodate 0.34 kg of oxide before it became saturated. If the source of the oxide was from moisture, saturation by oxide would correspond to complete reaction of 0.23 kg of HF with the containment vessel, from which 0.29 kg of Cr would be leached into the salt, increasing its concentration there by 59 ppm. It is thus evident that unless highly sensitive techniques were available for measuring the oxide concentration of the salt introduced from contamination of the salt by moisture, the initial indication of such contamination would be the increase of chromium. The 1σ sensitivity limit for zirconium corresponds to $\pm 0.24\%$, which corresponds to 1.75 kg of ZrO_2 . Although the solubility of ZrO_2 in the fuel salt is sufficiently temperature dependent to expect that on saturating the molten-salt solution with oxide and that further formation of oxide would result in the deposition of oxide crystals at the coldest point in the circuit, it has not been established experimentally that, with rapidly circulated streams, such crystal growth would actually occur. If not, significant amounts of zirconium might be carried in the salt in slurry form and an analysis of samples removed from the pump bowl would not signify a loss of zirconium from the salt as one might expect otherwise. It is thus clear that by the time it would have been possible to establish from zirconium analysis that the 1σ limit had been exceeded, at least 1.41 kg of ZrO_2 would have been precipitated and probably

carried by the salt as a slurry. Since, of all the fuel salt constituents, zirconium is the one whose reduction in concentration would independently reflect increasing amounts of oxide impurity, only perfunctory attention was given to the precision of the analyses of the carrier constituents. Analysis of these constituents was continued on a routine basis because of their use in providing general confirmation of the inference that the fuel was chemically stable and because the principal analytical costs were incurred from operations related to handling and processing the radioactive samples; laboratory tests which followed dissolution of the salts for analysis comprised a minor fraction of the overall charges. Mean values of the MSRE fuel-salt composition as determined from analysis of samples removed from the pump bowl are given in Table 3.2.

3.3 Oxide Analysis

Until the chemical equilibria involving H_2 , HF, and oxides in $LiF-BeF_2$ melts were defined completely,⁴ no satisfactory analytical method existed for determination of oxide in MSRE salts. The $KBrF_4$ method,⁵ while occasionally satisfactory, produced results that reflected the frequent contamination of samples after they were removed from the reactor by quantities of water adsorbed in transit and during storage, and were for the most part generally incredibly large and erratic.

Subsequently, an improved method of analysis was developed⁶ based on the equilibrium $O^{2-} + 2HF(g) \rightleftharpoons H_2O(g) + 2F^-$, which occurs when a molten-salt sample is purged with an HF- H_2 gas mixture. Although this hydrofluorination method was regarded as less sensitive than the inert-gas fusion method⁷ or the $KBrF_4$ method, satisfactory sensitivity was achieved by ~50-g samples. After development, only this method was used for analysis of MSRE salt samples. During the period when the MSRE was in operation it was important to know the approximate concentration of oxides in the fuel and coolant salts, but the information was not considered to be particularly relevant to a need to develop highly sensitive in-line analytical methods for reactors in which on-line fuel reprocessing is done. This arises from the fact that on-line reprocessing methods are likely to employ chemical processes in which, for rare earth removal, there is a complete turnaround in the uranium inventory. If this is done, the turnaround will be accomplished by fluorination, and the reconstituted stream will be adjusted in uranium (IV, III) concentration.

The fuel-salt mixtures which are most suited for use in breeder or converter systems employ a fertile carrier

Table 3.2. Mean values of the MSRE fuel composition from chemical analysis

Sample Group	No. of Samples	L1	Be	Zr (wt %)	U	F	LiF	BeF ₂ (mole %)	ZrF ₄	UF ₄	Cr	Fe	Ni (ppm)	Nom. Aver. Wt % U
Carrier ^a	36	10.79±0.33	7.25±0.18	11.93±0.31	-	70.17±0.62	62.24±0.90	32.48±0.90	5.28±0.16	22±5	102±54	14±9		
Run 2 ^a	8	10.44±0.19	6.79±0.31	11.26±0.13	3.04±0.02	67.50±0.62	62.84±1.08	31.46±1.12	5.16±0.11	0.54±0.01	19±8	98±51	23±3	3.038
Run 2	10	10.39±0.17	6.44±0.02	11.43±0.34	3.05±0.02	71.65±0.80	63.72±0.43	30.40±0.44	5.33±0.14	0.55±0.01	37±13	163±49	34±11	3.038
Run 3	51	10.45±0.21	6.49±0.21	11.22±0.35	3.98±0.71	69.80±1.72	63.46±0.83	30.60±0.84	5.23±0.17	0.71±0.12	37±8	154±55	48±19	
Run 4	22	10.51±0.14	6.55±0.16	11.14±0.30	4.642±0.028	67.17±1.44	63.36±0.57	30.65±0.58	5.15±0.12	0.83±0.01	48±7	131±65	40±20	4.648
Run 5-7	14	10.52±0.28	6.54±0.19	11.32±0.23	4.629±0.026	68.72±0.86	63.36±1.03	30.58±0.91	5.23±0.14	0.824±0.013	50±7	108±44	54±25	4.627
Run 4-7	47	10.52±0.18	6.57±0.18	11.24±0.27	4.638±0.025	67.96±1.36	63.29±0.72	30.70±0.70	5.19±0.13	0.824±0.011	49±7	114±55	46±21	
Run 8	8	11.78±1.41	6.53±0.20	11.16±0.19	4.632±0.011	69.77±1.49	65.84±2.49	28.57±2.12	4.82±0.35	0.771±0.058	64±7	122±45	61±36	4.605
Run 9	4	10.99±0.10	6.63±0.07	11.15±0.37	4.603±0.031	68.55±0.48	64.17±0.10	30.04±0.15	4.99±0.19	0.794±0.011	61±5	150±17	52±20	4.587
Run 10	10	11.14±0.08	6.58±0.19	11.05±0.15	4.609±0.020	67.82±1.38	64.65±0.45	29.64±0.48	4.92±0.06	0.791±0.010	60±4	150±30	74±35	4.567
Run 11A	31	10.80±0.35	6.46±0.15	10.97±0.18	4.570±0.018	67.81±1.46	64.30±0.90	29.88±0.82	5.02±0.13	0.804±0.018	64±6	131±48	54±16	4.557
Run 11B	6	10.89±0.36	6.53±0.09	10.97±0.17	4.579±0.023	68.94±1.66	64.27±1.00	29.96±0.85	4.97±0.14	0.799±0.017	64±11	144±46	54±18	4.565
Run 11	38	10.82±0.35	6.47±0.15	10.97±0.17	4.571±0.019	67.99±1.53	64.30±0.90	29.89±0.81	5.01±0.13	0.803±0.018	64±7	133±47	54±16	
Run 10-11A	41	10.89±0.34	6.49±0.17	11.00±0.17	4.580±0.024	67.83±1.43	64.34±0.82	29.81±0.76	4.99±0.13	0.801±0.017	63±6	136±45	59±24	
Run 10-11	48	10.88±0.34	6.49±0.16	10.99±0.17	4.579±0.024	67.95±1.47	64.37±0.83	29.84±0.76	4.99±0.13	0.801±0.017	63±7	136±44	58±23	
Run 12-A	15	11.00±0.45	6.50±0.18	10.75±0.21	4.544±0.023	66.79±1.10	64.65±0.96	29.70±0.90	4.85±0.13	0.790±0.020	71±9	166±54	61±11	4.535
Run 12-B	11	10.85±0.32	6.54±0.11	10.82±0.29	4.570±0.028	66.10±0.90	64.21±0.57	30.08±0.49	4.92±0.14	0.800±0.017	69±8	139±26	226±209	4.571
Run 12	26	10.93±0.40	6.52±0.15	10.78±0.24	4.555±0.027	66.50±1.06	64.46±0.83	29.86±0.77	4.88±0.14	0.794±0.021	70±9	154±46	110±?	
Run 13-14A	24	10.65±0.20	6.28±0.28	11.10±0.21	4.561±0.024	66.27±0.52	64.51±0.74	29.51±0.80	5.16±0.14	0.817±0.017	63±6	125±22	68±15	
Run 14B	20	10.35±0.28	6.39±0.16	10.91±0.24	4.523±0.030	66.49±0.32	63.55±0.92	30.48±0.86	5.15±0.14	0.821±0.012	82±7	121±14?	62±14	
Run 14	44	10.51±0.28	6.33±0.24	11.01±0.24	4.543±0.032	66.37±0.45	64.07±0.95	29.95±0.95	5.15±0.13	0.819±0.015	77±8	123±43	65±15	4.548
Run 4-14	176	10.75±0.50	6.48±0.21	11.04±0.27	4.585±0.046	67.44±1.49	64.09±1.11	30.05±1.00	5.06±0.19	0.809±0.024	64±13	130±45	67±67	
Run 16-18	21	11.33±0.39	6.71±0.30	10.99±0.29	0.809±0.011	68.71±1.26	65.08±0.91	29.93±0.93	4.85±0.14	0.137±0.004	72±9	135±24	49±12	0.8155
Run 19	11	10.95±0.34	6.83±0.48	11.08±0.27	0.791±0.013	69.40±1.66	63.94±1.67	30.96±1.74	4.97±0.18	0.137±0.005	93±8	186±38	38±13	0.8045
Run 19-20	13	10.86±0.40	6.85±0.45	11.05±0.26	0.791±0.012	69.83±1.86	63.68±1.75	31.21±1.79	4.97±0.17	0.137±0.005	93±8	193±41	41±16	
Run 16-20	33	11.14±0.45	6.76±0.37	11.02±0.28	0.802±0.015	69.18±1.60	64.53±1.46	30.43±1.46	4.90±0.16	0.137±0.004	80±14	157±43	46±14	
Run 2-20	258	10.79±0.50	6.53±0.25	11.05±0.28	3.881±1.462	67.87±1.65	64.10±1.24	30.16±1.08	5.05±0.19	0.685±0.261	62±17	136±58	62±58	

^a Analyses from the General Analysis Lab., all others from the HRLAL.

salt of the approximate composition $^7\text{LiF}-\text{BeF}_2-\text{ThF}_4$ (72-16-12 mole %). It has been deduced recently that in uraniferous fuel salts constituted from this base, the oxide tolerance at operating temperatures is in the range 30 to 70 ppm.⁸ Although there is no need for incorporation of an oxygen getter, such as ZrF_4 , in the salt directly, this low oxide tolerance indicates that there will be a need for swift, satisfactory, and preferably in-line methods for determination of O^{2-} (and UF_3) concentrations in the fuel after storage and during startup and operation. Further, it will be necessary to incorporate a demonstrated continuous process for removal of O^{2-} to a satisfactorily low level from a substantial side stream from the reactor. The results listed in Table 3.1 show that the concentration

of oxide never exceeded ~10% of saturation and were thus regarded, along with the corrosion data, as satisfactory evidence that the fuel system did not experience contamination during periods when fuel was circulated in it. Other material pertinent to this discussion is described in Chap. 6, concerning corrosion and anomalies in the behavior of UF_3 .

3.4 Uranium Concentration

One of the purposes of the Molten-Salt Reactor Experiment was to examine the applicability of various techniques for rapid, accurate, reliable means of establishing the inventory of uranium in the fuel-salt system. We projected that the experience gained with the MSRE

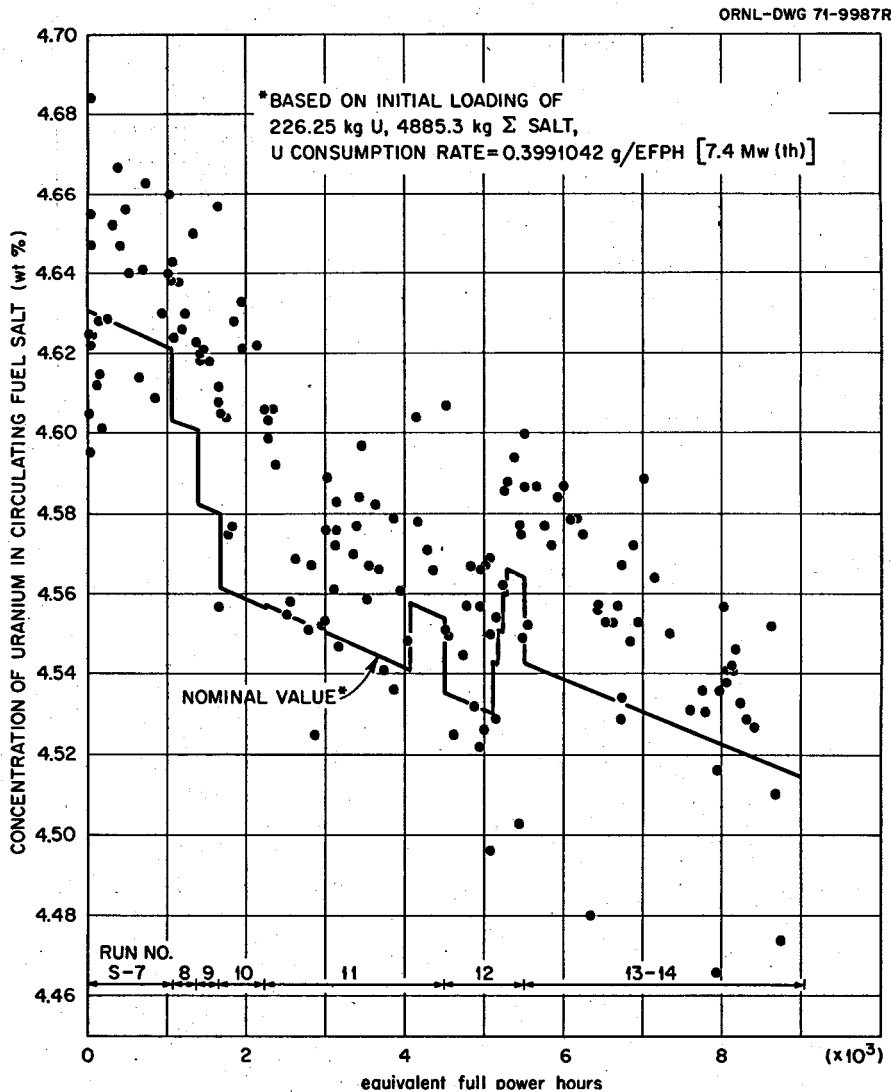


Fig. 3.1. Comparison of analytical and computed values of uranium in the MSRE fuel salt (^{235}U and ^{238}U fuel charge).

would fix the alternatives to be explored for the development of larger molten-salt reactors. When it was noted early in MSRE power operations that the sensitivity of on-site determination of uranium concentration coefficient in the reactivity balance was some tenfold greater than the statistical variation in chemical analysis, further consideration of the applicability of laboratory analysis of individual samples for operational control was abandoned.

Other sections of this report discuss uranium burnup rates (Chap. 7), fissile inventory (Sect. 2.4.2), and material balances (Sects. 3.6 and 3.7), the results of which led to the final estimates of the concentrations of uranium in the fuel salt as listed in Table 3.1. After final adjustments in the estimated amounts of salts contained in the reactor system and of the power

production rates, comparisons of the analytical data for uranium concentration were made with the nominal values for ^{235}U and ^{233}U fuel, respectively, in Figs. 3.1 and 3.2. It is evident in Fig. 3.1 that the analytical data contain a small positive bias in reference to nominal values. The bias is of little consequence, for with the average uranium inventory a difference in the estimated carrier salt mass of 1 kg changes the nominal concentration of uranium by 0.01 wt %.

3.5 Structural Metal Impurities

In the development of molten-salt reactor technology, continually recurring needs for accurate values of the properties of moving fluids become apparent. Consequences of ever increasing amounts of structural metal

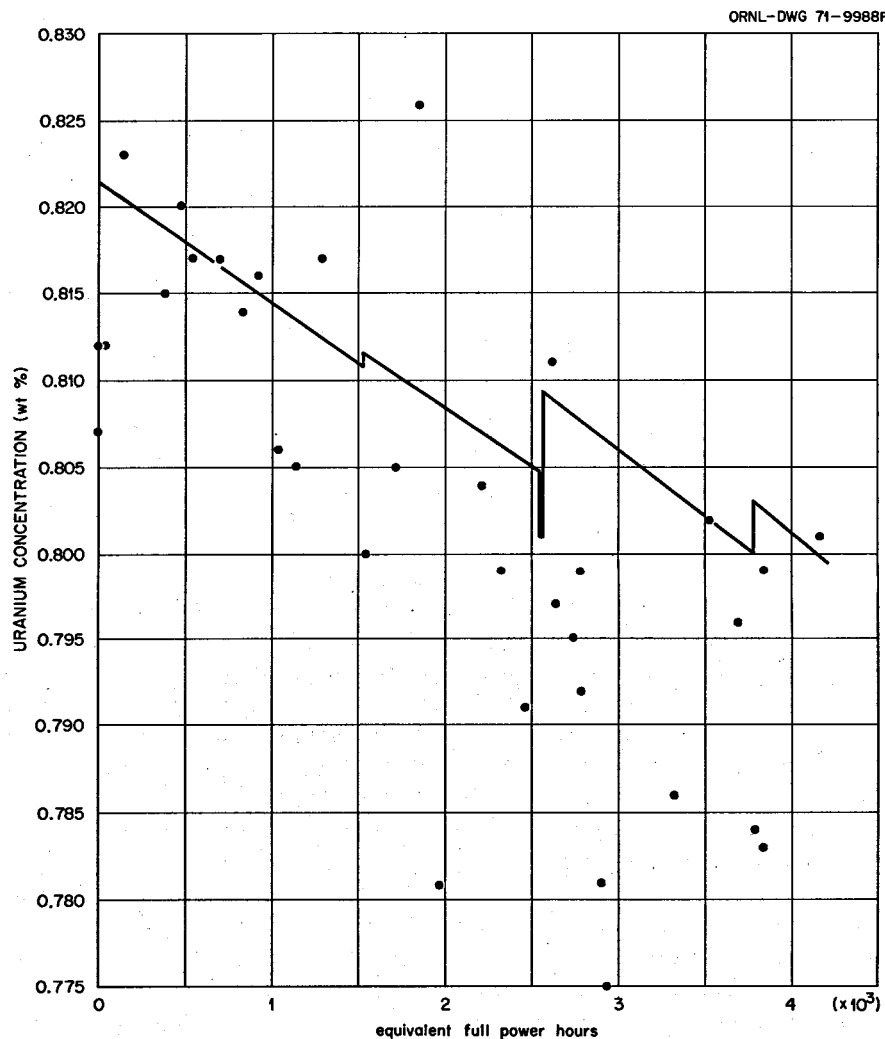


Fig. 3.2. Concentration of uranium (^{233}U) in the MSRE fuel circuit.

impurities that might be generated in the MSRE and that might alter the properties of the flowing salt streams into which they were released were envisioned at the outset of operations. With the possibility that impurities would exist both as ionic and metallic species, it was desirable to examine the interrelationships of their development with respect to corrosion of the container circuits, fission product transport, cavitation effects, changes in the flow characteristics, and their impact on MSBR reprocessing capability. Since all but the initial aspect of this behavior comprises an ongoing effort, the scope of the present report includes consideration of structural metal impurities in the MSRE only with respect to the implication of changes in their concentration as related to corrosion. Specific discussion of the chemical significance of the amounts of impurities and changes in the concentrations is deferred for consideration under Sects. 5 and 6, in which corrosion in the fuel and coolant circuits is discussed, and for subsequent reports where the relationships of physical and chemical properties of the MSRE to metallurgical behavior and to fission product behavior are assessed.

Midway through the experiment, phenomena were observed that led to the speculation that changes in the surface-related properties of the impurities were of possible significance to the changes observed. It was not experimentally feasible at that time to utilize the reactor as the experimental tool for studies of the interfacial behavior in salt-metal systems. By the time that laboratory studies had advanced to the stage where a program of studies with the reactor could be formulated, the schedule for operation of the reactor called for its termination.

The combined experience from laboratory investigations and from an extensive engineering test program in which various fluoride mixtures were circulated in thermal convection and forced circulation loops led to the expectation that the concentration of structural metals in the MSRE salts would increase only slightly throughout the planned period of reactor operation. As anticipated, only modest increases occurred.

The MSRE fuel was produced, as described in Sect. 2.4, from carrier salt and fuel concentrate, for which the chemical analyses indicated average concentrations of impurities were quite low. Chemical analyses were performed with samples of fuel salt removed regularly from the fuel pump bowl, and occasionally from the fuel drain tank. The average concentrations of the structural metal impurities found in these samples are listed in Table 3.2. Individual analyses are listed in Table 3.1.

Table 3.3. Average concentration of structural metal impurities in the MSRE fuel salt

Sample group	Number of samples	Impurity concentration (ppm)			
		Cr	Fe	Ni	
Fuel concentrate					
Run No.					
2					
3	34	37 ± 7	148 ± 59	55 ± 18	
4	69	53 ± 8	122 ± 51	52 ± 27	
5-7	14	50 ± 7	108 ± 44	54 ± 25	
8	8	64 ± 7	122 ± 45	61 ± 36	
9-10					
11	38	64 ± 7	133 ± 47	54 ± 16	
12	18	72 ± 9	160 ± 52	85 ± 73	
13-14					
Early stages	24	73 ± 6	125 ± 22	68 ± 15	
Latter stages	20	82 ± 7	121 ± 24	62 ± 14	
Total	44	77 ± 8	123 ± 23	65 ± 15	
15					
16-18	21	72 ± 9	135 ± 24	49 ± 12	
19-20	13	93 ± 8	193 ± 41	41 ± 16	

The methods employed by the analytical chemists for determination of structural metal impurities were described previously.⁹ Each of the methods employed is capable of approximately the same precision. Yet, as shown by the results in Table 3.3, the experimental precision obtained was much better for chromium than for either iron or nickel. Corrosion reactions in the MSRE were expected to produce only CrF₂ as a dissolved species in the salts; iron, nickel, and molybdenum, if present, were expected to persist in the metallic species. The differences in observed standard deviations for the three elements suggest that behavior very similar to that anticipated did result. Inspection of the individual results in Table 3.1 shows that the relative concentrations of iron and nickel found among individual samples rarely were constant. This is a somewhat surprising result since the excellent mixing conditions which existed in the circulating salt should have been conducive for allowing these metals to produce equilibrium solid solution alloys. The possibility that the metal particles might have deposited from the salt also was expected but seemingly did not occur either during circulation or during storage. In retrospect, these observations are compatible with the early conclusion that the pure salt fluids do not wet metal surfaces and with the fact that the low viscosities of the fluoride mixtures enable thermal convection currents to maintain the fluids in well-mixed condition during storage. That thermal mixing occurs in these tanks was substantiated by the first composition analysis in PC-2. As

evidenced by the composition of a sample which was obtained from No. 2 drain tank shortly after ^7LiF - $^{238}\text{UF}_4$ was added to the carrier salt, virtually complete mixing of ^7LiF - UF_4 and carrier salt was achieved before intertank transfers were made to ensure homogenization. Comparably efficient mixing is also probably adequate to prevent settling of the very fine (below the limit of microscopic detection) metallic particles of iron and nickel in the drain tanks.

A quality control program was initiated by the Analytical Chemistry Division as chemical surveillance of the reactor salt began. The results of this survey showed that comparable accuracy and precision were achieved in the analysis of structural metal impurities in the salt samples.¹⁰ From the beginning, molybdenum was not detected in the samples. Its absence then and later was interpreted to signify that such corrosion as occurred in the reactor was essentially diffusion limited.

3.6 Chemical Effects of Reprocessing

The MSRE included a fuel processing plant for removal of oxides, if necessary, from the fuel, flush, and coolant salts. The plant was also intended for use in recovering uranium from the fuel and flush salts after termination of experiments with the MSRE. A detailed description of the methods, operating procedures, and components is given in the *MSRE Design and Operations Report*.¹¹ It proved to be unnecessary to repurify any of the salt charges in MSRE maintenance operations, although flush salt was repurified after its initial use and prior to nuclear operations in order to remove from the salt the oxides that it had accumulated during its initial use in the fuel system. As planned, the $^{235},^{238}\text{U}$ fuel salt was fluorinated in the chemical reprocessing plant after completion of experiments with ^{235}U fuel salt. Decision to utilize ^{233}U as fuel entailed not only fluorination of the ^{235}U salt but subsequent reduction of the structural metal impurities that enter the salt as it is fluorinated. Decision to reuse the carrier to constitute ^{233}U fuel made it exigent to remove metal particulates from the salt carrier before returning it to the fuel system. Procedures for reduction of the fluorides were evaluated and tested, and an optimum filter medium was selected.¹² A sintered metal filter was then designed¹³ and incorporated in the return line from the processing plant.

Flush salt was reprocessed first to remove the uranium it had accumulated in use (see Sect. 4.2). Following fluorination, the fuel was treated, as was the flush salt, to reduce the structural metal fluorides present in their metallic forms.

The amounts of uranium which were recovered from the fuel and flush salts were estimated from the increases in weights of the NaF absorbers in which UF_6 was collected. The actual weights of UF_6 were not measurable because fluorination of the salts in Hastelloy N processing vessels converted small amounts of molybdenum to its volatile fluorides, which were absorbed along with UF_6 on the sodium fluoride beds. The approximate amounts of molybdenum absorbed on these beds were estimated from the proportionate amounts of iron, chromium, and nickel that were dissolved into the flush and carrier salts after fluorination. Estimates of the weights of uranium recovered were then obtained by subtraction of the probable amounts of molybdenum absorbed from the total weights gained by the absorbers. In a summary of experience with the processing plant, Lindauer has estimated that the amounts of uranium recovered from the flush and fuel salts at this time were ~6.5 and 217.85 kg respectively.¹⁴ The sodium fluoride absorbers were subsequently delivered to the Goodyear Atomic Plant in Portsmouth, Ohio, where wet chemical procedures were used to recover the uranium charge from the NaF absorbers. The results of these efforts and their significance are discussed in Sect. 3.7.

The reprocessing procedures were notably successful in decontaminating the uranium charge from fission products. The only activity collected in any measurable amount on the absorbers with UF_6 was ^{95}Nb . None of the filled absorber vessels exceeded maximum permissible radiation levels; each vessel could be removed from the processing plant without protective shielding.

At termination of operations of the MSRE with ^{235}U fuel, the concentration of structural metal contaminants in the flush and fuel salts was scarcely greater than when they were first used. Fluorination of the salts in the processing plant increased the concentrations of chromium, iron, and nickel contaminants temporarily. On completion of reprocessing procedures, their concentrations were reduced once again to satisfactorily low values. Changes in these concentrations as a result of processing the salts are listed in Table 3.4.

For operation of the reactor with ^{233}U fuel, a charge of only about 40 kg of uranium was required as compared with the some 220 kg of uranium that was used during ^{235}U operations. In order to provide a sufficient volume of the fluid fuel mixture, the reactor was loaded with a supplementary charge of fuel carrier salt amounting to 129.9 kg.

Methods for removal of the lanthanide element fission products from the fuel streams of molten-salt reactors using reductive extraction techniques were not fully

Table 3.4. Structural metal fluoride concentrations^a

	Concentration (ppm)		
	Cr \pm 10	Fe \pm 40	Ni \pm 15
Flush salt^b			
In reactor system	76	150	52
Before fluorination	104		
After fluorination	133	210	516
After 10.8 hr of H ₂ sparging		No sample taken	
After 604 g of Zr and 9 hr of H ₂ sparging	100 ^c	174 ^c	50 ^c
After 1074 g of Zr and 25 hr of H ₂ sparging		No sample taken	
After filtration	76 ^c	141 ^c	26
Fuel salt^b			
In reactor system	85	130	60
Before fluorination	170	131	36
After fluorination	420	400	840
After 17.1 hr of H ₂ sparging	420 ^c	430 ^c	^d
After 33.5 hr of H ₂ sparging	420 ^c	400 ^c	520 ^c
After 51.1 hr of H ₂ sparging	460 ^c	380 ^c	180 ^c
After 5000 g of Zr and 24 hr of H ₂ sparging	100 ^c	110 ^c	<10 ^c
After 5100 g of Zr and 32 hr of H ₂ sparging		No sample taken	
After filtration	34	110	60

^aFrom R. B. Lindauer, *Processing of the MSRE Flush and Fuel Salts*, ORNL-TM-2578 (August 1969).

^bH₂ sparging times are cumulative.

^cFiltered sample.

^dContaminated sample.

developed until after the MSRE had operated for some time. Until then the most promising method for their separation was the high-temperature low-pressure distillation of fuel carriers after removal of uranium. Tests of this method with irradiated salt were scheduled to take place at the MSRE on completion of ²³⁵U operations after removal of uranium from the fuel salt. Approximately 48 liters of irradiated carrier salt was allocated for this experiment; when the charge was delivered, however, it was found that only a total of 12 liters was transferred. Partly because of this anomalous behavior and because of its importance in the evaluation of the reactor fuel inventory, a considerable effort was made to obtain an accurate measurement of the volume of salt remaining in the fuel storage tank.

At the beginning of ²³³U operations, samples of fuel salt were removed from the MSRE pump bowl and analyzed regularly by coulometric methods which had been applied previously and which were checked against standards on a routine basis. Their precision and accuracy is regarded to be $\sim \pm 0.5\%$. The results of these analyses were, on the average, greater than the nominal values by 0.008 wt %, $\sim 1\%$ of the nominal value, and indicated (disregarding precision limits for purposes of this calculation) that the net weight of the carrier salt during this period was 4639 kg rather than 4708 kg, or

that an additional mass of 69.0 kg (1.13 ft³) of salt, that is, a total of 2.99 ft³ of the original carrier salt, was not returned to the reactor to constitute the ²³³U fuel charge. In an attempt to support the conclusion that some 3.0 ft³ of carrier salt was left in the fuel storage tank, an isotopic dilution experiment was performed in April 1969, in which two samples of ⁶LiF (35 g) were added to this tank. Retrieval of samples from the tank using a windlass and 10-g sample ladles was subsequently successful in removing small amounts of salt (which incidentally were found to be encrusted with metal residues) only through repeated attempts. The total weight of ⁶LiF added was 66.28 g (15.8 g of ⁶Li). Prior to ⁶LiF addition the carrier salt was found by analysis to have an average ⁷Li/ Σ Li concentration of 99.9905 ± 0.0015 wt %. The samples recovered after the addition had a concentration of 99.914 ± 0.024 wt %,¹⁵ which would indicate that the volume of the salt is 3.0 ± 0.84 ft³. However, samples of the carrier salt delivered to the still-pot section of the distillation apparatus were found to have concentrations of ⁶Li/ Σ Li = 1.59 and 2.85 wt %, indicating that the ⁶LiF was not dispersed homogeneously in the storage tank but instead had dissolved preferentially in the salt fraction delivered to the still pot. Homogeneous dispersal would have resulted in a higher average ⁶Li concentration in

Table 3.5. Chemical composition of the MSRE carrier salt as indicated by chemical analysis

Specimen	Number of samples	Chemical composition (mole %)		
		LiF	BeF ₂	ZrF ₄
Carrier salt, as produced	36	62.24 ± 0.90	32.48 ± 0.90	5.28 ± 0.16
Carrier salt, assuming transfer of 13.93 kg Zr ^a		62.33	32.58	5.15
Runs 4–14, all samples	176	64.61 ± 1.12	30.29 ± 1.0	5.10 ± 0.19
Run 14 (only)	44	64.61 ± 0.95	30.20 ± 0.95	5.19 ± 0.13
Runs 17–20, all samples	33	64.53 ± 1.46	30.43 ± 1.46	4.90 ± 0.16

^aAssumption of the removal of 13.93 kg of zirconium from this salt permits comparison after its dilution by six flush-salt residues.

the sample recovered from the fuel storage tank, and a lesser volume of salt would have been computed from the results of the isotopic dilution analysis experiment. Thus, although its lower limit cannot be deduced unequivocally from the isotopic data, the volume of salt retained in the storage tank cannot have been as high as 3.84 ft³.

The efforts to obtain samples from the storage tank provided additional information that allows a separate estimate of the salt volume. Sometimes small quantities of salt were obtained, sometimes none. If this is interpreted to mean that the salt level was at the point in the dished head directly below the samplers, the pool contained ~3.0 ft³ of salt. Assuming that the storage tank contained 3.0 ft³ of salt rather than 1.13 ft³ used before, we correct the earlier result 4707 – 182.6 (3.0 ft³) kg + 113.0 (1.13 ft³) kg and conclude that the drain tank contained 4638 kg of carrier salt at the beginning of ²³³U power operations. Thus the net weight of the fuel charge at the beginning of ²³³U power operations was 4638 kg + 38.3 kg = 4676 kg, and the uranium concentration was 0.819 wt %.

Ample thermodynamic evidence existed to indicate that reprocessing procedures would not change the average composition of the fuel carrier salt. This expectation was confirmed by comparison of the average composition of the fuel salt before and after reprocessing and by determination that the uranium concentration in the ²³³U fuel mixture conformed to our expectations. A discussion of the uranium assay during this period may be found in Sect. 7.3. The results of chemical analyses shown in Table 3.5 support the conclusion that the average composition of the fuel carrier salt remained essentially constant throughout the entire period of MSRE operations.

3.7 Material Balances for ²³⁵U and ²³³U Operations

3.7.1 Recovery of ²³⁵U and ²³⁸U. A material balance of the fuel and flush salts was maintained on a

continuous basis from the beginning of experimental operations with the MSRE. With refinements in physical property data for the salts, in neutron absorption cross-section data, and in analytical methods, the quality of the balance improved steadily. The accuracy afforded by these improvements was established finally by recovery operations at ORNL and at the Goodyear Atomic Corporation, Piketon, Ohio. There, the uranium hexafluoride removed from the ²³⁵U fuel and flush salts by chemical processing at ORNL was recovered by wet chemical methods. The amounts of uranium recovered using these methods were 6.420 ± 0.006 kg from absorbers 6, 7, and 8 (from the flush salt) and 214.572 ± 0.204 kg from the remaining 25 absorbers. The procedures employed in the recovery of uranium were described in detail in a report from the Goodyear Corporation as follows:¹⁶

The NaF material (25 absorbers) was processed using the continuous dissolver and resulted in 120 batches of solution, for a total of 46,049 liters containing 214,456 grams of uranium. These batches were measured and sampled, in duplicate, using the solution recovery accountability measuring columns. Batch samples were proportionally composited, in duplicate, representing from 10 to 20 batches of solution. All composite samples were analyzed for total uranium and weight percent U-235 by thermal mass spectrometer. In addition, the continuous dissolver operation generated 1,588 pounds of filter cake, containing 105 grams of uranium. This material was also sampled in duplicate and composited on a weight basis. Vent losses resulting from steam effluent were calculated to be 11 grams of uranium.

The limits of error used for the measurement of solution and filter cake resulting from processing the remaining sodium fluoride were ±0.18 and ±10 percent of the reported value per composite analyzed. The limit of error for the total uranium recovered was based on propagation of error applicable to each composite group measured. Also, included in the limit of error is a bias estimate for the volume measurements of ±0.25 liter per batch, equivalent to ±126 grams of uranium.

These limits of error are based on previously determined precision and accuracy estimates. Statistical evaluation of the analyses obtained was not performed at this time since the

variation between samples indicates the precision will be well within the estimated values. Analyses of standard samples for comparison to known uranium value were made during the processing period and showed excellent agreement.

The following precautions and special consideration were taken while processing the NaF material to minimize measurement uncertainty:

1. The continuous dissolver and solution recovery systems were dedicated to processing NaF material exclusively from mid-March through June, 1970, to minimize rinsing of equipment as well as possible crossover of other material in process.
2. The accountability measuring columns were recalibrated on a weight basis and the recycle time required for representative sampling was determined by test data.
3. The accountability measuring columns were rinsed twice, 30 liters per rinse, between each batch measured and sampled.
4. All containers, plastic, and miscellaneous scrap generated during opening the 25 absorbers were decontaminated and the resulting solution processed through the dissolver.
5. Vent losses, even though minimal, were calculated based on total steam flow to atmosphere and the uranium concentration determined by analyses of condensate samples throughout the processing period.
6. System clean-out was initiated after processing the solution generated from the last three absorbers which were estimated at zero uranium content. This solution, 4,210 liters, contained an average of 0.033 grams of uranium per liter. Final rinse of the system averaged less than 0.002 grams U/liter.

A disparity between the ORNL material balance and the Goodyear results of 0.83 kg of ^{235}U was evident. In an attempt to resolve this discrepancy we requested the Goodyear Corporation to retain the absorber vessels until investigation of the cause of the disparity was identified. In a telephone conversation between R. B.

Lindauer and J. G. Crawford,¹⁷ two pertinent details were disclosed: the few fines remaining in the absorber tanks were removed (by wiping the interior surfaces with moistened tissues) and added to the process solutions. Further, the interior surfaces of the absorbers were noted to be bright and shiny, a condition which seems to preclude the possibility that significant amounts of uranium were retained on these surfaces.

The overall results strongly suggest that rationalization of the disparity in the amount of uranium which we anticipated would be recovered by the Goodyear plant and that which was actually recovered would be possible only through a careful review of MSRE operations. In this connection, two possibilities were suggested, by J. R. Engel and R. B. Lindauer, respectively.¹⁸

Engel noted that the particle filter (a 9-ft filter designed to remove corrosion product solids from the

fluorinated salt before its reuse in the reactor) in the line between the fuel storage tank and the processing tanks could, after treatment of the flush salt was completed, have contained an unknown amount of zirconium metal, delivered to this location as the processed flush salt was returned to the reactor system. It is difficult to assign high probability to the events which could have reduced the uranium from the fuel charge as, subsequently, it passed through this filter, in such a way that some 2 kg of uranium remained in the filter; however, the possibility cannot be excluded and merits further examination.

Another possible site where uranium may have been retained, as has been suggested by R. B. Lindauer, is the high-temperature sodium fluoride absorber bed which is positioned between the fuel storage tank and the NaF absorbers. The design temperature for operation of this absorber is 750°F, based on previous laboratory studies.¹⁹ The laboratory studies indicate that this absorber would not retain UF₆ at the operating temperature; the possibility that temperature gradients prevailed within the absorber at periods near the end of fluorination operations which allowed the retention of some uranium within the absorber should now be examined.

The possibilities that such errors as might be ascribed to misestimates of power output of the reactor, reactivity anomalies, and implications of short-term trends in the results of chemical analyses, have been reexamined; we conclude that their possible contribution to the disparity described is negligible.

The possibility that the retention of uranium in either site might be established with certainty by application of newly developed neutron interrogation techniques using a californium source seemed favorable. Mockup experiments were devised and tested in the remote maintenance practice cell at the MSRE with a neutron source and an ORR fuel element. These tests showed, however, that the method could not be used without considerable modification, including procurement of a more intense source, and the effort was abandoned. Although confirmation of the results of the existing isotopic dilution analyses would be desirable by direct experiments such as were planned, the data which were used to monitor the transfers of uranium and plutonium within the reactor system appear to be sufficiently reliable to estimate the amounts of ^{235}U and ^{238}U retained in the reprocessing system and for computation of final inventory distribution.

3.7.2 Inventories for stored salts. Later in this report, methods for establishment of the power output of the MSRE are described (see Sect. 7). By application of the

Table 3.6. Inventory of residual uranium and plutonium in the MSRE^a

	A. Uranium					
	²³³ U	²³⁴ U	²³⁵ U	²³⁶ U	²³⁸ U	Σ U
Fuel-circuit inventory, run 20-I, kg	28.782	2.545	0.876	0.036	2.035	34.274
Total inventory, run 20-I, kg	31.052	2.746	0.945	0.039	2.196	36.978
Drain-tank inventory, run 20-I, kg	2.270	0.201	0.069	0.003	0.161	2.704
Fuel-circuit inventory, run 20-F, kg	28.739	2.563	0.876	0.036	2.035	34.249
Transfer to flush salt, run 20-F, kg	0.411	0.037	0.013	0.001	0.029	0.491
Charged into drain tank, run 20-F, kg	28.328	2.526	0.863	0.035	2.006	33.758
Drain tank residue, kg	2.270	0.201	0.069	0.003	0.161	2.704
Final drain tank inventory, kg	30.598	2.727	0.932	0.038	2.167	36.462
U/ Σ U, wt %	83.918	7.479	2.556	0.104	5.943	

	B. Plutonium			
	²³⁹ Pu	²⁴⁰ Pu	^{238,241,242} Pu	Σ Pu
Fuel circuit inventory, run 20-I, g	625.8	61.81	2.39	690.0
Total inventory, run 20-I, g	680.2	67.19	2.60	749.99
Drain tank inventory, run 20-I, g	54.4	5.38	0.21	59.99
Fuel-circuit inventory, run 20-F, g	615.6	65.43	2.37	683.4
Transfer to flush salt, run 20-F, ^b g	61.8	6.57	0.23	68.6
Charged into drain tank, run 20-F, g	553.8	58.86	2.14	614.8
Drain tank residue, g	54.4	5.38	0.21	59.99
Final drain tank inventory, g	608.2	64.24	2.35	674.79
Pu/ Σ Pu, wt %	90.13	9.52	0.35	

^aWeights are based on comparisons of analytical results and computed values. These comparisons indicate that maximum power output was 7.4 MW(t). Final estimates assume 4167 EFPH (equivalent full-power hours) at 7.4 MW(t).

^bThis item makes the simplifying assumption that the total amount of plutonium estimated to be transferred to the flush salt was transferred during the final flush of the fuel circuit.

isotopic analyses used for this determination, together with other analytical methods, it became possible to establish the power output of the reactor with good precision, and accordingly to compute final material balances for the fuel and flush salt systems. The results of these computations are listed in Table 3.6.

In storage, the fuel salt is divided equally between the two drain tanks. Both fuel and flush salt were frozen in storage and are maintained between 232 and 343°C to minimize the evolution of fluorine from the frozen salts.

An inventory of the uranium and plutonium contained in the drain tanks, based on data listed in Table 3.6, together with results of mass spectrometric analyses, is shown in Table 3.7. Using the values in this inventory the composition of the fuel salt was calculated. Nominal values are compared with analytical data in Table 3.8.

3.7.3 Salt loss from leakage. Experiments with the MSRE were terminated on December 12, 1969. The fuel and coolant salts were drained for storage in the

drain tanks. After the fuel was drained, and while the freeze valves were being frozen, an increase in the radioactivity in the reactor containment cell was observed, which indicated that a very small leak had occurred in the primary containment. After several hours the activity began to decrease after having driven the monitor on the recirculating cell atmosphere to a maximum of 35 mR/hr. The fuel loop and drain tanks were pressurized without causing an apparent effect on the activity. A sample of the cell atmosphere indicated that the activity was caused primarily from ¹³³Xe. Since leakage had apparently stopped, flush salt was charged into the fuel system and circulated for 17 hr. Before flush salt was drained from the circuit the system was pressurized to 20 psig for 2 hr without showing any signs of leakage. It was concluded after further investigation that the leak was in freeze valve FV-105 or in the immediate vicinity of this valve. To conclude operations with the fuel circuit, flush salt was transferred through the fill line to ensure that FV-105 and the adjacent line were filled with salt.

Table 3.7. Material balance for the MSRE fuel and flush salts

	Inventory (kg)			Uranium concentration (wt %)	
	Uranium	Fuel salt	Carrier salt	Calculated	Observed
Total uranium charged to the MSRE, 1964	229.020				
Correction to ^{238}U inventory ^a	-2.0				
Fuel inventory at termination of run No. 3	227.02	4883.8	4656.8	4.648	4.648
Total uranium burned in ^{235}U operations, 9057 EFPH at 7.4 MW(t) ^b	-3.615	-3.615	0		
Uranium added as fuel replenishment	+2.461	+3.074	+0.613		
Total uranium removed in samples	-0.256 ^c	-5.583	-5.327		
Uranium returned to circuit with ^{233}U charge	-1.935	0	0		
Transfer balance, fuel to flush salt	-6.420	-12.0	-12.0		
Maximum amount of uranium recoverable	217.255	4865.68	4648.42		
Maximum amount of uranium recovered (ORNL) ^d	217.99				
Maximum amount of uranium recovered (Goodyear) ^e	214.776				
ORNL inventory minus Goodyear recovery value	-2.479				
Carrier salt retained in storage tank (3.0 ft ³)			-182.6		
Supplementary addition of carrier salt			+129.9		
$\text{LiF} \cdot 2^{233}\text{UF}_4$ (including 1.935 kg $^{235},^{238}\text{U}$ residue)	38.298	57.367	+21.00		
Fuel salt charge at beginning of run No. 16	38.298	4654.80	4616.50	0.823	0.820
Total uranium burned in ^{233}U operations	-1.316	-1.316	0		
Uranium added as fuel replacement	+0.389	+0.630	+0.241		
Transfer balance, fuel to flush salt	-0.289	-0.289	0		
Total uranium removed in samples	-0.025	-3.167	-3.142		
Fuel inventory at termination of MSRE operations	37.057	4650.5	4613.6	0.797	0.792 ^f

^aSee sect. 2.4.2.^bBurnup rate: -0.3991042 g/EFPH. See B. E. Prince, *MSR Program Semiannual Prog. Rep. Aug. 31, 1969*, ORNL-4449, p. 25.^cJ. R. Engel, *MSRE Book Uranium Inventories at Recovery of ^{235}U Fuel Charge*, MSR-68-79 (May 15, 1968).^dR. B. Lindauer, *Chem. Technol. Div. Annu. Prog. Rep. May 31, 1969*, ORNL-4422, p. 40.^eSee sect. 3.7.1.^fAverage of four samples obtained during run 20.

Table 3.8. Composition of fuel salt stored in the MSRE drain tanks

	^7LiF	BeF_2	ZrF_4	$^{233},^{42}\text{UF}_4$	$^{239},^{11}\text{PuF}_3$
Mole Percent					
Nominal	64.50	30.18	5.19 ^a	0.134	2.38×10^{-3}
Analytical ^b	64.53	30.43	4.90	0.137	
Weight Percent					
Nominal	41.87	35.44	21.67	1.033	0.0177
Analytical ^b	41.37	35.27	20.19	1.06	

^aCurrent calculations do not include corrections for transfer of carrier solvent residues to flush salt or flush salt residues to fuel. Disparity between nominal and analytical values for zirconium will be reduced by introduction of this correction factor.

^bRun 17-20, average of 33 samples.

References

1. E. S. Bettis et al., *Nucl. Sci. Eng.* **2**, 841 (1957).
2. J. A. Lane, H. G. MacPherson, and Frank Maslan (eds.), *Fluid Fuel Reactors*, p. 590, Addison-Wesley, Reading, Mass., 1958.
3. F. F. Blankenship, E. G. Bohlmann, S. S. Kirslis, and E. L. Compere, *Fission Product Behavior in the MSRE*, ORNL-4684 (in preparation).
4. A. L. Mathews and C. F. Baes, Jr., *Oxide Chemistry and Thermodynamics of Molten Lithium Fluoride-Beryllium Fluoride by Equilibration with Gaseous Water-Hydrogen Fluoride Mixtures*, thesis, ORNL-TM-1129 (May 7, 1965).
5. G. Goldberg, A. S. Meyer, Jr., and J. C. White, *Anal. Chem.* **32**, 314 (1960).
6. *MSR Program Semiannual Prog. Rep. Aug. 31, 1965*, ORNL-3872, p. 140.

7. *MSR Program Semiannu. Progr. Rep. Feb. 28, 1965*, ORNL-3812, p. 160.
8. C. E. Bamberger and C. F. Baes, Jr., *MSR Program Semiannu. Progr. Rep. Aug. 31, 1970*, ORNL-4622, p. 91.
9. *MSR Program Semiannu. Progr. Rep. Feb. 28, 1966*, ORNL-3936, p. 168; *ibid.*, *Aug. 31, 1966*, ORNL-4037, p. 200; *ibid.*, *Feb. 28, 1967*, ORNL-4119, p. 165.
10. M. T. Kelley, *Statistical Quality Control Report, January–March 1969*, ORNL-CF-69-4-30; *April–June 1969*, ORNL-CF-69-7-65; *July–September 1969*, ORNL-CF-69-10-36; *October–December 1969*, ORNL-CF-70-1-37.
11. R. B. Lindauer, *MSRE Design and Operations Report, Part VII*, ORNL-TM-907 (May 1965).
12. R. B. Lindauer and C. K. McGlothlan, *Design, Construction, and Testing of a Large Molten-Salt Filter*, ORNL-TM-2478 (March 1969).
13. J. H. Shaffer and L. E. McNeese, *Removal of Ni, Fe, and Cr Fluorides from Simulated MSRE Fuel Carrier Salt*, ORNL-CF-68-4-41 (April 1968).
14. R. B. Lindauer, *Processing of the MSRE Flush and Fuel Salts*, ORNL-TM-2578 (August 1969).
15. Analyses performed by J. R. Sites, Analytical Chemistry Division.
16. Correspondence from W. B. Thompson, Supervisor of Process Engineering, Goodyear Atomic Corporation, Piketon, Ohio, to the Oak Ridge National Laboratory, September 2, 1970.
17. Goodyear Atomic Corporation, Piketon, Ohio.
18. Personal communication.
19. G. I. Cathers, M. R. Bennett, and C. J. Shipman, *MSR Program Semiannu. Progr. Rep. Aug. 31, 1968*, ORNL-4344, p. 321.

4. CHEMICAL COMPOSITION OF THE FLUSH SALT DURING NUCLEAR OPERATIONS

4.1 Role of Flush Salt Analysis in the Determination of Salt Residue Masses

The potential utility of a flush salt to scour contaminants from the MSRE fuel circuit was recognized early in the MSRE development program; the sagacity of the choice to use this salt was confirmed immediately after preliminary experiments with the reactor — experiments in which the flush salt was repurified after its first period of circulation through the fuel system.¹ The repurification procedures employed at that time showed that in its first use the salt had served to remove

a considerable amount of contaminants from the fuel and moderator graphite system. Not foreseen, however, was the fact that it would function later to have a significant influence on evaluations of reactor performance. This arose from the fact that the quantities of residues of fuel and flush salt, intermittently cross-transferred before and after reactor maintenance, could not be adduced from on-site inferences. Soon after experiments began with the circulating fuel salt, it became evident that only the results of highly accurate chemical analysis of the flush salt would make it possible to establish reliable values for the amounts of fuel and flush salt residues left in the reactor fuel system after it was drained. Accuracy in these values was also necessary in order to compute changes in nominal values of the concentration of fissionable material in the fuel circuit as the reactor experiment proceeded.

Results of chemical analyses indicated that after the fuel salt was drained, circulation of the flush salt removed an average of 20 kg of fuel salt from the drained circuit. Refinements in the values for the physical properties of the fuel and flush salts allowed an estimation from the relative density of the flush and fuel salts that the average mass of flush salt residues would be ~17.5 kg. With these values, nominal values for the composition of the fuel salt were calculated for the period when experiments were conducted with ^{235}U fuel.

The total mass of flush salt originally charged into the MSRE was about 4190 kg. From averages of the increments in the changes in concentration of uranium which developed in the flush salt in use, it was expected that after its final use with ^{235}U fuel the flush salt would contain uranium at a concentration of 1500 ppm, representing a total pickup of 6.29 kg of uranium. Analysis of the flush salt after its final use to remove ^{235}U fuel residue from the fuel circuit showed that the concentration of uranium was 1488 ppm and, therefore, that the amount of uranium which was recoverable from the salt was 6.23 kg; the actual amount of uranium recovered was 6.420 kg. With the final amount of uranium in the flush salt established as 6.420 kg, the average increments were established as 0.917 kg, and the average mass of fuel residue as 20.0 kg.

Complete results of the chemical analyses performed with the flush-salt samples removed from the MSRE are listed in Table 4.1. The average concentrations of uranium in the samples removed from the system during ^{235}U operations are shown in Fig. 4.1.

Flush salt was circulated in the MSRE fuel-salt circuitry 13 times as a part of the ^{235}U operations and

Table 4.1. Summary of MSRE salt analyses, flush salt

Date	Sample	Weight %						Parts per million				
		Li	Be	Zr	U ^a		F	Σ	Fe	Cr	Ni	O ^b
					Book	Analytical						
	PC-1	13.12	9.68				77.08	99.93	45	45	7	432 ^b
	FP-3-36	13.70	9.71	0.021		0.0195	77.68	101.17	144	64	75	1205 ^b
12/15/65	FP-4-1											35 ^b
12/16/65	FP-4-2	13.65	9.83	<0.0025		0.0210	80.52	104.04	110	<10	33	56 ^b
12/16/65	FP-4-3											46 ^c
12/16/65	FP-4-4	13.55	9.35	<0.0025		0.0207	79.34	102.30	212	62	30	74 ^b
12/17/65	FP-4-5											72 ^c
12/17/65	FP-4-6	13.50	9.96	<0.0025		0.0200	80.07	103.58	125	<10	<20	180 ^b
12/17/65	FP-4-7	13.65	9.46	<0.0025		0.0241	77.85	101.03	180	54	<20	150 ^b
12/17/65	FP-4-8											106 ^c
12/17/65	FP-4-9	13.35	9.98	<0.0025		0.0221	75.80	99.20	210	57	<20	142 ^b
12/18/65	FP-4-10		9.49	<0.0025		0.0230	75.05	98.26	128	60	<20	1300 ^b
9/28/66	FP-8-1	12.40	9.79	0.02		0.0409	80.70	102.99	262	75	31	
9/29/66	FP-8-2	12.40	9.66	0.25		0.505	78.14	101.01	197	82	225	
9/30/66	FP-8-3											22 ^b
9/30/66	FP-8-4	12.43	9.02	0.22		0.458	75.75	98.93	382	53	74	
11/2/66	FP-8-15		9.34	<0.01		0.0578	78.74		128	65	<15	
11/3/66	FP-8-16	13.50	9.24	<0.10		0.0715	78.01	100.94	125	61	<15	
11/4/66	FP-8-17	13.40	8.62	<0.10		0.0556	73.63	95.81	76	52	<15	
11/24/66	FP-9-8	13.35	9.59	0.24		0.0840	72.15	95.43	175	53	26	
12/11/66	FP-10-1	13.15	8.90	0.145		0.0828	72.67	94.98	169	71	53	
12/11/66	FP-10-2	13.10	8.41	0.190		0.0747	73.03	94.84	194	75	42	
5/10/67	FP-11-59	13.43	7.57	0.345		0.0292	76.10	97.50	222	68	40	
5/10/67	FP-11-59					0.930 ^d						
5/10/67	FP-11-59					0.1080 ^e						
5/11/67	FP-11-60	13.40	9.36	0.260		0.0268	79.23	102.30	119	74	34	
6/16/67	FP-12-1	13.40	8.64	<0.2		0.0778	80.22	102.56	108	66	26	
6/16/67	FP-12-2	13.70	9.50	<0.2		0.0793	75.40	98.89	104	70	23	
6/17/67	FP-12-3	13.60	9.38	<0.2		0.0826	77.40	100.68	93	68	24	
6/17/67	FP-12-4	50-g sample for oxide analysis										
9/8/67	FP-13-1	12.70	8.42	<0.2		0.1392	75.14	96.64	106	82	260	
9/10/67	FP-13-2	12.80	8.84	0.72		0.1084	76.12	98.72	140	60	250	
9/11/67	FP-13-3	12.80	10.04	0.70		0.1069	77.72	101.42	202	76	232	
4/28/68	FP-14-72	12.53	9.66	0.42		0.1507	73.85	96.64	150	76	52	
4/28/68	FP-14-72					0.1488 ^e						
8/2/68	FST-11					0.1172				104	(before F ₂)	
8/4/68	FST-12					24 ppm			176	119	(after F ₂)	
8/4/68	FST-13					7 ppm			232	112	516 (after F ₂)	
8/5/68	FST-14					6 ppm			174	133	543 (after F ₂)	
8/8/68	FST-15	No sample obtained										
8/8/68	FST-16			0.30					206	136	36	
8/8/68	FST-17	50-g FVS capsule after Zr addition							174	100	50	
8/10/68	FST-18	No sample obtained										
8/14/68	FP-15-1	13.43	9.16	0.546		0.0036			152	76	26	
8/15/68	FP-15-2	50-g sample for eta experiment - no sample retrieved										
8/15/68	FP-15-3	25-g sample for eta experiment										
8/16/68	FP-15-4	25-g sample for eta experiment										
8/11/69	FV-19-1S											
8/12/69	FP-19-2	12.43	9.64	0.51		0.0072	79.7	102.30	128	81	23	
8/13/69	FP-19-3	50-g sample for oxide determination										
8/13/69	FP-19-4	12.50	9.53	0.41		0.0065	79.2	101.68	197	74	25	
8/13/69	FP-19-5	11.55	7.55	0.49		0.0075	80.5	100.14	241	80	40	
12/13/69	FP-20-33	11.55	8.19	0.430		0.0118	77.40	103.59	146	93	49	
12/13/69	FP-20-34	50-g sample of flush salt for oxide analysis										71
12/14/69	FP-20-35	11.50	8.45	0.540		0.0108	77.90	103.4	155	88	46	

^aValues corrected to 33.696 at. % ²³⁵U.^bKBrF₄ method employed unless otherwise noted.^cHF purge method used.^dRecheck by fluorometric method.^eDelayed neutron activation analysis.

ORNL-DWG 71-9989

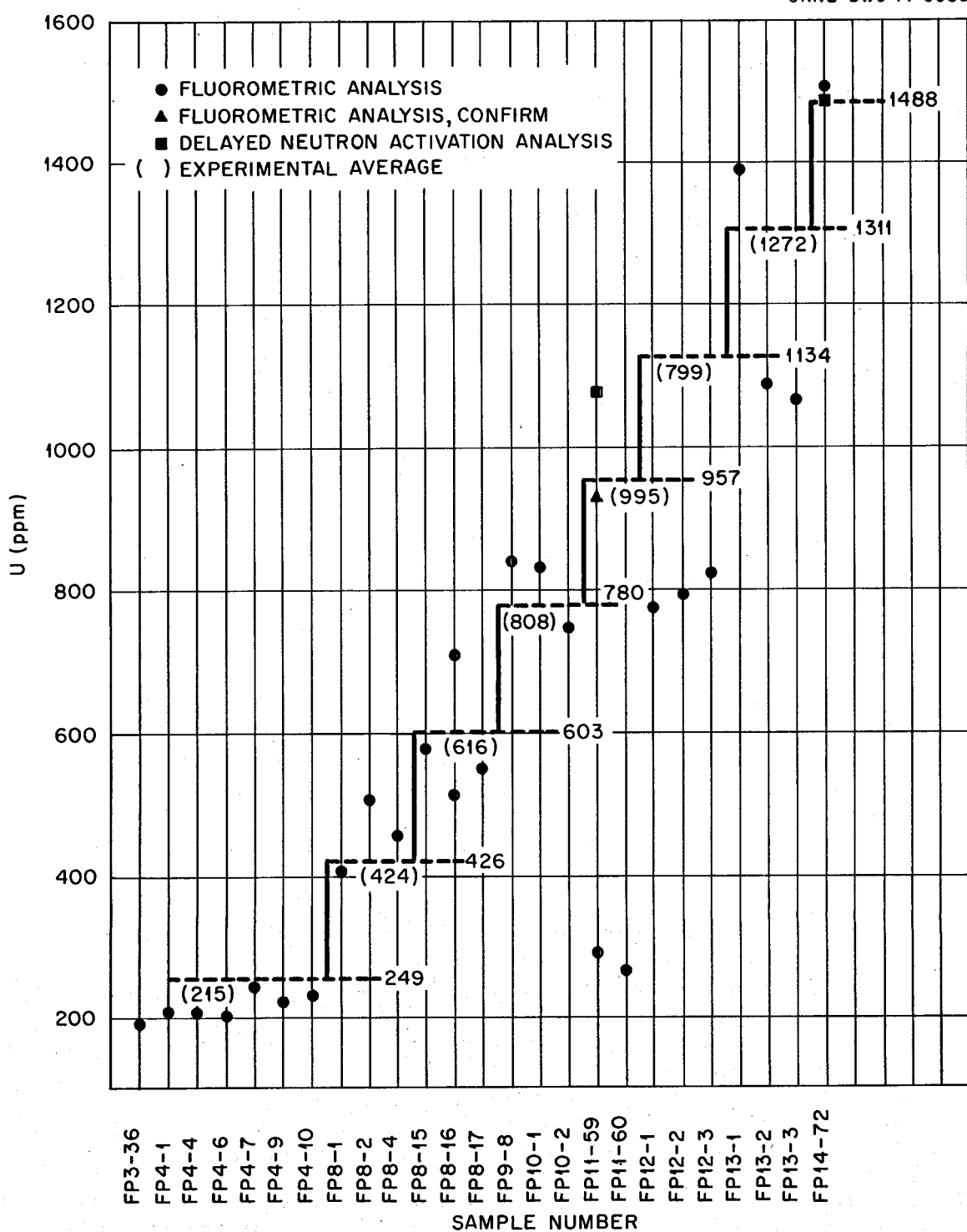


Fig. 4.1. Uranium concentration in MSRE flush salt. Calculated average increment = 177 ppm (includes transfers of five fuel residues totaling 11.34 kg from fill line).

three times as part of ^{233}U operations, once on each occasion before the fuel was constituted in the reactor system, and thereafter whenever the fuel system was to be opened for maintenance. If during the maintenance period, the possibility developed that the fuel circuit was exposed to ambient cell atmosphere, the circuit was again washed with the molten flush salt before resumption of experiments with the fuel salt. In use, the flush salt was circulated for brief periods, usually 24 to 48 hr, because it was assumed that molten LiF-BeF_2 flowing in the metal circuit at 650°C would be extremely effective as a solvent for contaminants that may have entered the system during the previous maintenance period. Gross exposures of the circuit to potentially contaminating atmospheres were avoided during the maintenance periods first by flushing the reactor system with argon, and subsequently by maintaining a nitrogen atmosphere in the standpipe column through which access to the reactor core was gained. Neither blanket gas was specially purified for this application.

It was judged that the flush salt was circulated for sufficient periods of time to be effective, because, in use, major increases were not observed in the concentration of contaminants in the salt nor were there major increases in the concentration of chromium in the fuel salt on initiation of the subsequent experiments with fuel salt. After each of these occasions, however, the chromium concentration of the fuel salt gradually rose to a higher value than had preceded the maintenance period. The significance of these changes is discussed in Sect. 6.

4.2 Transfer of Uranium and Plutonium to Flush Salt in ^{233}U Operations

Reclamation of 6.420 kg of uranium from the flush salt indicates that the average increase in uranium concentration developed from the removal of a single fuel-salt heel during ^{235}U operations was 219 ppm rather than the average 215 ppm we had observed from analyses performed during the course of reactor operations. With the ^{233}U fuel salt, a reduction of the concentration increments was anticipated proportionate to the lower concentration of uranium in the fuel salt, and should have resulted in an average increase of ~40 ppm per flush operation. The average of the two results obtained with the flush salt after completion of run No. 20 shows that the final concentration of uranium in the salt was 113 ppm, or that for each of the three times flush salt was used to remove fuel salt residues, the average increase in the concentration was 38 ppm, in good agreement with the anticipated value.

Table 4.2. Results of mass spectrometric analysis of MSRE flush salt

In weight percent

Sample No.	Uranium				
	^{233}U	^{234}U	^{235}U	^{236}U	^{238}U
FP-20-33	40.55	3.73	17.67	0.25	37.80
FP-20-35	38.20	3.47	17.06	0.24	41.03

Sample No.	Plutonium			
	^{233}Pu	^{240}Pu	^{241}Pu	^{242}Pu
FP-20-33	94.74	4.78	0.44	0.04
FP-20-35	94.63	4.87	0.45	0.05

After termination of experiments with ^{233}U fuel the reactor was drained and flushed. Two samples of flush salt were obtained (FP-20-33 and -35) in which the average concentration of uranium was 113 ppm, an increase of 42 ppm over that found during the single previous use in which it removed a fuel-salt heel in ^{233}U operations (the beginning of run No. 19). The single flush-salt sample obtained during the startup operation preceding the introduction of ^{233}U fuel into the system was reported to have contained 36 ppm of uranium. The three groups of data are thus consistent — an indication that the concentration of uranium increased as predicted. They also suggest that the flush salt contained 35 to 40 ppm of uranium when it was returned from the chemical reprocessing plant.

Isotopic analyses obtained from the last two samples of flush salt are shown in Table 4.2. The isotopic composition of the uranium contained in these samples indicates that (correcting for the contribution from the fuel of 0.023 kg and neglecting a correction for ^{238}U burnout) the flush salt contained ~50 ppm (0.21 kg) of uranium. This is somewhat more than one would expect considering the excellent agreement between expected and observed amounts of uranium previously recovered from the flush salt, and from analyses obtained during the uranium recovery experiments with flush salt in which results indicated the residual concentration was no higher than 24 ppm, and possibly as low as 4 ppm.¹

4.3 Flush Salt Loss to Off-Gas Holdup Tank

The results of the chemical and mass spectrometric analyses described above provide a basis for the conclusion that only very small amounts of either fuel or flush salt could have been lost from the primary containment or came in contact with the cell atmosphere through the leak that developed adjacent to the

freeze valves (see Sect. 3.6.3). If cell air were aspirated into the fuel salt as it drained from the reactor at termination of run No. 20, a probable consequence would have been that ZrO_2 deposits may have formed in the region of the break, later to be dissolved in the flush salt. Possibly, some uranium would have been deposited as well, along with the ZrO_2 . Small amounts of ZrF_4 are transferred to the flush salt as a part of fuel residues, yet, as shown in Table 4.1, the concentration of zirconium in the flush salt after its final use does not seem to have increased. Second, sizable amounts of uranium deposited in the area of the break would both increase the anticipated concentration in the flush salt and alter the isotopic ratio in favor of an anomalous increase in ^{233}U fraction. The isotopic analyses shown in Table 4.2 denote a slight anomaly in isotopic ratios of uranium, but of opposite character than suggested above; that is, they indicate that slightly more ^{235}U and ^{238}U were present than was expected from the prior reprocessing operations. In one previous incident, the possibility developed that flush salt was inadvertently² lost from the salt system.

In Piper's account² of operations in July 1966, he notes that the fuel loop was filled with flush salt in preparation for maintenance work in the reactor cell. Flush salt was transferred into the overflow tank to flush out the residual fuel and to check the indicated level in the pump bowl at the overflow point, and transfer began when the indicated level was 9.6 in. (In January the indicated level at the overflow point had been 9.2 in.) After approximately 0.6 ft³ of salt was transferred, the fuel pump level suddenly rose off scale. Rising level in the overflow tank triggered a drain, but not before salt had entered some of the lines connected to the top of the pump bowl. This behavior resulted from an operational error which allowed the salt level in the flush tank to be lowered too far, and also allowed the pressurizing gas to enter the fill line and pass up into the reactor vessel. The gas expanded rapidly as it rose through the salt, causing salt to flood the pump bowl. The pump bowl reference line was plugged with frozen salt, and enough salt was frozen in the sampler tube to obstruct passage of the latch. A thermocouple indicated that some salt also entered the off-gas line, but this line was not plugged. Salt also froze on the annulus around the fuel-pump shaft, preventing its rotation. In subsequent maintenance operations electric heaters were applied to the outside of the lines to melt out the salt in the bubbler reference line and the sampler tube. The short flexible portion of the off-gas line was replaced because of uncertainty over the possible effects of salt in the convolutions.

We noted above that for the increments observed in the change of concentration in the flush salt the projected amount of uranium recoverable for the salt was ~ 6.3 kg, and that a total of 6.42 kg was recovered. The projected value was calculated from the final analytical values, $1488 \text{ ppm} \times [4187 + 7 \times 2.6 \text{ kg}]$ (the average mass increase from fuel-flush cross transfer) = 6.257 kg. The fact that 6.42 kg of uranium was recovered suggests that if the analytical data are free of bias, only a small volume of flush salt could have transferred to the off-gas in the overflow accident. For example, if 50 kg of flush salt were lost by transfer the maximum amount of uranium which could be recovered from the flush salt at a concentration of 1488 ppm would not exceed 6.18 kg. Although it cannot be contended that the above results unequivocally demonstrate that the amount of flush salt transferred was negligible, they provide convincing evidence that the amount was indeed small.

In retrospect, the flush salt has served as the source of several kinds of valuable information pertaining to the performance of the MSRE. It now seems evident that it could have been used more effectively as a more valuable source if the periods of its use had been extended and designated for additional chemical investigations.

References

1. R. B. Lindauer, *Processing of the MSRE Flush and Fuel Salts*, ORNL-TM-2578 (August 1969).
2. H. B. Piper, *MSR Program Semiannual Progr. Rep. Aug. 31, 1966*, ORNL-4037, p. 24.

5. CHEMICAL BEHAVIOR OF THE COOLANT SALT

Of some 7000 kg of $LiF-BeF_2$ (66-34 mole %) prepared for the MSRE, 2610 kg was designated for use as the coolant salt and the remainder as flush salt. This coolant was circulated by a 75-hp motor and pump through a circuit which included a tube and shell heat exchanger and an air-cooled radiator. Detailed descriptions of this coolant system are given in the *MSRE Design and Operations Report*.¹ At termination of the Molten-Salt Reactor Experiment the salt had circulated in the system for a period of $\sim 26,000$ hr. With the reactor at full power, coolant salt entered the tube bundle of the heat exchanger (Fig. 5.1) at a temperature of $546^\circ C$ ($1015^\circ F$) and at 77 psig, removing heat from the fuel salt as it circulated through the shell side of the exchanger, and flowed on to the air-cooled

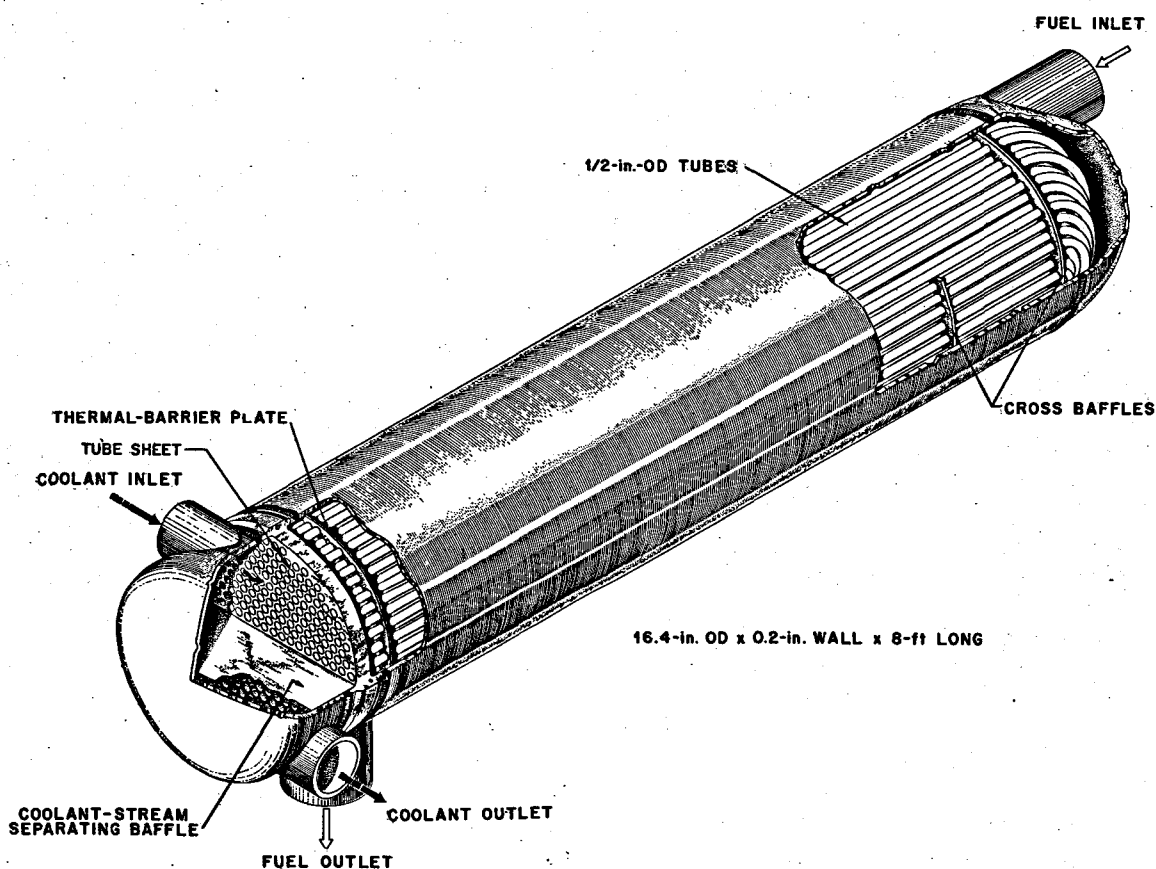


Fig. 5.1. Primary heat exchanger.

radiator (Fig. 5.2). On reentry to the heat exchanger, the salt was at a temperature of 579°C (1075°F). The coolant was circulated under these conditions for approximately half the period of its use. At zero or low power the salt was circulated isothermally, at about 650°C (1200°F). The coolant pump operated at constant speed, developing a salt flow of 6286 kg/min (793 gpm).

5.1 Composition Analysis

The salt was circulated for some 1200 hr during the prenuclear test period. Since flush and coolant salts were supplied from the same inventory, the coolant salt was analyzed during this period only for impurities.

At the end of prenuclear testing, concentrations of the structural metal impurities, chromium, iron, and

nickel, were established to be approximately 30, 90, and 7 ppm respectively — remarkably low considering that the circuit had not been flushed previously with molten salt. The results of spectrochemical analyses showed that no significant amounts of additional impurities were introduced during this period. As the reactor was brought to full power early in 1966, coolant salt was again circulated, sampled regularly, and subjected to compositional and impurity analysis. The results of these analyses, together with all other analyses of the coolant salt, are listed in Table 5.1.

It was stipulated that the chemical analyses include a determination of zirconium concentration as part of the procedures for coolant-salt analysis. Although such analyses were not conceivably applicable as primary indicators of fuel leakage, their incorporation supplied base-line data for the contingency that possible analysis

ORNL-LR-DWG 55841R2

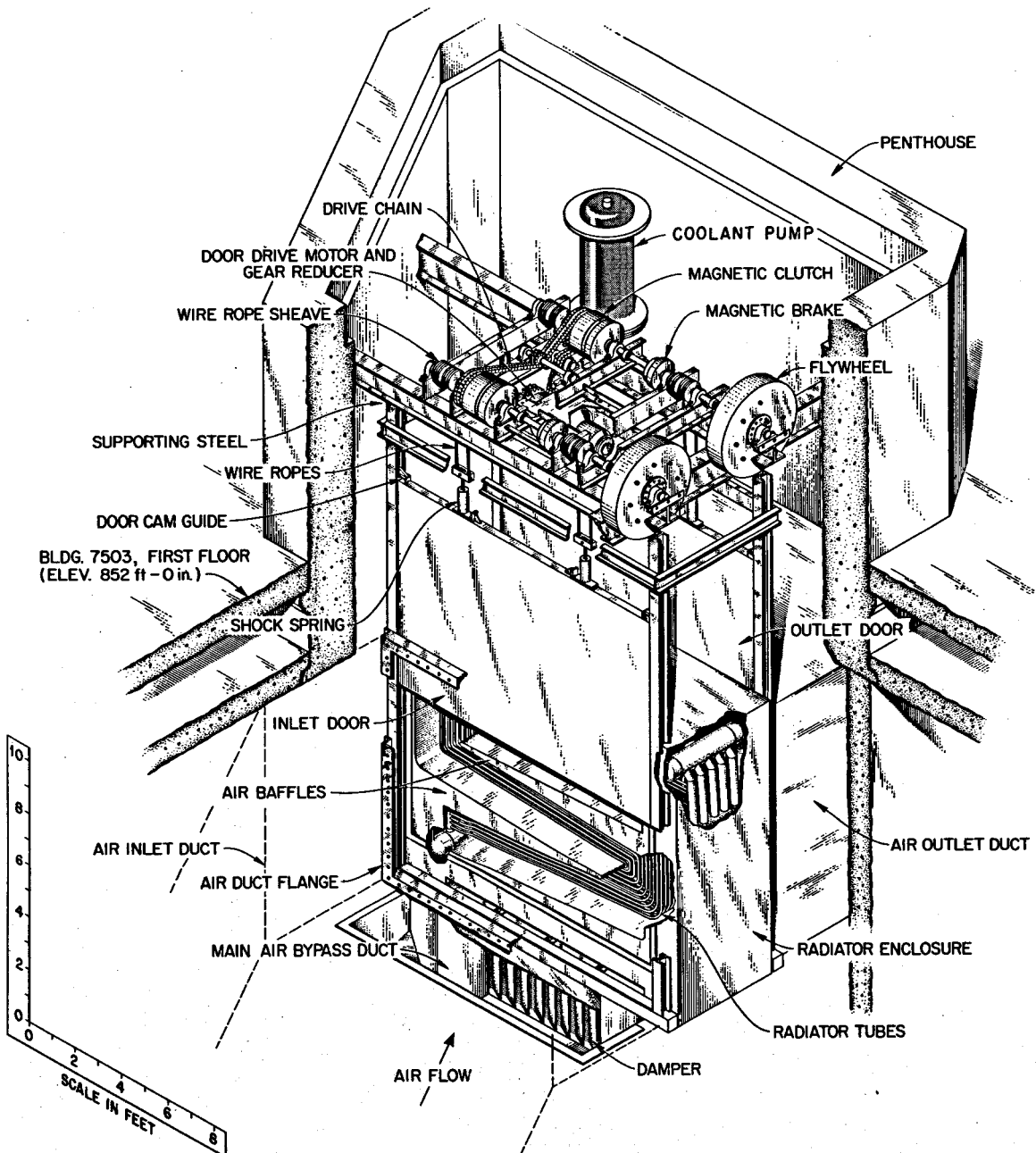


Fig. 5.2. MSRE radiator coil and enclosure.

Table 5.1. Summary of analytical chemical data for the MSRE coolant circuit

Table 5.1 (continued)

Date	Total Number Hr. in circuit	Sample Design	L1	Be (wt %)	Zr	F	Cr	Fe (ppm)	Ni	O ^a
8/29/67		Run 13,14-I								
9/8/67	12150	CP13-1	12.40	9.27	0.0045	73.80	<15	62	<20	264
9/29/67	12550	CP14-1	12.60	9.87	0.0098	72.80	24	<10	<20	158
10/25/67	13174	CP14-2	14.30	8.86	0.0011	76.32	24	25	37	210
11/27/67	13966	CP14-3	15.20	9.35	0.0100	75.50	24	61	<10	348
1/18/68	15214	CP14-4	12.50	10.10	0.0019	76.10	25	21	<20	197
3/20/68	16702	CP14-5	14.60	9.61	0.0078	77.20	<15	38	<25	104
3/28/68	16894	Run 14-F								
9/ /68		Run 15-I								
9/17/68	17714	CP15-1								
11/27/68	19414	Run 15-F								
12/ /68		Run 16-I								
12/10/68	19524	CP16-1								
12/ /68		Run 16-F								
1/12/69		Run 17-I								
2/4/69	20076	CP17-1	13.10	9.26	<0.0020	76.60	26	21	7	372
3/6/69	20796	CP17-2	13.40	9.49	0.0021	77.00	25	15	<10	2200
		Run 17-F								
		Run 18-I								
4/27/69	22044	CP18-1	13.00	9.52	0.0013	77.60	25	12	<5	720
5/29/69	22812	CP18-2	13.70	9.22	0.0014	77.50	25	14	<10	780
		Run 18-F								
		Run 19-I								
8/10/69	22870	CP19-1	13.40	9.44	<0.0019	77.30	35	<5	10	1850
9/14/69	22966	CP19-2 ^c	13.40	9.25	0.112	77.60	35	143	6	-
9/14/69	22966	CP19-3 ^c	13.85	9.13	0.103	78.30	35	128	6	
11/2/69	23084	Run 19-F								
11/26/69	23084	Run 20-I								
11/26/69	23094	CP20-1	14.00	9.55	0.0019	77.20	46	32	11	3200
12/10/69	23430	CP20-2	13.70	9.31	0.0206	77.20	60	114	10	1700 ^b
12/11/69	23454	CP20-3			Ni bar, exposed to coolant for tritium experiments					
12/11/69	23454	CP20-4			Ni bar, exposed to coolant for tritium experiments					
12/12/69	23479	CP20-5			CuO specimens, exposed to coolant for tritium experiments.					
12/16/69	23479	CP20-6			CuO specimens, exposed to coolant for tritium experiments.					
12/12/69		Run 20-F								

^a Unless otherwise noted, oxygen analyses were obtained by the KBrF₄ method.

^b Results obtained by HF-H₂ transpiration method.

^c Samples analyzed by HRLAL personnel.

of fuel-coolant mixing accidents might arise. Results are omitted from Table 5.1, because in none of the analyses of the coolant salt was zirconium detected.

As noted in Sect. 3.3, procedures used for the determination of the concentrations of oxides in MSRE samples were unsatisfactory until development of the HF-H₂ transpiration method was completed. Not until late in the program of reactor operations was this method applied to coolant-salt samples, and then, for the single sample available, it produced questionable results. The results of analyses for oxides listed in Table 5.1 were obtained with the KBrF₄ method, a method which is generally satisfactory for nonhygroscopic materials, but which was applied to samples which are hygroscopic and had not remained isolated from ambient atmospheres after their removal from the reactor. In view of the established absence of corrosion in the coolant circuit, their credibility is dubious.

Analyses of coolant salts were conducted by the General Analysis Laboratory of the ORNL Analytical Chemistry Division, while those for the fuel were obtained from the High-Radiation-Level Analytical Laboratory of that Division.

5.2 Corrosion Behavior

Corrosion of Hastelloy N as a container for molten LiF-BeF₂ mixtures may originate from a very limited number of sources: from impurities in the melt, from oxide films on the metal, and from mass transfer of metal constituents in the fluoride. Of these sources, only the latter, which is caused by the differential temperature coefficient for solubility of metals in salts, affords a mode of continuous attack in reactor systems that are protected from inleakage of contaminants.

Since the procedures adopted for MSRE operations assured that the circuit would be free from chronic sources of contaminants, it was anticipated that surveillance of the coolant salt would indicate imperceptibly low corrosion throughout the experiment.

In the early stages of MSRE operations, samples of the flush salt were removed from the circuit at a rate of one per week. However, as our experience developed, and it was confirmed that chronic sources of oxidizing impurities were absent, the frequency was decreased, finally to intervals of a month or longer. In contrast to the fuel system, the coolant salt system was not

ORNL-DWG 71-9990

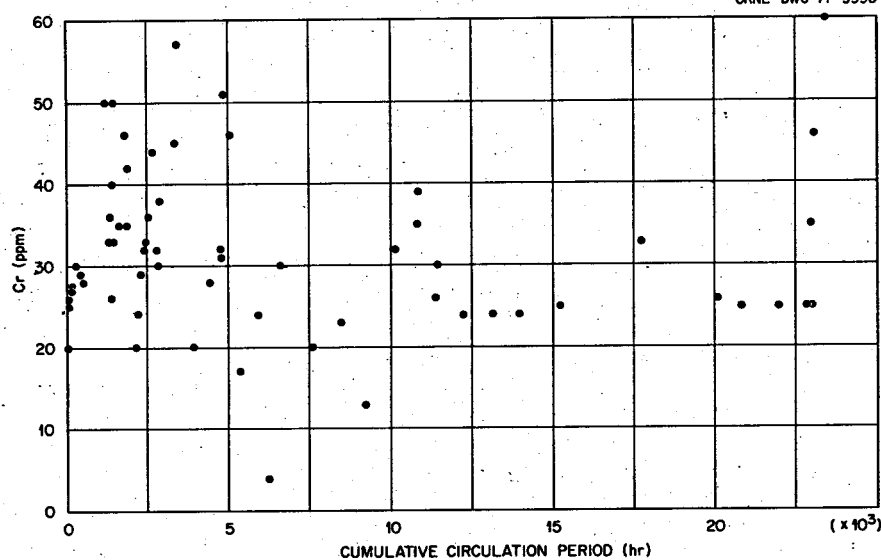


Fig. 5.3. Concentration of chromium in the MSRE coolant circuit salt.

exposed to the cell atmosphere during the course of MSRE operations. Under these circumstances, it was reasonable to expect that corrosion would not occur in the circuit, and these expectations were borne out in MSRE operations as indicated by the results of chemical analyses, and later in the postoperational examinations of the radiator (see below).

The results of the chemical analyses performed with coolant-salt samples showed that no measurable increase in the concentration of Cr, Fe, and Ni (with average values of 32, 64, and 20 ppm respectively) developed after the coolant salt was first charged into the MSRE. The concentrations of chromium in the coolant-salt samples, as determined in chemical analyses, are shown in Fig. 5.3. The fact that the chromium concentration remained unchanged is remarkable, since it indicates that within the limitation of the analytical precision (± 7 ppm) no corrosion, excepting that possibly resulting from mass transfer, occurred in the coolant circuit during the entire period of MSRE operations. The demonstrated compatibility of the coolant salt with its containment alloy is believed to be unmatched in any prior experience with either molten salts or liquid metals as recirculating heat-exchange media.

The average value of the chromium concentration in the coolant salt remained at 32 ppm for the entire period of reactor operation. The apparent trend toward higher values toward the end of the use period, as is reflected in Fig. 5.3, tends to discount the credibility of the view that the system remained free of contami-

nants. However, the results of postoperational examinations support this view completely and indicate thereby that continued use and analysis of the salt would have shown that the data were not indicative of a trend, but rather represented normal scatter. As part of the postoperational examination of MSRE components, sections of the radiator tubing were removed from the inlet and outlet ends and tested by ORNL metallurgists. Their analysis of the surfaces of the alloy that were exposed to the coolant salt by electron microprobe techniques disclosed that no compositional variations in Cr, Mo, Ni, or Fe existed within 2μ (the allowable working range on these samples) of the surfaces.²

Comparisons of the chemical composition of sections of this tubing with machined turnings showed a higher concentration of carbon at the salt interface after service, as was suggested from examinations of the microstructure.² However, changes in the tensile strength of the alloy were found to be slight and did not indicate serious embrittlement of the alloy.

The chemical behavior of the coolant salt in the MSRE is a unique demonstration of the compatibility of pure fluoride mixtures with nickel-based alloys, and shows as well that, with normal precautions to ensure that oxidizing contaminants are prevented from entering these systems, corrosion will not occur. The behavior of the coolant salt in the MSRE is a benign indicator of the potential application of LiF-BeF₂ based systems, but has only marginal implication with respect to the coolant salt of larger-scale molten-salt reactors in which lower liquidus temperatures are

mandatory for the coolant, and where the capital cost of the coolant salt will have a pronounced effect on power economics. These factors seem to preclude the choice of $^7\text{LiF-BeF}_2$ mixtures as coolants in such reactors. The current choice for the MSBR coolant salt is the NaF-NaBF_4 eutectic mixture. The highly successful performance of the molten fluoride salt $^7\text{LiF-BeF}_2$ in the MSRE is, however, of special significance in that it leads to the recognition that the possibilities of materials combinations are more flexible than was estimable prior to operation of the MSRE.

References

1. R. C. Robertson, *MSRE Design and Operations Report, Part I*, ORNL-TM-728 (January 1965).
2. H. E. McCoy and B. McNabb, *MSR Program Semiannual Progr. Rep. Aug. 31, 1970*, ORNL-4622, p. 120.

6. CORROSION IN THE FUEL CIRCUIT

6.1 Modes of Corrosion

Early recognition that numerous inorganic fluorides are among the most chemically stable materials in nature supplied the initial impetus for investigation of the chemical feasibility of molten-salt reactors. It was noted that the fluorides of commonplace alloy constituents such as iron, nickel, chromium, and molybdenum were less stable than the various compounds which might serve as components of molten-salt reactor fuels and coolants, and thus good alloys were potentially available as containers for molten fluoride mixtures (see Table 6.1). Subsequently, a materials development program was initiated culminating in the development of the alloy now designated as Hastelloy N specifically for use in constructing the MSRE; its approximate composition was Ni-Mo-Cr-Fe (71-17-7.5 wt %). The basis for the selection of this exact composition is described by Taboada¹ in a detailed review of the alloy development program.

Since the major components of the MSRE salts, LiF , BeF_2 , ZrF_4 , and UF_4 , are much more stable than the fluorides which can result from the corrosion of Hastelloy N, that is, MoF_3 , NiF_2 , and FeF_2 , compatibility of the molten-salt mixtures and the alloy was essentially assured.

The most probable mechanisms by which corrosion might occur in the MSRE were identified and examined extensively prior to operation of the reactor. The chemistry of such processes was reviewed recently by

Table 6.1. Relative stability^a of fluorides for use in molten-salt reactors

Compound	Free energy of formation at 1000°K (kcal per F atom)	Melting point (°C)	Absorption cross section ^b for thermal neutrons (barns)
Structural metal fluorides			
CrF_2	-74	1100	3.1
FeF_2	-66.5	930	2.5
NiF_2	-58	1330	4.6
MoF_6	-50	17	2.4
Diluent fluorides			
CaF_2	-125	1330	0.43
LiF	-125	848	0.033 ^c
BaF_2	-124	1280	1.17
SrF_2	-123	1400	1.16
CeF_3	-118	1430	0.7
YF_3	-113	1144	1.27
MgF_2	-113	1270	0.063
RbF	-112	792	0.70
NaF	-112	995	0.53
KF	-109	856	1.97
BeF_2	-104	548	0.010
ZrF_4	-94	903	0.180
AlF_3	-90	1404	0.23
SnF_2	-62	213	0.6
PbF_2	-62	850	0.17
BiF_3	-50	727	0.032
Active fluorides			
ThF_4	-101	1111	
UF_4	-95.3	1035	
UF_3	-100.4	1495	

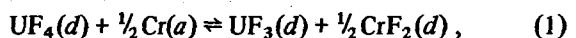
^aReference state is the pure crystalline solid; these values are, accordingly, only very approximately those for solutions in molten mixtures.

^bOf metallic ion.

^cCross section for ^7Li .

Grimes.² In the absence of impurities, corrosion proceeds through two mechanisms, by mass transfer and by selective oxidation of chromium, the most chemically active constituent of the container alloy. Both types of corrosion are limited by self-diffusion of chromium in the alloy and by temperature, which in the MSRE fuel reached extremes of 654°C (1210°F) and 632°C (1170°F).

Preponderantly, oxidation-reduction reactions are responsible for all the corrosion in molten-salt reactor fuel systems. The principal reaction which controls the process is



for which the standard free energy at 1000°K (727°C) is +15.1 kcal; at this temperature the equilibrium constant for the reaction is

$$K = \frac{N_{UF_3} N_{CrF_2}^{1/2}}{N_{UF_4} \alpha_{Cr}} = 5 \times 10^{-4}, \quad (2)$$

where N is mole fraction of a reactant or product and α is the activity coefficient. For purposes of examining the way this equilibrium affects corrosion behavior, assume conditions similar to those existent with ^{233}U fuel, where $N_{UF_4} = 1.38 \times 10^{-3}$, $Cr^{2+} = 5.15 \times 10^{-5}$ (150 ppm), $\alpha_{Cr} = 3 \times 10^{-2}$.³ The equilibrium concentration of UF_3 thus becomes 2.832×10^{-6} and

$$N_{UF_3}/N_{UF_4} = 2.832 \times 10^{-6}/1.38 \times 10^{-3} = 0.205\%.$$

These results illustrate that the reaction tends to come to equilibrium with a small fraction of the uranium in the trivalent state. Chemical factors which remove UF_3 from the salt system promote the forward reaction (1) and tend to remove chromium from the container alloy by selective oxidation.

Fission in molten-salt reactor fuel systems causes a gradual increase in the oxidation potential in molten-salt fuels (based on UF_4) as uranium is consumed. From estimates of fission yields⁴ and probable oxidation states of the species produced, the effect of fuel burnup on corrosion can be evaluated. A recent appraisal of this balance indicates that when reducing conditions are maintained and xenon and krypton are removed rapidly from the fuel, the sum of the electrical charges on the fission product cations is less than an average value of +4 per mole of uranium burned, and ~0.76 equivalent of oxidation results from the fission of one gram atomic weight of uranium.⁵ It was useful for this reason to increase the N_{UF_3}/N_{UF_4} concentration in the fuel salt occasionally as a means of minimizing corrosion.

Self-diffusion coefficients of chromium in nickel-base alloys in the temperature range 600 to 900°C were determined by Watson and co-workers⁶ by monitoring the total intake of ^{51}Cr by the alloys exposed to salt solutions containing this radiotracer and by measuring the tracer concentration profiles through successive electropolishing of the specimens.

They found from the loop experiments that the diffusion coefficient of ^{51}Cr in Hastelloy N at 650°C (1200°F), the mean temperature of the MSRE fuel, was $1 \times 10^{-14} \text{ cm}^2/\text{sec}$. In recent examination of metal surveillance specimens from the MSRE core,⁷ evidence

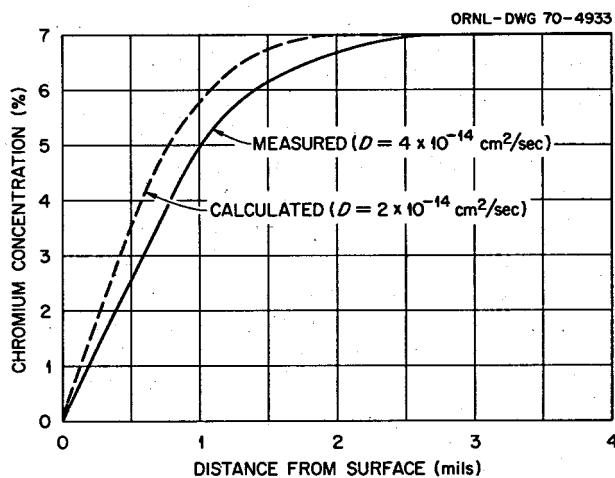


Fig. 6.1. Chromium gradient in Hastelloy N sample exposed in MSRE core for 22,533 hr.

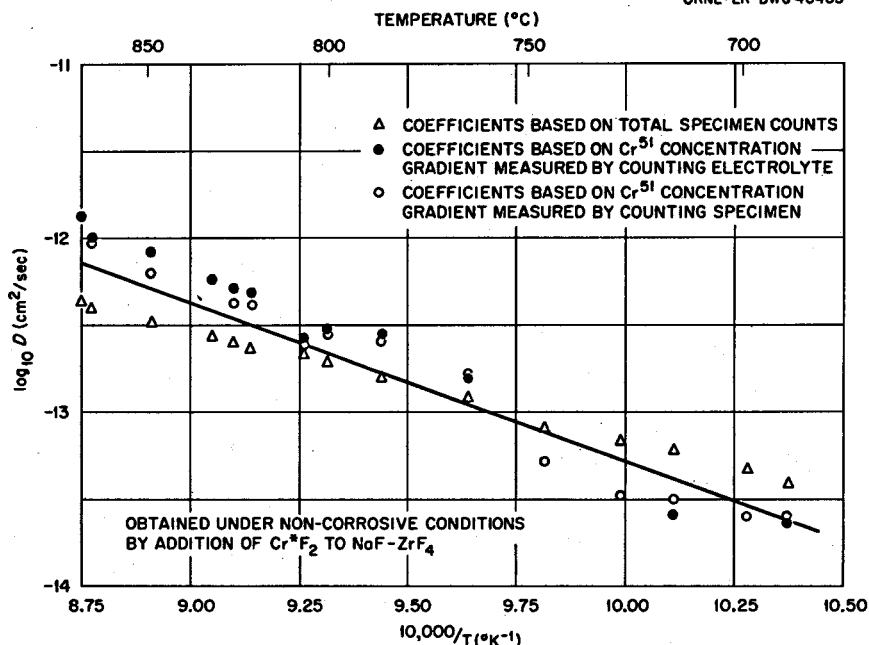
was found that indicated the diffusion coefficient of chromium in the core specimens may have been as high as $4 \times 10^{-14} \text{ cm}^2/\text{sec}$ (Fig. 6.1). The fact that the data from the MSRE samples were of necessity obtained from hot-cell operations, whereas no such constraints were imposed in the original laboratory measurement of self-diffusion coefficients, lends somewhat greater credibility to Watson's values. Both values may be accurate, however, because Watson noted that for Inconel the self-diffusion coefficients of chromium were strongly dependent on annealing conditions at low temperatures. Conditions leading to large grains led to low diffusion coefficients and vice versa.

Extrapolation of Watson's data for Hastelloy N (see Fig. 6.2) indicates that the self-diffusion coefficient for Cr in Hastelloy N at the lowest temperature of the MSRE fuel circuit is $8 \times 10^{-15} \text{ cm}^2/\text{sec}$. The rate of mass transfer is limited by the rate of diffusion of chromium into the alloy in the coolest area of the system. Corrosion from mass transfer was therefore expected to be of little consequence in the MSRE.*

Fick's equation, $M_t = 2C_0(Dt/\pi)^{1/2}$ (where C_0 = concentration of the diffusing element in the bulk species, D = diffusion coefficient, t = time) can be used to predict the quantity of material removed by dif-

*Postoperational examination of sections of Hastelloy N from the heat exchanger disclosed no evidence of an enrichment of chromium at the salt-metal interface. This observation has led to a suggestion, by F. F. Blankenship that since the coolest location in the fuel circuit is in the area of freeze valve 103, it would be useful in a future examination to determine the profile of chromium concentration in the alloy at this location.

ORNL-LR-DWG 46403

Fig. 6.2. Self-diffusion coefficients for ${}^{51}\text{Cr}$ in INOR-8; loop 1248. (from ref. 3).Table 6.2. Comparison of predicted and observed amounts of chromium in ${}^{235}\text{U}$ fuel saltDiffusion coefficient = D

Time (hr)	Predicted						Observed (ppm)
	$D = 1 \times 10^{-14}$ cm/sec	$D = 2 \times 10^{-14}$ cm ² /sec	$D = 4 \times 10^{-14}$ cm ² /sec	$D = 1 \times 10^{-14}$ cm ² /sec	$D = 2 \times 10^{-14}$ cm ² /sec	$D = 4 \times 10^{-14}$ cm ² /sec	
1,000	263	372	525	54	76	108	48
2,000	371	525	743	76	108	152	48
4,000	548	775	1097	112	159	225	48
6,000	643	910	1286	136	186	263	48
8,000	743	1050	1486	152	215	304	62
10,000	837	1184	1674	171	242	343	64
12,000	909	1286	1819	186	263	372	64
14,000	982	1387	1965	201	284	402	70
16,000	1050	1486	2101	215	304	430	72
18,000	1114	1575	2227	228	322	455	82
20,000	1174	1661	2349	240	340	480	82

fusion under conditions where the surface concentration of the diffusing element is zero. Table 6.2 lists the amounts of chromium which might have been expected to appear in the fuel salt during ${}^{235}\text{U}$ operations if all the chromium accessible to the salt were oxidized to CrF_2 . It is apparent from these data that generalized corrosion, as inferred from increases in chromium concentration of the fuel salt, was only one-fourth to one-third of that expected from the

diffusion coefficients. By contrast, the apparent corrosion rates that were observed during the initial stages of MSRE operations with ${}^{233}\text{U}$ fuel and again in the beginning of run 19 were approximately 5.4 and 3.84 times as rapid as predicted using a diffusion coefficient of 2×10^{-14} cm²/sec. Such rates were inconsistent with previous observations and more rapid than the maximum allowed by the maximum value observed for the diffusion coefficient, 4×10^{-14} cm²/sec. Since the

rates of corrosion on these occasions were unlikely to be permitted by chromium diffusion, it seems likely that bulk diffusion involving other constituents of the alloy was operative.

From the following argument it is concluded that the anomalously rapid corrosion during these periods and occasionally during ^{235}U operations was caused by contaminants introduced into the fuel system during periods of maintenance.

6.2 Corrosion in Prenuclear Operations

As noted in Chap. 2, chemical analyses were performed concurrently in the General Analysis Laboratory and in the High-Radiation-Level Analytical Laboratory with salt samples removed from the MSRE during the period before nuclear operations began. This procedure reflected that a slight operational bias existed in the results of the two laboratories⁸ for some of the species and enabled us to use those biases as correction factors for assessment of changes in the salt. With respect to chromium analyses as a corrosion indicator, the data corrected by this factor showed that at the average value of its concentration, 37 ± 7 ppm, no change in the chromium concentration of the fuel circuit salt had occurred throughout the period ending with the completion of the zero-power experiments. In

the low-power experiments following the first maintenance period, during which time the pump rotor was removed for examination, the new average value of chromium in the fuel salt was 48 ± 7 ppm. Since the standard deviations for these two values overlap, it can be inferred that the flushing operation preceding the low-power operation (run 4) effectively removed corrosion-inducing contaminants that might have entered the system during the maintenance period.

6.3 Corrosion in Power Operations

In Fig. 6.3 the results of all chemical analyses of fuel salt samples for chromium are summarized for power runs. The scattered data are described most simply as increasing linearly with time and correspond to an increase in chromium concentration in the salt at a rate of 12 ppm per year. Statistical analyses of the individual groups of data, however, indicate that the average values (least-squares method) are as listed in Table 3.3.

In operation of the reactor with ^{233}U fuel, the concentration of chromium in the samples of fuel salt increased sharply only during two periods, during the initial stages of run Nos. 15 and 19. One interpretation of these analytical results is that corrosion rates exceeded those predicted by diffusion data only after

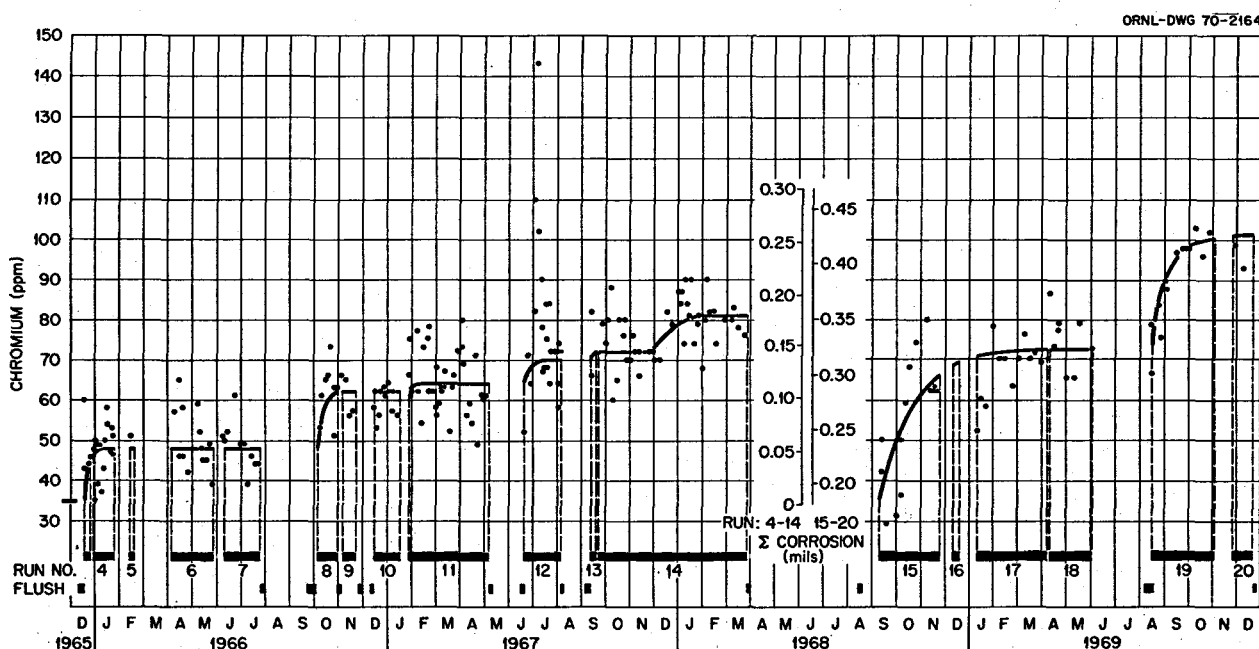


Fig. 6.3. Corrosion of the MSRE fuel circuit in ^{235}U and ^{233}U power operation.

some specific event. A significant increase in the concentration of chromium in fuel salt samples was noted only during the *initial* stages of runs Nos. 4, 8, 12, 15, and 19, with an apparent increase partway through run No. 14. In the beginning periods of run Nos. 4, 8, 12, 15, and 19, we find that in each instance a common set of circumstances existed: the reactor core vessel had been opened previously, either for maintenance or to exchange test arrays positioned within the graphite moderator. Although reasonable measures were adopted to minimize the amount of airborne contaminants that might be introduced into the system during these periods, the possibility that significant amounts of oxidants were introduced into the open vessel cannot be excluded. During the first period of power operation, when a significant temperature differential was imposed on the circuit for the first time (run 4), some corrosion was anticipated as the $\text{Cr}^0 + 2\text{UF}_4 \rightleftharpoons \text{CrF}_2 + 2\text{UF}_3$ equilibrium reaction adjusted to the temperature profile of the circuit. Under these conditions the increase in the concentration of chromium in the fuel salt could have resulted from the establishment of the equilibrium reaction and was not necessarily a signal of the presence of oxidizing contaminants.

The increase in the concentration of chromium in the fuel salt well after run 14 began (see Fig. 6.3) seems to be inconsistent with the premise that external contaminants were the principal cause of corrosion. However, in the period preceding run 14 part of the graphite and metal specimens in the core were removed and replaced. It seems quite possible, therefore, that the residual concentration of reductant which was generated within the fuel salt during run 12 was sufficient to offset the combined oxidizing effects of whatever contamination was incurred during shutdown and that characteristic of the fission reaction⁵ only through the early part of run 14 and that the subsequent rise in chromium concentration represents the normal compensating shift in the equilibrium corrosion reaction. Generally, it is assumed that the contaminant most likely to be responsible for corrosion is moisture.

The inference that moist air was the corrosion-inducing contaminant calls into question the efficacy of the flush salt. As an agent for removal of adsorbed moisture, molten LiF-BeF₂ flush salt is extremely effective, as demonstrated in numerous laboratory experiments, and unquestionably was an effective moisture scavenger. If an oxidizing contaminant or contaminants were capable of diffusion within the graphite or reacting with species deposited in the surface layers of the graphite, the probability of its removal by brief

circulation of flush salt might be slight; instead it might be released into the salt gradually after the moderator was heated to high temperatures. Thus, oxygen (perhaps as CO), rather than water, seems more likely to be the cause of the observed corrosion. This conclusion is supported by the fact that the scale found on the nickel cages which were used to expose Be⁰ to the salt during run 15 was comprised preponderantly of iron, whereas on other occasions the principal structural metal in such scales was chromium. Results of chemical analyses showed that the prior fuel reprocessing treatment was effective in reducing the concentration of chromium in the salt from 133 to 34 ppm and of iron from 174 to 110 ppm. The effectiveness of the reprocessing operations in reducing Cr²⁺ precludes the likelihood that significant amounts of Fe²⁺ were delivered to the fuel circuit from the chemical reprocessing plant. The reduction of Fe²⁺ to Fe⁰ by Be⁰ suggests rather that Fe²⁺ was generated after the beginning of fuel circulation by an oxidizing contaminant contained in the closed fuel circuit. As increasing amounts of Be⁰ were added to the salt mixture, the ratio of metallic Fe/Cr found on the nickel metal cages was reduced until a normal balance was reestablished and corrosion ceased (see Tables 6.3 and 6.4).

Laboratory studies of the stability of FeF₂ have led to the conclusion that at equilibrium little or no Fe²⁺ should exist in the MSRE fuel (see Sect. 2.4.7). The results of these tests confirmed that, of the structural metal impurities in the melt, iron and nickel persist almost entirely as metallic species. The results of other laboratory studies, particularly those concerned with the reduction of Fe²⁺ by hydrogen,⁹ suggest that even in concentrations as large as was found by Manning, the presence of divalent iron was likely to have resulted from reoxidation after transfer and remelting of the salt samples. Subsequent laboratory tests with the MSRE fuel were precluded by the generation of fission products in the salt.

Appraisal of the premise that maintenance operations might possibly permit the ingress of enough oxygen to account for the analytical results requires the following considerations. The cumulative amount of oxidation introduced into the fuel salt (during both ²³⁵U and ²³³U operations) based on the increases of chromium at the beginning of run Nos. 8, 12, 15, and 19 and on the apparent losses of UF₃ at the end of runs 7, 18, and 19 amounts to 51.31 equivalents, or 410.5 g of O²⁻, and corresponds to a cumulative exposure of ~50 ft³ of air. During ²³³U operations, the amount of oxygen entering the salt might have been expected to increase the concentration of oxide by 83 ppm, in excess of the

Table 6.3. MSRE fuel salt analyses, run No. 15

Sample	Be^0 added (g)	Weight percent				% M/ Σ Fe + Cr + Ni		
		Be	Fe	Cr	Ni	Fe	Cr	Ni
Carrier, before Zr^0 addition		0.0380	0.0460	0.0180		3.72	45.2	17.6
Carrier, after Zr^0 addition		0.0110	0.0034	<0.0010		71.4	22.0	6.5
FP-15-7	10.08							
Scale from Ni cage		12.0	0.106	8.03		59.7	0.53	39.8
FP-15-30	8.34							
Scale from Be^0 rod		Σ mg:	(31.1)	(42.8)	(11.2)	36.5	50.3	13.2
Scale from Ni cage		Σ mg:	(96.1)	(4.93)	(21.2)	78.6	4.0	17.4
FP-15-62	9.38							
Loose particles		6.06	3.83	3.75	1.44	42.5	41.6	15.9
Scale from top		6.29	4.72	3.26	4.71	37.2	25.7	37.1
Scale from cage		7.34	2.74	4.53	0.096	37.2	61.5	1.3
Salt average, 11/23/68	6.59	0.0140	0.0067	0.005		55	26	19

Table 6.4. Relative fractions of Fe^0 and Cr^0 reduced from MSRE fuel salt in run No. 15

Sample No.	Equivalents of Be^0 added	Corrosion rate (mils/year)	Fe^0/Cr^0 on nickel cage ^a
FP-15-7	2.24	0.88	113
FP-15-30	4.09	0.54	19.5
FP-15-62	6.17	0.35	0.61

^aAverage Fe/Cr in carrier salt was 2.24 at the inception of run No. 15.

sensitivity limits for the analytical method and well above that observed. It must be recalled, however, that early in ^{235}U power operations the concentration of O_2^- , as measured experimentally, declined from 120 to 60 ppm, suggesting that under power operation O_2^- is partially removed from the salt as a volatile species. It may be concluded, therefore, that the corrosion observed in the MSRE is likely to have been caused as described above but that the mechanism has, as yet, not been demonstrated unequivocally.

The rationale proposed above has several implications concerning the behavior of the MSRE during ^{233}U operations. During the first 16 hr in which fuel salt was circulated at the beginning of run No. 15, the salt did not transfer to the overflow tank and behaved as though it contained a negligibly small bubble fraction. Thereafter, Be^0 was introduced, and the bubble fraction began to increase; with further exposures of the salt to Be^0 the fraction varied erratically.¹⁰ Certainly the Be^0 reduced the surface tension and thereby allowed easier transport of gas from graphite to salt, followed probably by oxidation of the metallic iron impurity, which acts as an oxidant to the circuit walls.

Corrosion would continue until the oxidants were consumed. The model of corrosion proposed here has a relation to the changes in bubble fraction. The corrosion data suggest that with respect to its physical and chemical properties, the fuel did not achieve a reference state until the beginning of run 17. That its bubble fraction then was greater than observed in ^{235}U operations probably was related principally to its lower density.

The probability that atmospheric oxygen was the primary causative agent of corrosion in the MSRE was discounted by Grimes in the following appraisal of the observed behavior:¹¹

We find no evidence whatsoever that air was introduced into MSRE during its periods of normal high temperature operation. There is, on the other hand, no doubt that air in appreciable quantities was admitted to this reactor system during shutdowns when the reactor circuit was at temperatures of 300°F or below. Only a small fraction of the oxygen admitted at such low temperatures should have reacted with the reactor metal and should have been available to cause subsequent corrosion. Flushing of the reactor circuit with helium during the reactor heatup should have removed most of the unreacted air (oxygen). Moreover, use of the flush salt before admission of the fuel should have removed some (and perhaps a large fraction) of the reacted oxygen. However, some oxidant was admitted, and some corrosion from this source probably occurred in MSRE. The evidence suggests that corrosion from admitted air must have been a small fraction of the minor amount which took place.

Since a detailed description of the corrosion picture in MSRE at all times is not yet available, it is not possible to define the precise amount of corrosion due to ingress of oxygen. It is easily possible, however, to set upper limits upon the amounts of oxygen that could have been involved. These amounts are small. If all the observed corrosion (as evidenced by rise in CrF_2 concentration) in MSRE Runs 1 thru 9 is attributed to ingress

of oxygen the oxide ion concentration of the fuel should have risen by about 11 ppm. If corrosion (by the same indicator) in Runs 10 thru 14 were due to oxygen ingress, and if this oxygen ingress were also responsible for oxidizing all the UF_3 created by the Be^0 added during those runs, the oxide ion concentration of the fuel should have risen by about 25 ppm. During the entire sequence of runs with $^{235}\text{UF}_4$, therefore, all the chemically observed corrosion could be due (it seems very certain that it was not) to the ingress of oxygen resulting in less than 40 ppm of added oxide ion in the fuel. Our systematic chemical analyses for O^{2-} in the MSRE fuel showed no evidence of such an increase. MSRE was provided with no mechanism intended to remove O^{2-} , and we have been unable to postulate — much less to demonstrate — an inadvertent mechanism for O^{2-} removal. Our methods for determination of O^{2-} might possibly fail to find this <40 ppm increase. It seems much more plausible, however, that the actual increase in O^{2-} was a small fraction of this figure and that the observed corrosion was due to oxidation of chromium by UF_4 through mechanisms similar to those postulated from many years of testing. It is true that we have drawn detailed curves of the chromium behavior of the individual MSRE runs with $^{235}\text{UF}_4$, and we have been tempted to speculate about them. However, the marked scatter in the chromium data gives such curves little or no statistical significance.

Rise in the chromium concentrations in MSRE Runs 15 thru 19 (that is in the runs fueled with $^{233}\text{UF}_4$) was more dramatic and the initial increases were almost certainly more statistically significant. Several pieces of evidence suggest that the $^{233}\text{UF}_4$ fuel, which by virtue of reuse of the carrier salt was necessarily less well characterized and probably less pure than was the $^{235}\text{UF}_4$ initial fuel charge, was relatively oxidizing. This may have been due to oxygen ingress and oxidation of the MSRE metal surfaces during the long fuel-change shutdown between Run 14 and Run 15. If all the corrosion during Runs 15 thru terminal Run 19, again as adduced from increases in chromium concentration of the fuel and allowing for oxidation of all reductant added, is attributed to admitted oxygen, the oxide ion concentration of the fuel should have increased by some 45 ppm; this increase, again, seems conceivable but unlikely.

In summary, the corrosion picture shows that the quantity of oxide ion which could have entered the fuel during the whole MSRE operation (involving 20 separate shutdowns) was less than 100 ppm. It seems virtually certain that the actual amount which entered was much less than this. The ZrF_4 present in this fuel would have prevented precipitation of appreciable UO_2 even if much larger quantities had entered; oxide ion at the maximum levels suggested above would not have precipitated ZrO_2 . Subsequent corrosion of the reactor circuit through ingress of oxygen would, however, not have been prevented (or appreciably affected) by the presence of ZrF_4 in the MSRE; this would be equally true for ZrF_4 in the MSBR fuel.

It has been postulated that one of the principal reasons for the expectedly low corrosion observed is that the metal surfaces of the fuel circuit have been covered with a film of the noble-metal fission products Nb, Mo, Tc, and Ru about 10 Å thick. Results of electron microprobe analysis of the metal surveillance specimens¹² removed from the MSRE in May 1967 lend support to this view in that they did not reveal any

change in chromium concentration below a depth of 10 μ , the limit of measurement, as do the results of electron microscopic investigation of the specimens,¹² which indicated that the surface was covered to a depth of several thousand angstroms by those metals. Although the postulate of a dynamically produced and autoregenerative noble metal film is an attractive rationale of the very low corrosion observed in ^{235}U operations, it fails when the behavior of the MSRE during the early stages of run 19 is considered. Here, rapid corrosion was proceeding concurrently with the generation and presumably the deposition of the same noble metal fission products which seemed earlier to have restricted the corrosion of the fuel circuit walls.

Another hypothesis has been suggested recently by Grimes¹³ as an alternate rationale of data that indicate the almost complete absence of corrosion during extended periods of operation, while at other times rates were more rapid than could be accounted for by diffusion-controlled mechanisms. It presupposes that the presence of UF_3 in the fuel salt does not counter the corrosion of Hastelloy N effectively once the concentration of Cr^{2+} in the salt has risen to a level of ~70 to 80 ppm. Rather, at concentrations of this order and in the presence of the intense radioactive flux in the reactor core, chromium carbide, Cr_3C_2 , is formed at the surfaces of the graphite moderator. The formation of such a phase thus causes the graphite moderator to act as a sink for chromium and promotes corrosion of the container alloy at the most rapid rate allowed by the diffusion coefficient of chromium. If such a mechanism operates, the difference in the chromium concentration as observed in the fuel salt samples and the maximum possible concentration represents the quantity of chromium which was deposited at the surface of the moderator graphite. On occasions when the oxidation potential of the salt increased substantially, this carbide coating would then decompose and release large amounts of Cr^{2+} to the salt, thus causing rapid changes in the concentration of chromium in the salt samples submitted for chemical analysis to suggest that the corrosion rate was increasing rapidly. This hypothesis is attractive for a variety of reasons: (1) it implies that throughout the operation of the MSRE the corrosion rate was invariant and diffusion limited; (2) the $[\text{UF}_3]/[\text{UF}_4]$ remains so low in such systems at all times that attempts to repress corrosion in MSBR fuels by external adjustment of the $[\text{UF}_3]/[\text{UF}_4]$ are needless, as well as the previously foreseen need to develop in-line analytical methods for its determination; and (3) the hypothesis provides a rationale for the otherwise inexplicably low rates of corrosion which

seemed to characterize operations of the MSRE with ^{235}U fuel.

It seems unlikely that significant quantities of chromium carbides will have formed on the moderator graphite surfaces for the following reasons:

1. In run No. 15, the principal constituent of the slag found on the nickel cages used for the introduction of beryllium was iron (see Sect. 6.7). Presumably, this iron deposit was formed by reduction of Fe^{2+} from the melt and represents a condition in the melt which is so oxidizing that, if present, the relatively unstable compound Cr_3C_2 ($\Delta G_{1000^\circ\text{K}} = -23 \text{ kcal}$) should have decomposed completely during this period. The possible amount of chromium which should have been released to the fuel salt by such decomposition, as calculated using diffusion coefficients from 1×10^{-14} to $4 \times 10^{-14} \text{ cm}^2/\text{sec}$, would increase the concentration of chromium in the fuel salt to values of 240 to 480 ppm (see Table 6.2), that is, to much higher concentrations than were observed at any time during MSRE operations.
2. The coincidence of apparently stepwise increases in Cr followed maintenance periods (as noted previously).
3. The carbides of niobium are more stable than is Cr_3C_2 ; in ^{233}U operations the oxidation potential of the salt increased gradually during runs by fission to the point that niobium entered the salt (see Sect. 6.5) and was subsequently reduced and removed from the salt by Be addition; under these conditions, Cr_3C_2 should have become reoxidized, entered the salt, and increased the chromium concentration of the samples sharply, where, in fact, no perturbation of the average concentration of chromium was noted.

In postoperational examinations with one of the stringer bars from the reactor core, a search was made to ascertain whether or not a coating of chromium carbides adhered to the surface. No evidence of such a coating was found.

A surprising result of the postoperational tests performed with specimens of the MSRE control rod thimbles was the observation of anomalous intergranular penetration of the alloy which had been exposed to the fuel salt. Occasionally, inspection of Hastelloy N specimens removed from the reactor core showed grain boundary cracks at the surfaces of specimens subjected to tensile tests. These cracks appeared in material strained at room temperature, which is not normal for Hastelloy N, but they penetrated only a few mils and

had no detectable effect of the mechanical properties of the specimens. The cracks in the control rod thimbles, however, were deeper than previously observed, at some locations as deep as 7 mils,¹⁴ some ten times the depth of the generalized attack indicated by changes in the concentration of chromium in the fuel salt. Curiously, several fission products, preponderantly tellurium, had penetrated to depths comparable with those of the cracks.

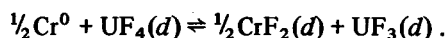
It is not possible to ascribe this attack to radiation effects per se, for in-pile tests with salt-graphite-alloy assemblages prior to tests with the MSRE showed no corresponding effects. These unpredicted results have caused a renewal of the investigation of materials removed from the MSRE, with the initial objectives to determine if fission products are indeed the cause of grain boundary separation.

While the initial results seem to implicate tellurium as a causative agent, its role is not positively identified. One mechanism, proposed before tellurium was believed to have deposited preferentially, relates the attack to impurities in the following way. Electron microscopic examinations of Hastelloy N show typically that an unidentified group of complex phases comprised of Mo, Cr, C, N, and B, morphologically similar to face-centered M_2C carbides, are deposited preferentially at intergranular surfaces. It is also observed that the loss of ductility that occurs with Hastelloy N after irradiation correlates with more pronounced intergranular fracture. Such behavior very possibly means that the chemical activity of the carbide-like phases deposited in these locations is increased. If so, it would not be surprising to find that these phases were highly susceptible to oxidative corrosion. It was noted previously that two unusually oxidative regimes occurred in the MSRE, at the beginning of run 15 and again at the beginning of run 19. In an earlier assessment of corrosion of the MSRE fuel circuit we have deduced that the most probable oxidant at those periods was atmospheric oxygen.¹⁵ We reach the tentative conclusion, therefore, that the intergranular attack noted was a result of attack by oxygen on the carbide-like phases deposited at intergranular surfaces. If oxygen were released from the moderator, as suggested previously, the first metal which it might contact would be the control-rod thimbles. It seems likely, therefore, that the intergranular penetration observed in the postoperational tests resulted from the development of unusually oxidative conditions in the MSRE and is atypical of normal reactor behavior. The overall results of corrosion surveillance in the MSRE, while not totally

unequivocal, appear to indicate that corrosion behavior in molten-salt reactors can properly be anticipated to be negligible over the planned use period of these reactors. Furthermore, the probability of recurrence of the anomalous penetration in future reactors can be assessed in tests with the modified alloys which are currently under development and which will contain a group of carbides perhaps unlike those found in the MSRE alloy.

6.4 Additions of Reductants and Oxidants to the Fuel Salt

As discussed earlier in this report (Sect. 6.3) the fuel salt, free of moisture and HF, should remove chromium from Hastelloy N only by the equilibrium reaction



When the above corrosion equilibrium was first established in MSRE power operations, the UF_3 produced in this reaction, together with that originally added to the fuel concentrate, should have totaled 1500 g, with the result that as much as 0.65% of the uranium of the system could have been trivalent soon after the beginning of power operation. The UF_3 content of the MSRE fuel was determined after approximately 11,000 MWhr of operation to be no greater than 0.05%. The fuel salt was considered to be far more oxidizing than was necessary and certain to become more so as additional power was produced unless adjustment was made in the UF_3 concentration. A program was initiated early in 1967 to reduce 1 to 1.5% of the uranium inventory to the trivalent state.

On the basis that it met chemical criteria and that its introduction into fuel salt could be accomplished conveniently, beryllium metal was selected as the most suitable substance to use for in-situ reduction of U(IV) in the fuel salt. Results of laboratory tests had shown that the metal would be sufficiently reductive to require exposure for conveniently short periods of time but was not so reductive as to cause concern that it might reduce U(IV) to the metallic state. The pure material was available in forms that were easily accommodated for use with the sampler-enricher device, and the metal afforded a maximum of reductive equivalents per unit mass.

Initially, 4 g of beryllium was introduced into the salt by melting a mixture of ^7LiF - BeF_2 carrier salt and powdered beryllium in the MSRE pump bowl sampler cage. Subsequently, three additions were made by suspending specimens of $\frac{3}{8}$ -in.-diam beryllium rods in

the salt in the pump bowl. The capsules used for adding beryllium were similar in size to those used for sampling for oxide analysis but were penetrated with numerous holes to permit reasonable flow of fuel salt. The beryllium rods were found to react with fuel salt at a steady rate, dissolving at approximately 1.5 g/hr. A summary of all the additions of reductants and oxidants introduced into the fuel salt system via the sampler-enricher apparatus is given in Table 6.5.

With ^{235}U fuel salt, all dissolutions of beryllium metal into the fuel salt proceeded smoothly; the bar stock which was withdrawn after exposure to the fuel was observed to be smooth and of symmetrically reduced shape.

No significant effects on reactivity were observed during or following the beryllium additions, nor did the results of chemical analyses indicate that the actual concentration of U(III) had increased until after run 12 had begun (see Table 6.6). The additions preceding run 12 had increased the U^{3+} concentration in the total uranium by approximately 0.6%. Four exposures of beryllium were made at close intervals during the early part of that run. Samples taken shortly after the last of these four exposures (FP-12-16 et seq., Table 3.1) began to show an unprecedented increase in the concentration of chromium in the specimens, followed by a similar decrease during the subsequent sampling period.

Previous laboratory experience has not disclosed comparable behavior, and no well-defined mechanism was available at the time to account satisfactorily for the observed behavior. Speculation as to the cause, partially supported by experimental data, included the following consideration.

On the two occasions when the most rapid rates of dissolution of the beryllium rods were observed, chromium values for the next several fuel samples, FP-11-10 et seq. and FP-12-16 et seq., rose temporarily above the 1σ level and subsequently returned to normal. That the increase in chromium levels in samples FP-12-16 to -19 was temporary indicates that the high chromium concentration of fuel samples removed from the pump bowl was atypical of the salt in the fuel circuit and implies that surface-active solids were in suspension at the salt-gas interfaces in the pump bowl.

That atypical distribution of species in this location does indeed take place was demonstrated earlier by the analysis of sample capsule support wires that were (1) submerged below the pump-bowl salt surface, (2) exposed to the salt-gas interface, and (3) exposed to the pump-bowl cover gas. The results showed that the noble-metal fission products, Mo, Nb, and Ru, were

Table 6.5. Summary of adjustments of $[U^{3+}]/[\Sigma U]$ in the MSRE fuel salt

Date	Sample Number	Reducant or oxidant added		Equivalents of reductant added	$[U^{3+}/\Sigma U]$ (%), nominal
		Form	Weight (g)		
2/13/66	Runs 5-I				0.41
1/1/67	FP-10-14	Be powder	3.0	0.67	0.22
1/3/67	FP-10-16	Be powder	1.0	0.89	0.25
1/4/67	FP-10-18	Be rod	1.63	1.25	0.29
1/13/67	FP-10-23	Be rod	10.65	3.61	0.51
2/15/67	FP-11-10	Be rod	11.66	6.20	0.74
4/10/67	FP-11-40	Be rod	8.40	8.06	0.79
6/21/67	FP-12-8	Be rod	7.93	9.82	0.87
6/23/67	FP-12-9	Be rod	9.84	12.01	1.12
7/3/67	FP-12-13	Be rod	8.33	13.86	1.30
7/6/67	FP-12-15	Be rod	11.68	16.45	1.59
8/3/67	FP-12-56	Be rod	9.71	18.60	1.72
9/15/68	FP-15-7	Be rod	10.08	2.24	0
10/13/68	FP-15-30	Be rod	8.34	4.09	0
11/15/68	FP-15-62	Be rod	9.38	6.17	0
11/20/68	FP-15-66	Be washer	1.00	6.39	0
1/22/69	FP-17-8	Be rod	8.57	8.29	1.19
1/30/69	FP-17-11	Cr rod	4.73	8.48	1.19
4/15/69	FP-18-3	Zr rod	20.24	9.37	0.65
4/26/69	FP-18-7	Zr rod	24.04	10.42	1.19
5/8/69	FP-18-17	FeF ₂ powder	30.00	9.78	0.52
5/15/69	FP-18-23	Be rod	5.68	11.04	1.20
5/20/69	FP-18-28	Be rod	3.17	11.74	1.59
9/12/69	FP-19-25,26	Zr foil	0.62	11.77	0
9/24/69	FP-19-31-4	Zr foil	1.20	11.82	0
10/2/69	FP-19-40	Be rod	2.87	12.46	0.99
10/8/69	FP-19-48	Be rod	4.91	13.55	1.61
10/21/69	FP-19-51	Nb foil	0.018	13.55	1.37
11/29/69	FP-20-7	Be rod	6.974	15.10	1.16
12/9/69	FP-20-22	Be rod	9.894	17.30	2.49
12/9/69	FP-20-22	Be rod	3.019	17.97	2.95

deposited in abnormally high concentrations at the salt-gas interface. Such behavior suggests that the high chromium concentrations in the fuel specimens were caused by the occurrence of chromium in the pump bowl in nonwetted, surface-active phases in which its activity was low. A possible mechanism which would cause such a phenomenon is the reduction of Cr²⁺ by Be⁰ with the concurrent reaction of Cr⁰ with graphite present on the salt surface to form one or more of the chromium carbides, for example, Cr₃C₂ ($\Delta H_f^\circ = -21$ kcal at 298°K). Such phases possess relatively low stability and could be expected to decompose, once dispersed in the fuel-circuit salt.

The possibility that surface-active solids were formed as a consequence of the Be⁰ additions was tested late in run 12 by obtaining salt specimens at the salt-gas interface as well as below the surface. First, specimens were obtained in a three-compartment sample capsule that was immersed so that the center hole was expected

to be at the interface (Fig. 6.4). Next, a beryllium metal rod was exposed to the fuel salt for 8 hr with the result that 9.71 g of beryllium metal was introduced into the fuel salt. Twelve hours later a second three-compartment capsule was immersed in the pump bowl. Its appearance after removal from the pump bowl is shown in Fig. 6.5. Chemical analyses of the fuel-salt specimens FP-12-55 and -57 did not show significant differences in chromium; however, the salt-gas interface in FP-12-57 was blackened as compared with FP-12-55 (Fig. 6.6).

An additional purpose of sampling with the three-compartment capsule was to determine whether foam-like material was present in the sampler area and would be collected in the upper compartment. Globules were noted on the upper part of FP-12-57 (Fig. 6.5), indicating that conditions in the pump bowl were substantially different after beryllium was added to the fuel salt.

Table 6.6. Concentration of UF_3 in the MSRE fuel salt^a

Date	Sample No.	Megawatt-Hours	Uranium Consumed	Uranium Consumed	Net Equivalents of Oxidation	Total Be Added (g)	Net Equivalents of Reductant Added	Net Equivalents of Reductant	$\text{U}^{3+}/\Sigma\text{U} (\%)$	
			(kg)	(moles)					Calculated	Analytical
11/14/66	FP9-14	0	0	2.67	2.14	0	3.13	3.13	0.33	0.33
1/1/67	FP10-14	12,345	0.632	3.23	2.58	3	3.80	0.99	0.10	0.10
1/3/67	FP10-16	14,950	0.766	3.25	2.60	6	4.46	1.22	0.13	0.13
1/4/67	FP10-18	15,050	0.771	3.70	2.96	7.63	4.82	1.80	0.19	0.19
1/13/67	FP10-23	17,100	0.877	3.86	2.96	18.28	7.19	1.86	0.20	0.20
1/15/67	FP10-25	17,852	0.915	3.90	3.08	18.28	7.19	4.11	0.43	0.43
2/6/67	FP11-5	18,050	0.924	4.26	3.10	18.28	7.19	4.09	0.43	0.66
2/15/67	FP11-10	19,712	1.010	4.60	3.40	18.28	7.19	3.79	0.39	0.60
2/22/67	FP11-13	21,272	1.090	4.60	3.68	29.94	9.77	6.09	0.64	0.64
3/28/67	FP11-32	22,649	1.161	4.90	3.90	29.94	9.77	5.87	0.62	0.69
4/10/67	FP11-40	28,342	1.453	6.13	4.90	29.94	9.77	4.87	0.51	0.45
6/21/67	FP12-6	30,900	1.584	6.68	5.34	38.34	11.64	6.30	0.66	0.66
6/21/67	FP12-8	36,055	1.663	7.01	5.61	38.34	11.64	6.03	0.64	0.71
6/23/67	FP12-9	36,055	1.663	7.01	5.61	46.27	13.40	7.79	0.82	0.82
6/29/67	FP12-11	36,416	1.866	7.87	6.30	56.11	15.58	9.28	0.98	0.98
7/3/67	FP12-13	37,400	1.932	8.15	6.52	56.11	15.58	9.06	0.95	1.30
7/13/67	FP12-15	37,856	1.940	8.19	6.55	64.24	17.38	10.83	1.14	1.14
7/13/67	FP12-15	38,345	1.966	8.30	6.64	76.12	20.02	13.38	1.40	1.40
7/13/67	FP12-21	39,500	2.023	8.54	6.83	76.12	20.02	13.19	1.39	1.0
8/3/67	FP12-56	43,872	2.248	9.49	7.59	85.83	22.18	14.59	1.54	1.54
9/15/67	FP13-5	44,781	2.314	9.76	7.81	85.83	22.18	12.42	1.31	1.60
3/26/68	FP14-(F)	72,454	3.743	15.79	12.63	85.83	22.18	9.55	1.01	1.01
9/15/68	FP15-7	0	0	0	0	10.08	2.23	0	0	0
10/13/68	FP15-30	0	0	0	0	18.42	4.09	0	0	0
11/15/68	FP15-62	0	0	0	0	27.80	6.17	0	0	0
11/20/68	FP15-66	0	0	0	0	28.80	6.39	0.22	0.15	0.15
1/22/69	FP17-8	850	0.044	0.19	0.15	37.37	8.29	1.97	1.31	1.31

^aThese numbers assume that the ^{235}U salt originally was 0.16% reduced; that the increase in Cr before initial ^{235}U power operations was real, occurred before 11/14/66, and resulted in reduction of U^{4+} to U^{3+} ; that each fission results in oxidation of 0.8 atom of U^{3+} ; and that there have been no other losses of U^{3+} .

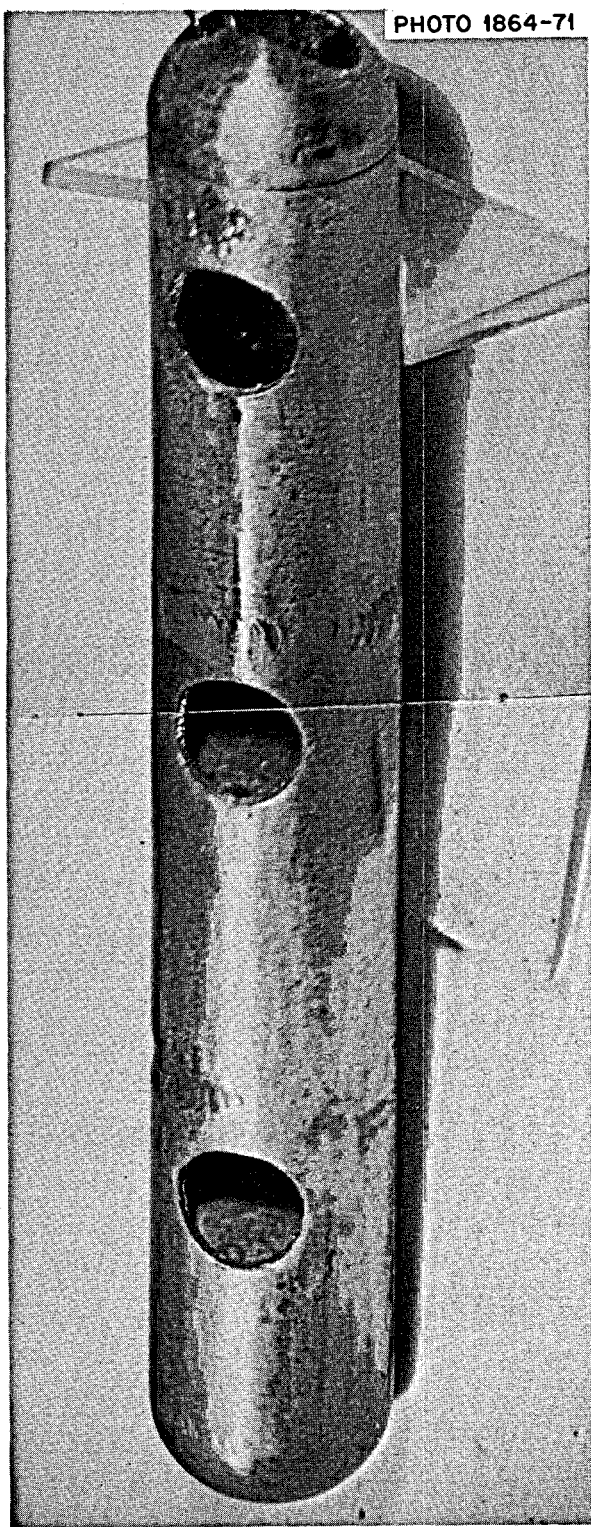


Fig. 6.4. Three-compartment nickel capsule suspended in MSRE pump bowl before exposure of beryllium to ^{235}U fuel salt. August 2, 1967, FP-12-55.

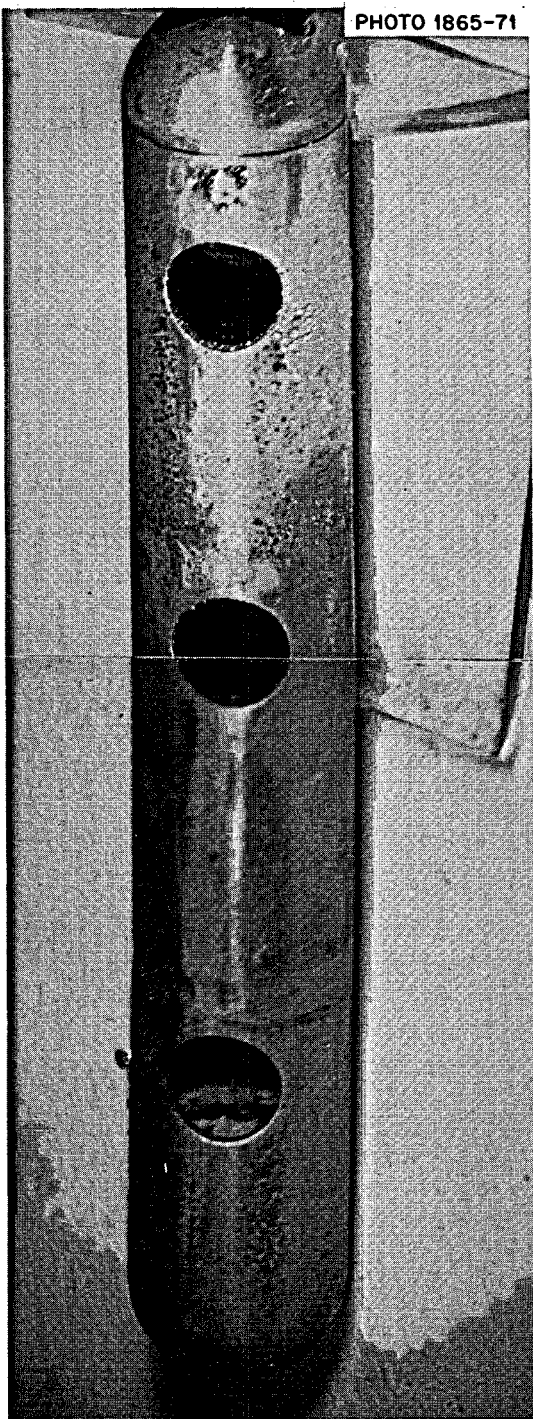


Fig. 6.5. Three-compartment nickel capsule suspended in MSRE pump bowl after exposure of beryllium to ^{235}U fuel salt. August 3, 1967, FP-12-57. Each of the three compartments in the capsules shown in Figs. 6.4 and 6.5 was open to the outside by two holes as shown here. The capsules were positioned approximately so that the center compartment was expected to be at the salt-gas interface to collect surface-active solids. The upper compartment was to serve as a collector of foam if it were present. No appreciable residue was found in the upper compartment.

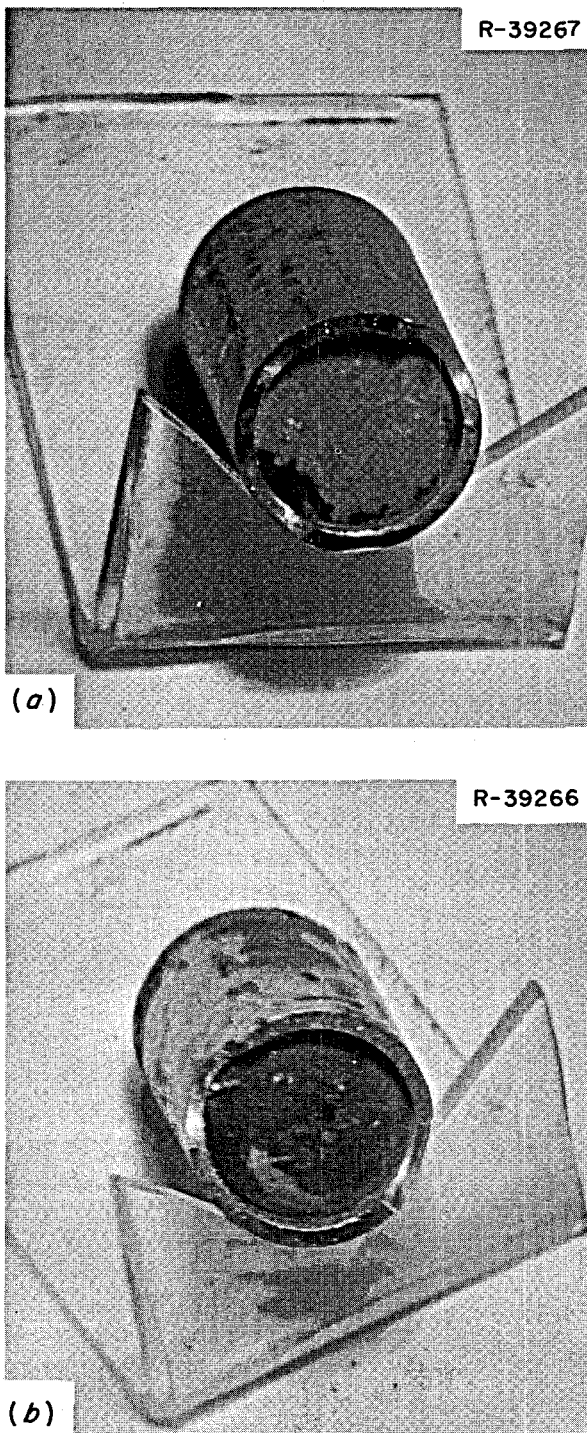


Fig. 6.6. Surface appearance of fuel salt before and after beryllium exposure to ^{235}U fuel salt. (a) FP-12-55, (b) FP-12-57. Salt analyses did not reflect significant differences in chromium concentration nor were they indicative of the identity of the material at the blackened surface.

Examination of the metal basket that contained the beryllium rod while it was exposed to the fuel showed the presence of dendritic crystals along with a small amount of salt residue (Fig. 6.7). Spectrochemical analysis of material removed from the basket (Fig. 6.7) indicated that the material contained 7.8 wt % chromium and less than 10 ppm of iron and nickel.

The evidence obtained did not permit inference as to the identity of the phases which formed within the pump bowl as a consequence of the beryllium additions. It strongly implied that nonwetted flotsam can be formed and accumulated temporarily in the MSRE pump bowl.

During this period, fuel salt accumulated in the overflow tank steadily during operation and remained there in relative isolation from the fuel stream. At intervals of about one day, part of the salt (60 lb) was returned to the fuel stream. Recognizing that chromium might be injected into the pump bowl as the salt returned, we performed an experiment in which salt samples were obtained from the pump bowl within an hour after fuel was returned from the overflow tank to the pump bowl. The purpose of the experiment was to determine whether material from the overflow tank contributed appreciably to the perturbations in the chromium concentration. The results were negative, possibly, in part, because sampling and salt-transfer operations were not performed concurrently for safety reasons.

In view of the mechanism developed recently¹⁶ to account for the transport behavior of the noble metal fission products in the MSRE, we can infer that the exposures of beryllium which generated high concentrations of chromium in the salt samples simply reduced the Cr^{2+} in the flowing fuel salt to the metal, which in turn became a part of the particulate pool of suspended metals at the surface of the salt in the pump bowl. It remained there temporarily, gradually oxidizing to the fluoride as it reacted with the fuel salt.

In their examinations of the behavior of the noble metal fission products, Kirslis and Blankenship¹⁷ did not observe a significant effect of fuel reduction on the noble-metal concentrations in the fuel. The concentrations frequently rose rather than fell, as expected, after adding beryllium. They noted that the ^{99}Mo , ^{103}Ru , ^{106}Ru , and ^{132}Te showed parallel rises and falls. The ^{99}Mo results were extraordinarily high for samples FP-11-8 and FP-11-12. The high values were checked by reruns on fresh samples. If all the ^{99}Mo produced by fission remained uniformly distributed in the fuel, the calculated concentration would be 1.4×10^{11} dis-

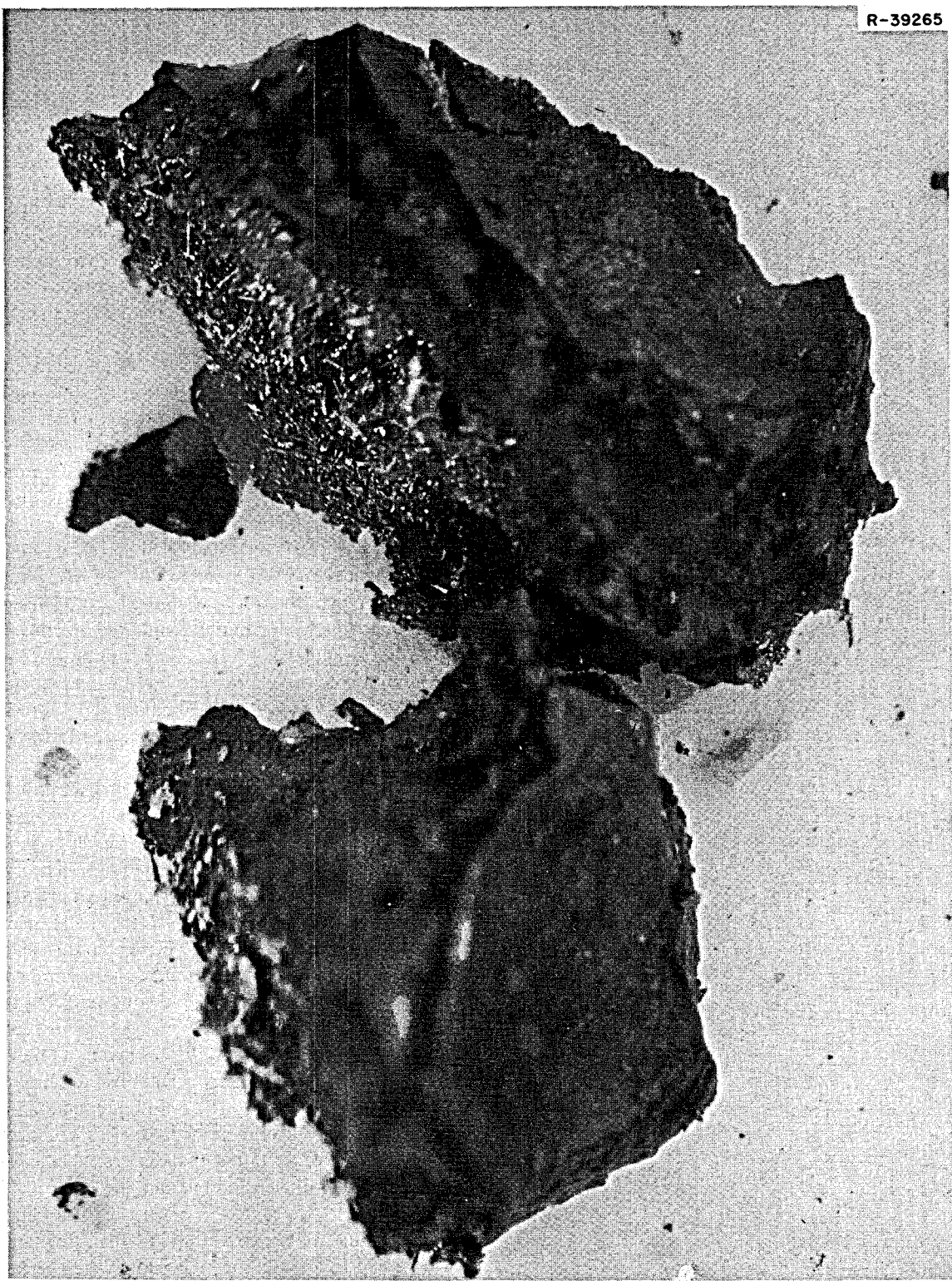


Fig. 6.7. Residue from beryllium addition capsule FP-12-56, August 3, 1967. Capsule was exposed to fuel salt for 8 hr; 9.71 g of Be^0 dissolved. Residue contained 7.8 wt % Cr and less than a total of 10 ppm Fe and Ni.

$\text{min}^{-1} \text{ g}^{-1}$. A calculation showed that if all the ^{99}Mo produced by neutron activation of the ^{98}Mo in the first 0.1-mm thickness of the Hastelloy N reactor containment vessel diffused instantaneously into the fuel melt, the increase in ^{99}Mo concentration would be only about 10^9 dis/min per gram of fuel. It thus appeared that a mechanism was operating which either concentrated fission-produced ^{99}Mo and other noble metals in the pump bowl or resulted in large temporal and spatial variations in their concentrations. Dissolved ^{99}Mo would undoubtedly be uniformly distributed. If the noble metals circulated as a suspension of insoluble metal particles, it was reasoned that they might concentrate in the pump bowl or vary in concentration with pump bowl level, cover gas pressure, and other operating variables. Since clean metal surfaces are not wetted by the fuel salt, there might also be a tendency for metal particles to collect around helium bubbles, which are probably most numerous in the pump bowl.

The ^{95}Nb concentrations varied erratically and did not parallel the behavior of the other noble metals. This was ascribed to analytical difficulties. An unavoidable difficulty was that a large correction for ^{95}Zr decay must be made for each salt analysis.

From the beginning of operations of the MSRE with ^{233}U fuel, the behavior of the fuel salt during and after exposure to the beryllium rods was markedly different than previously observed. A detailed description of the changes in fluid salt and gas behavior during these periods is described in a separate report.¹⁰ Introduction of beryllium metal into the ^{233}U fuel salt apparently caused a major perturbation of salt-gas interactions and resulted in an increase in void fraction of the fuel salt. The exact reasons for development of the greater void fraction that persisted throughout ^{233}U operations have not been completely determined. In addition to the purely chemical effects which resulted from the addition of beryllium and other reductants, other factors such as pump speed, variation in the solubility of inert gases as a function of hydrostatic pressure, difference in density of the ^{235}U and ^{233}U fuel salt, and changes in interfacial tension were recognized to be related. Interaction of beryllium with the fuel salt during run 15 caused a major change in only one physical property of the fuel — its surface tension. This is the most puzzling aspect of the effect of beryllium on the fuel salt in run 15 since the effect was unprecedented in the fuel system. However, slight changes in interfacial energies in fluid systems are known to account for marked changes in hydraulic behavior. Since the addition of beryllium in the early part of the ^{233}U operations effected both chemical and physical

changes concurrently, the exact way in which these changes altered the void fraction of the salt cannot, therefore, be evaluated exactly, although some aspects of the observed phenomenon can be attributed tentatively to the additions.

If, as inferred in Sect. 6.3, atmospheric oxygen was the causative agent for the increased oxidation potential of the salt, release of the gas from the moderator graphite might well have been triggered by a reduction in the salt-gas interfacial tension, resulting in an increase in the bubble fraction of the salt.

Photographs of the cage assemblies removed from the fuel pump bowl after exposure to the fuel salt are shown in Figs. 6.8–6.23. While none of these cages appeared to have been wetted by salt during ^{235}U operations, each of those removed after treatment of the ^{233}U salt showed evidence that salt had wetted the nickel cage and had adhered to it. A typical example is shown in Fig. 6.17. The presence of bubbles is suggested by the appearance of the upper part of capsule FP-17-8 (Fig. 6.17), on which structures of collapsed bubbles seem to be visible.

Of particular significance to the interpretation of the behavior of the fuel salt from August 1968 to January 1969 are the changes in the relative amounts of iron and chromium contained in the deposits on the nickel cages that were used to suspend beryllium into the pump bowl (Table 6.5). From this and other chemical evidence we deduced that corrosion in the fuel circuit was not checked until early in 1969. By that time, the bubble fraction in excess of that observed in ^{235}U operations was reduced to a fraction that could in general be accounted for by the other factors mentioned above. It may be speculated that the coincidence of the disappearance of reactivity blips with reestablishment of the expected ratio of structural metal fractions in the residues adhering to the nickel cages was indicative of the removal of the last fraction of anomalous excess of bubbles in the fuel salt.

Among the conjectures advanced to account for the excessive rates of salt transfer during this period was one based on the recognition that sharp gradients in the density profile of the fuel salt in the pump bowl existed; from this it was suggested that voluminous amounts of foam were developed in the pump bowl. There was no evidence that such foam had existed in ^{235}U operations, but rather that a salt mist was present in the pump bowl. Indication that such a mist existed was obtained by suspension of a cage-rod assembly of nickel into the pump bowl during run 14. Photographs of the assembly after removal from the pump bowl (Fig. 6.10) show that the surfaces of the rod exposed to

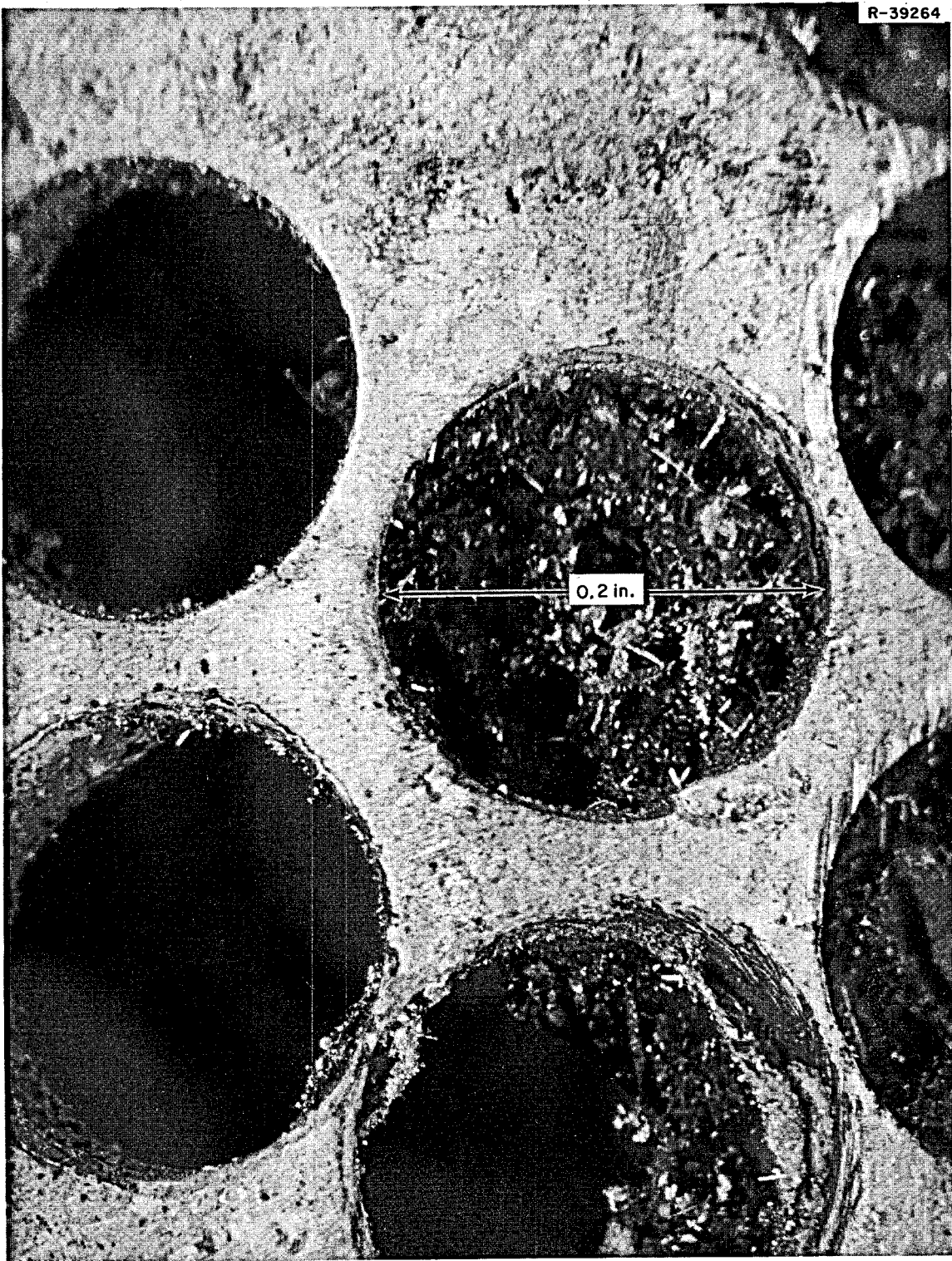


Fig. 6.8. Dendritic crystals and salt on basket of nickel capsule used to expose beryllium to ^{235}U fuel salt. August 3, 1967,
FP-12-56..

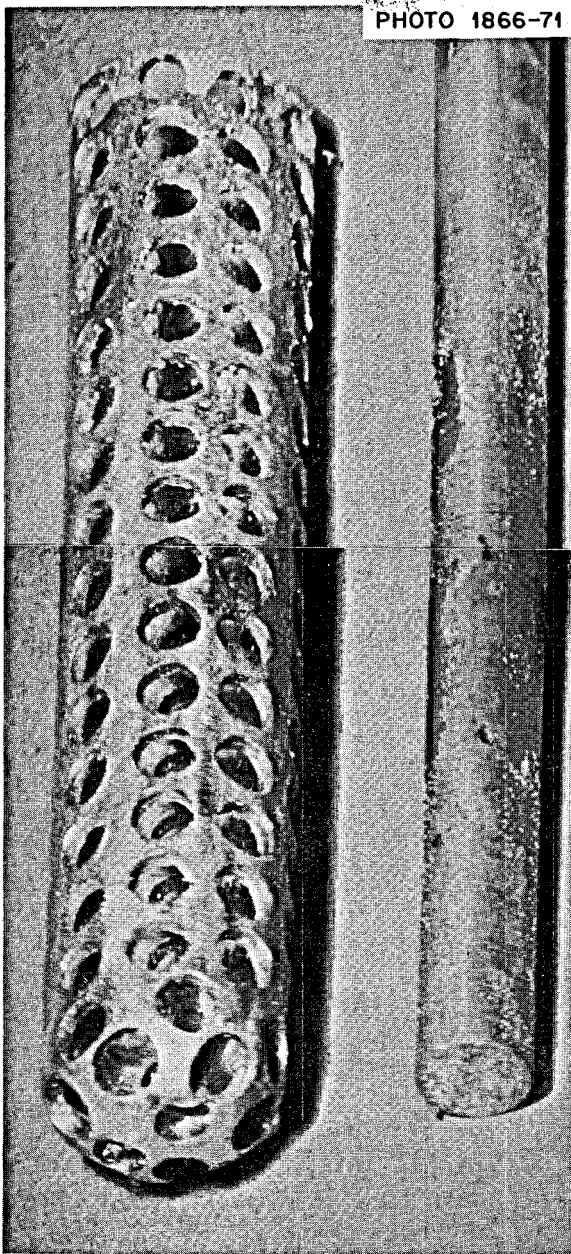


Fig. 6.9. Appearance of nickel basket and rod after suspension in MSRE fuel salt for 2 hr. FP-14-55.

the vapor just above the salt were coated with condensed droplets. Although the vapor space in the sample shroud was probably more quiescent than that in the pump, it was reasoned that foam should also appear here if it were prevalent in the pump bowl.

Attempts to produce foam were performed in the laboratory¹⁸ but were unsuccessful. Tests for foam production consisted of measurements of the fuel salt level in a 10-in.-diam nickel vessel at intervals during the reduction of essentially all of the uranium to its trivalent state and after stepwise oxidation of the nickel with nickel fluoride. Melt levels were determined by the abrupt change in electrical resistance noted as the insulated nickel rods made contact with the salt mixture. Without exception, the tests showed no evidence of the development of a foam either by increasing or decreasing the oxidation potential of the salt.

In an attempt to identify other possible agents which might cause development of foams in fluoride melts, Kohn and Blankenship¹⁹ tested the effect of each of the additives: carbon dust, graphite powder, beryllium metal, finely divided nickel metal, and pump oil vapor. They were unable to promote the development of stable foams with any of these additives in clean melts. Foams were formed only by introducing enough water into the melt, either in the sweep gas or by adding solid hydrates, to give a definite cloudiness. Even so, the foam would collapse very quickly after the purge gas stream was removed.

The phenomena observed in run 15 and later remain as puzzling because the opportunity to perform realistic tests to resolve unanswered questions was lost with the termination of operations of the reactor. It appears that development of a void fraction of unprecedented magnitude took place during a period of rapid corrosion of the containment system and that contaminants which entered the core of the reactor while it was exposed to the atmosphere during maintenance were the source of the corrosion. These contaminants markedly affected the interfacial energies of salt-metal, salt-gas, and salt-graphite surfaces but did not generate foam in the fuel circuit. The conditions which allowed these events to occur are avoidable and are atypical of the operating procedures that are projected for future MSR's.

Additional investigation of the physical properties of molten salts will be necessary to establish quantitatively the relationships of interfacial energies in salt systems to the retention of and stability of bubbles in flowing streams. The initial stages of these investigations can properly be carried out in the laboratory; however, the results may prove to be irrelevant unless the effect of highly radioactive fluxes on the properties is shown to be inconsequential.

PHOTO 1867-71

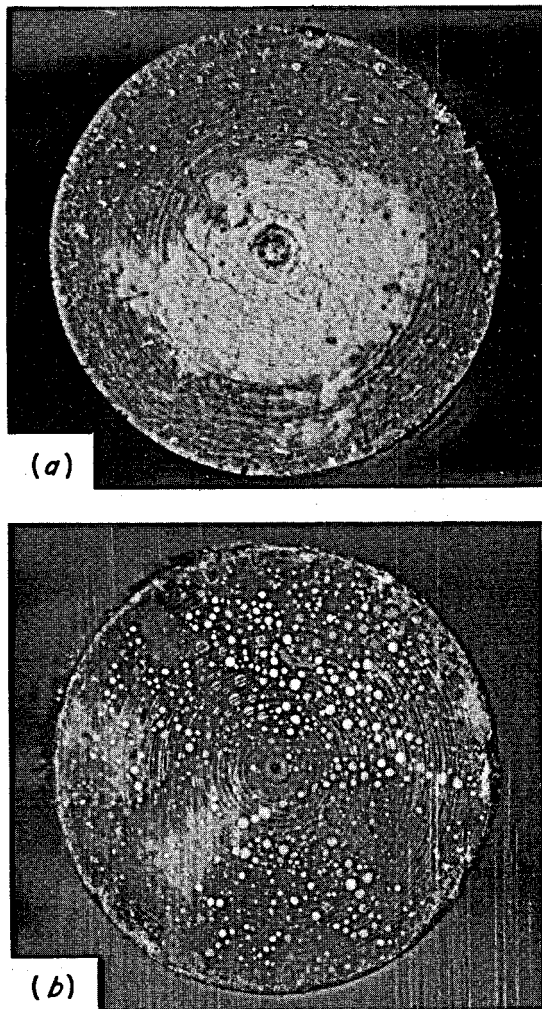


Fig. 6.10. Appearance of nickel rod from FP-14-55 after suspension in MSRE pump bowl for 2 hr. (a) Upper end, (b) lower end.

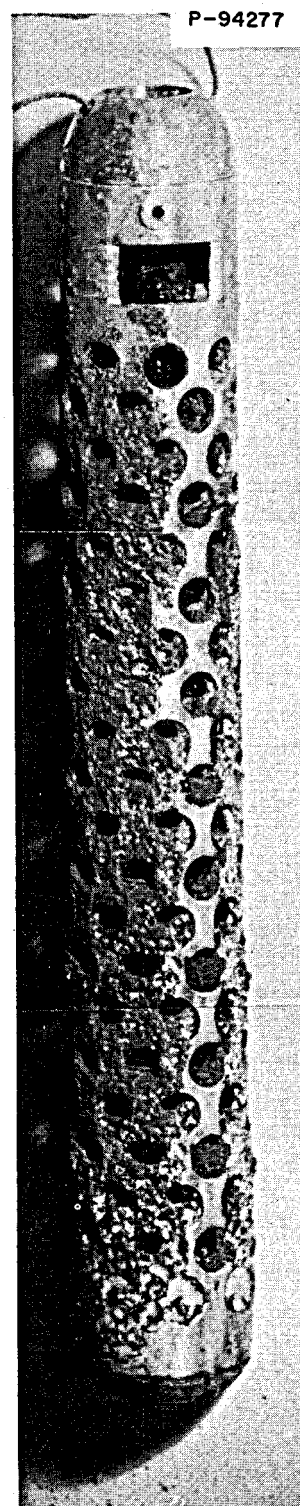


Fig. 6.11. Nickel cage after second exposure of beryllium to ^{233}U fuel salt. October 13, 1968, FP-15-30; 8.34 g Be^0 dissolved from Be rod.

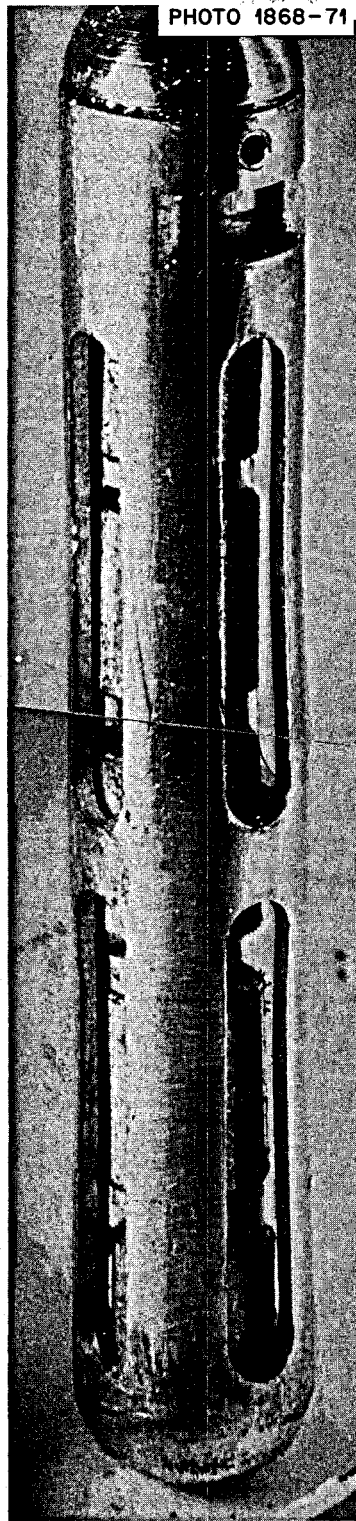


Fig. 6.12. Copper capsule containing several short magnets before exposure to ^{233}U fuel salt.



Fig. 6.13. Metallic particles on copper capsule used to expose a magnet to ^{233}U fuel salt. November 15, 1968, FP-15-61. Dendrites on capsule were composed of fine particles of iron.

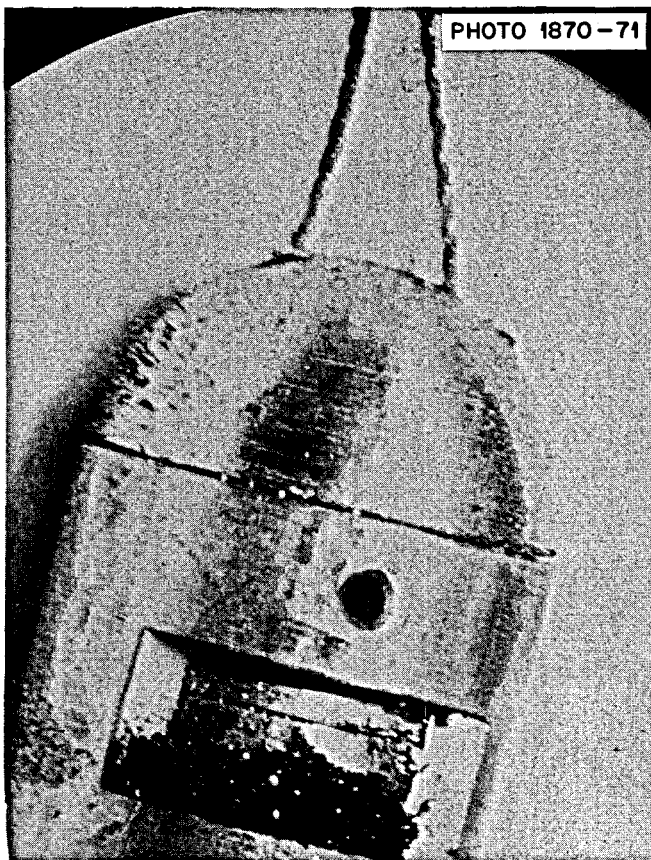


Fig. 6.14. Upper end of magnet capsule FP-15-61 showing collected material.



Fig. 6.15. Copper capsule used to expose beryllium and magnets simultaneously. November 20, 1968, FP-15-66; 1 g Be⁰ dissolved from beryllium metal spacers.

PHOTO 1872-71

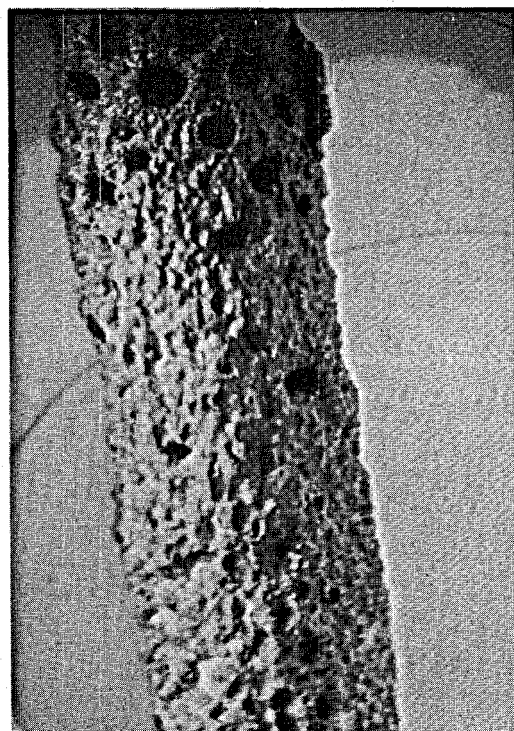
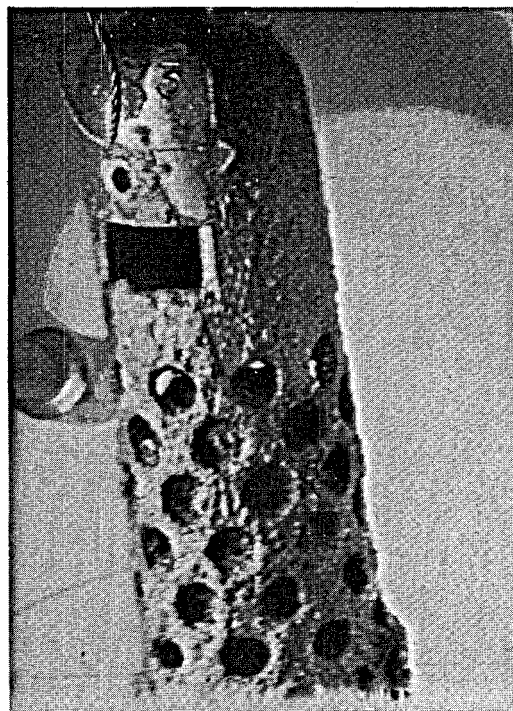
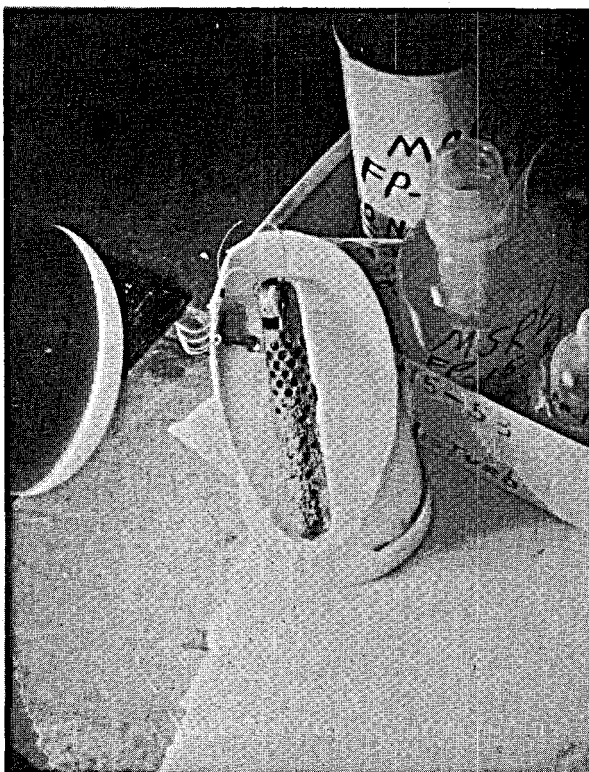


Fig. 6.16. Nickel cage from third beryllium exposure in ^{233}U fuel salt. November 15, 1968, FP-15-62; 9.38 g Be⁰ dissolved from rod.

PHOTO 94278

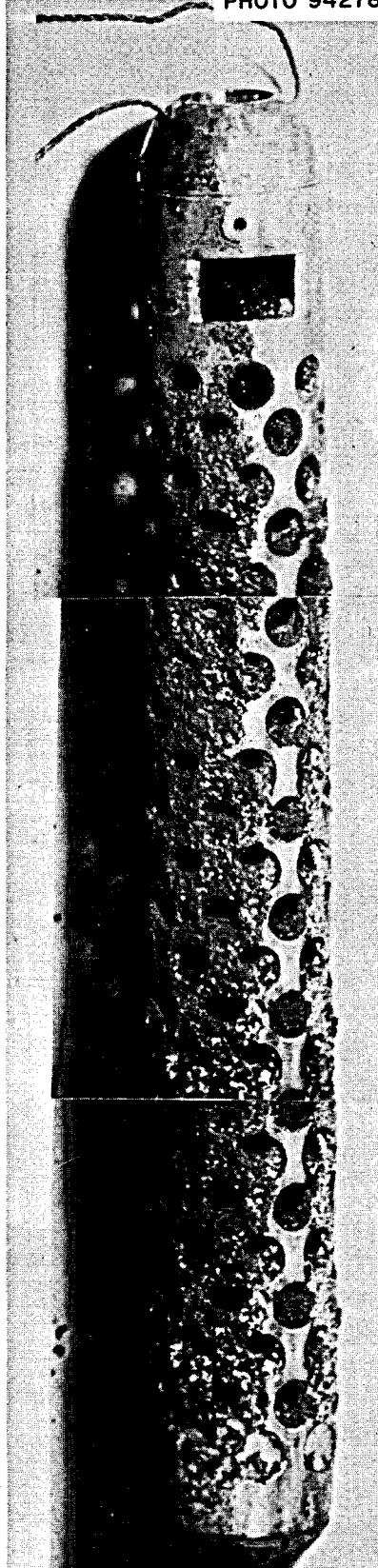


Fig. 6.17. Nickel cage after fourth exposure of beryllium to ^{233}U fuel salt. November 15, 1968, FP-17-8; 8.57 g of Be^0 dissolved from rod.

PHOTO 94273

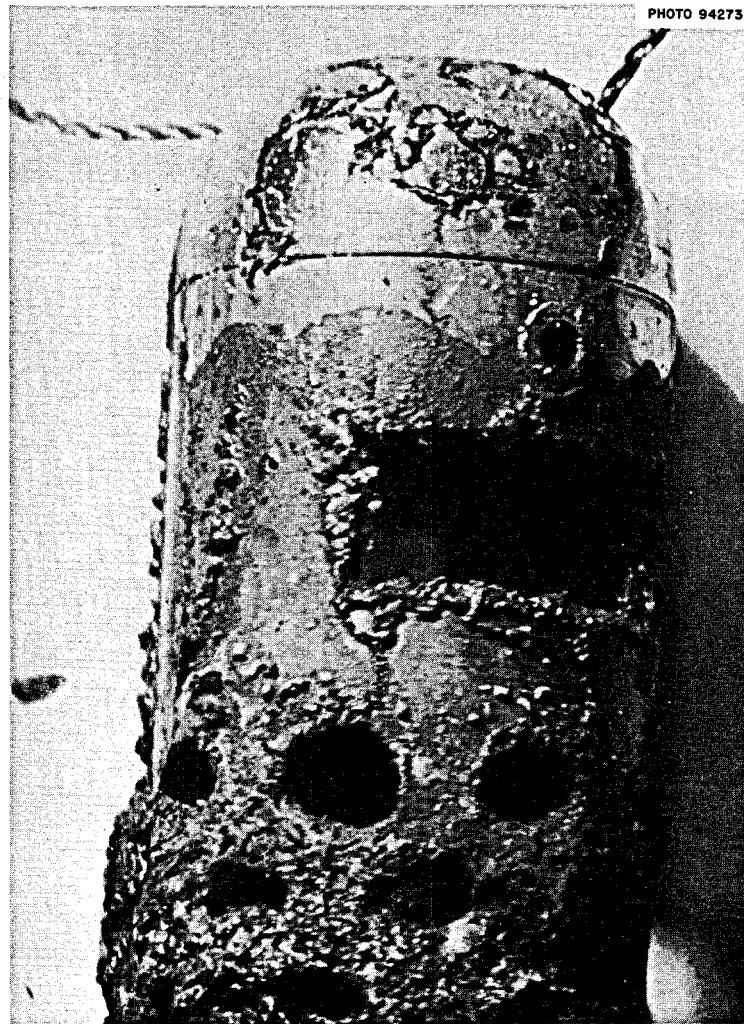


Fig. 6.18. Top of nickel cage from fourth beryllium exposure in ^{233}U fuel salt. January 22, 1969, FP-17-8; 8.57 g Be^0 dissolved from rod. After leach treatment with Verbocit and nitric acid solutions.

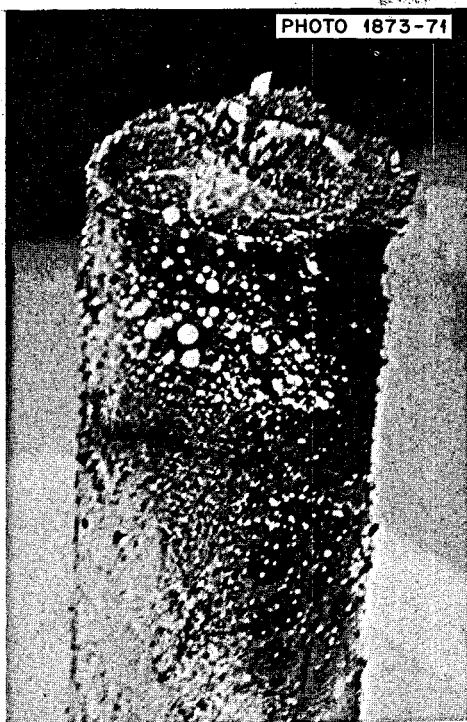


Fig. 6.19. Chromium rod exposed to ^{233}U fuel salt.
January 30, 1969, FP-17-11.

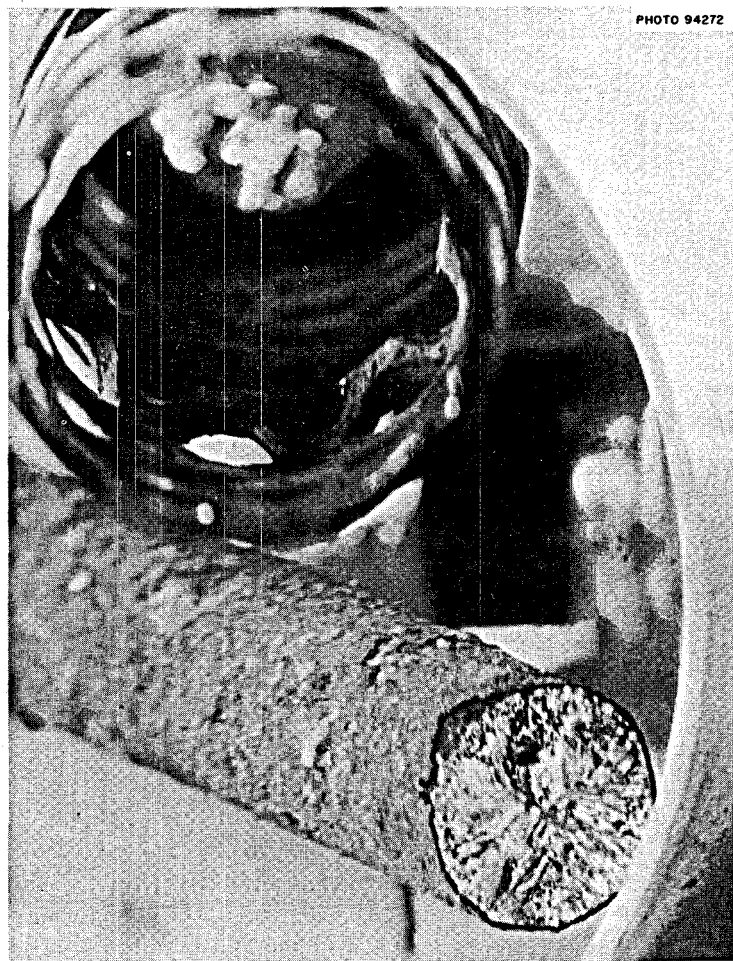


Fig. 6.20. Cross section of chromium rod showing
surface deposit. January 30, 1969, FP-17-11.

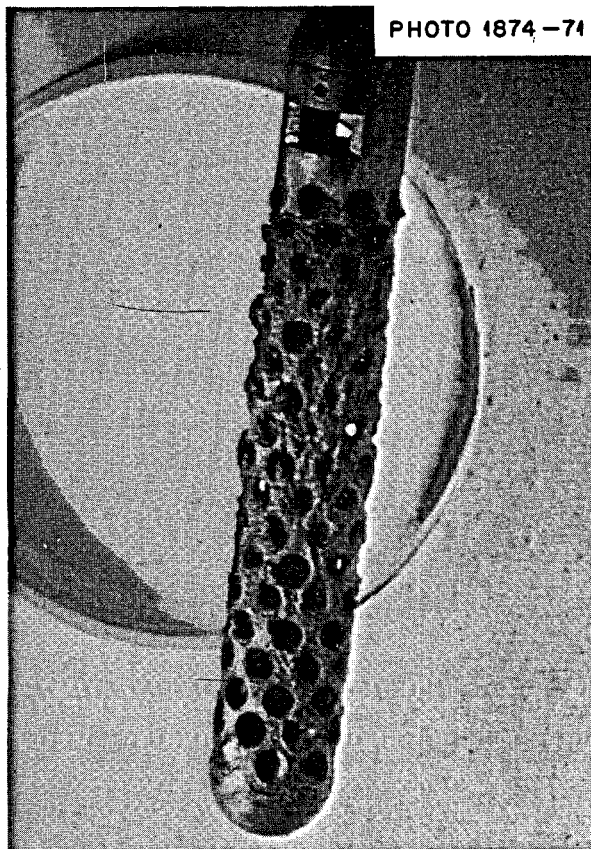


Fig. 6.21. Nickel cage after exposure of beryllium rod to ^{233}U fuel salt. October 8, 1969, FP-19-48; 4.91 g Be^0 dissolved from rod.

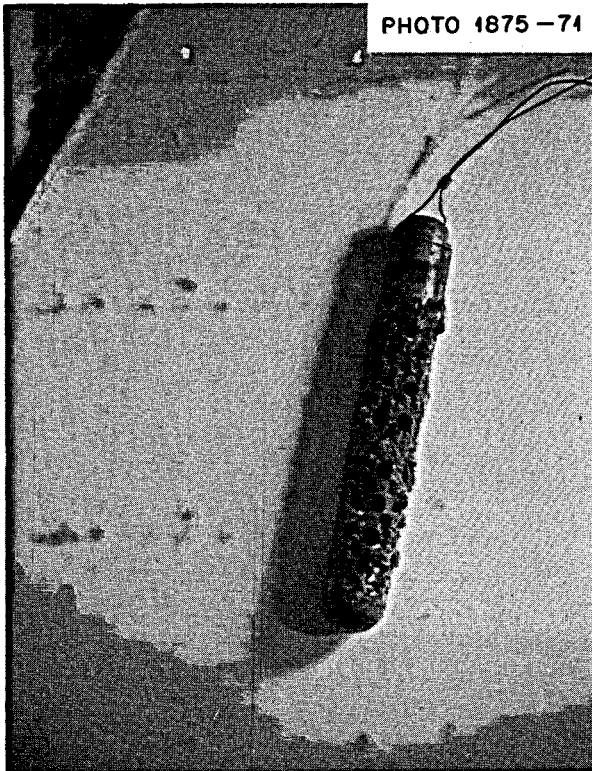


Fig. 6.22. Nickel cage from exposure of beryllium rod to ^{233}U fuel salt. November 29, 1969, FP-20-7; 6.97 g Be^0 dissolved from rod.

6.5 Effect of Uranium Trifluoride on the ^{95}Nb Concentration of the Fuel Salt

Minor adjustments in the concentration of uranium trifluoride in the MSRE fuel salt were made occasionally during the period when the MSRE was operated with ^{235}U fuel. Their primary purpose was to offset the oxidizing effects anticipated to result from the fission reaction. Within this period the $[\text{U}^{3+}] / [\Sigma\text{U}]$ concentration ratio was estimated to have varied within the range 0.1 to $\sim 1.7\%$ (Fig. 6.24). No evidence was found that indicated that such variation effected significant changes in either corrosion rate or fission product behavior in the fuel salt within the reactor. This derives from the fact that the ^{235}U fuel was a highly buffered system in comparison with the ^{233}U fuel used later; that is, the total amount of uranium in the ^{235}U fuel exceeded that contained in the ^{233}U fuel by sixfold. In contrast, operation of the MSRE with

^{233}U fuel showed pronounced changes in the corrosion rates and fission product chemistry as the concentration of UF_3 was altered. Of considerable interest was the appearance of ^{95}Nb in the fuel salt, noted for the first time in initial operations with ^{233}U fuel.²⁰ This observation signaled the potential application of the disposition of ^{95}Nb as an in-line redox indicator for molten-salt reactors.

Operation of the MSRE with ^{233}U fuel thus gave evidence that pronounced changes in fission product and corrosion chemistry resulted as variations of the concentration of UF_3 in the fuel salt were made. The ^{233}U fuel was experimentally more tractable for study than the previous charge of $^{235},^{238}\text{U}$ fuel because of the much lower uranium inventory carried in the ^{233}U fuel. A serious disadvantage was realized, however, when it was discovered that the total amounts of UF_3 which were obtainable in samples of the ^{233}U fuel caused the previously satisfactory method²¹ used for

PHOTO 1876-71

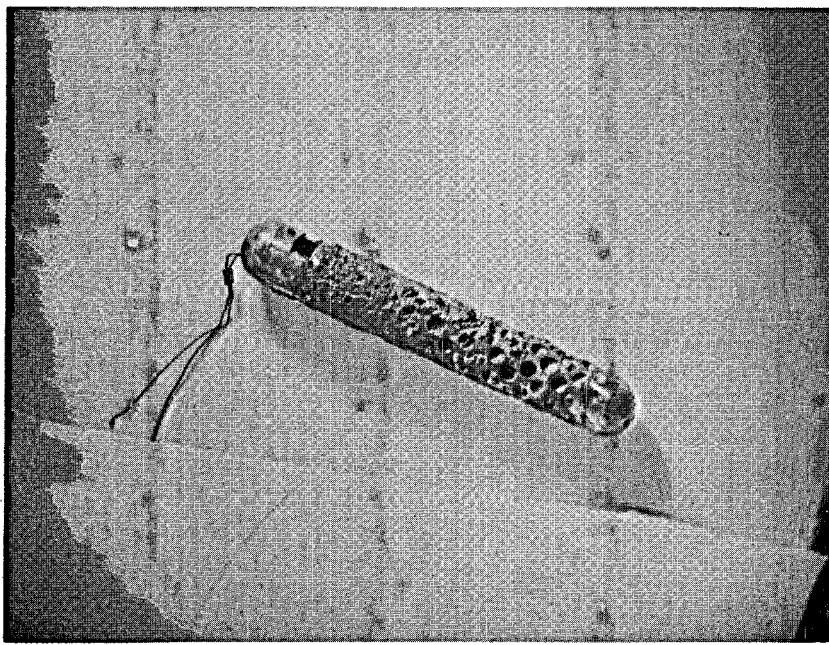
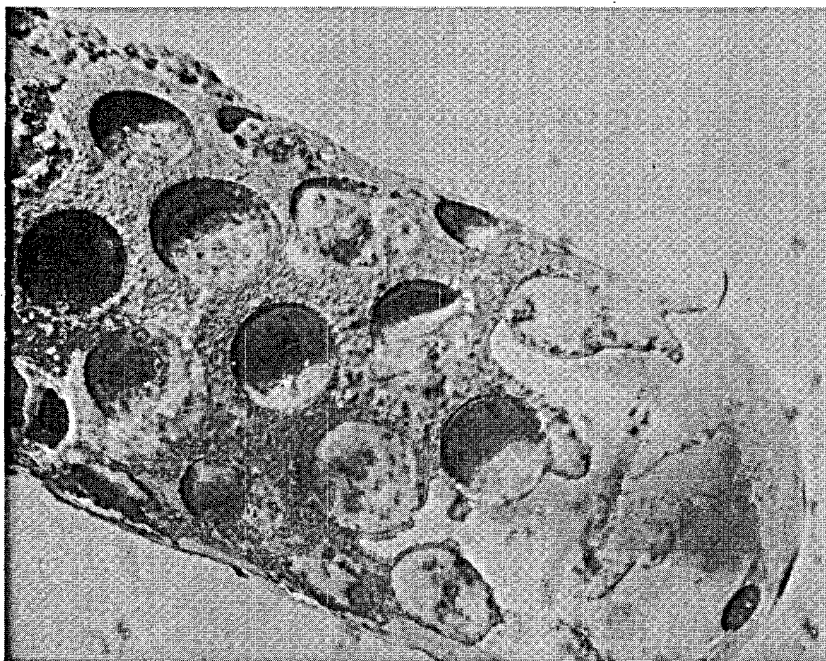


Fig. 6.23. Nickel cage from exposure of beryllium rod to ^{233}U fuel salt. December 9, 1969, FP-20-22; 9.87 g Be^0 dissolved.

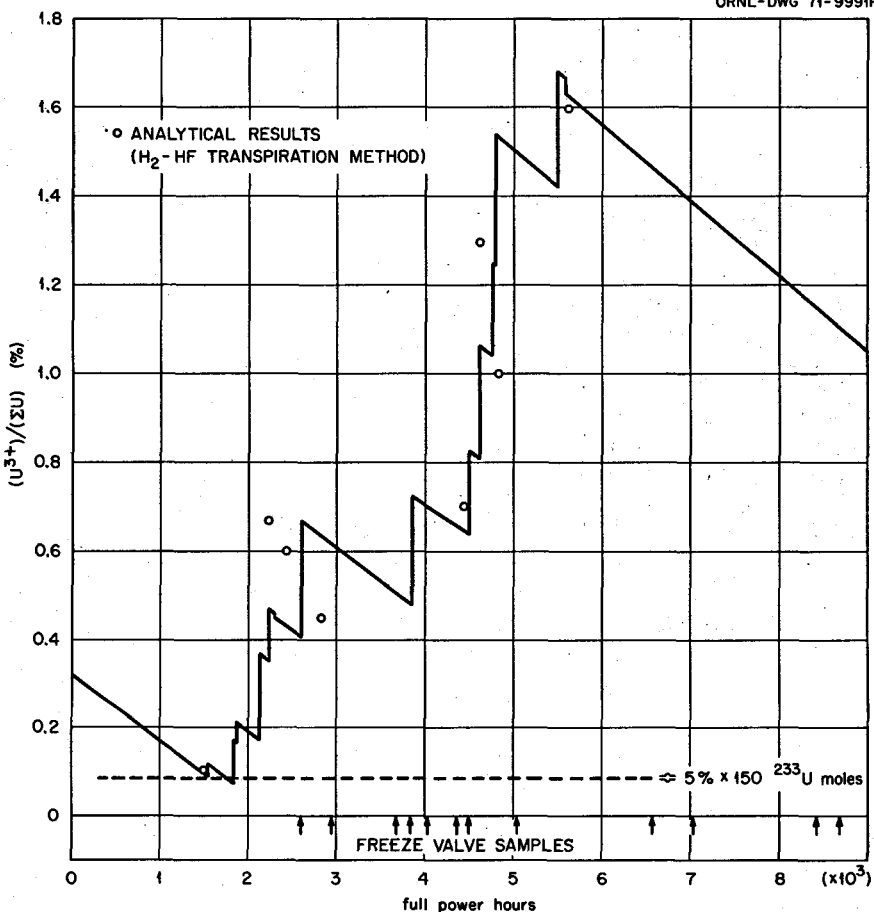


Fig. 6.24. $[\text{U}^{3+}] / [\Sigma \text{U}]$ in the MSRE fuel salt, runs 5-14. Assumed maximum power, 7.4 MW(t):

determination of U^{3+} in the fuel salt to be of little value and required the development of new methods of analysis.

Adjustments of the uranium trifluoride concentration of the MSRE fuel salt were made frequently during ^{233}U operations in order to study the inhibition of corrosion by control of the $[\text{U}^{3+}] / [\Sigma \text{U}]$ concentration ratio and to evaluate the possible application of ^{95}Nb disposition as a redox indicator. The experimental results obtained during this period of operations provided concrete evidence that values of the equilibrium constant for the reaction $\text{Cr}^0 + 2\text{UF}_4 \rightleftharpoons \text{CrF}_2 + 2\text{UF}_3$, as assigned from standard free energy and activity data, are reasonably accurate. Together with niobium distribution data they show that after the fuel system had been opened for maintenance the fuel salt subsequently appeared to become oxidizing with respect to the MSRE containment circuit even though it did not seem to have caused corrosion in the drain tanks. Comparisons of the relative fraction of the ^{95}Nb inventory

which appeared in the fuel salt as the redox potential of the salt changed indicated that when mildly reducing conditions were imposed, as for steady-state operation of the MSRE, niobium very likely became involved in reaction with the moderator graphite to form niobium carbide.

During August and September 1968 the ^{233}U fuel charge was constituted from ^7LiF - $^{233}\text{UF}_4$ and ^7LiF - BeF_2 - ZrF_4 carrier salt which had previously contained $^{235},^{238}\text{UF}_4$. Concurrent with the inception of corrosion in the fuel circuit, as evidenced by a rapid increase in the concentration of Cr in the fuel salt (Fig. 6.25), niobium began to appear in the fuel salt for the first time²¹ and persisted there until 28.80 g (6.54 equivalents) of Be^0 had been added. During this period the concentration of chromium in the salt rose from 35 to 65 ppm, indicating the removal of 140 g (5.89 equivalents) of chromium from the circuit walls. Thus, when ^{95}Nb disappeared from the fuel salt after the final addition of beryllium (sample FP-15-62), a total of

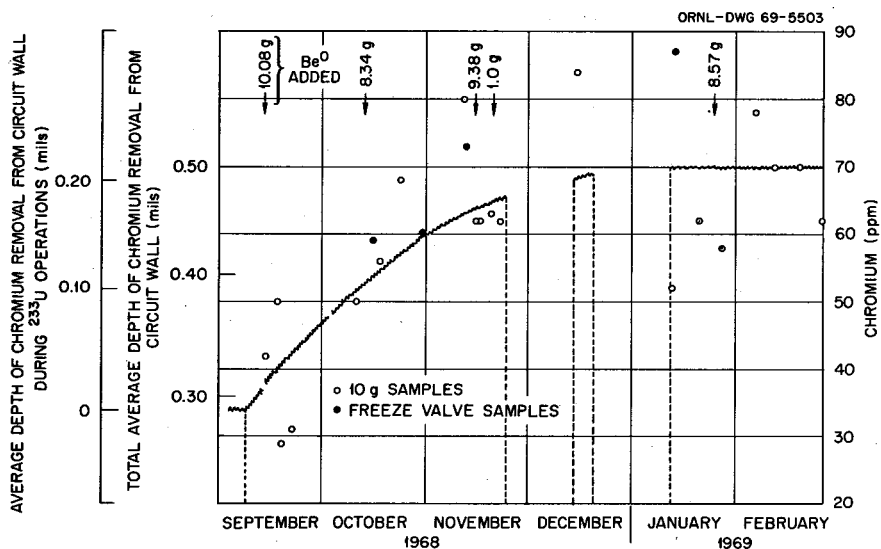


Fig. 6.25. Corrosion of the MSRE fuel circuit in run Nos. 15 and 16, September–December 1968.

12.43 equivalents were involved in the reduction of Fe^{2+} and establishment of the $\text{Cr}^0 + 2\text{UF}_4 \rightleftharpoons 2\text{UF}_3 + \text{CrF}_2$ equilibrium. Samples of the salt obtained during the brief period of the subsequent run (No. 16) as well as the beginning of ^{233}U power operations in run No. 17 (FP-16-4 and FP-17-2) showed the presence of 52 and 29% of the ^{95}Nb inventory respectively.

In Fig. 6.26, nominal values of $[\text{U}^{3+}]/[\Sigma\text{U}]$ are shown for runs 17–20. These operations comprise nearly the total power operation of the MSRE with ^{233}U fuel. The concentrations of UF_3 shown in Fig. 6.26 are based on the assumption that 0.76 equivalent of oxidation results from the fission of 1 at. wt of uranium⁵ and that the maximum power achieved by the MSRE was 7.4 MW(t). They also assume that the observed increases in the concentration of chromium in the fuel salt at the beginning of runs 19 and 20 are indicative of the total loss of U^{3+} from the salt; the nominal values for $[\text{U}^{3+}]/[\Sigma\text{U}]$ at these instants are thus shown as zero. The equilibrium constant for the corrosion equilibrium $\text{Cr}^0 + 2\text{UF}_4 \rightleftharpoons 2\text{UF}_3 + \text{CrF}_2$ reaction at 650°C, assuming an activity for Cr^0 in the Hastelloy to be 0.03,³ is 1.271×10^7 . Thus, in a regime such as that which prevailed during the initial stages of run No. 19, the rate at which Cr^0 is leached from the Hastelloy N circuit gradually decreases as the Cr^{2+} concentration of the fuel salt increases. During the initial period of run No. 19 the Cr^{2+} concentration of the circulating fuel salt rose from 72 to 100 ppm. At that point the equilibrium concentration of $[\text{U}^{3+}]/[\Sigma\text{U}]$ in the fuel salt anticipated from free energy and activity data is $\sim 0.5\%$.

The disposition of ^{95}Nb in the ^{233}U fuel during the initial period of run No. 19 indicates that when $[\text{U}^{3+}]/[\Sigma\text{U}]$ was less than $\sim 0.5\%$, Nb became oxidized and entered the salt, possibly as Nb^{3+} or Nb^{4+} . Then, as the corrosion reaction $\text{Cr}^0 + 2\text{UF}_4 \rightleftharpoons 2\text{UF}_3 + \text{CrF}_2$ proceeded to equilibrium, the $\text{U}^{3+}/\Sigma\text{U}$ concentration ratio increased, and at a $[\text{U}^{3+}]/[\Sigma\text{U}]$ value of 0.5%, ^{95}Nb precipitated from the fuel salt. Two levels of nominal $\text{U}^{3+}/\Sigma\text{U}$ concentration are given during run Nos. 17 and 18, the higher values based on the assumption that corrosion of the fuel circuit during the early stages of run No. 17 may have accounted for a fraction of $[\text{U}^{3+}]/[\Sigma\text{U}]$. The extent to which this reaction might contribute to the total concentration of UF_3 in the fuel at the beginning of run No. 17 is obscure, because the MSRE was operated at full power at the inception of run No. 17. Such operation deposits the noble metal fission products on the surface of the Hastelloy N, causing the activity of Cr^0 at the alloy surface to be effectively reduced. The beginning period of run No. 19 is not analogous, for not until the corrosion equilibrium was established was the reactor operated at full power for sustained periods.

Freeze-valve samples were obtained at the request of E. G. Bohlmann and E. L. Compere during runs Nos. 17–20. Their analyses of the salt removed from the pump bowl showed ^{95}Nb disposition as indicated by the data points in Fig. 6.26. It is evident that, as $[\text{U}^{3+}]/[\Sigma\text{U}]$ decreased below 0.5% in run No. 17, ^{95}Nb was oxidized and distributed to the fuel salt, to be removed subsequently as this concentration ratio was exceeded. Of the data shown in Fig. 6.26 only the

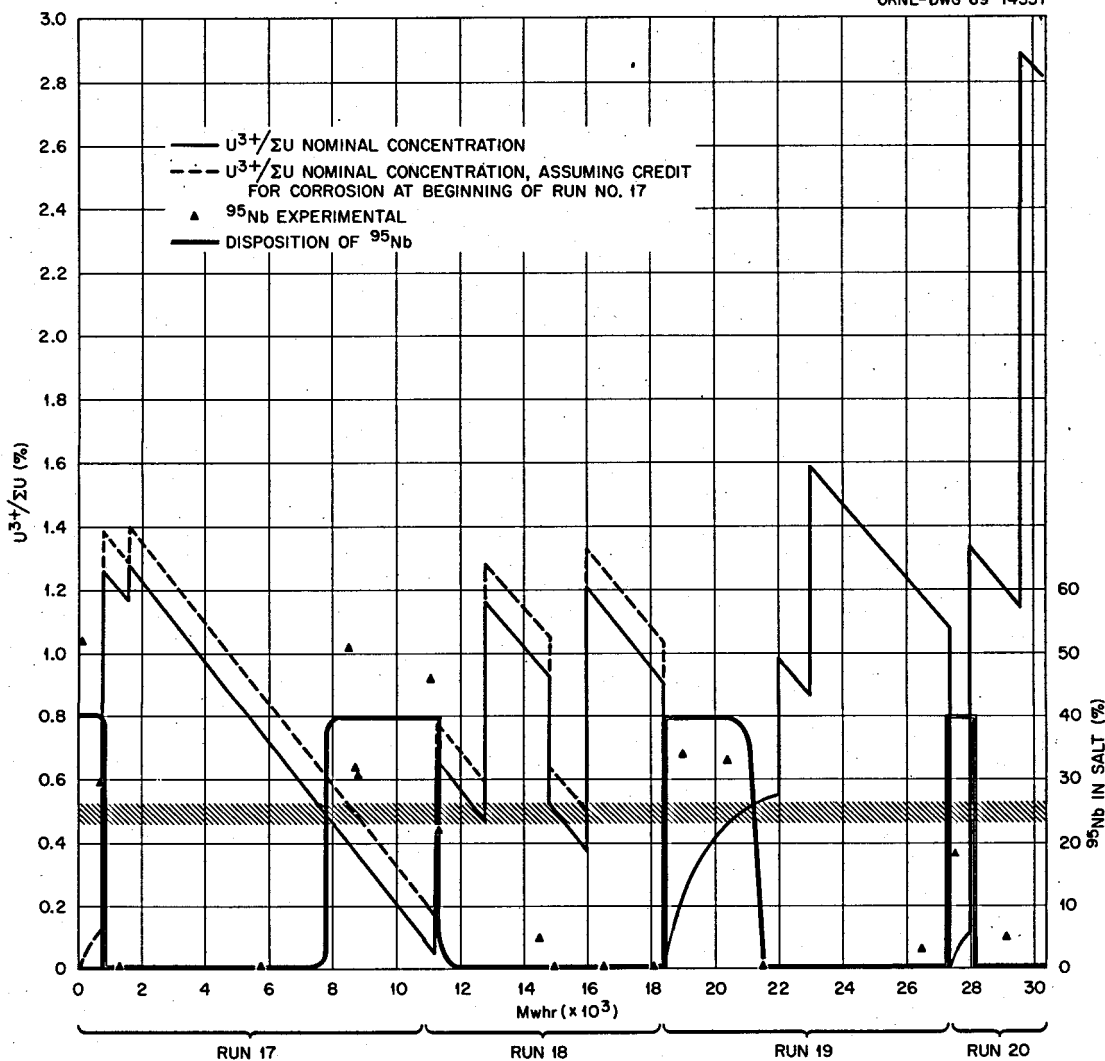


Fig. 6.26. Effect of $U^{3+}/\Sigma U$ on distribution of ^{95}Nb in the MSRE fuel salt.

second data point in run 18 appears to be anomalous. It seems likely that this result represents incomplete equilibrium since the sample was obtained just after $[U^{3+}]/[\Sigma U]$ had been adjusted to a nominal value of 0.7%. In view of the fact that Be^0 , in contact with the molten fuel, generates reduction potential gradients which result in the reduction not only of U^{4+} to U^{3+} but of Cr^{2+} to Cr^0 as well, one might anticipate a kinetic factor to be significant in $\text{Be}^0 \rightleftharpoons \text{Be}^{2+}$, $\text{U}^{4+} \rightleftharpoons \text{U}^{3+}$, $\text{Cr}^{2+} \rightleftharpoons \text{Cr}^0$, $\text{Nb}^{3+} \rightleftharpoons \text{Nb}^0$ equilibria in the MSRE fuel salt.

The results described in Fig. 6.26 indicate that when the $[U^{3+}]/[\Sigma U]$ of the ^{233}U MSRE fuel was poised at ~0.5%, disposition of ^{95}Nb toward solution in the salt or deposition within the reactor was at a null point,

and, as indicated by behavior during ^{235}U operations, the $\text{U}^{3+}/^{95}\text{Nb}$ ratio is the controlling factor. At 0.5% U^{3+} this ratio is 8.5/1.

Little is known concerning the chemistry of niobium in the MSRE fuel salt. Preliminary results of laboratory experiments indicate²² that under mildly oxidative conditions niobium assumes an oxidation number of ~3.7. The fact that during run 15, when the oxidation potential of the fuel salt was sufficiently high to permit Fe^{2+} to exist in the salt in significant concentrations, nearly all of the ^{95}Nb inventory of the fuel salt was in solution, whereas in subsequent operations when the oxidation potential was less, no greater than ~50% of the ^{95}Nb was found in the salt. This behavior seems to indicate that when niobium was deposited on the

moderator graphite it reacted to form niobium carbide and that under the various redox regimes which were established in the MSRE during runs 17 to 20 niobium carbide was not removed from the moderator graphite. The prevalence of niobium as the carbide is compatible with the experimental observations by Blankenship et al.¹⁶ and as noted by Cuneo and Robertson,²³ who found that the concentration of ⁹⁵Nb at all profiles in three different types of graphite was greater than would have been anticipated if after deposition the isotope remained as the metallic species.

References

1. A. Taboada, *MSR Program Semiannu. Progr. Rep. July 31, 1964*, ORNL-3708, p. 330.
2. W. R. Grimes, *Nucl. Sci. Appl. Technol.* 8, 138 (1970).
3. M. B. Panish, R. F. Newton, W. R. Grimes, and F. F. Blankenship, *J. Phys. Chem.* 62, 980 (1962).
4. J. O. Blomeke and M. F. Todd, "Uranium-235 Fission Product Production as a Function of Thermal Neutron Flux, Irradiation Time, and Decay Time," USAEC report ORNL-2127, Oak Ridge National Laboratory (November 1958).
5. C. F. Baes, "The Chemistry and Thermodynamics of Molten Salt Reactor Fluoride Solutions," *Proc. IAEA Symposium on Thermodynamics with Emphasis on Nuclear Materials and Atomic Transport in Solids, Vienna, Austria, July 1965*.
6. W. R. Grimes, G. M. Watson, J. H. DeVan, and R. B. Evans, "Radiotracer Techniques in the Study of Corrosion by Molten Fluorides," *Proceedings of the Conference on the Use of Radioisotopes in the Physical Sciences and Industry, Sept. 6-17, 1960*, vol. III, p. 559, International Atomic Energy Agency, Vienna, Austria, 1962.
7. H. E. McCoy, *An Evaluation of the Molten Salt Reactor Experiment Hastelloy-N Surveillance Specimens - Fourth Group*, ORNL-TM-3063 (1970).
8. *MSR Program Semiannu. Progr. Rep. Aug. 31, 1965*, ORNL-3872, p. 113.
9. *MSR Program Semiannu. Progr. Rep. July 31, 1963*, ORNL-3529, p. 130.
10. J. F. Engel, P. N. Haubenreich, and A. Houtzeel, *Spray, Mist, Bubbles, and Foam in the Molten Salt Reactor Experiment*, ORNL-TM-3027 (June 1970).
11. Letter dated February 9, 1971, from D. B. Trauger to M. Shaw, *Assessment of Need for Oxygen Getter in MSBR Fuel*.
12. Furnished through the courtesy of C. Crouthamel, Chemical Engineering Division, Argonne National Laboratory, Argonne, Ill.
13. W. R. Grimes, unpublished work, 1970.
14. B. McNabb and H. E. McCoy, internal correspondence, March 31, 1971.
15. R. E. Thoma, *MSR Program Semiannu. Progr. Rep. Feb. 28, 1970*, ORNL-4548, p. 93.
16. F. F. Blankenship, E. G. Bohlmann, S. S. Kirslis, and E. L. Compere, *Fission Product Behavior in MSRE*, ORNL-4684 (in preparation).
17. S. S. Kirslis and F. F. Blankenship, *MSR Program Semiannu. Progr. Rep. Feb. 28, 1967*, ORNL-4119, p. 131.
18. J. H. Shaffer and W. R. Grimes, *MSR Program Semiannu. Progr. Rep. Feb. 28, 1969*, ORNL-4396, p. 135.
19. H. W. Kohn and F. F. Blankenship, *ibid.*, p. 137.
20. J. M. Dale, *MSR Program Semiannu. Progr. Rep. Aug. 31, 1967*, ORNL-4191, p. 167.
21. E. L. Compere and E. G. Bohlmann, *MSR Program Semiannu. Progr. Rep. Feb. 28, 1969*, ORNL-4396, p. 139.
22. C. F. Weaver, private communication.
23. D. R. Cuneo and H. E. Robertson, *MSR Program Semiannu. Progr. Rep. Aug. 31, 1968*, ORNL-4344, p. 141.

7. DETERMINATION OF REACTOR POWER

7.1 Power Estimates with ²³⁵U Fuel from Heat Balance and Other Methods

Estimates of the power developed by the MSRE can be derived from nuclear and heat balance data. Both bases were used from the beginning of power operations with the MSRE. As refinements and corrections were introduced into the physical property and nuclear data, new estimates were made. Consequently, MSR Program progress reports cite various values for the maximum average power of the reactor ranging between 7 and 8 MW(t).

The results of the investigation described in this chapter fixed the maximum power of the MSRE at 7.4 MW(t), a value with which other estimates have more recently agreed.

The power generation rate of the MSRE was calculated routinely by an on-line computer; power production was determined from computation of the heat balance in the fuel and coolant systems. Details of the methods employed are described elsewhere.^{1,2} Once heat balances were established, nuclear instrumentation systems were calibrated to correspond to the nuclear power indicated by the heat balance.

The results of chemical and isotopic analysis of fuel salt were assessed carefully throughout the period when the MSRE was operated with ^{235}U fuel and later when the fuel charge was comprised of ^{233}U and plutonium, with the purpose of employing these results to monitor, if possible, the power generated by the reactor. Attempts to use chemically determined values of the concentration of uranium in the fuel-salt samples were generally unsatisfactory because of the point-to-point scatter in these data and because of the overwhelming effect that the use of flush salt in the fuel circuit had on the uranium concentration base lines. The amounts of fuel- and flush-salt residues remaining in the fuel circuit after drains were estimated by comparisons of the chemical analyses of uranium in the flush salt with those in the fuel salt during each period of use. Not until the uranium concentration of the flush salt had undergone several increments was the precision of the average mass of fuel-salt residues narrowed to within ± 5 kg. This was, however, of insufficient precision to afford a sufficiently accurate base line for computation of the power generation. It was thus evident that the results of wet chemical analyses for uranium in the fuel salt would be of potential use in establishing burnup rates only after long periods of power generation which were free from drain-flush-fill interruptions.

Until March 1968, calculations of the heat balance indicated that the maximum power generated by the MSRE was 7.2 MW(t). By that time, a discrepancy between nominal concentration and analytical values for uranium in the circulating fuel salt began to appear; the analytical data over an extended period in run No. 10 showed a negative divergence from the nominal concentration of the uranium in the fuel of about 10%. During this period, however, computations of the reactivity balance did not indicate corresponding or anomalous decreases in the fissile concentration of the salt. Reactivity balance calculations had previously indicated that this method of evaluating reactor performance was sensitive to a factor of 10 greater than chemical analysis with respect to detection of changes in uranium concentration of the fuel. The chemical data suggested that the maximum actual power output of the reactor was ~ 8.0 MW rather than 7.2 MW. However, little credibility could be accorded to this conclusion for the reasons cited above.

By early 1968 a sufficient amount of ^{236}U was generated in the fuel salt to suggest that comparison of the analytical results of mass spectrometric measurements would provide a good measure of the integrated power. Tests of this comparison³ yielded a slope that was within 1% of the theoretical slope for a power

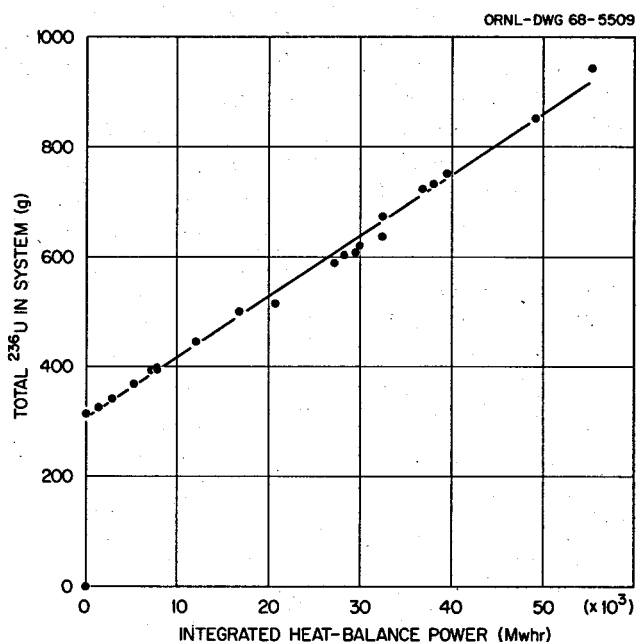


Fig. 7.1. ^{236}U buildup in MSRE vs power production.

generation rate of 7.2 MW. The uncertainty in the theoretical slope was regarded to be probably less than 10%, and the actual integrated power was probably within 10% of the value indicated by the heat balances (see Fig. 7.1).

Although the ^{236}U production rate seemed to confirm estimates that indicated the maximum power output to be 7.2 MW, suspicion was growing that the heat balance calculations were in error, for data collected at different power levels indicated that the value employed for the specific heat of the LiF-BeF_2 coolant salt was not temperature dependent,⁴ whereas a temperature-dependent relationship was employed in the heat balance.⁵

A program of laboratory measurements of the enthalpy of solid and liquid Li_2BeF_4 from 273 to 900°K was completed at this time, by investigators at the National Bureau of Standards,⁶ from which it was shown that the heat capacity was $0.56 \text{ cal g}^{-1}(\text{°C})^{-1}$. A fluoride mixture was synthesized for confirmation at ORNL of the NBS value. Results of these measurements indicated that the derived heat capacity of the coolant salt was $0.577 \pm 0.008 \text{ cal g}^{-1}(\text{°C})^{-1}$,⁷ in good agreement with the NBS investigations but substantially higher in the operating temperature range of the MSRE than the previously used value, and showed essentially no variation with temperature. The new value of the specific heat was incorporated into the computerized heat balance computations prior to the beginning of

operation with ^{233}U fuel. Calculated full-power level was changed from 7.2 to 8.0 MW as a result of the revision in the value for specific heat and in accord with the analytical chemical results.

Throughout this entire period, changes in the nominal amounts of uranium isotopes in the fuel salt were computed based on average cross-section data for thermal and epithermal neutron reactions in the MSRE spectrum that were current to 1965.^{8,9} The consumption and production rates were:

^{234}U	$-2.167 \times 10^{-4} \text{ g/MWhr}$
^{235}U	$-5.417 \times 10^{-2} \text{ g/MWhr}$
^{236}U	$+1.083 \times 10^{-1} \text{ g/MWhr}$
^{238}U	$-7.017 \times 10^{-2} \text{ g/MWhr}$
Total	$-5.146 \times 10^{-2} \text{ g/MWhr}^a$

^aRef. 9.

7.2 Power Output of the MSBR Based on the Isotopic Composition of Plutonium

The potential use of plutonium as a fuel for molten-salt reactors has been assessed periodically for more than a decade. The results of one early study¹⁰ showed that a PuF_3 -fueled two-region homogeneous fluoride salt reactor was operable, although its performance was poor. Further development was not pursued for neither the chemical feasibility nor methods for improving its performance were obvious. Although the thermochemical properties of the plutonium fluorides were not well established at that time, it was clear that the most soluble fluoride, PuF_4 , was too strong an oxidant for use with the available structural alloys. The solubility of PuF_3 , while sufficient for criticality even in the presence of fission fragments and nonfissionable isotopes of Pu, was assumed¹¹ to limit the amount of ThF_4 which could be added to the fuel salt. This limitation, coupled with the condition that the continuous use of ^{239}Pu as a fuel would result in poor neutron economy in comparison with that of ^{233}U -fueled reactors, vitiated further efforts to exploit the plutonium fluorides for application in two-region MSBRs.

Recent developments in fuel reprocessing chemistry and in reactor design have established the feasibility of single-fluid molten-salt breeder reactors. One of the alternative modes of operating such reactors is to employ plutonium in place of enriched ^{235}U for the

initial fuel loading and startup of the reactors. Assessments of plutonium to start up MSBRs in this way have concluded that plutonium should prove to be a very satisfactory alternative to enriched uranium, either as initial fuel for a molten-salt breeder reactor or as initial fuel and subsequent feed material.¹²⁻¹⁴

It now appears that it will be possible to operate an $\text{LiF}-\text{BeF}_2-\text{ThF}_4-\text{PuF}_3$ single-fluid molten-salt reactor with lower concentrations of thorium and plutonium than earlier considerations required, for example, with thorium fluoride concentrations of 8 to 12 mole % and with a plutonium fluoride concentration of approximately 25% less than required for ^{233}U loading, that is, ≤ 0.2 mole %. These conclusions indicated the desirability of demonstration experiments to examine, in as nearly similar application as possible, the behavior of plutonium in an MSBR. The chemical feasibility of this application was evaluated¹⁵ and found to hold promise for successful application. Therefore, when the MSRE resumed operations with ^{233}U fuel, plans were made to include plutonium as a constituent of the fuel. Using pre-1965 cross-section data and assuming that the maximum operating power of the reactor was 8.0 MW, efforts were initiated to establish a material balance for plutonium.

During the final period of operation with $^{235},^{238}\text{U}$ fuel, a sufficient amount of plutonium was generated for its detection in salt samples to be tractable by standard analytical methods. Approximately 600 g of plutonium was generated in the MSRE fuel as it was operated with ^{235}U fuel by neutron absorptions in ^{238}U , enough to afford a comparison of the analytical data with anticipated values. The results of that comparison, expressed as a material balance for plutonium, showed that the analytical chemical methods, which were previously satisfactory for determination of the concentration of plutonium in the fuel salt, were of questionable utility for use with the ^{233}U fuel charge and that isotopic dilution methods, using mass spectrometric analyses, afforded the most satisfactory means of analysis. They indicated, in addition, that at the maximum concentrations in which plutonium occurred in the MSRE fuel salt, it existed as a stable chemical entity and, by inference, that Pu_2O_3 is not precipitated in the presence of low concentrations (50 to 60 ppm) of oxide ion.

The net production rates for plutonium generated in the $^{235},^{238}\text{U}$ fuel salt have been estimated¹⁶ to be

$$G^{239} = G^{238} \cdot 0.018584(e^{-0.60537^{-7}T})$$

$$- e^{-0.3318^{-5}T},$$

$$G^{240} = G^{238} \cdot (0.008233e^{-0.29166^{-5}T} - 0.0648799e^{-0.29166^{-5}T} + 0.056647e^{-0.33318^{-5}T}),$$

where

G^k = mass of k in circulation (g) ($k = 238, 239, 240$ refers to ^{238}U , ^{239}Pu , and ^{240}Pu respectively),

T = time-integrated power (MWhr).

At termination of the ^{235}U experiment, 589 g of plutonium should have been generated in the fuel salt with the reactor operating at a maximum power of 8.0 MW. For a fuel charge of 4900 kg, this corresponds to 120 ppm. The average concentration of plutonium in the fuel salt, as determined from the results of analyses of 18 fuel-salt samples obtained during the latter period of power operations with $^{235},^{238}\text{U}$ fuel, was 118 ppm. The analytical data do not show a significant trend and are probably not sufficiently precise to use as a basis to infer that a real difference exists between calculated and analytical values. On completion of these power operations, uranium was removed from the fuel salt by fluorination.¹⁷ It was anticipated that the plutonium would remain in the carrier salt. Five samples of the carrier salt were removed from the fuel drain after fluorination and found to have an average concentration of 120 ppm of plutonium, representing a total of 562 g, as compared with an expected value of 125 ppm; that is, 27 g of plutonium is not accounted for by the results of these analyses.

The concentration of plutonium in a salt specimen is calculated from the relation:

$$\begin{aligned} \text{Concentration of Pu (ppm)} &= \text{dpm/g} \times 3.97 \times 10^{-8} \\ &\div (^{238}N \times 1.470 + ^{239}N \times 5.402 \times 10^{-3} + ^{240}N \\ &\quad \times 2.00 \times 10^{-2} + ^{241}N \times 4.10 \times 10^{-4} \\ &\quad + ^{242}N \times 3.5 \times 10^{-4}), \end{aligned}$$

where N is the atom fraction of plutonium as the isotope designated.

The concentration of plutonium in each of the 10-g samples of fuel salt taken since the beginning of ^{233}U operations was determined using conversion factors which assumed that the plutonium in the MSRE consisted entirely of ^{239}Pu and ^{240}Pu . The average concentration of plutonium after full loading of the reactor was achieved was found to be 147 ppm (Table

7.1). This value indicates the presence of a total of 689 g of plutonium; thus the enriching salt might then have been expected to contain 100 g of plutonium. In an attempt to substantiate this conclusion, a sample of the $^7\text{LiF}-^{233}\text{UF}_4$ enriching salt was obtained from a section of transfer line at the TURF and submitted for chemical and mass spectrometric analysis. The salt residue which was contained in the line was considered to be typical of that delivered for use in the MSRE. The results of mass spectrometric analysis showed that this salt contained plutonium, 1.64 wt % of which was ^{238}Pu . Revised conversion factors were therefore required for calculation of the total plutonium concentration of the TURF salt and ^{233}U fuel salt because of the high specific activity, $6.46 \times 10^5 \text{ dis sec}^{-1} \mu\text{g}^{-1}$, for ^{238}Pu . The plutonium concentration of the TURF salt appears now to have been 249 ppm using the revised factor and corresponds to the addition of 16.4 g of plutonium along with the $^7\text{LiF}-^{233}\text{UF}_4$ eutectic. Current estimates of the nominal concentration of plutonium are now based on the assumption that this amount of plutonium was added to the fuel salt and, therefore, that the MSRE contained ~ 605 g of plutonium at the beginning of ^{233}U power operations.

A plutonium inventory of the MSRE fuel was computed, both before and after loading with ^{233}U fuel, based on Prince's estimates of the production and fission rates for plutonium and on the assumption that 16.4 g of plutonium was contained in the enriching salt. These values showed that the plutonium production rate during ^{235}U operations was greater than previously anticipated and, correspondingly, that the relative changes in ^{240}Pu and ^{239}Pu during ^{233}U operations were also slightly different.

Estimates of the variation of ^{239}Pu and ^{240}Pu during recent power operations require that the quantity and composition of the final plutonium inventory be known accurately. As noted previously,¹⁸ and as shown in Fig. 7.2, attempts to determine the concentration of plutonium in the fuel salt from gross alpha count measurements were not very satisfactory because of the high specific activity of ^{238}Pu . An improved estimate of the plutonium inventory of the system was made from extrapolations of the observed changes in ^{239}Pu and ^{240}Pu in the beginning stages of power operation with ^{233}U fuel. The initial $^{240}\text{Pu}/^{239}\text{Pu}$ concentration ratio was computed to be 0.0453, with the plutonium of the reactor at that point as 568 g, approximately 2% more than estimated from previous analyses. Current estimates of inventory values have been computed for this revised starting inventory. The values obtaining at the time the samples were taken were based on estimated

Table 7.1. Summary of MSRE fuel-salt analyses: plutonium

Sample No.	Mwhr	Net Weight of Pu in Fuel Salt (g)			Weight % Pu/ Σ Pu				Concentration of Pu (ppm)	
		^{239}Pu	^{240}Pu	Σ	Calculated	Analytical	Calculated ^a	Analytical		
					^{239}Pu	^{240}Pu	^{239}Pu	^{240}Pu		
FP14-41	67,767	487	18.6	506	96.32	3.68	96.46	3.31	94	95
FP14-42	62,305	492	18.8	511					95	120
FP14-43	62,705	495	19.0	514					95	125
FP14-44	63,251	498	19.3	517					96	128
FP14-46	63,537	500	19.5	520					96	127
FP14-47	63,671	501	19.6	521					97	122
FP14-48	64,211	505	19.8	525					97	126
FP14-49	64,232	505	19.8	525					97	125
FP14-50	64,234	505	19.8	525					97	123
FP14-51	64,367	507	20.0	527					97	119
FP14-52	64,994	510	20.3	530					98	111
FP14-54	65,397	513	20.5	534					99	98
FP14-56	65,809	517	20.8	538					100	119
FP14-58	66,351	521	21.2	542					101	118
FP14-59	66,982	525	21.5	547					102	120
FP14-64	68,720	537	22.7	560	95.94	4.06	96.05	3.67	104	145
FP14-65	69,481	543	23.3	566					114	97
FP14-68	69,838	546	23.5	570					115	102
FP14-Final	72,454	563	25.6	589					120	120
FP15-6	72,454	571	27.1	599					128	113
FP15-9	72,454	573	27.5	602					128	112
FP15-10	72,454	575	27.9	604					129	96
FP15-12	72,454	575	27.9	604					129	112
FP15-18	72,454	575	27.9	604					129	100
FP15-33	72,454	575	27.9	604					129	134
FP15-38	72,454	576	28.0	605					129	143
FP15-42	72,454	576	28.0	605					129	135
FP15-60	72,454	576	28.0	605					129	129
FP15-63	72,454	576	28.0	605					129	141
FP15-65	72,454	576	28.0	605					129	159
FP15-68	72,454	576	28.0	605	95.85	3.99	95.43	4.12	129	157
FP17-1	72,454	576	28.0	605					129	130
FP17-4	73,127	575	28.0	605					129	134
FP17-9	73,830	572	29.4	602					128	148
FP17-12	75,434	569	30.4	598					128	138
FP17-18	76,183	564	31.9	597					127	149
FP17-19	76,791	563	32.5	596					127	147
FP17-20	78,026	560	32.7	594					127	141
FP17-23	79,154	557	34.8	593					127	130
FP17-24	79,814	555	35.5	592					126	142
FP17-27	80,828	552	36.4	589					126	140
FP17-28	81,610	550	37.2	588					125	134
FP17-30	82,771	547	38.3	586					125	149
FP18-1	84,741	542	40.1	583					124	160
FP18-5	86,454	538	41.8	581					124	162
FP18-10	87,267	536	42.5	580					124	145
FP18-13	88,265	533	43.5	578					123	154
FP18-22	89,886	529	44.8	575	92.63	7.20	91.81	7.33	122	164
FP18-27	90,898	527	45.7	574					122	144
FP18-43	92,142	524	46.9	570	92.30	7.53	91.38	7.70	122	171
FP18-Final	92,985	524	47.3	570					122	

^aBased on total fuel charge.

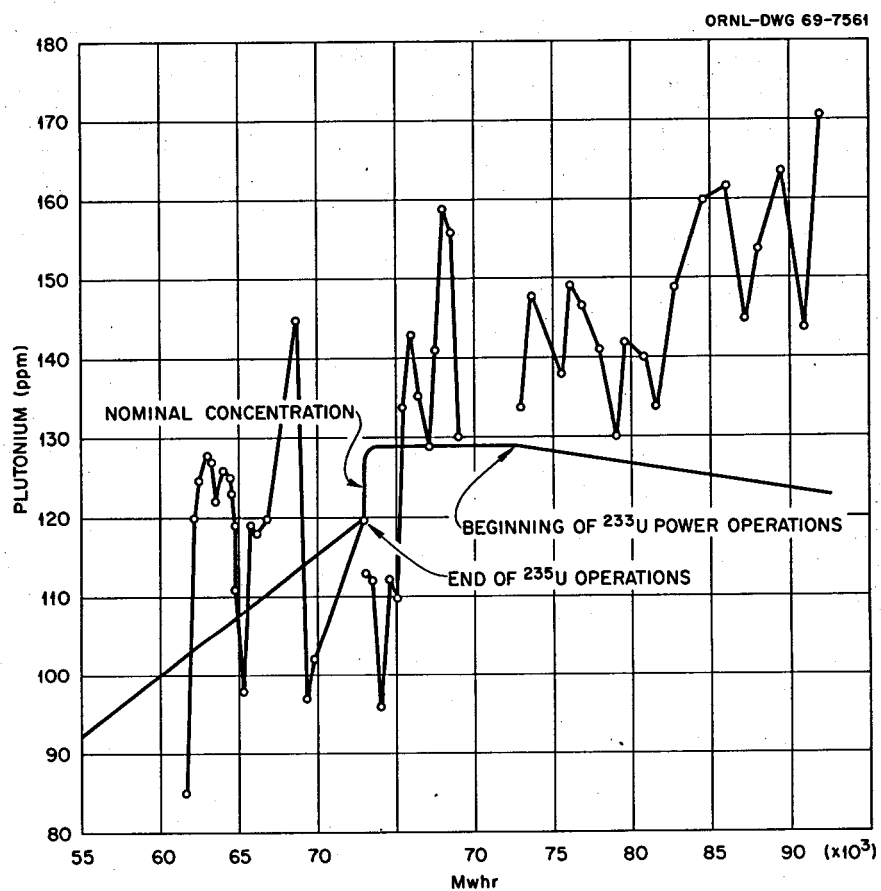


Fig. 7.2. Comparison of nominal and analytical values for the concentration of plutonium in the MSRE fuel salt.

Table 7.2. Isotopic composition of plutonium in MSRE fuel salt

Sample No.	Description	^{238}Pu	^{239}Pu	^{240}Pu	^{241}Pu	^{242}Pu
FP14-41	$\Sigma \text{ g (calculated)}$		487	18.6	<i>a</i>	<i>a</i>
	% calculated		96.32	3.68		
	% analytical	0.011	96.45	3.32	0.22	0.002
FP14-64	$\Sigma \text{ g (calculated)}$		537	22.7		
	% calculated		95.94	4.06		
	% analytical ^b	≤ 0.015	96.05	3.67	0.28	0.005
FP15-68	$\Sigma \text{ g generated in MSRE (calculated)}$		563	25.6		
	$\Sigma \text{ g added with } ^7\text{LiF-}^{233}\text{UF}_4$	0.27	12.9	2.44	0.37	0.33
	$\Sigma \text{ g}$	0.27	575.90	28.04	0.37	0.33
	% calculated	0.04	95.20	4.64	0.06	0.06
	% analytical	≤ 0.08	95.43	4.12	0.34	0.13

^a ^{241}Pu and ^{242}Pu not included; B. E. Prince estimates $\Sigma \text{ g } ^{241,242}\text{Pu} \leq 1.8 \text{ g}$.

^bAnalyses performed by R. E. Eby.

average values for the rates of change of ^{239}Pu and ^{240}Pu in the period between samples (Table 7.2).

In the MSRE, fluid fuel was circulated at rates which were sufficiently rapid with respect to changes in the isotopic composition of the fissile species that the salt samples removed from the pump bowl were representative of the circulating stream. This characteristic of molten-salt reactors makes it possible to use the results of isotopic analyses for a variety of purposes. One potential application, that of appraising the cumulative power generated by the MSRE at various periods, became apparent with the initiation of ^{233}U operations, for with ^{233}U fuel the isotopic composition of the plutonium inventory (produced partly by that generated in ^{235}U operations as well as from that added later) would change significantly during power production and would possibly serve as an accurate indicator of the power produced.

About 600 g of plutonium was produced during power operations with ^{235}U fuel. Thereafter, additional plutonium was introduced into the fuel salt as a contaminant of ^7LiF - $^{233}\text{UF}_4$ enriching salt and later to replenish the fissile inventory of the MSRE during ^{233}U power operations.

Additions of plutonium to the fuel salt as PuF_3 were accomplished smoothly by use of capsules sealed by 12 zirconium disks. These containers were designed and loaded by Carr et al.,¹⁹ a typical capsule is shown in Fig. 7.3. In contact with the fuel salt the zirconium dissolved, permitting the PuF_3 to disperse and to dissolve in the fuel salt. Photographs of one of the capsules after use are shown in Fig. 7.4.

Resolution of the analytical problems with plutonium showed that estimated production rates of plutonium in the ^{235}U fuel salt, based on pre-1965 cross-section data, were low. The programs used for reactor physics calculations were revised using post-1965 data, and as a consequence, both consumption and production rates for plutonium and uranium isotopes were revised significantly.²⁰

Samples of the MSRE fuel salt were submitted routinely for determination of the isotopic composition of the contained fissile species. Comparisons of the results of plutonium assays with nominal values that should result from operations at various power levels from ~7 to 8 MW were made. Within this range, best agreement between calculated and experimental values was obtained for a maximum power output of ~7.40

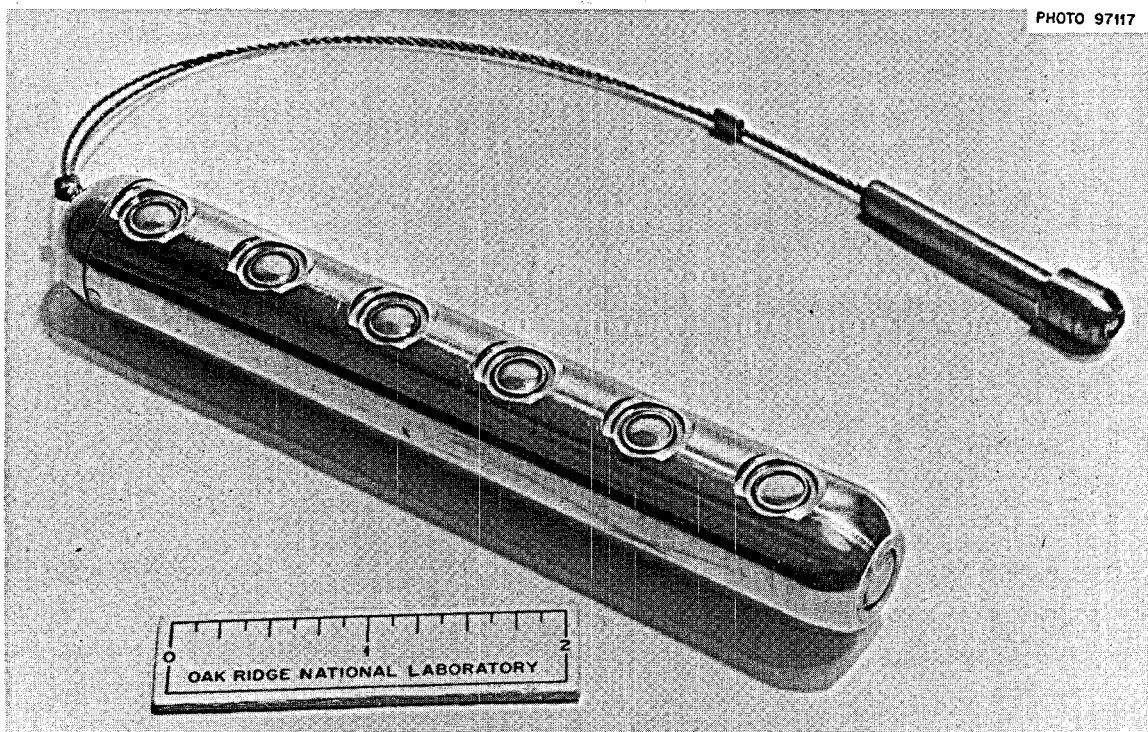
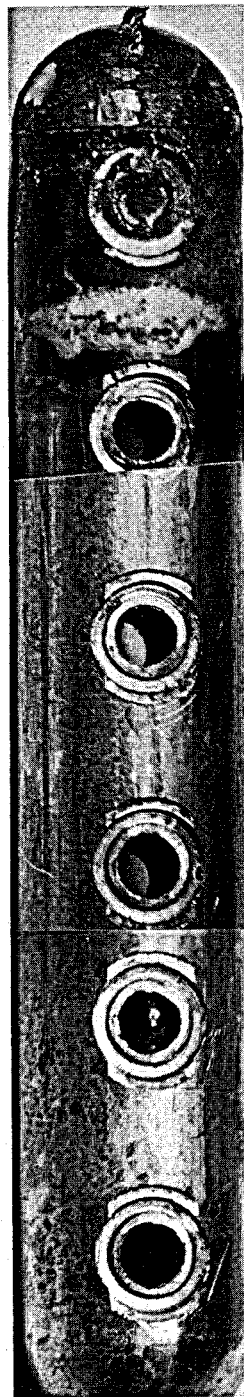


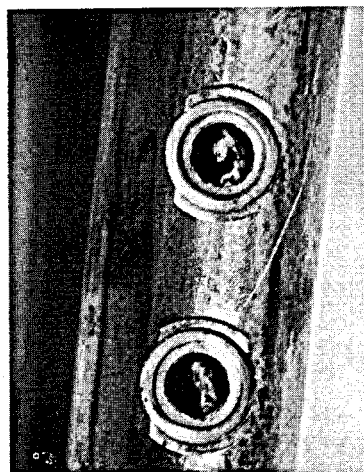
Fig. 7.3. $^{239}\text{PuF}_3$ capsule for MSRE refueling.



FP 19-25 TOP SECTION, OPPOSITE SIDE FROM
THAT SHOWN IN OVERALL VIEW.



FP 19-25 FIRST CAPSULE
USED TO ADD PuF_3 TO THE
MSRE FUEL SALT. CAPSULE
WAS PARTIALLY SUBMERGED
IN FUEL SALT FOR FOUR HOURS



FP 19-25 BOTTOM SECTION, OPPOSITE SIDE
FROM THAT SHOWN IN OVERALL VIEW. SALT
RESIDUE MORE CLEARLY EVIDENT HERE THAN
IN OVERALL VIEW.



FP 19-25 CAPSULE VIEWED FROM BOTTOM,
SHOWING SALT RESIDUE IN CAPSULE.

Fig. 7.4. Capsule sections.

Table 7.3. Isotopic composition of plutonium in the MSRE fuel salt at a power generation rate of 7.40 Mw(th)

Sample No.	Full-Power Hours	Mwhr ^a	$\Delta^{239}\text{Pu}$ (g per 1000 Mwhr)	$\Delta^{240}\text{Pu}$ (g per 1000 Mwhr)	Fuel Circuit Inventory (Calculated) (g) ^b			Isotopic Composition (Calculated)			Isotopic Composition (Analytical)		
					^{239}Pu	^{240}Pu	ΣPu	Wt % Pu/ ΣPu ^{239}Pu	Wt % Pu/ ΣPu ^{240}Pu	$^{240}\text{Pu}/^{239}\text{Pu}$	Wt % Pu/ ΣPu ^{239}Pu	Wt % Pu/ ΣPu ^{240}Pu	$^{240}\text{Pu}/^{239}\text{Pu}$
Run 17-I	0	0			541.5	24.53	568.4	95.26	4.32	0.0453			
FP 17-9	148	537	-3.025	+1.178	539.8	25.16	567.4	95.14	4.43	0.0466	95.26	4.35	0.0457
FP 17-18	466	2,227	-2.996	+1.144	534.8	27.09	564.3	94.76	4.80	0.0507	94.28	5.16	0.0547
FP 17-19	542	3,656	-2.949	+1.180	530.6	28.78	561.8	94.44	5.12	0.0542	94.48	5.00	0.0508
FP 17-20	697	4,492	-2.924	+1.105	528.1	29.70	560.3	94.26	5.30	0.0562	94.20	5.25	0.0557
FP 17-23	920	5,862	-2.894	+1.086	524.2	31.18	557.8	93.97	5.95	0.0595			
FP 17-27	1047	7,131	-2.871	+1.072	520.5	32.54	555.5	93.70	5.86	0.0625	93.58	5.80	0.0620
FP 17-28	1145	7,946	-2.854	+1.063	518.2	33.42	554.0	93.53	6.03	0.0645	94.30	5.97	0.0639
FP 17-30	1290	8,827	-2.845	+1.054	515.7	34.35	551.5	93.51	6.23	0.0666	93.16	6.18	0.0663
Run 17-F	1536	10,245	-2.824	+1.039	511.7	35.82	549.9	93.04	6.51	0.0700			
FP 18-I	1536	10,245			514.1	34.91	551.4	93.22	6.33	0.0679			
FP 18-1	1536	10,245	-2.875	+1.075	514.1	34.91	551.4	93.22	6.33	0.0679	92.92	6.36	0.0684
FP 18-5	1562	11,231	-2.860	+1.066	513.5	35.11	551.1	93.18	6.37	0.0684	92.65	6.61	0.0713
FP 18-10	1851	12,373	-2.843	+1.055	507.6	37.32	547.3	92.73	6.82	0.0735	92.38	6.84	0.0740
FP 18-13	1976	13,873	-2.826	+1.038	505.0	38.26	545.7	92.54	7.01	0.0757	92.16	7.04	0.0764
FP 18-22	1976	13,873	-2.826	+1.038	505.0	38.26	545.7	92.54	7.01	0.0757	91.80	7.36	0.0802
FP 18-27	2306	15,523	-2.799	+1.017	498.3	40.69	541.4	92.03	7.52	0.0817	91.63	7.49	0.0817
FP 18-43	2461	17,281	-2.773	+0.999	495.2	41.81	539.5	91.80	7.75	0.0844	91.48	7.63	0.0834
Run 18-F	2544	18,143	-2.758	+0.989	493.5	42.41	538.4	91.67	7.87	0.0859			
Run 19-I	2544	18,143			495.2	41.81	539.4	91.79	7.75	0.0844			
FP 19-17	2625	18,739	-2.770	+0.993	493.5	42.39	538.4	91.67	7.87	0.0858	91.22	7.84	0.0860
FP 19-18	2642	19,093	-2.763	+0.989	493.2	42.51	538.2	91.65	7.90	0.0862	91.19	7.87	0.0863
FP 19-21	2724	19,449	-2.755	+0.985	491.6	43.10	537.1	91.52	8.02	0.0877	91.02	8.03	0.0882
FP 19-22	2791	19,693	-2.752	+0.985	490.2	43.58	536.3	91.42	8.13	0.0889	90.90	8.11	0.0892
FP 19-24	2791	19,693	-2.752	+0.985	490.2	43.58	536.3	91.42	8.13	0.0889	89.88	8.99	0.1000
FP 19-25-6	2791	19,693	-2.760	+0.983	541.1	46.74	590.6	91.62	7.91	0.0864			
FP 19-27	2791	19,693	-2.760	+0.983	541.1	46.74	590.6	91.62	7.91	0.0864	91.01	8.03	0.0882
FP 19-30	2818	19,693	-2.760	+0.983	540.5	46.93	589.9	91.63	7.96	0.0868	90.89	8.13	0.0895
FP 19-31-4	2818	19,693	-2.750	+0.983	662.6	54.51	719.6	92.08	7.58	0.0823			
FP 19-35	2964	20,961	-3.820	+1.369	658.6	55.96	717.1	91.85	7.80	0.0850	91.35	7.77	0.0851
FP 19-43	3102	21,989	-3.810	+1.357	654.8	57.32	714.5	91.64	8.02	0.0875	91.18	7.90	0.0866
FP 19-53	3294	23,185	-3.795	+1.339	649.5	59.18	711.1	91.33	8.32	0.0911	90.88	8.25	0.0908
FP 19-63	3561	24,631	-3.775	+1.339	642.2	61.77	706.4	90.91	8.74	0.0962	90.49	8.50	0.0939
FP 19-74	3693	26,078	-3.750	+1.316	639.3	62.77	704.5	89.09	8.91	0.0982	90.15	8.78	0.0974
Run 19-F	3774	27,069	-3.720	+1.302	637.1	63.54	703.1	90.62	9.04	0.0997			
Run 20-I	3774	27,069			625.8	61.81	690.0	90.69	8.96	0.0988			
FP 20-6	3820	27,236	-3.670	+1.309	624.6	62.25	689.3	90.61	9.03	0.0996	89.89	8.99	0.1000
FP 20-31	4159	28,294	-3.660	+1.293	615.6	65.43	683.4	90.07	9.57	0.1062	89.36	9.43	0.1055
Run 20-F	4159	28,294	-3.660	+1.293	615.6	65.43	683.4	90.07	9.57	0.1062			

^aAverage for period between samples.^bAssumes 92% fuel charge in circulation.

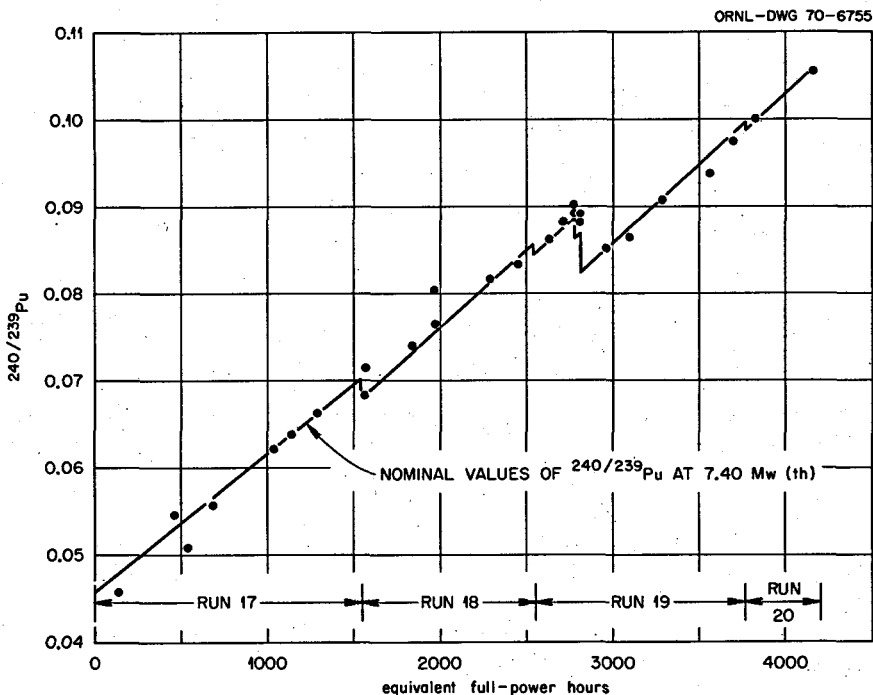


Fig. 7.5. $[^{240}/^{239}\text{Pu}]$ in the MSRE fuel salt circuit during ^{233}U operations.

MW(t). A comparison of calculated and observed values for the isotopic composition of plutonium which should result from a maximum power output of 7.40 MW is shown in Table 7.3 and in Fig. 7.5. Agreement tests indicate that the standard deviation between calculated and observed values is $\pm 0.63\%$ and that the average positive bias in the experimental data is 0.093% . On this basis the maximum power output was 7.41 ± 0.05 MW(t). The precision of this value seems to be adequate for related analyses of reactor operations.

It is considered unlikely that further refinements in cross-section data for the plutonium isotopes will require any substantial changes in the calculated inventories used for this comparison. However, for the purpose of estimating uncertainty in the combined cross-section data and neutronic model used to calculate reaction rates, an equivalent of $\pm 2\%$ in the power output is judged conservative. The results of experiments designed to measure the ^{233}U capture-to-absorption ratio in the fuel of the MSRE were reported recently by Ragan.²¹ From these results he concluded that the full-power output of the reactor was 7.34 ± 0.09 MW, in excellent agreement with our value. Further corroboration of these estimates was provided by Gabbard²² in a recent reevaluation of the accuracy of the data produced by the MSRE coolant salt flow transmitters. He found that either the pressure trans-

mitter or the square-root converter component, which generated 2- to 10-v signals for the computer, was faulty and caused the device to indicate higher than actual flows. Using a corrected flow rate of 793 gpm rather than a nominal flow rate of 850 gpm, as indicated by the computer, to recompute the heat balance power, he estimated that the full-power output of the reactor was 7.65 MW rather than the previous value of 8.2 MW.

7.3 Isotopic Composition of Uranium during ^{233}U Operations

For operation of the MSRE with ^{233}U fuel, estimation of the power output of the MSRE from measured changes in isotopic composition of the fissile material is achieved with considerably greater precision from analyses of plutonium than from uranium. This arises from the fact that the rate of change in the relative fraction of the most abundant isotopes for plutonium, ^{239}Pu and ^{240}Pu , is some four times that for the uranium pair, ^{233}U and ^{234}U . Analyses of the isotopic composition of uranium in the fuel circuit during ^{233}U operations were employed, therefore, primarily to determine whether they afforded approximate confirmation of the power estimate as inferred from the plutonium data (Sect. 7.2). Calculations of the

Table 7.4. Isotopic composition of uranium in the MSRE fuel-salt circuit^a

Sample No.	EFPH ^b	U/ Σ U (wt %)					$[^{234}\text{U}]/[^{233}\text{U}]$
		^{233}U	^{234}U	^{235}U	^{236}U	^{238}U	
Run 17-I	0	84.687	6.948	2.477	0.0808	5.807	0.08204
FP 17-18	466	84.590	7.011	2.489	0.084	5.828	0.08288
		84.690	6.990	2.470	0.084	5.771	0.08253
FP 17-24	920	84.489	7.073	2.501	0.087	5.849	0.08371
		84.382	7.058	2.487	0.089	5.986	0.08364
FP 17-32	1338	84.440	7.131	2.510	0.090	5.867	0.08445
		84.445	7.128	2.487	0.087	5.843	0.08440
Run 17-F	1536	84.363	7.152	2.513	0.091	5.875	0.08477
Run 18-I	1536	84.393	7.136	2.511	0.091	5.870	0.08455
Run 18-2	1536	84.199	7.138	2.507	0.089	6.067	0.08477
FP 18-4	1563	84.385	7.141	2.511	0.091	5.871	0.08462
		84.249	7.158	2.527	0.091	5.975	0.08496
FO 18-10	1852	84.326	7.180	2.518	0.092	5.883	0.08514
		84.269	7.178	2.507	0.091	5.955	0.08517
FP 18-13	1976	84.298	7.199	2.521	0.092	5.890	0.08539
		84.060	7.203	2.517	0.087	6.133	0.08568
FP 18-22	2221	84.241	7.232	2.529	0.095	5.902	0.08584
		84.167	7.208	2.517	0.098	6.016	0.08563
FP 18-43	2461	84.189	7.265	2.534	0.097	5.912	0.08629
		84.041	7.232	2.537	0.093	6.097	0.08605
Run 18-F	2544	84.169	7.279	2.536	0.098	5.916	0.08648
Run 19-I	2544	84.185	7.267	2.534	0.097	5.913	0.08632
FP 19 10-12 ^c	2544	84.224	7.268	2.526	0.097	5.882	0.08629
FP 19-35	2964	84.377	7.349	2.543	0.100	5.919	0.08709
		83.987	7.338	2.537	0.099	6.036	0.08737
FP 19-43	3102	84.103	7.348	2.539	0.101	5.909	0.08726
		83.994	7.328	2.533	0.099	6.047	0.08724
FP 19-53	3294	84.060	7.375	2.546	0.102	5.917	0.08773
		83.912	7.358	2.537	0.101	6.092	0.08768
FP 19-63	3561	84.000	7.413	2.553	0.104	5.931	0.08825
		83.927	7.408	2.542	0.102	6.021	0.08826
FP 19-74	3693	83.971	7.430	2.555	0.105	5.937	0.08848
		83.801	7.418	2.569	0.102	6.102	0.08851
Run 19-F	3774	83.953	7.442	2.557	0.105	5.942	0.08864
Run 20-I	3774	83.973	7.427	2.555	0.105	5.938	0.08844
FP 20-3 ^c	3774	83.996	7.426	2.549	0.105	5.923	0.08840
FP 20-6	3820	83.986	7.433	2.550	0.105	5.925	0.08850
		83.614	7.435	2.577	0.104	6.271	0.08892
FP 20-31	4159	83.911	7.482	2.558	0.108	5.940	0.08916
		83.742	7.484	2.577	0.105	6.092	0.08936

^aUpright type indicates values computed on the basis that the maximum power generated by the MSRE was 7.41 Mw(th). The following rates (furnished by B. E. Prince) were used: ^{233}U : -4.643×10^{-2} g/Mwhr; ^{234}U : $+3.6325 \times 10^{-3}$ g/Mwhr; ^{235}U : $+9.5596 \times 10^{-5}$ g/Mwhr; ^{236}U : $+3.0725 \times 10^{-4}$ g/Mwhr; ^{238}U : -2.90×10^{-4} g/Mwhr. Results of mass spectrometric analyses are listed in italicized type.

^bEquivalent full-power hours.

^cFuel addition.

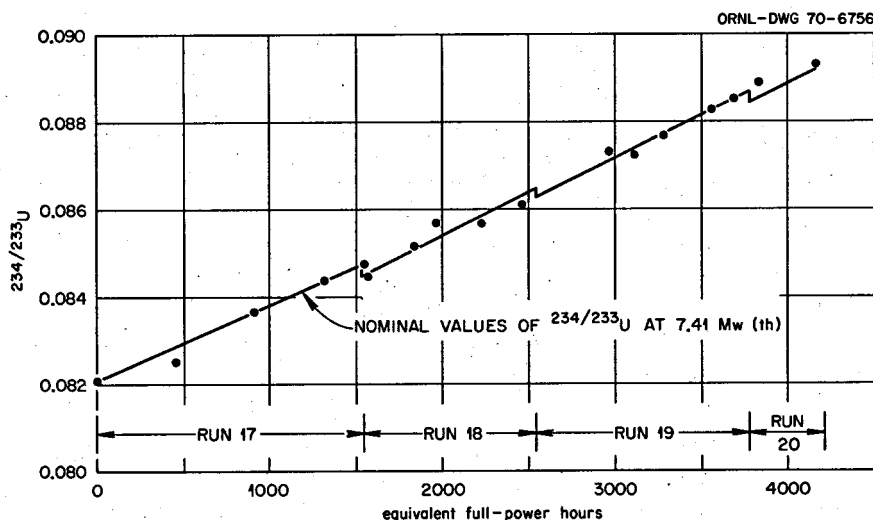


Fig. 7.6. $^{234}/^{233}\text{U}$ in the MSRE fuel circuit during ^{233}U operations.

isotopic composition changes of the uranium in the MSRE fuel circuit that should have accompanied operation of the reactor at a maximum power output of 7.41 MW(t) were made and compared with the results of mass spectrometric analyses. The results of this comparison are shown in Table 7.4 and in Fig. 7.6; they indicate that the changes observed in the isotopic composition of the uranium were in excellent agreement with those of plutonium.

7.4 Isotopic Composition of Uranium during ^{235}U Operations

Once the anomalies in the power production of the MSRE were resolved by analysis of the mass spectrometric data, and assisted by refinements in the cross-section data, internal consistency developed quickly among various other analytical results. In particular, use of the final estimate of power generation at a maximum rate of 7.4 MW to appraise both isotopic analysis and chemical analyses for uranium during the ^{235}U operational period showed that these results were entirely consistent with those for uranium and plutonium during ^{233}U operations. In addition, the revised estimates in the changes in consumption and production rates for ^{234}U , ^{235}U , ^{236}U , and ^{238}U , together with improved values for the amounts of uranium transferred to the flush salt, brought nominal and analytical values for the concentration of uranium in the fuel into good agreement as shown in Table 7.5.

Isotopic composition of the uranium in the circulating fuel salt was recalculated on the basis that the

reactor had operated at 7.4 MW and that the consumption and production rates of the uranium isotopes at this power level were those given in Prince's revised estimates.²⁰ A comparison of the results obtained is shown in Table 7.5. It will be noted that the greatest disparity in nominal and analytical values listed in Table 7.5 is observed for ^{238}U . In Sect. 3.6 it is noted that further analysis of these data led to the conclusion that, of the ^{238}U nominally charged to the MSRE drain tanks, some 2 kg was probably not delivered. Recomputation of these results in line with that conclusion would bring the nominal and observed values for the relative fractions of uranium isotopes, as listed in Table 7.5, into even closer agreement.

References

1. R. H. Guymon, *MSRE Design and Operations Report, Part VIII, Operating Procedures*, ORNL-TM-908, vol. II (January 1966).
2. G. H. Burger, J. R. Engel, and C. D. Martin, *Computer Manual for MSRE Operators*, internal memorandum, MSR-67-19 (March 1967).
3. R. C. Steffey, Jr., and J. R. Engel, *MSR Program Semiannual Progr. Rep. Feb. 29, 1968*, ORNL-4254, p. 10.
4. C. H. Gabbard, *Specific Heats of MSRE Fuel and Coolant Salts*, internal memorandum, MSR-67-19 (March 1967).
5. R. B. Lindauer, *Revisions to MSRE Design Data Sheets, Issue No. 9*, ORNL-CF-64-6-43 (June 1964).

Table 7.5. Isotopic composition of uranium in the MSRE fuel system^a

Sample No.	EFPH ^b	^{234}U	^{235}U (kg)	^{236}U	^{238}U	ΣU	^{234}U	^{235}U (wt %)	^{236}U	^{238}U
Initial Loading ^c		-	0.325	-	147.272	147.60	-	0.222	-	99.778 ^d
		0.775	75.645	0.320	4.640	81.38	0.952	92.953	0.393	5.702 ^d
		0.775	75.973	0.320	151.912	228.980	0.339	33.179	0.140	66.342
Run 3-F ^c	0	0.711	69.660	0.294	139.288	209.953	0.339	33.179	0.140	66.342
Run 4-I	0						0.350	33.250	0.140	66.260
FP 4-14	0						0.350	33.249	0.141	66.360
FP 4-28	0						0.344	33.132	0.137	66.387
FP 4-33	0						0.343	33.168	0.138	66.351
FP 4-37	0						0.339	33.157	0.147	66.357
FP 6-14	166	0.712	69.594	0.308	139.276	209.889	0.349	33.534	0.144	66.973
FP 6-19	400	0.712	69.498	0.327	139.258	209.795	0.339	33.127	0.156	66.378
FP 7-8	725	0.710	69.366	0.353	139.235	209.664	0.339	33.445	0.151	66.060
FP 7-12	1012	0.709	69.250	0.376	139.213	209.548	0.338	38.084	0.168	66.408
FP 7-15	1047	0.709	69.236	0.379	139.211	209.535	0.336	33.592	0.178	66.876
FP 8-5	1047	0.707	68.992	0.371	138.657	208.727	0.339	33.047	0.179	66.435
FP 10-7	1677	0.700	68.203	0.414	137.494	206.811	0.338	32.978	0.200	66.484
FP 11-14	2884	0.698	67.732	0.509	137.409	206.348	0.338	32.259	0.196	66.198
FP 11-39	3856	0.697	67.340	0.588	137.337	205.962	0.338	32.824	0.247	66.591
FP 11-44	3937	0.696	67.305	0.595	137.331	205.927	0.338	32.695	0.286	66.681
FP 11-44 ^e	4107	0.704	67.997	0.611	137.365	206.677	0.347	32.973	0.276	66.402
FP 11-48	4172	0.704	67.971	0.617	137.361	206.653	0.347	32.684	0.289	66.689
FP 12-5	4513	0.700	67.568	0.627	136.784	205.679	0.347	32.962	0.283	66.404
FP 12-29	5121	0.700	67.321	0.677	136.740	205.438	0.341	32.900	0.296	66.463
FP 12-51 ^f	5296	0.714	68.777	0.697	136.822	207.010	0.344	32.987	0.287	66.378
FP 12-58	5500	0.714	68.695	0.715	136.807	206.931	0.345	32.891	0.299	66.469
FP 14-25	6848	0.708	67.788	0.813	136.147	205.456	0.344	33.067	0.292	66.290
FP 14-46	7953	0.703	67.337	0.903	136.064	205.007	0.343	32.851	0.305	66.504
FP 14-68	8742	0.701	67.017	0.968	136.008	204.694	0.342	33.733	0.296	66.217
FP 14-72	9006	0.701	66.910	0.989	135.988	204.588	0.343	32.769	0.330	66.560
							0.355	32.963	0.320	66.386
							0.357	33.224	0.337	66.095
							0.355	33.475	0.325	65.845
							0.353	33.197	0.346	66.112
							0.353	33.350	0.333	65.964
							0.357	32.994	0.396	66.266
							0.357	33.390	0.379	65.874
							0.355	32.846	0.441	66.370
							0.355	33.171	0.422	66.052
							0.342	32.740	0.473	66.445
							0.354	32.945	0.450	66.251
							0.343	32.705	0.483	66.469
							0.350	33.083	0.260	66.307

^aBold faced type indicates values computed on the basis that the maximum power generated by the MSRE was 7.40 Mwth. The following rates were used: ^{234}U : - 1.665×10^{-3} g/EFPH, ^{235}U : - 4.05150×10^{-1} g/EFPH, ^{236}U : + 8.14×10^{-2} g/EFPH, ^{238}U : - 7.3691 g/EFPH (see ORNL-4449, p. 25). Results of mass spectrometric analyses are listed in italicized type.

^bEquivalent full power hours.

^cRefers to total inventory in fuel system. All following items refer to fuel circuit inventory only.

^dJ. H. Shaffer memorandum to R. E. Thoma, Sept. 28, 1970.

^e0.819 kg uranium added.

^f1.642 kg uranium added.

6. T. B. Douglas and Wm. H. Payne, *J. Res. NBS, Ser. A*, 73A, 479 (1969).
7. J. W. Cooke, L. G. Alexander, and H. W. Hoffman, *MSR Program Semiannu. Progr. Rep.* Aug. 31, 1968, ORNL-4344, p. 100.
8. B. E. Prince, *MSR Program Semiannu. Progr. Rep.* Feb. 28, 1967, ORNL-4119, p. 79; B. E. Prince, J. R. Engel, and C. H. Gabbard, *Reactivity Balance Calculations and Long-Term Reactivity Behavior with ^{235}U in the MSRE*, ORNL-4674 (in preparation).
9. B. E. Prince, *MSR Program Semiannu. Progr. Rep.* Aug. 31, 1969, ORNL-4449, p. 25.
10. D. B. Grimes, *MSR Program Quart. Progr. Rep.* June 30, 1958, ORNL-2551, p. 13.
11. J. A. Lane, H. G. MacPherson, and F. Maslan, *Fluid Fuel Reactors*, p. 656, Addison-Wesley, Reading, Mass., 1958.
12. P. R. Kasten, ORNL Reactor Division, personal communication, 1968.
13. P. R. Kasten, J. A. Lane, and L. L. Bennett, *Fuel Value Studies of Plutonium and U-233*, unpublished work, 1962.
14. A. M. Perry, unpublished work, 1971.
15. R. E. Thoma, *Chemical Feasibility of Fueling Molten-Salt Reactors with PuF₃*, ORNL-TM-2256 (June 1968).
16. B. E. Prince, personal communication.
17. R. B. Lindauer, *Processing of the MSRE Flush and Fuel Salts*, ORNL-TM-2578 (July 1969).
18. R. E. Thoma, *MSR Program Semiannu. Progr. Rep.* Aug. 31, 1969, ORNL-4449, p. 98.
19. W. H. Carr, W. F. Shaffer, and E. L. Nicholson, *MSR Program Semiannu. Progr. Rep.* Aug. 31, 1969, ORNL-4449, p. 245.
20. B. E. Prince, *MSR Program Semiannu. Progr. Rep.* Aug. 31, 1969, ORNL-4449, p. 22.
21. G. L. Ragan, *MSR Program Semiannu. Progr. Rep.* Aug. 31, 1970, ORNL-4622, p. 31.
22. C. H. Gabbard, internal correspondence, Mar. 22, 1971.

8. PHYSICAL PROPERTIES

8.1 General Properties

Successive refinements in the design or in operational criteria for molten-salt reactors evoke repeated reappraisals of the accuracy and precision of the available physical property data for reactor materials.

As experience with the MSRE grew, most of the values for physical properties of the fuel, flush, and

coolant salts were reconfirmed, while for some properties, the values originally employed appeared to be of questionable accuracy. The properties of greatest significance in these respects were viscosity, thermal conductivity, electrical conductivity, phase transition behavior, heat capacity, heat of fusion, density, expansivity, compressibility, vapor pressure, surface tension, solubility of the gases helium, krypton, and xenon, isochoric heat capacity, sonic velocity, thermal diffusivity, kinematic viscosity, and Prandtl number. Of these, the precision and accuracy are intrinsically variable and depend on methods of measurement or estimation. While the accuracy for some classes of properties, for example, liquidus-solidus temperatures, developed to be of minor concern, others, such as surface tension and heat capacity, had neither been measured nor were measurable with the precision that was desirable for reactor performance evaluations. In response to MSRE program requirements, reappraisals and refinements of physical property data were repeatedly made whenever it was feasible. The final evaluation led to values which, for the coolant and flush salt, are summarized in Table 8.1 and, for the fuel salt, are summarized in Table 8.2.

8.2 Density of Fuel and Coolant Salts

Laboratory measurements of the density of molten fluoride mixtures were performed by various groups of investigators before the MSRE was operated. The precision in the results, however, was considered to be less than desirable for use in on-site calculations of reactivity balances and for appraisal of temperature effects. An effort was made, therefore, to make direct measurements with the reactor that would serve these purposes and that would afford independent measurement of the salt inventories. An early account gives a perspective on the success of these efforts:¹

The weigh cells on all the salt drain tanks were calibrated with lead weights shortly after the equipment was installed and before the tanks and connected piping were heated. Additional data were obtained with the tanks hot during various salt-charging and transfer operations. These data served both to calibrate the weighing systems and to give a measure of the density of the salts at operating temperature. Throughout the operation, salt inventories were computed from weigh-cell readings, using scale factors and tare corrections obtained from the calibration tests.

Cold and hot calibration of the coolant drain-tank weigh cells gave scale factors differing by less than 0.5%. Fuel drain tank 2 (FD-2) was calibrated hot twice, with flush salt and with fuel carrier salt; scale factors were within 0.2% of each other but were about 4% higher than the original, cold calibration. The reason for this discrepancy has not been established.

The coolant-salt density was measured in the reactor by three different methods; values ranged from 121.3 to 122.3 lb/ft³ at 1200°F, with an average of 121.9 lb/ft³. When flush salt, which

Table 8.1. Physical properties of lithium fluoroberyllate, $\text{Li}_2\text{BeF}_4^a$

Property	Value	Estimated precision
Viscosity	η (centipoises) = $0.116 \exp [3755/T(\text{°K})]$	±7
Thermal conductivity	$0.010 \text{ watt cm}^{-1} \text{ °C}^{-1}$	±10%
Electrical conductivity	$\kappa = 1.54 \times 6.0 \times 10^{-3} (\text{ohm}\cdot\text{cm})^{-1}$ at 500°C	±10%
Melting point ^b	459.1°C	±0.2°C
Crystal structure	Hexagonal; space group: $R\bar{3}$; $a = 13.29\text{\AA}$, $c = 8.91\text{\AA}$	±0.01 Å
Heat capacity		
Liquid	$C_p = 0.57 \text{ cal g}^{-1} \text{ °C}^{-1}$	±3%
Solid	$C_p = 0.31 + 3.61 \times 10^{-4} T(\text{°C}) \text{ cal g}^{-1} \text{ °C}^{-1}$	±3%
Density		
Liquid	$\rho = 2.214 - 4.2 \times 10^{-4} T(\text{°C}) \text{ g/cm}^3$ $= 122 \text{ lb/ft}^3$ at 650°C	±1%
Solid	$\rho = 2.1953 \text{ g/cm}^3$	
Expansivity	$2.14 \times 10^{-4}/\text{°C}$ at 600°C	±10%
Compressibility	$\beta_T(\text{°K}) = 2.3 \times 10^{-12} \exp [1.0 \times 10^{-3} T(\text{°K})] \text{ cm}^2/\text{dyne}$	Factor 3
Vapor pressure	$\log P(\text{torrs}) = 8.0 - 10,000/T(\text{°K})$	Factor 50 from 500 to 700°C
Surface tension	$\gamma = 260 - 0.12T(\text{°C}) \text{ dynes/cm}$	+30, -10%
Solubility of He, Kr, Xe	$T(\text{°C}) \quad \text{He} \quad \text{Kr} \quad \text{Xe}$ 500 6.6 0.13 0.03 600 10.6 0.55 0.17 700 15.1 1.7 0.67 800 20.1 4.4 2.0 $\times 10^{-8} \text{ moles cm}^{-3} \text{ melt atm}^{-1}$	≥ Factor 10
Isochoric heat capacity, C_v	C_v $T(\text{°C}) \quad \frac{\text{cal g}^{-1}}{\text{°K}^{-1}} \quad \frac{\text{cal g-mole}^{-1}}{\text{°K}^{-1}} \quad \frac{\text{cal g-atom}^{-1}}{\text{°K}^{-1}} \quad \frac{C_p}{C_v}$ 500 0.48 ₉ 16.2 6.9 ₁ 1.1 ₇ 600 0.48 ₂ 15.9 6.8 ₁ 1.1 ₈ 700 0.47 ₅ 15.7 6.7 ₂ 1.2 ₀	
Sonic velocity	$500^\circ\text{C}: \mu = 3420 \text{ m/sec}$ $600^\circ\text{C}: \mu = 3310 \text{ m/sec}$ $700^\circ\text{C}: \mu = 3200 \text{ m/sec}$	
Thermal diffusivity	$500^\circ\text{C}: D = 2.0_9 \times 10^{-3} \text{ cm}^2/\text{sec}$ $600^\circ\text{C}: D = 2.1_4 \times 10^{-3} \text{ cm}^2/\text{sec}$ $700^\circ\text{C}: D = 2.1_8 \times 10^{-3} \text{ cm}^2/\text{sec}$	
Kinematic viscosity	$500^\circ\text{C}: \nu = 7.4_4 \times 10^{-2} \text{ cm}^2/\text{sec}$ $600^\circ\text{C}: \nu = 4.3_6 \times 10^{-2} \text{ cm}^2/\text{sec}$ $700^\circ\text{C}: \nu = 2.8_6 \times 10^{-2} \text{ cm}^2/\text{sec}$	
Prandtl number	$500^\circ\text{C}: \text{Pr} = 35.6$ $600^\circ\text{C}: \text{Pr} = 20.4$ $700^\circ\text{C}: \text{Pr} = 13.1$	

^aPhysical properties for the pure compound Li_2BeF_4 approximate those for the MSRE flush and coolant salts within limits of experimental uncertainty. Unless otherwise noted, property values correspond to those reported in *Physical Properties of Molten-Salt Reactor Fuel, Coolant and Flush Salts*, S. Cantor, ed., ORNL-TM-2316 (August 1968).

^bK. A. Romberger and J. Braunstein, *MSR Program Semiannual Progr. Rep. Feb. 28, 1970*, ORNL-4548, p. 161.

^cJ. H. Burns and E. K. Gordon, *Acta Cryst.* **20**, 135 (1966).

Table 8.2. Physical properties of the MSRE fuel salt

Property	Value			Estimated precision
Viscosity	η (centipoises) = $0.116 \exp [3755/T(\text{°K})]$			±7
Thermal conductivity	$0.010 \text{ watt cm}^{-1} \text{ °C}^{-1}$			±10%
Electrical conductivity	$\kappa = -2.22 + 6.81 \times 10^{-3} T(\text{°C})^a$			±10%
Liquidus temperature	434°C			±3°C
Heat capacity				
Liquid	$C_p = 0.57 \text{ cal g}^{-1} \text{ °C}^{-1}$			±3%
Solid	$C_p = 0.31 + 3.61 \times 10^{-4} T(\text{°C}) \text{ cal g}^{-1} \text{ °C}^{-1}$			±3%
Density				
Liquid	$\rho = 2.575 - 5.13 \times 10^{-4} T(\text{°C})$ $= 139.9 \text{ lb/ft}^3 \text{ at } 650^\circ\text{C}$			±1%
Expansivity	$2.14 \times 10^{-4}/\text{°C}$ at 600°C			±10%
Compressibility	$\beta_T(\text{°K}) = 2.3 \times 10^{-12} \exp [1.0 \times 10^{-3} T(\text{°K})] \text{ cm}^2/\text{dyne}$			Factor 3
Vapor pressure	$\log P(\text{torrs}) = 8.0 - 10,000/T(\text{°K})$			Factor 50 from 500 to 700°C
Surface tension	$\gamma = 260 - 0.12T(\text{°C}) \text{ dynes/cm}$			+30, -10%
Solubility of He, Kr, Xe	$T(\text{°C})$	He	Kr	Xe
	500	6.6	0.13	0.03
	600	10.6	0.55	0.17
	700	15.1	1.7	0.67
	800	20.1	4.4	2.0
		$\times 10^{-8} \text{ moles cm}^{-3} \text{ melt atm}^{-1}$		
Isochoric heat capacity, C_v		C_v		
	$T(\text{°C})$	$\text{cal g}^{-1} \text{ }^{\circ}\text{K}^{-1}$	$\text{cal g-mole}^{-1} \text{ }^{\circ}\text{K}^{-1}$	$\text{cal g-atom}^{-1} \text{ }^{\circ}\text{K}^{-1}$
	500	0.48 ₉	16.2	6.9 ₁
	600	0.48 ₂	15.9	6.8 ₁
	700	0.47 ₅	15.7	6.7 ₂
				$\frac{C_p}{C_v}$
				1.1 ₇
				1.1 ₈
				1.2 ₀
Sonic velocity				
500°C: $\mu = 3420 \text{ m/sec}$				
600°C: $\mu = 3310 \text{ m/sec}$				
700°C: $\mu = 3200 \text{ m/sec}$				
Thermal diffusivity				
500°C: $D = 2.0_9 \times 10^{-3} \text{ cm}^2/\text{sec}$				
600°C: $D = 2.1_4 \times 10^{-3} \text{ cm}^2/\text{sec}$				
700°C: $D = 2.1_8 \times 10^{-3} \text{ cm}^2/\text{sec}$				
Kinematic viscosity				
500°C: $\nu = 7.4_4 \times 10^{-2} \text{ cm}^2/\text{sec}$				
600°C: $\nu = 4.3_6 \times 10^{-2} \text{ cm}^2/\text{sec}$				
700°C: $\nu = 2.8_6 \times 10^{-2} \text{ cm}^2/\text{sec}$				
Prandtl number				
500°C: $Pr = 35.6$				
600°C: $Pr = 20.4$				
700°C: $Pr = 13.1$				

^aApplicable over the temperature range 530 to 650°C. The value of electrical conductivity given here was estimated by G. D. Robbins and is based on the assumption that ZrF₄ and UF₄ behave identically with ThF₄; see G. D. Robbins and A. S. Gallanter, *MSR Program Semiannual Prog. Rep.* Aug. 31, 1970, ORNL-4548, p. 159; ibid., ORNL-4622, p. 101.

is identical with coolant salt, was charged into FD-2, the amount of salt added between two level probes indicated a density of 124.5 lb/ft³. A density of 120.9 lb/ft³ was computed from the pressure required to lift salt from the drain tank to the fuel loop. Weigh-cell indications of flush-salt density, using the "hot" calibration factor, ranged from 123.2 to 131.5 lb/ft³ at 1200°F; the "cold" calibration factor would have given 118.4 to 126.3 lb/ft³. The data on coolant- and flush-salt densities thus tend to support the "cold" calibration factor for FD-2.

The density of the fuel carrier salt, LiF-BeF₂-ZrF₄ (65-30-5 mole %) was measured as the salt was being charged to FD-2. This measured density, computed from externally measured weights and the volume between the level probes in FD-2, was 140.6 lb/ft³ at 1200°F. Addition of all the uranium added through run 3 would be expected to increase the density by about 5.3 lb/ft³. Four measurements were made after the uranium was added, using the weigh cells and the level probes. Densities based on the "hot" calibration of the weigh cells ranged from 149.9 to 152.2 lb/ft³, with an average of 151.0 lb/ft³ at 1200°F. With the "cold" scale factor the average was 145.1 lb/ft³, very close to the expected density.

Salt densities were computed on several occasions from the change in weigh-cell readings as the fuel loop was filled. In every case the computed density was less than given by other means, suggesting that a full loop volume may not have been transferred.

The temperature coefficients of density for the salts were computed from the change in salt level with loop temperature. Measured values of $(\Delta\rho/\rho)/\Delta T$ were: for the coolant salt, -1.06×10^{-4} (°F)⁻¹ (average of three measurements); for the flush, -1.15×10^{-4} (°F)⁻¹; and for the fuel salt, -1.09×10^{-4} and -1.15×10^{-4} (°F)⁻¹ (two measurements).

The bulk of the inventory data accumulated to date is on the flush salt, because more transfer and fill-and-drain operations have been done with this salt. Calculated inventories (using "hot" scale factors) have ranged from 1.7% below to 2.6% above the nominal or "book" inventory for no ascribable reason.

With continued experience it became evident that on-site measurements of salt masses were less and less reliable and would have little consequence in appraising reactor performance because of inaccuracies in the weigh-cell measurements. In the absence of such information the amounts of salts delivered to the circulating system or remaining in the drain tanks were approximated from values of the density of the salt mixtures and the dimensions of the container vessels. Efforts were initiated to appraise and improve, if feasible, the accuracy and precision of data pertaining to the densities of molten fluoride mixtures.

Relatively few measurements of the densities of liquid salt mixtures were made in the development of molten-salt technology at ORNL prior to MSRE operations. Experimental values for the densities of a number of ZrF₄-containing mixtures were made as a part of the Aircraft Nuclear Propulsion program.² Similar measurements, which employed the buoyancy principle, as did

the ORNL program, were made later with LiF-BeF₂-UF₄ mixtures by the Mound Laboratory³ under contract work with ORNL. Most density values for the mixtures used in the MSR program, however, were estimated by the method of mixtures.² This method was believed to have an accuracy of approximately ±5%.

In an effort to obtain more accurate values for the salt mixtures used in the MSRE, attempts were made to develop new methods for the laboratory determination of the densities of molten salt mixtures. Employing a new technique, Sturm and Thoma⁴ obtained density measurements for the MSRE fuel and coolant-salt mixtures. Measurements of the depth of salt in a cylindrical container of accurately known dimensions, which was contained in a controlled atmosphere glove box, were obtained using an electrical probe attached to a vernier caliper. Contact of the probe with the melt was indicated by completion of an electrical circuit through the caliper and the melt. Appropriate corrections for thermal expansion at a particular temperature were applied for the container and the probe. Although some shortcomings were evident in the procedure, principally owing to the effects of small amounts of liquid adhering to the probe, it afforded a direct measurement of the densities of liquids which were visually observable during measurement. The results of the measurements were found to be in satisfactory agreement with on-site measurements of the densities of the salt stored in the drain tanks.⁵ Laboratory efforts were therefore discontinued. Concurrently, a method for estimating densities which assumes additivity of molar volumes was devised by Cantor.⁶ With continued refinement, the method was developed to the extent that its accuracy was within 5%. A comparison of the densities of the MSRE fuel and coolant salts, as found using the several methods described above, is given in Table 8.3.

On the basis of reactor physics analysis, it was estimated that the average fraction of the fuel charge circulated during power runs with the MSRE was 92%. This value, together with a value of the volume of the circuit computed from component dimensions, 71.3 ft³, and the mass of the circulated charge as deduced from chemical and isotopic analyses (Table 2.6), indicates that the density of the ²³⁵U fuel at the beginning of power operations was 139.01 lb/ft³, whereas the value computed by Cantor's method is 139.9 lb/ft³. In more recent application of Cantor's method to other salt mixtures, excellent agreement has been found between estimated and observed values. Such confirmation, along with its apparent precision for MSRE fuel

Table 8.3. Density of MSRE salt mixtures at 650°C (1200°F)
 $\rho = a - bT(\text{°C}) \text{ g/cm}^3$

Composition (mole %)	Source	Density parameters		ρ , density	
		a	b	g/cm^3	lb/ft^3
$\times 10^{-4}$					
LiF-BeF ₂ (66-34)	Method of mixtures ^a	2.24	6	1.85	115.5
	Mound Laboratory ^b	2.158	3.7	1.921	119.9
	On-site estimate (see text)			1.89-2.11	118-132
	Electrical probe	2.296	4.82	1.983	123.8
	Molar volume estimate ^c	2.214	4.2	1.941	121.8
LiF-BeF ₂ -ZrF ₄ (64.7-30.1-5.2)	Molar volume estimate ^c	2.471	4.95	2.15	134.2
	On-site estimate			2.25	140.6
LiF-BeF ₂ -ZrF ₄ -UF ₄ (64.7-29.38-5.1-0.82)	Method of mixtures ^a	2.61	7	2.15	134.2
	On-site estimate			2.32-2.44	145-152
	Electrical probe	2.848	7.69	2.35	146.6
	Molar volume estimate ^c	2.575	5.13	2.24	139.9

^aS. I. Cohen and T. N. Jones, *A Summary of Density Measurements on Molten Fluoride Mixtures and a Correlation for Predicting Densities of Fluoride Mixtures*, ORNL-1702 (July 1954, declassified Nov. 2, 1961).

^bMound Laboratory report MLM-1086 (see ref. 3).

^cS. Cantor, unpublished work, 1969.

salt, permits the inference that the most accurate values of MSRE salt densities have been derived by this method.

An important characteristic that easily tends to pass unnoticed from attention is that Li₂BeF₄ is unique among the complex fluorides which have significance in molten-salt reactor technology, in that it undergoes the least volume change associated with the melting-freezing transition of any of the compounds encountered. This value has not been measured directly but can be estimated by assuming that the linear coefficients of thermal expansion for Li₂BeF₄ and LiF are similar enough to be used interchangeably. If this assumption is valid, the density of Li₂BeF₄ is 2.064 g/cm³ at the melting point, about 6% less than at room temperature. The density of liquid of the stoichiometric composition at the melting point, as indicated by the density expression in Table 8.1 is 2.021 g/cm³. These two values indicate that, on melting Li₂BeF₄, the density is reduced only about 2.07%.

It is important to recognize that the MSRE fuel, coolant, and flush salts were nearly of the composition Li₂BeF₄, and to some extent the freedom that the MSRE showed from difficulties with freeze valves and from distortion of the radiator tubes under off-specification cooling conditions⁷ is due to the very small volume change this compound undergoes at the melting point.

8.3 Crystallization of the MSRE Fuel

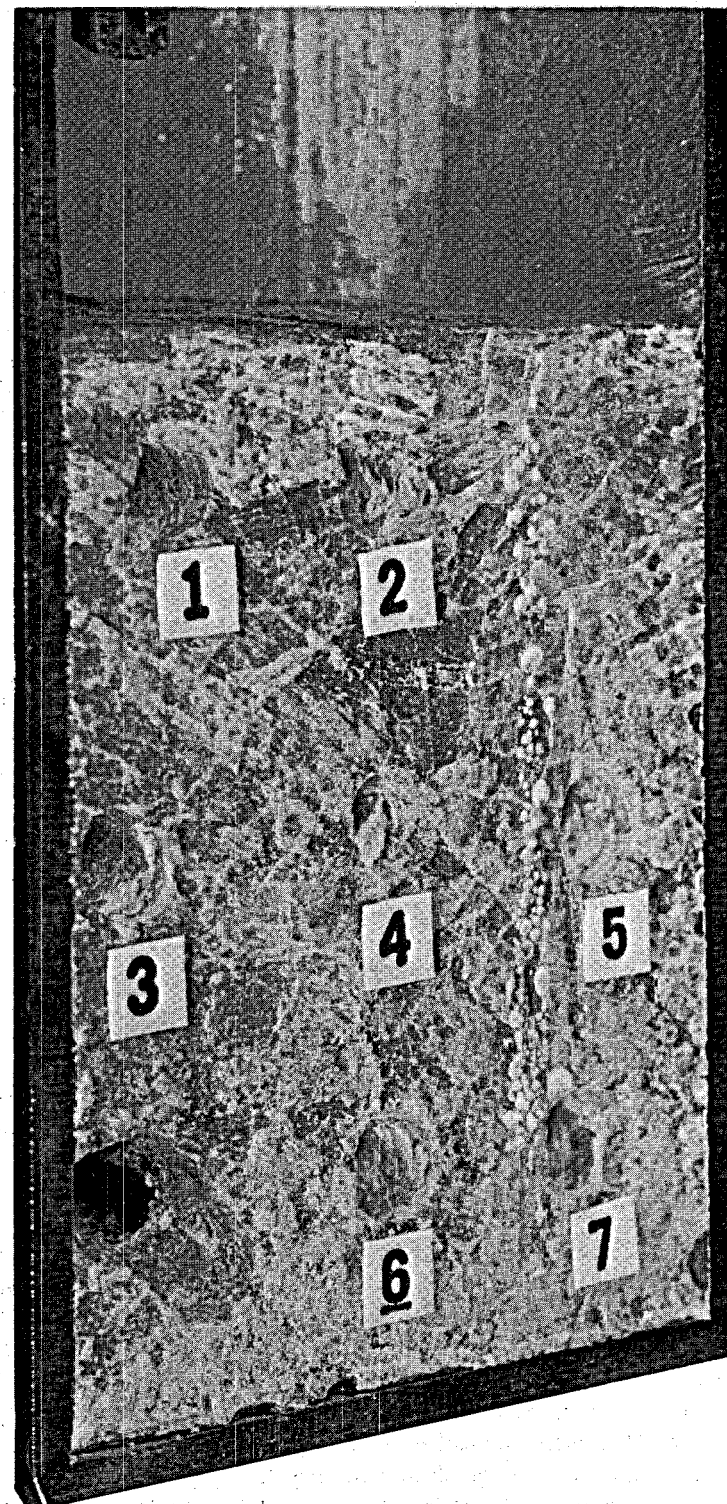
Laboratory studies of fluoride mixtures were carried on for some years before the MSRE was operated. In these studies, the crystallization behavior of the LiF-BeF₂-ZrF₄-UF₄ (65-29.1-5-0.9 mole %) mixture was established to approximate that of the MSRE fuel salt when it operated with ²³⁵U fuel. Crystallization was found to follow the equilibrium crystallization sequence described below:

On cooling the liquid mixture to 434°C, crystalline Li₂BeF₄ is formed. This phase continues to precipitate on further cooling, and at 431°C, Li₂ZrF₆ begins to crystallize; the onset of crystallization by the tertiary phase, LiUF₅, begins at 416°C. The liquid portion of the mixture decreases but is present down to temperatures as low as ~350°C. When completely frozen, the fuel at equilibrium should be composed of crystalline Li₂BeF₄, Li₂ZrF₆, LiUF₅, and BeF₂ in volume fractions of 0.735, 0.204, 0.032, and 0.029 respectively. The usual cooling paths for LiF-BeF₂-ZrF₄-UF₄ mixtures of compositions similar to the MSRE fuel involve a glassing of the BeF₂-rich liquids that are low melting and, thus, the last to freeze. Hence, crystals of pure BeF₂ are generally not expected; rather, the last liquid solidifies as glass which incorporates variable amounts of the phases listed above with BeF₂.

PHOTO 67747AR



Fig. 8.1. MSRE fuel ingot resulting from slower cooling rate.



The homogeneity generally characteristic of multicomponent salt mixtures in the liquid state is progressively destroyed as the mixture undergoes gradual crystallization. The possibility that the MSRE fuel mixture, $\text{LiF}-\text{BeF}_2-\text{ZrF}_4-\text{UF}_4$ (65.29.1.5.0.0.9 mole %), might, on cooling in the MSRE drain tanks, experience sufficient solid-phase fractionation to create potentially hazardous conditions was examined in laboratory-scale experiments. Some 650 g of simulated fuel salt was cooled at rates approximating that expected of the entire drain tank assembly and that expected of the fuel alone, 3.46 and 0.387°C/hr respectively. In both cases the radiative cooling geometry was controlled to simulate as nearly as possible that expected in the drain tanks, even though it was realized that the horizontal ΔT profile in the cooling radioactive fuel mixture would probably be substantially different from that prevailing in the laboratory experiment.

The concentrations of uranium were found to be identical at the top and bottom fractions of each of the two ingots, irrespective of cooling rate. A photograph of the ingot resulting from the slower cooling rate experiments is shown in Fig. 8.1. Chemical analyses of the salt specimens from each of the locations designated in Fig. 8.1 were obtained. For areas 1 to 7, the uranium concentrations were found to be 2.94, 3.49, 4.15, 3.32, 4.28, 4.62, and 5.74 wt %. In comparison with the nominal concentration of uranium in the MSRE fuel, 5.13 wt %, these experiments show a maximum increase of 23.4% in uranium concentration on very slow static cooling. A fact which accounts for the small degree of segregation of the uranium phases in these experiments is that, at the onset of crystallization of LiUF_5 , simultaneous crystallization of the three solid phases Li_2BeF_4 , Li_2ZrF_6 , and LiUF_5 takes place. In addition, the volume of the liquid phase is being reduced steadily, so sharply, in fact, that in this experiment as well as in similar previous ones, some of the liquid phase was apparently occluded among dendritic-like crystals of the solidified phase, a phenomenon which helps prevent compositional variation in the mixture.

In the freezing of multicomponent mixtures, maximum segregation of crystalline phases takes place under equilibrium cooling conditions. The segregation represented by the results obtained in the fractionation experiments described here represents, in a practical way, the nearest approach to equilibrium cooling that the MSRE fuel salt may experience in a single crystallization sequence.

The crystallization behavior described above pertains exclusively to the fuel-salt mixtures used in the MSRE and is, of course, quite unlike that for fuel mixtures

proposed for use in a molten-salt breeder reactor. Crystallization equilibria similar to those for the breeder fuel are described elsewhere by Thoma and Ricci.⁸

References

1. P. N. Haubenreich et al., *MSR Program Semiannual Progr. Rep. Aug. 31, 1965*, ORNL-3872, p. 30; see also Sect. 2.4.2 of this report.
2. S. I. Cohen and T. N. Jones, *A Summary of Density Measurements on Molten Fluoride Mixtures and a Correlation for Predicting Densities of Fluoride Mixtures*, ORNL-1702 (July 19, 1954, declassified Nov. 2, 1961).
3. *Density and Viscosity of Fused Mixtures of Lithium, Beryllium and Uranium Fluorides*, Mound Laboratory report MLM-1086 (December 1956).
4. B. J. Sturm and R. E. Thoma, *Reactor Chem. Div. Annu. Progr. Rep. Jan. 31, 1965*, ORNL-3789, p. 83.
5. P. N. Haubenreich, private communication, Aug. 16, 1965.
6. S. Cantor, *Reactor Chem. Div. Annu. Progr. Rep. Jan. 31, 1962*, ORNL-3262, p. 38.
7. T. L. Hudson, C. H. Gabbard, and D. M. Richardson, *MSR Program Semiannual Progr. Rep. Aug. 31, 1966*, ORNL-4119, p. 41.
8. R. E. Thoma and J. E. Ricci, *Fractional Crystallization in the System $\text{LiF}-\text{BeF}_2-\text{ThF}_4$* , ORNL-TM-2596 (July 1969).

9. INTERACTIONS OF FUEL SALT WITH MODERATOR GRAPHITE AND SURVEILLANCE SAMPLE MATERIALS

A new method of in-situ analysis for lithium, beryllium, and fluorine was invented by Macklin, Gibbons, and Handley¹ in response to our appeal for their assistance in examination of graphite specimens removed from the MSRE core. The method they devised employed proton bombardment of target nuclides and measurement of the yields of neutrons and gamma rays produced. It was found to be applicable for measurement of the concentration of target nuclides in graphite at the few-parts-per-million level as a means to determine the extent to which MSRE fuel salt components penetrated into the graphite under radiation. This method has the advantage of applicability to matrix-dispersed samples and in the presence of considerable radioactivity from fission products, features which make it well suited to the examination of MSRE graphite.

The results obtained by these workers were reported in detail previously.^{2,3} There remain several puzzling aspects of their findings, and because of this the results are reviewed here.

Data were obtained from three samples, (1) a control sample (Y-5 from CGB bar 635) exposed to nonradioactive salt, (2) sample Y-7, removed from the reactor core after 33,400 MWhr of exposure in May 1967, and (3) sample X 13, removed March 25, 1968, after 66,637 MWhr of exposure.

Specimens were moved across a beam of 2.06-MeV protons collimated through a slit of 0.0075 cm width at the ORNL 3-MV Van de Graaff accelerator. Measurement of the resulting prompt gamma rays from $^{19}\text{F}(p,\gamma)^{16}\text{O}$ showed that fluorine varied in sample X-13 from 350 ppm near the surface to 60 ppm at the center (Fig. 9.1). The observed ratio of fluorine to lithium was near that characteristic of the MSRE fuel (Fig. 9.2). However, as shown in Figs. 9.1 and 9.3, the lithium and fluorine did not show a simple dependence on depth.

Results of the examination of sample X-13 suggested that much of the Li and F came from bulk intrusion, a finding which differed from that resulting from the previous examination of sample Y-7 (Fig. 9.4), where

the Li/F ratio became increasingly higher at greater distances from the surface. Equally puzzling is that comparisons with the results of the analysis for ^{235}U by Kirslis and Blankenship⁴ (see Figs. 9.1 and 9.3) showed that the relative concentrations of F and ^{235}U became steadily divergent with penetration depth and thus seemed to rule out bulk salt intrusion as a mechanism. Further, in the absence of radiation, a control specimen showed less penetration of both salt and uranium by a factor of 100. The possibility was considered that introduction of a fuel aerosol from the gas phase, as was suggested to rationalize the intrusion of certain fission products,⁴ was responsible for fuel having penetrated the graphite voids as an aerosol. The cause of this phenomenon is still not resolved.

The uranium profiles shown in Figs. 9.1 and 9.3 were derived in the investigation by Kirslis and Blankenship, in which it was found, from delayed neutron activation analysis, that the uranium concentration profile ranges from values as high as 100 ppm at the surface to 6.5 ppm at 50 mils depth, but "in most cases, the total range of variation of the ^{235}U concentration in 50 mils penetration was less than two orders of magnitude. This moderate slope indicates a higher mobility for uranium in graphite than for most fission products [but] . . . represents only 1 g of ^{235}U per 1000 kg of graphite."⁴

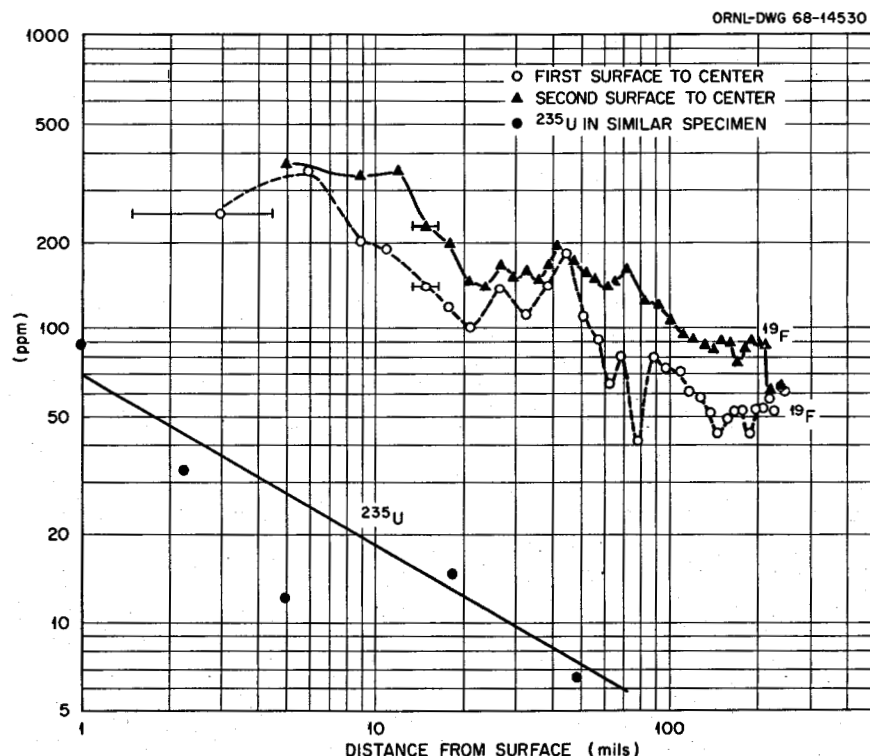


Fig. 9.1. Fluorine concentration as a function of distance from the surface.

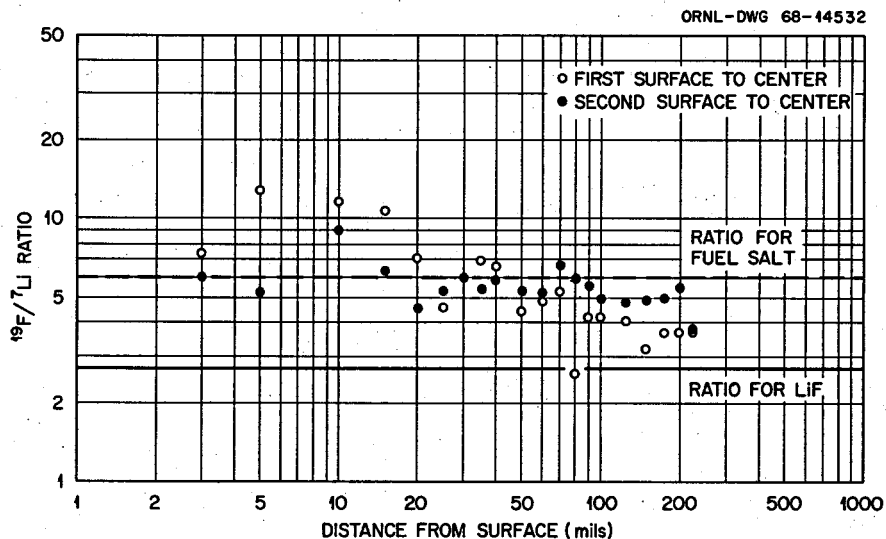


Fig. 9.2. Mass concentration ratio, F/Li, vs depth.

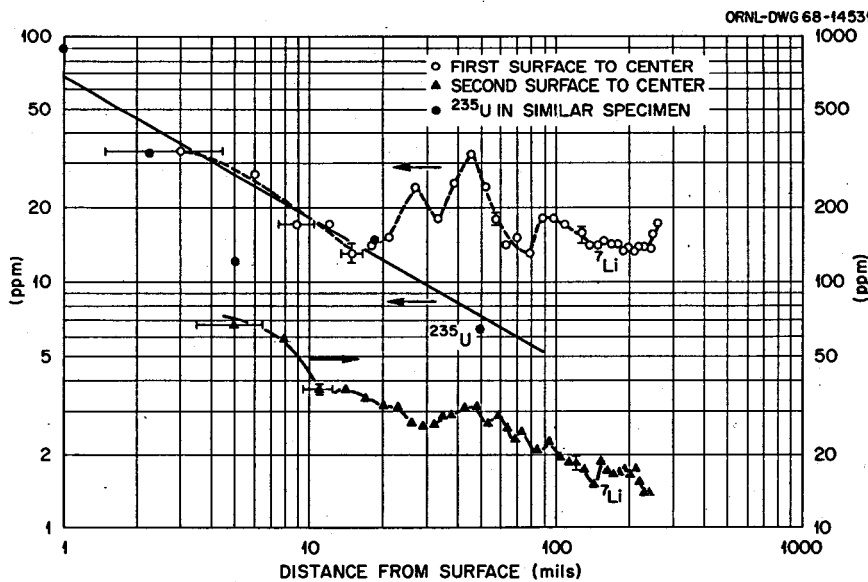


Fig. 9.3. Lithium concentration as a function of distance from the surface.

Although the results of the proton reaction analysis described by Macklin and co-workers do not seem to permit quantitative generalization, they do suggest several points of significance to further development of molten-salt reactor technology:

1. The penetration of the graphite moderator by lithium and fluorine appears to be real, if not massive. Only samples of CGB graphite were examined in the experiments performed by Macklin et al. Whether similar penetrations of more dense or

coated graphites can be expected for improved MSBR graphites is not estimable from the current results.

2. Effects of salt-gas-graphite interfacial properties on transport of lithium and fluorine through films is unknown at present.
3. The current data were derived from a fuel salt with a composition, $\text{LiF-BeF}_2\text{-ZrF}_4\text{-UF}_4$ (65-29.2-5.0-0.8 mole %), whose effect on transport conceivably may differ from that for the MSBR. Whether the trans-

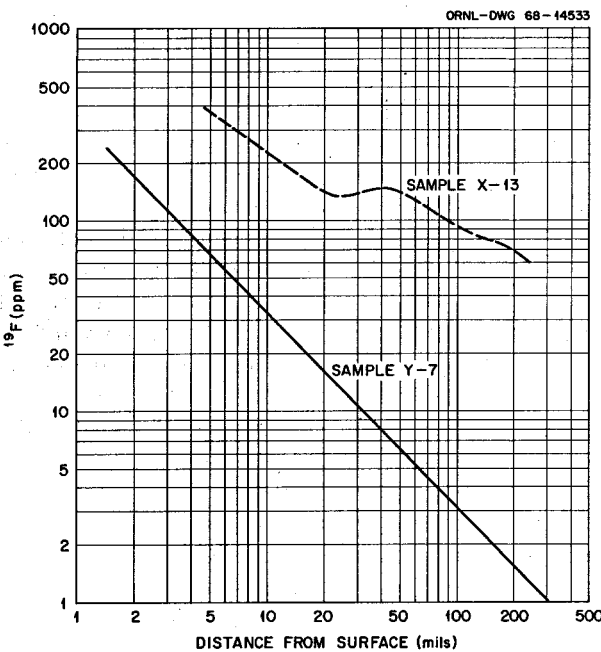


Fig. 9.4. Comparison of fluorine concentrations in samples Y-7 and X-13, a smooth line having been drawn through the data points.

port would be markedly affected by the large heavy-metal concentration of the MSBR fuel, containing a total of 12 mole % $\text{ThF}_4 + \text{UF}_4$, is of justifiable curiosity.

The results obtained indicated with ^{235}U fuel salt that there are a number of parameters whose quantitative relationship to the transport of salt species to moderator graphites should be examined by further examination of graphite specimens, especially those removed from the MSRE core after completion of the ^{233}U experiments. Several notable differences between ^{233}U and ^{235}U operations existed, including for ^{233}U operation a uranium concentration less than 20% of that with ^{235}U , a continuously higher void fraction in the fuel salt, and variable differences in the gas-salt interfacial tension. The latter two of these factors were regarded as possibly conducive to enhanced transfer of materials to the graphite moderator and prompted further examination of graphite specimens from the MSRE.

In postoperational examinations of a graphite stringer from the MSRE core vessel, Kirslis and Blankenship⁵ obtained spectrochemical and delayed neutron analyses of the graphite milled from the surface of the stringer. Analyses by the proton bombardment method were not performed. The analytical results that were obtained were in partial agreement with the earlier results of Macklin and co-workers and indicated bulk penetration

of the fuel salt, probably via cracks in the graphite, to a depth of ~ 2 mils. In contrast, however, they did not indicate penetration to greater depths. Although the results of the two groups of analyses are in good agreement with respect to penetration of the outermost layers, Kirslis and Blankenship did not find anomalous divergence in the relative concentration of any of the components, nor did they find that uranium penetration had occurred to greater depths. The absence of detectable amounts of uranium in the graphite at depths where uranium had been detected with samples from ^{235}U tests tends to support a model of bulk salt penetration, since the ^{233}U concentration of the fuel was less than 20% of that of the ^{235}U fuel.

Applications of new and increasingly sensitive methods of analysis, such as the proton bombardment method, in molten-salt research and development programs are significant to the continued development of the technology. Continued refinement and adaptation of this new method are highly desirable within the framework of future research programs for possible application to MSBR development.

References

1. R. L. Macklin, J. H. Gibbons, and T. H. Handley, *Proton Reaction Analysis for Lithium and Fluorine in Graphite Using a Slit Scanning Technique*, ORNL-TM-2238 (July 1968).
2. R. L. Macklin et al., *MSR Program Semiannual Progr. Rep. Feb. 9, 1968*, ORNL-4254, p. 119.
3. R. L. Macklin et al., *MSR Program Semiannual Progr. Rep. Aug. 31, 1969*, ORNL-4344, p. 146.
4. S. S. Kirslis and F. F. Blankenship, *MSR Program Semiannual Progr. Rep. Aug. 31, 1969*, ORNL-4344, p. 115.
5. S. S. Kirslis and F. F. Blankenship, *MSR Program Semiannual Progr. Rep. Feb. 28, 1971*, ORNL-4676, p. 73.

10. CHEMICAL SURVEILLANCE OF AUXILIARY FLUID SYSTEMS

10.1 Water Systems

Potable water from the ORNL distribution system was supplied to the MSRE for a variety of uses as described in the *MSRE Design and Operations Report*.¹

After passing through a backflow preventer, the water is used in the liquid waste system, in the vapor-condensing system, for general cleanup of equipment, as makeup for the cooling tower water system, and for cooling of the charcoal beds. Two

520-gpm centrifugal pumps are provided for circulating cooling tower water, which is cooled by a two-fan induced draft cooling tower. The cooling tower water is used for air compressors, air conditioners, in the chemical plant, for the lube-oil systems, in the charcoal beds, and for condensing steam from the drain tank steam domes. (Process water can also be used for this.) Cooling tower water is also used in a shell-and-tube heat exchanger to provide cooling for the treated water system. Two 230-gpm centrifugal pumps circulate treated water in a closed loop to cool in cell components. Makeup water is supplied by condensing building steam in a shell and tube heat exchanger using cooling tower water as the coolant. Treated water is also used to fill the Nuclear Instrument penetration. This water is continuously recirculated through a closed loop by a 5-gpm pump to maintain uniformity of the water condition throughout the penetration. In order to minimize corrosion, potassium tetraborate and potassium nitrite were added to the water supply and maintained at concentrations of 500 and 1500 ppm, respectively. Steam condensate is also used to supply water to the feedwater tanks. This untreated water is used in the drain tank bayonets to remove decay heat from the reactor fuel after the reactor has been drained.

The several water systems at the MSRE were sampled periodically and analyzed to determine corrosion rates, buildup of contaminants, loss of corrosion-inhibiting chemicals, etc. Water samples were submitted regularly for chemical analysis in the General Analysis Laboratory. At more frequent intervals, on-site tests were performed to give continuity to the control data and to reduce dependency on analyses from the laboratory. Details of sampling procedures, methods of additions of corrosion inhibitors, and of on-site testing procedures are given in the *MSRE Design and Operations Report*, Sect. 6-1.¹

10.1.1 Cooling tower water. Samples of the cooling tower water were tested on-site daily to check the concentration of its chromate ion, which served as a corrosion inhibitor, pH, and hardness. Samples were submitted on a weekly basis for laboratory analysis, where more complete analyses were performed. In use, the cooling tower water supply was maintained in the pH range 7 to 8, concentration of chromate ion at 30 to 50 ppm, hardness ≤ 250 ppm (as CaCO_3), and $\text{Fe} \leq 0.03$ ppm. The results of laboratory analyses with cooling tower water samples are listed in Table 10.1.

10.1.2 Treated water supply. A supply of treated water was circulated within a closed system to remove heat from the thermal shield and other equipment in the reactor and drain cells. A program of water system surveillance was incorporated into the procedures employed at the MSRE to minimize the probability that operational difficulties would arise from this auxiliary system. Since standardized methods for control of the water chemistry of auxiliary systems such as those which existed in the MSRE were fairly well stand-

ardized, it was anticipated that surveillance of the water supply would require only cursory attention. However, when power was first generated with the MSRE, it was found that the chemicals used in the treated water system had become activated. The source of the activity was identified as ^{42}K , produced from the potassium nitrite-potassium tetraborate mixture used to inhibit corrosion in the system. Extrapolation of the radiation levels observed at low power indicated that if the reactor were operated for extended periods at full power, equilibrium radiation levels of about 400 mR/hr would prevail in the heat exchanger in the diesel equipment room and in the water control room.

As the alternative, the potassium-containing inhibitors were discarded and replaced with an analogous lithium-based mixture, highly enriched in the ^7Li isotope to minimize tritium production. Lithium nitrite was prepared commercially by ion exchange from potassium nitrite and lithium hydroxide for this use. After the 4000-gal treated-water system was diluted with demineralized water to reduce the potassium from 800 to 3 ppm, the desired inhibitor concentration was attained by adding ^7Li nitrite, boric acid, and ^7Li hydroxide.

When the reactor was next operated at power, in run 5, activation again occurred, this time caused by the presence of sodium, ~ 1 ppm of which was present in the demineralized water from the ORNL facility. Condensate was produced at the MSRE with less than 0.1 ppm of sodium and used to dilute the sodium in the treated-water system to 0.3 ppm. The concentrations of sodium and ^6Li were thereafter reduced to sufficiently low concentrations that shielding and zero-leakage containment of the water system were not required.

Criteria were established for the treated water after replacement of the inhibitor mixture to meet the following specifications: pH: 7.0 to 9.0, $\text{Na}^+ \leq 3$ ppm, $\text{NO}_2 = 760$ to 860 ppm, $\text{B} \geq 57$ ppm, $\text{K}^+ \leq 8$ ppm, $\Delta\text{Al} = 0$ ppm, $\text{Fe} = 0$ ppm, tritium $\leq 2.2 \times 10^5$ dis $\text{min}^{-1} \text{cm}^{-3}$, ΔZ hardness (as CaCO_3) = 0 ppm.

Chemical analyses of treated-water samples were obtained at frequent intervals in order to maintain these specifications and as guides for adjustments of the concentrations of chemicals in the treated-water system supply. On-site tests were also performed with greater frequency than laboratory analyses for control of operations, with supplementary analyses obtained from the Analytical Chemistry laboratory at approximately biweekly intervals. The results of the chemical analyses obtained for treated-water samples obtained from the circulating system are listed in Table 10.2. Those obtained from the nuclear instrument penetration are listed in Table 10.3.

The results listed in Tables 10.2 and 10.3 do not warrant detailed comment or interpretation because they were used primarily as guides for controlling the concentrations of the corrosion inhibitors. It is evident from the results listed that they served satisfactorily for this purpose, and that the treated-water systems were essentially free of operational difficulties.

10.1.3 Vapor condensing system. Among the water supplies which were subjected to routine chemical

surveillance was included in the reservoir of the vapor condensing system. This system was incorporated into the MSRE for service only under the accident conditions described in the *MSRE Design and Operations Report, Part I*.² If an accident occurred in which hot fuel salt and the water used to cool equipment inside the cells became mixed, it would be necessary to contain within the MSRE the steam generated by the accident. A vapor condensing system, shown sche-

Table 10.1. Results of chemical analysis of MSRE cooling tower water

CTW Sample No.	Date	Total Hardness	CrO ₄ (ppm)	pH	Fe	CTW Sample No.	Date	Total Hardness	CrO ₄ (ppm)	pH	Fe
8	6/18/65	214	39	8.53	<2.0	456	12/2/66	178	12	8.00	<0.3
9	6/25/65	185	13	8.63	<2.0	458	12/4/66	251	68	8.00	<1.0
10	7/2/65	284	39	8.70	<2.0	467	12/12/66	197	4	-	<0.3
11	7/9/65	133	141	8.10	-	473	12/18/66	176	14	-	<2.0
12	7/23/65	105	21	9.58	<1.0	482	12/27/66	187	28	817	<0.3
13	7/30/65	105	30	7.97	<1.0	494	1/8/67	178	16	8.37	0.5
14	8/6/65	185	72	7.80	<1.0	502	1/15/67	175	18	-	<0.3
15	8/23/65	194	-	8.51	<0.3	512	1/30/67	171	9	8.10	<0.3
16	9/4/65	248	-	6.90	4.0	516	2/5/67	165	11	8.28	<0.3
18	9/17/65	3.0	37	8.77	1.0	524	2/13/67	171	-	-	<0.3
26	9/24/65	223	25	8.60	-	532	2/21/67	161	26	8.02	<0.3
32	10/8/65	111	44	8.00	0.5	538	2/27/67	175	17	8.10	<0.3
33	10/15/65	30	32	8.10	0.5	546	3/6/67	231	27	8.77	<0.3
48	11/10/65	121	14	8.08	0.3	559	3/19/67	223	79	8.36	<0.3
55	11/17/65	141	15	8.22	0.2	575	4/3/67	-	23	8.57	<0.3
67	11/29/65	161	16	7.0	<0.2	581	4/8/67	342	36	8.60	<0.3
79	12/10/65	129	29	7.37	-	588	4/18/67	241	-	8.30	<1.0
83	12/15/65	137	21	8.0	<0.3	596	4/24/67	239	29	8.50	<1.0
97	12/28/65	143	-	7.80	<0.3	603	5/2/67	235	26	8.47	<0.3
105	1/5/66	-	-	8.32	<0.3	607	5/7/67	286	66	-	<0.5
109	1/9/66	157	20	8.17	0.5	615	5/15/67	193	50	8.30	<0.3
118	1/19/66	151	17	8.30	<0.3	622	5/22/67	143	54	8.07	<0.3
123	1/23/66	153	17	8.25	<0.3	630	5/30/67	152	53	8.00	<0.3
142	2/12/66	150	15	8.35	<0.3	634	6/4/67	132	59	7.77	0.5
145	2/13/66	169	13	-	<0.5	641	6/12/67	155	44	7.93	<0.3
162	2/28/66	262	42	8.40	<0.5	655	6/26/67	217	108	8.31	<0.3
164	3/3/66	128	-	8.20	<0.5	661	7/2/67	-	71	8.33	<0.3
172	3/12/66	153	17	8.07	<0.3	669	7/10/67	245	58	7.3	<0.3
181	3/19/66	151	17	8.38	<0.3	676	7/16/67	260	58	8.0	<0.3
186	3/23/66	186	19	7.90	<0.3	689	7/30/69	149	-	-	<0.3
189	3/27/66	156	19	8.20	<0.3	697	8/7/67	152	68	8.54	<0.3
209	4/18/66	179	17	8.14	<0.5	704	8/14/67	214	54	8.40	0.35
219	4/27/66	-	17	-	<0.3	711	8/21/67	176	42	8.51	<0.2
224	5/1/66	178	20	8.4	<0.3	721	8/31/67	199	67	8.22	<0.3
232	5/8/66	194	21	8.42	<0.5	725	9/3/67	155	40	8.44	<0.3
240	5/15/66	-	18	8.32	<0.3	734	9/12/67	212	56	8.53	<0.4
248	5/22/66	200	20	8.28	<0.3	740	9/18/67	248	71	8.50	<0.4
256	5/30/66	198	15	8.22	<0.3	748	9/25/67	248	71	8.38	1.1
262	6/5/66	187	14	8.24	<0.3	756	10/2/67	268	71	8.55	0.62
269	6/12/66	183	21	8.08	<0.3	763	10/9/67	247	56	8.40	<0.4
277	6/19/66	212	20	8.45	<0.3	769	10/16/67	276	129	8.35	<0.3
285	6/26/66	218	17	8.37	<0.3	776	10/23/67	250	62	6.80	<0.2
292	7/2/66	210	8	8.55	<0.3	783	10/30/67	228	72	8.10	<0.4
300	7/10/66	216	20	8.40	<0.3	790	11/6/67	205	58	8.0	<0.5
307	7/17/66	203	20	8.05	<0.3	795	11/13/67	213	56	8.3	<0.5
315	7/23/66	156	20	8.38	<0.3	800	11/18/67	215	58	8.46	<0.5
317	7/24/66	172	17	8.46	<0.3	810	11/27/67	54	67	8.50	<0.2
325	7/31/66	20	20	-	<0.3	824	12/10/68	273	67	8.40	<0.4
332	8/6/66	126	15	7.71	<1.0	844	1/1/68	-	-	8.24	<0.2
340	8/15/66	129	32	-	<0.3	921	3/30/68	168	60	8.12	<0.4
346	8/21/66	130	21	7.70	<0.3	928	4/8/68	151	69	7.48	<2.0
354	8/29/66	121	13	-	-	964	6/21/68	160	100	8.98	0.1
360	9/5/66	127	17	8.10	<0.4	992	6/30/68	150	76	8.24	<0.4
366	9/11/66	260	90	-	<0.3	1027	8/4/68	193	47	8.44	<0.3
375	9/19/66	145	12	8.20	<0.3	1186	1/8/69	177	60	8.05	<0.1
383	9/25/66	158	11	8.20	<0.3	1241	3/2/69	409	155	8.50	<0.3
392	10/3/66	-	18	8.50	<0.4	1274	4/6/69	186	36	8.32	<0.1
414	10/24/66	294	30	-	<0.5	1359	7/6/69	209	65	7.76	0.12
422	10/30/66	210	17	8.57	-	1385	8/3/69	228	112	7.57	0.08
433	11/10/66	185	14	8.70	<2.0	1413	8/31/69	275	76	8.06	7.0
438	11/14/66	198	16	8.70	<0.3	1491	10/9/69	270	46	8.59	<0.1
444	11/20/66	187	13	-	<0.3	1503	10/20/69	493	98	8.82	<0.2
452	11/28/66	176	21	8.16	<1.0	1539	12/4/69	225	71	8.32	<0.1

matically in Fig. 10.1, was provided to prevent steam pressure from rising above the 40 psig allowable pressure for the cells and to retain the noncondensable gases. The vapor condensing tank in this system was kept about two-thirds full of potable water at all times from 1964 to 1969.

Corrosion inhibition in the water reservoir tank was effected by addition of potassium nitrite and potassium tetraborate, as in the recirculated water systems. The water supply in the water reservoir tank was to meet the same specifications as the circulating systems.

Table 10.2. Chemical analysis of treated-water samples from the MSRE circulating system

Date	Treated Water Sample No.	pH	NO_2^-	β	Al (ppm)	Fe	Σ Hardness	Tritium dpm/cm^3
3/2/66	129	9.45	720	60	<1.0	<0.5	-	
3/7/66	132	9.40	860	61	<1.0	-	-	
3/17/66	137	9.40	760	57	<1.0	<0.3	15	
3/19/66	138	8.98	760	57	<0.5	<0.3	20	
3/19/66	139	9.40	750	57	<1.0	<0.3	20	
3/23/66	141	9.30	740	56	-	<0.3	19	
4/3/66	145	9.50	710	56	<1.0	<0.5	27	
4/3/66	146	8.45	740	57	<1.0	<0.3	25	
4/18/66	149	9.33	630	56	<1.0	<0.5	22	
4/22/66	152	9.34	670	70	-	-	-	
5/1/66	156	9.28	600	70	<1.0	<0.3	25	
5/10/66	158	9.27	590	60	<1.0	<0.5	28	
5/16/66	169	9.17	460	67	<1.0	<0.3	25	
5/16/66	170	-	-	-	-	-	-	9.04×10^3
5/27/66	179	-	-	-	-	-	-	1.72×10^4
5/27/66	180	9.07	7.60	-	-	-	-	
6/5/66	187	9.10	720	64	<1.0	<0.3	26	
7/3/66	208	9.20	690	64	<1.0	<0.3	26	1.96×10^4
9/7/66	224	9.38	520	42	-	<0.3		
9/19/66	227	9.00	540	44	<1.0	<0.3	14	
10/3/66	233	10.10	500	51	13	<0.3	7	
10/5/66	235	10.10	1204	51	15	<0.3	12	
10/30/66	244	9.62	560	68	22	<0.3	16	
11/10/66	245	9.50	740	69	26	<0.2	26	1.4×10^4
12/4/66	250	9.40	1020	67	12	<1.0	18	
1/24/67	260	9.20	860	58	49	<0.3	20	
2/5/67	263	9.17	810	59	1.0	<0.3	16	
3/6/67	268	9.07	840	58	31	<0.3	16	8.07×10^4
3/9/67	271	9.14	732	58	5	<0.3	17	1.1×10^6
4/3/67	274	9.07	715	58	27	<0.3	19	7.85×10^4
5/7/67	279	9.17	640	73	4	<0.3	14	1.26×10^5
5/9/67	280	9.27	790	71	<1.0	<0.5	13	1.48×10^5
6/4/67	283	9.08	752	70	0.5	<0.5	18	1.76×10^5
6/14/67	285	9.07	900	72	1.0	<0.3	13	1.37×10^5
6/26/67	286	9.18	840	66	1.0	<0.3	-	1.33×10^5
7/2/67	287	9.17	890	65	<0.4	<0.3	13	1.42×10^5
7/5/67	288	9.18	850	65	0.5	<0.3	12	1.33×10^5
8/7/67	294	9.20	810	64	0.8	<0.3	8	5.0×10^4
9/3/67	298	8.81	820	69	<0.4	<0.4	17	1.57×10^5
10/2/67	302	9.25	790	63	<0.4	<0.5	21	1.59×10^5
1/1/68	312	9.20	850	60	<0.2	0.5	10	2.23×10^5
3/30/68	320	9.12	800	60	<0.5	<0.4	9	2.44×10^5
6/2/68	327	9.22	760	58	<1.0	0.3	10	2.32×10^5
6/30/68	331	9.34	780	55	<0.5	<0.4	9	2.47×10^5
8/4/68	333	9.23	730	56	0.18	<0.1	10	1.11×10^5
1/7/69	343	9.08	746	45	<0.2	0.12	10	
3/2/69	349	9.14	700	67	0.6	<0.3	10	2.26×10^5
4/6/69	352	9.16	800	67	0.4	0.2	10	2.57×10^5
7/6/69	355	8.84	758	71	<0.4	<0.3	10	2.85×10^5
8/3/69	357	9.10	742	70	0.73	<0.3	-	2.83×10^5
8/31/69	359	9.19	765	70	0.74	<0.3	9	2.82×10^5
10/9/69	361	9.15	730	69	1.0	<0.1	10	4.41×10^5
10/19/69	362	9.18	686	67	<0.2	<0.2	10	3.10×10^5
11/4/69	363	9.18	723	68	<0.2	<0.2	8	2.98×10^5
12/4/69	365	9.17	660	69	<0.7	<0.1	9	3.00×10^5

Table 10.3. Chemical analyses of treated water from the MSRE instrument shaft

Date	Treated Water Sample No.	pH	NO_2^-	β	A1	Fe	Σ Hardness	Tritium dpm/cm ³
9/24/65	18	9.71	120	46	2	<0.5	4	-
10/8/65	20	9.51	1250	60	2	0.5	8	-
10/15/65	21	9.47	1240	60	2	0.5	9	-
11/10/65	22	9.60	1110	58	5	0.3	6	-
11/17/65	23	9.55	1110	59	3	0.2	9	-
11/29/65	24	9.52	-	59	2	<0.2	10	-
12/15/65	28	9.50	1170	59	2	<0.3	35	-
12/28/65	33	9.50	1050	60	2	<0.3	6	-
1/5/66	36	9.50	1060	58	1	<0.3	-	-
1/9/66	37	9.53	1100	59	2	0.5	9	-
1/15/66	39	9.18	1100	91	2	<0.3	11	-
1/23/66	42	9.15	1280	91	1	<0.3	-	-
2/16/66	48	9.22	740	61	1	<0.3	12	-
3/2/66	53	9.25	720	60	1	<0.5	20	-
3/7/66	56	9.20	860	60	1	-	-	-
3/12/66	58	9.07	830	58	<1	<0.3	16	-
3/19/66	61	9.15	810	58	1.0	<0.3	11	-
3/23/66	63	9.12	820	60	-	<0.3	13	-
3/23/66	64	9.25	820	61	1.0	<0.3	16	-
4/8/66	67	9.16	820	62	1.0	<0.5	13	-
5/1/66	69	9.10	700	62	<1.0	0.3	14	-
5/10/66	71	9.08	700	61	<1.0	<0.5	20	-
7/3/66	79	8.90	600	65	<1.0	<0.3	17	5.76×10^3
7/31/66	87	8.90	800	60	<1.0	<0.3	20	-
8/29/66	91	8.70	760	62	10	<0.3	18	-
9/5/66	92	8.75	770	60	11	<0.4	19	-
10/3/66	97	8.82	780	61	11	-	-	-
10/30/66	103	8.84	670	61	11	<0.3	21	9.88×10^3
11/1/66	105	8.85	920	-	23	<2.0	27	-
12/4/66	109	8.82	830	62	11	<1.0	19	-
12/31/66	115	8.26	750	63	<0.5	<0.3	19	-
2/5/67	120	8.78	690	60	1.0	<0.3	20	-
3/6/67	125	8.96	830	72	8	<0.3	18	2.30×10^4
3/19/67	128	8.78	878	71	4	<0.3	20	2.99×10^4
4/3/67	131	8.76	822	72	3	<0.3	20	3.90×10^5
4/16/67	132	8.75	840	71	<1	<1	18	3.63×10^5
5/7/67	134	8.73	690	72	4.0	<0.3	17	5.23×10^4
5/9/67	135	8.70	740	71	<1.0	<0.5	15	5.16×10^4
6/4/67	137	8.67	780	68	0.5	0.5	22	7.14×10^4
7/2/67	139	8.68	830	70	0.5	<0.3	16	-
7/24/67	142	8.78	790	70	0.8	0.3	49	1.24×10^5
8/7/67	147	8.74	860	69	0.8	<0.3	11	1.46×10^5
9/3/67	151	8.81	820	69	<0.4	<0.4	17	5.36×10^4
10/2/67	155	8.80	890	67	0.5	0.9	21	4.77×10^4
11/6/67	160	8.70	895	69	<1	0.7	16	6.41×10^4
1/1/68	164	8.81	1060	68	0.6	0.4	16	6.75×10^4
3/30/68	173	8.73	1070	67	1.0	<0.4	13	8.09×10^4
6/2/68	179	8.77	990	66	<1	0.3	14	7.74×10^4
6/30/68	183	8.91	1040	62	<0.5	<0.4	13	8.01×10^4
8/4/68	185	8.83	1040	66	<0.5	<0.3	13	7.25×10^4
1/7/69	194	8.88	965	63	<0.2	<0.3	12	-
3/2/69	200	8.96	1040	64	1.2	<0.3	10	7.63×10^4
4/6/69	203	8.99	1070	64	1.4	<0.3	9	8.44×10^4
7/6/69	206	9.02	1090	61	<0.4	<0.3	7	9.07×10^4
8/3/69	208	9.10	1058	62	0.9	0.3	6	8.75×10^4
8/31/69	210	9.07	993	62	0.7	0.34	17	9.08×10^4
9/14/69	211	9.0	1040	62	1.0	<0.3	8	-
10/9/69	212	9.01	1040	62	1.0	<0.3	8	1.03×10^6
11/4/69	214	9.01	1030	63	1.3	<0.3	8	1.02×10^5
12/4/69	216	8.99	890	64	0.7	<0.3	8	9.83×10^4

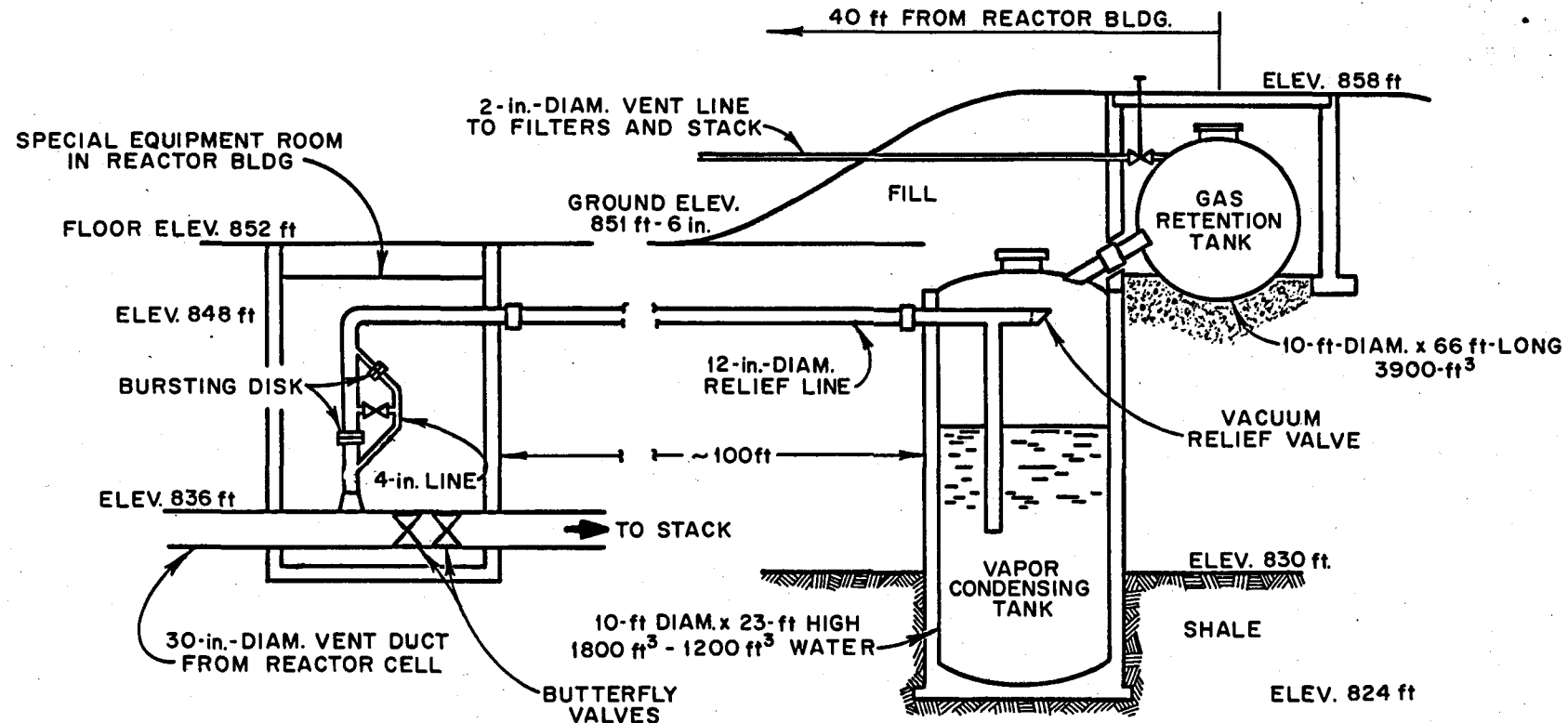


Fig. 10.1. Diagram of MSRE vapor-condensing system.

Samples obtained from the vapor condensing tank were analyzed at approximately semiannual intervals. The results of these analyses are listed in Table 10.4. It may be noted from the last entry in Table 10.4 that the final analysis of the vapor condensing system water reservoir was made more than one year before termination of the reactor experiment. The reason is implicit in the results listed, which show adequate stability of the corrosion inhibitor during the entire period water was stored in the reservoir tank.

10.2 Helium Cover Gas

Helium was used to fill voids in the salt circulation systems with an inert protective gas. Commercial helium, supplied from tank trucks, was passed through a purification system to reduce the oxygen and water content to below 1 ppm before the gas was admitted to the reactor. The helium supply was passed continuously through the fuel pump bowl at $\sim 200 \text{ ft}^3/\text{day}$ (STP) to

transport the fission product gases to activated charcoal absorber beds. The cover gas system was also used to pressurize the drain tanks to move molten salts into the fuel and coolant systems. Exhaust gas from these operations was discharged through the charcoal beds and filters to the atmosphere via the off-gas stack.

Incoming helium gas was passed through hot titanium sponge and then through a moisture analyzer to ensure that the purity of the gas was not degraded by inleakage of moisture at faulty connections. Samples of the helium supply were obtained from each new trailer of the gas delivered to the reactor site and were analyzed using mass spectrometric methods. The upper limits of the allowable concentrations of contaminants in the gas prescribed in design and operations specifications were set at $\leq 1 \text{ ppm}$ oxygen and $\leq 6 \text{ ppm}$ water. Results of the mass spectrometric analyses performed with samples of the helium gas supply (Table 10.5) showed that the supply was consistently of adequate quality for use in the MSRE.

Table 10.4. Chemical analysis of water samples from the MSRE vapor condensing system

Date	Sample	pH	Parts per million						
			Li	Na	K	Al	B	Fe	NO_2^-
2/7/66	VCS-1	8.70	0.1	6.3	935	10	82	<0.3	590
8/31/66	VCS-3	9.00	1.1	6.3	748	15	70	<0.3	690
5/27/67	VCS-4	8.86	1.1	6.6	800	1.0	63	<0.3	690
5/24/68	VCS-5	8.77	6.4	6.6	758	<1.0	61	<0.1	560

Table 10.5. Purity of helium cover gas for the MSRE as measured by mass spectrometric methods

Date	Laboratory No.	Weight percent						
		He	H_2	H_2O	$\text{N}_2 + \text{CO}$	O_2	Ar	CO_2
10/28/65	6639	99.998	<0.0004	0.0003	0.0010	0.0002	<0.0001	0.0001
1/3/66	6806	99.981	0.0004	<0.0001	0.0187	<0.0001	0.0001	<0.0001
1/5/66	6827	99.977	0.0004	0.0002	0.0222	0.0004		0.0001
3/25/66	7050	99.990	0.0006	0.0003	0.0084	0.0001	<0.0001	<0.0001
6/2/66	7253	99.995	0.0004	0.0001	0.0059	0.0001	0.0001	0.0001
8/9/66	7456	99.996	<0.0001	0.0001	0.0033	0.0001	0.0002	0.0001
10/18/66	7665	99.996	0.0002	<0.0001	0.0035	0.0004	0.0002	0.0001
12/22/66	7865	99.998	0.0003	<0.0001	0.0009	0.0002	0.0001	0.0001
3/8/67	9410	99.998	<0.0002	<0.0002		<0.0001		0.0001
8/8/68		99.997	<0.0001	<0.0007	0.0018	0.0004	0.0002	0.0001
8/15/68		99.997	0.0001	0.0009	0.0017	0.0002	<0.0005	<0.0001
9/16/68	473	99.997	0.0001	0.0006	0.0019	0.0003	0.0002	<0.0001
4/11/69	1192	99.995	0.0004	0.0026	0.0015	0.0002	0.0001	0.0001
6/17/69	1438	99.998	0.0003	0.0002	0.0014	0.0001	0.0001	<0.0001
10/10/69	1812	99.995	0.0005	0.0001	0.0034	0.0007	0.0002	0.0001
10/28/69	1952	99.995	0.0003	<0.0001	0.0016	0.0003	0.0024	0.0001

^aEach entry represents the supply from one trailer (39,000 ft^3) charge as delivered to the MSRE site.

10.3 Reactor Cell Air

Composition of the reactor cell atmosphere was adjusted to consist primarily of nitrogen containing less than 5% oxygen. Oxygen was maintained at this low concentration to minimize the possibility of combustion hazards which might occur if lubricating oil leaked from the fuel salt circulation pump system. Nitrogen was added to the cell as needed to make up for air inleakage. The normal cell pressure was 12.7 psia, with a maximum permissible air inleakage rate of 0.42 scfh. Under these conditions the required nitrogen purge rate was 1.5 scfh. Samples of the atmosphere of the reactor cell were obtained periodically and submitted for mass spectrometric analysis in order to ensure that the specifications were met. Results of these analyses are listed in Table 10.6.

Table 10.6. Chemical analyses of MSRE reactor cell air samples

Date	Cell air sample No.	vol %		
		O ₂	CO ₂	H ₂ O
4/19/66	2	1.52		
5/8/55	3	5.01		
5/24/66	4	2.35		
5/30/66	5	1.26		
6/12/66	6	2.53		
6/21/66	7	2.09		
6/30/66	8	2.29		
7/3/66	9	2.34		
7/10/66	10	2.9		
7/17/66	11	2.36		
7/25/66	12	1.88		
1/4/67	13	9.45		
1/5/67	14	6.67		
1/9/67	15	4.7		
8/2/67	16	7.0	0.09	
12/14/67	18	3.6	0.02	
1/4/68	19	2.63	0.11	3.29
1/23/68	21	3.04		
2/5/69	23	2.92		

At termination of operations with the MSRE, inspection of the reactor cell components was initiated, the preliminary results of which indicated that the machinery in the cell remained relatively free of atmospheric corrosion. The details of these examinations were not complete at the time this report was made and will appear subsequently in progress reports of the Molten Salt Reactor Program.

10.4 Oil Lubrication Systems

Each of the two salt pumps in the MSRE was served by an independent lubrication oil system, interconnected so that either system could serve both pumps in an emergency. These oil systems supplied both oil for lubrication of bearings and seals, as well as for cooling pump radiation shields. Details of the oil circulation systems are described elsewhere.³ Specifications of the oil to be used in the MSRE were recommended by Grindell in 1960.⁴

The MSRE employed a turbine-grade paraffinic-base lubricating oil having a viscosity of 66 SSU at 100°F, commercially available as Gulfspin-35. No attempts were made to characterize the lubricating oil completely during reactor operations, for in these operations the principal concern was that its lubricating properties would not be degraded in use. Composition and physical property analyses were performed routinely to provide this assurance. The composition analysis conformed with the average specifications for the product; for Gulfspin-35 analytical specifications fixed the carbon content of the paraffinic hydrocarbon at 85.4 wt %. The average formula of the paraffinic compound conforming to this fraction is C₃₉H₇₈.

Little was known about the identity of the additives in the MSRE lubricating oil, except that nominally they were thermally stable through the operating temperature range to which the oil would be subjected in MSRE usage. Analyses normally requested were for carbon, sulfur, moisture, total solids, bromine number, acid number, flash point, viscosity at 100 and 210°F, infrared and spectrographic analyses. In operation, an acid number of 0.06 was to be maintained as indicative of oxidation-free performance; the interfacial tension was not to exceed 18 dynes/cm at 77°C. The results of these analyses are summarized in Table 10.7.

It was recognized that migration of the fission gases from the pump tank to the region of the shaft lower seal via the shaft annulus could polymerize oil as it leaked down the shaft, plugging the drain line. The pump was designed accordingly with a flow of purge gas down the shaft annulus to minimize this migration.⁵ It was concluded that the oil to be used in the MSRE could withstand radiation doses of as high as 10⁷ rads/g without significant degradation of its properties and that this amount of radiation would still permit the oil to flow from the oil catch basin. Although this conclusion, which proved to be valid, led to the expectation of satisfactory performance of the MSRE lubrication oil in service with components that were exposed to highly radioactive fluxes, early experience

Table 10.7. Properties of MSRE lubricating oil as measured in laboratory tests

Date	Sample Desig. ^a	Viscosity (Centistokes)		Bromine Number	Interfacial Tension (dyne/cm)	Composition (wt %)			Total Solids (ppm)	Flash Point (°C)	Acid Number
		38°C	99°C			Carbon	Sulfur	Water			
8/25/66	1-N			1.95		86.37	1.13	<0.04	-	163	
8/25/66	2-N			1.86		86.43	1.01	<0.04	-	158	
8/25/66	3-N			1.67		85.68	1.67	<0.04	-	158	
8/25/66	4-N			1.56		85.52	0.98	<0.04	-	162	
8/25/66	5-N			1.86		85.82	0.92	<0.04	-	163	
3/27/66	16-C										1.78
4/3/66	17-C										1.35
4/3/66	18-F										1.40
4/15/66	19-F										1.26
4/15/66	20-C										1.24
4/18/66	21-C				9.60						1.18
4/18/66	22-F				9.22						1.27
4/29/66	23-F				9.32						1.48
4/29/66	24-C				9.89						1.44
5/1/66	25-F				8.65						1.42
5/1/66	26-F				9.89						1.39
5/8/66	27-F				8.43						1.47
5/8/66	28-C				10.05						1.44
5/24/66	29-C				10.77						1.67
5/24/66	30-C				10.13						1.64
6/3/66	31-F						0.03				0.78
6/3/66	32-C						0.04				0.81
6/3/66	33-N						0.03				0.61
6/21/66	34-C				9.48						1.38
6/21/66	35-F				9.20						1.33
6/26/66	36-C				10.60						1.58
6/26/66	37-F				10.70						1.59
7/3/66	38-F				10.14						1.76
7/3/66	39-C				10.33						1.86
7/10/66	40-F				10.25						1.50
7/10/66	41-C										1.40
7/17/66	42-F				10.13						1.10
7/17/66	43-F				10.71						1.00
7/24/66	44-F	10.51	2.77	1.70	10.63	85.04	0.032	0.20	2120	165	0.83
7/24/66	45-C	10.27	2.07	1.60	10.56	85.28	0.045	0.15	2076	166	0.88
8/12/66	46-F	10.00	2.60		17.35						0.92
8/8/66	47-N	9.94	2.64	1.26	17.46	86.88	0.012	0.16	1872	155	0.93
8/16/66	48-C	10.00	2.27		17.55						0.93
8/13/66	49-N			1.30	18.32	86.21	0.029	0.017	1874	156	0.96
10/17/66	50-F	10.16	2.60		16.40						0.33
10/17/66	51-C	10.06	2.58		16.59						0.30
10/25/66	52-C				17.5						0.26
10/25/66	53-F				17.10						0.29
10/30/66	54-F				17.18						0.79
10/30/66	55-C				16.80						0.60
11/10/66	56-F				16.50						0.57
11/11/66	57-C				16.75						0.55
12/18/66	58-C				15.80						1.01
12/18/66	59-F				15.40						0.83
12/27/66	60-C				15.81						0.90
12/27/66	61-F				16.97						0.85
1/3/67	62-C				16.08						1.32
1/3/67	63-F				16.13						1.30
1/9/67	64-C				15.70						1.30
1/9/67	65-F				16.00						1.30
2/2/67	66-C	9.93	2.64		15.70						1.40
2/2/67	67-F				16.00						
2/10/67	68-F				15.60						1.4
2/13/67	69-C	9.94	2.64	1.90	15.40	86.21	0.10	0.06		161	1.21
2/13/67	70-F	10.26	2.67	1.70	16.00	86.60	0.07	0.09		164	1.15
3/2/67	71-C	9.88	2.63		15.70						1.40
3/2/67	72-F	10.20	1.66		15.80						1.26
3/21/67	75-C				14.88						1.05
3/21/67	76-F				15.07						1.01
3/27/67	77-C				14.40						1.28
3/27/67	78-F				15.70						1.15
4/3/67	80-C				14.60						1.25
4/3/67	81-F				15.60						1.21
4/10/67	82-C	9.97	2.60		14.40						1.41
4/10/67	83-F	10.40	2.65	2.06	14.90	85.90	0.025	<0.05		158	1.27

Table 10.7 (continued)

Date	Sample Desig. ^a	Viscosity (Centistokes)		Bromine Number	Interfacial Tension (dyne/cm)	Composition (wt %)			Total Solids (ppm)	Flash Point (°C)	Acid Number
		38°C	99°C			Carbon	Sulfur	Water			
4/17/67	84-C				11.30						1.30
4/17/67	85-F				14.20						1.30
4/24/67	86-C				14.80						1.31
4/24/67	87-F				16.10						1.24
5/1/67	88-C				15.80						1.35
5/1/67	89-F				14.40						1.40
5/7/67	90-C				15.10						1.39
5/7/67	91-F				16.80						1.30
7/3/67	95-N				15.60						1.30
7/3/67	96-N				16.20						1.36
7/10/67	97-C	6.01	2.57		16.43						1.30
7/10/67	98-F	10.15	2.57		15.50						1.30
7/17/67	99-C	10.01	2.56		15.80						1.31
7/17/67	100-F	10.16	2.57		15.80						1.31
7/24/67	101-C				15.60						1.38
7/24/67	102-F				15.90						1.29
7/31/67	103-C				15.83						1.36
7/31/67	104-F				15.05						1.43
8/7/67	105-C				15.66						1.52
8/7/67	106-F				15.47						1.42
8/13/67	107-C	9.92	2.55	1.96	11.78	83.30	0.011	0.013	1809	157	1.12
9/18/67	108-F				15.95						1.30
9/18/67	109-C				16.14						1.30
9/25/67	110-F				16.50						1.38
9/25/67	111-C				16.50						1.40
10/2/67	112-F				16.50						1.01
10/2/67	113-C				16.30						1.11
10/9/67	114-F				16.40						0.84
10/9/67	115-C				16.30						1.03
10/16/67	116-F				17.10						1.14
10/16/67	117-C				17.10						1.21
10/23/67	118-F				16.10						1.22
10/23/67	119-C				15.90						1.40
10/30/67	120-F				15.64						1.38
10/30/67	121-C				15.17						1.46
11/6/67	122-C				15.47						1.35
11/6/67	123-F				14.81						1.23
11/13/67	124-F				15.84						1.27
11/13/67	125-C				15.94						1.35
11/27/67	126-F				16.19						1.15
11/27/67	127-C				15.62						1.35
12/10/67	128-C				15.61						0.83
12/10/67	129-F				15.04						0.85
12/19/67	130-C				14.60						1.31
12/19/67	131-F				15.36						1.23
1/1/68	132-F				16.33						1.36
1/1/68	133-C				15.48						1.51
3/2/69	146-C				13.70						1.11
3/2/69	147-F				16.10						0.86
3/16/69	148-F				15.80						0.96
4/6/69	149-F				15.80						1.08
4/6/69	150-C				13.70						1.30
4/20/69	151-F				15.60						1.00
4/11/69	152	10.55	2.67	1.69	13.00	85.60	0.016	0.090	1780	164	1.06
4/11/69	153	9.90	2.64	0.63	11.00	85.70	0.045	0.080	1640	159	0.91
5/19/69	154-F	9.94	2.58	1.29	14.15	78.00	0.012	0.015	1800	163	1.43
5/19/69	155-C	10.52	2.67	1.55	16.41	76.70	0.050	0.020	1800	167	1.20
9/14/69	156-C	9.93	2.73	0.63	12.78	86.30	0.019	0.002	1730	168	1.10
9/14/69	157-F	10.19	2.73	1.10	15.89	86.30	0.021	0.006	1810	175	0.90
9/14/69	158-F	9.80	2.60	1.11	16.10	85.90	0.021	0.003	1840	180	0.81
10/9/69	159-F				15.45						0.88
10/9/69	160-C				10.14						1.14
10/19/69	161-F	10.58	3.80	1.35	15.60	85.40	0.018	0.002	1940	174	0.88
12/4/69	167-F				15.90						1.02
12/4/69	168-C				13.40						1.22

^aletter designations with sample numbers denote source of sample, N = unused oil from storage, C = sample from coolant system, F = sample from fuel system.

with the MSRE in power operations showed that oil vapors transported to restricted areas could certainly polymerize (see Sect. 11.1). We had no foreknowledge as to whether polymerization of the recirculated oil might occur, although we faced this prospect with trepidation because of the formation of varnishes from oil vapors in the off-gas valves. This fear seems to have been unwarranted, for throughout the operation of the MSRE the properties of the oil apparently remained unchanged, both as judged on the basis of performance of the components in which it was used as well as from the results of the analyses listed in Table 10.7.

On one occasion, at the time when hydrocarbon varnishes were plugging the off-gas stream valves, the lubricating oil was fractionally distilled and the refractive index of each 10% volume cut was measured. The range was found to include refractive indices from 1.4726 to 1.4817, as compared with the refractive index of the undistilled oil of 1.4738.

Surveillance analysis included infrared absorption tests to determine whether oxidation was occurring. Occasionally these tests indicated that C-O bands were present, but these bands were only slightly more intense than in the reference sample and seemed not to become more so with continued use of the oil.

Among the least well-understood chemical phenomena governing behavior in the MSRE and, as well, among the least tractable for experimental investigation with the MSRE were the chemical relationships involving oil from the MSRE fuel pump and the transport and distribution of fission products and tritium within the reactor system. The properties of the oil, as determined through the chemical monitoring program, disclosed little that was significant concerning these matters. Unquestionably, the thermal degradation products formed in the pump bowl were of some significance in the transport behavior of fission products and tritium. Resolution of their exact effects on reactor operations, however, will be derived from future investigations rather than from further scrutiny of MSRE behavior.

References

1. R. H. Guymon, *MSRE Design and Operations Report, Part VIII, Operating Procedures*, ORNL-TM-908, vol. I, p. 3C-1.
2. R. C. Robertson, *MSRE Design and Operations Report, Part I*, ORNL-TM-728, p. 444.
3. R. C. Robertson, *ibid.*, p. 144.
4. A. G. Grindell, *Specification of a Lubricant for MSRE Pumps*, ORNL-MSR-60-37.

S. A. G. Grindell and P. G. Smith, *MSR Program Semiannual Progr. Rep. July 31, 1964*, ORNL-3708, p. 155.

11. TRANSPORT OF MATERIALS FROM SALT TO COVER GAS SYSTEMS

11.1 Fission Products

In solid fuel reactors, knowledge of the modes of fission product distribution is of utmost importance to the assessment of reactor safety and control and for the development of reprocessing methods. Changes in state and distribution of fission product species in solid fuel matrices have been examined so intensely and for so long a period of time that only problems related to accident conditions remain as challenging to the understanding. For molten-salt reactors it is necessary that an even more comprehensive understanding of fission product behavior be achieved, for with fission products intentionally circulated with fuel salt, their disposition, as controlled by mechanical and chemical influences, is of considerably greater importance than in static fuel systems. In MSRs, some fission products are removed from the fuel salt continuously and become distributed to the off-gas system, to the fuel storage tanks, and to the processing plant. They must be contained and their decay heat removed under all conceivable circumstances.

The probable fates of fission products produced in molten-salt reactors were deduced from thermodynamic considerations, from laboratory studies, and from in-pile static capsule tests. From the results of these studies, one may group fission product elements in categories according to general chemical properties: noble gases: Kr, Xe; noble metals: Pd, Rh, Ru, Mo, Ag, Te, Tc, Nb, Se, As; transition metals: Sn, Sb, In, Cd, Ga, Zr, Zn; lanthanides: Y, La, Ce, Pr, Nd, Pm, Sm, Eu, Gd, Tb, Dy, Ho, Er; active metals: Cs, Rb, Ba, Sr; halides: Br, I.

Of the elements produced in high yields, only the lanthanides developed concentrations in the MSRE that were in the range of chemical detection. This group accounts for 53.8% of the fission products. Operation of the MSRE resulted in the fissioning of 2.88 kg of ^{235}U fuel and 1.32 kg of ^{233}U , a total of 17.92 g-atoms of uranium. From fission, therefore, 9.64 g-atoms of lanthanides, about 1.5 kg, were produced ultimately to produce a final concentration of 300 ppm of these elements in the fuel salt. At the very low concentrations which prevailed in the fuel salt, the

lanthanides were of little consequence with respect to general chemical surveillance, and no special effort was made to monitor their concentrations or distributions directly. One method for their removal from MSR carrier salts relies on high-temperature distillation. Tests of this separation method with MSRE fuel carrier salt disclosed that the measured concentrations of the lanthanides in the salt agreed well with computed values.¹

The MSRE provided the first opportunity to begin studies of fission product transport in circulating salt systems. Although some preliminary information was derived from the results of experiments with the Aircraft Reactor Experiment, its scheduled period of operation was so brief as to obviate any real opportunity for such studies. Recognition that the knowledge of fission product behavior was in a rudimentary condition required that programs for their investigation proceed independently from that for general chemical surveillance. Detailed results of the studies of fission product behavior are therefore excluded from the present report and will be described separately.²

11.2 Restrictions in the Off-Gas System

In both the fuel and coolant systems, control of the pressure in the cover-gas systems over extended periods proved to be difficult and unpredictable. The cause was the accumulation of solids and tarry deposits, mostly originating from lubricating oil, in the off-gas throttling valve used for fuel-system pressure control and in the filter just upstream of the coolant-system pressure-control valve.

During the initial period of circulation of coolant salt in the reactor, a period of 1200 hr, the off-gas filter plugged and was replaced twice. Examination of the filter medium showed that it was covered with amorphous carbon containing traces of the constituents of the coolant salt and Hastelloy N. Although the filter was replaced by another one with some 35 times the surface area, pressure control again became erratic. It was realized that oil seepage took place down the shaft of both the fuel pump and the coolant pump. Rates of seepage were determined and found to be variable, ranging from indicated rates of zero to 4 cm³ of oil per day seeping into the pump bowl.

The rates did not seem to increase appreciably from time to time, nor was their variation clearly related to any operational practice. It became routine to replace the filter in the coolant salt off-gas system after several months' use. Each time the filter was replaced, it was found to be covered with oil residues.

Pressure control of the fuel system became erratic toward the end of the first extended operation with salt in the circuit. During this period, ⁸⁵Kr was used for tests of the stripping efficiency of the noble gas from the helium stream. After saturation of the salt to near equilibrium concentrations, the inflow of ⁸⁵Kr was stopped and the gas purged from the system. As one part of the tests, the effect of salt level in the pump bowl was examined with the LiF-BeF₂ (66-34 mole %) salt at three levels. At this time the void fraction of the salt in the fuel loop was measured for the first time and found to be 0.6%. At termination of these tests the off-gas filter was removed and examined. It was found to be free of deposits. Examination of the pressure control valve showed that it was partially plugged. The residue was washed out with acetone. The liquid suspension was dark in color, and the residue left after evaporation of the acetone consisted of spheres of a glassy material, 1 to 5 μ in diameter. Shortly after the cleaned control valve was reinstalled, it became partially restricted again. It was then replaced with another one of greater flow-through capacity. Inspection of the original valve revealed that a black deposit partially covered the tapered stem. The deposit was about 20% amorphous carbon and the remainder was again 1- to 5- μ spheres that were found to have the composition of the flush salt.

The program for bringing the MSRE to full-power operation was interrupted on two occasions by flow restrictions in the off-gas system. Symptoms of plugging became pronounced in each case after about 12 hr of operation at 1 MW. Restrictions were first noted in the capillary restrictor in line 521; at the same time, check valve HCV-533 became inoperative. Restriction was also noted in the stainless steel line filter and 522 valve assembly. In order to resume operation of the reactor, the capillary restrictor and HCV-533 check valve were replaced by nonrestrictive sections, and the filter-valve assembly was replaced. The filter element which was removed was capable of blocking passage of more than 90% of the particulate matter of $\geq 0.7 \mu$ in diameter. It was replaced by a filter designed to block particulates of $< 50 \mu$ in diameter.

Continued difficulty was experienced with restrictions in the off-gas system of the fuel circuit for some time during the early stages of power operation with the MSRE. These difficulties led to a practice which relieved excess pressure in the fuel system by venting gas through HCV-533 to the auxiliary charcoal bed. During this period, evidence of restrictions in the charcoal beds began to appear. On resuming operation at 1 MW, restrictions appeared to develop in three

locations: at valve 522B, at the entries to charcoal beds 1A and 1B, and in the lines ahead of the auxiliary charcoal bed. Small specimens of the materials which were suspected to have caused plugging were removed from the affected parts of the off-gas system and subjected to laboratory tests in an attempt to determine

the reasons for flow restrictions. The results of these examinations are summarized in Table 11.1.³

The results shown in Table 11.1 indicate that the restriction in the off-gas system may be attributed to varnish-like organic materials whose origin was the Gulfspin-35 lubricating oil. The refractive index of the

Table 11.1. Results of examinations of specimens removed from the MSRE off-gas lines

Specimen description and origin	Morphology	Refractive index	Activity at contact (R/hr)	Predominant isotopes (from gamma scan)	Spectrochemical data
1. Deposit from exit orifice of capillary restrictor	Isotropic particles, appearing as partly coalesced amber globules	1.520		Li, 99 μ g; Be, 124 μ g; Zr, 100 μ g	
2. Scrapings from spool piece adjacent to capillary	Same as 1	1.540			
3. Deposit from check valve 533	Isotropic, amber, varnish-like particle, ~50 X 100 μ			Be, 0.95 μ g; Li, 2 μ g; Zr, <0.5 μ g	
4. Scrapings from valve 522 poppet	Isotropic, amber, varnish-like matrix containing embedded isotropic(?) crystalline material of lower refractive index	~1.540	2.5	No Zr, Nb, Ce	
5. Scrapings from valve 522 seat	Same as 4	1.544 to 1.550	1.5	^{89}Sr , ^{140}Ba , ^{140}La	
6. Oil drops from valve 522 body		1.509		No Zr, Nb, Ce	
7. Scrapings from stainless steel filter element	Isotropic, faintly colored material, more nearly scalelike than glassy in appearance	1.524 to 1.526		^{140}Ba , ^{140}La , ^{103}Ru , ^{137}Cs ; no Ce, Zr, Nb	
8. Metallic scrapings from stainless steel filter element	Granular opaque particles; low index, transparent, birefringent crystalline material spalled off metal on microscope slide				
9. Deposit from HV-621 valve stem	Isotropic, faintly colored material, varnish-like in appearance with pebbly surface	~1.526		^{132}Te	

heaviest 10% volume fraction obtained on vacuum distillation⁴ of the oil (see Sect. 10.4) was found to be approximately 1.50. The high refractive index of the varnish-like materials removed from the off-gas system suggests that oil vapor and fractionation products carried into the off-gas were polymerized in transit to and on the surfaces of the valve parts, and thus plugged the system. This inference is strengthened further by the observation that the varnish-like materials were found to have limited or no solubility at room temperature in xylene, petroleum ether, carbon tetrachloride, or acetone.

Typical examples of the deposits removed from the MSRE and examined in the laboratory are shown in Figs. 11.1–11.4. In one attempt to identify the materials that were causing the restrictions, the reactor was drained, and for several days after, all helium flow through the fuel loop was stopped⁵ and the contained helium was recirculated at 100°F. Three samples of the recirculated gas were isolated for analysis, but the results were inconclusive.

The appearance of restrictions in the off-gas system of the fuel circuit comprised a major operational impediment. Considerable effort was expended to identify the causes of these restrictions and to alleviate the concomitant problems. In April 1966 a particle trap was installed in the fuel system off-gas line, just downstream from the first holdup section. It was replaced in August 1966 with an identical unit. In January 1967 an improved unit was used to replace the original one and

remained in service throughout the remainder of operations with the MSRE. Each of the particle traps employed stainless steel mesh as the roughing section; in addition, finer media, both fibrous metal (Feltmetal) and Fiberfrax, served to block passage of the smallest particles. It served to alleviate the major part of the difficulties that had beset previous operations, but because it was not capable of completely blocking the passage of volatile hydrocarbons, it was ineffective for providing complete freedom from the development of restrictions in the charcoal beds. The system was operable throughout the remainder of MSRE tests, although with chronic indications that oil fractionation products were being transferred downstream to the charcoal beds.

A particle trap that had been installed in the fuel system off-gas line in April 1966 was examined, and samples were removed from the trap for analysis. The results of the examination of this trap were described in detail by Scott and Smith.⁶ The chemical results are summarized below.

Mass spectrometric analysis of material leached from Yorkmesh matting at the inlet section of the filter indicated that it had collected a number of fission products. The eluted material contained 20 wt % Ba, 15 wt % Sr, and 0.2 wt % Y. In the same analysis the salt constituents Be and Zr were estimated to be 0.01 and 0.05 wt % respectively. Other samples removed from the metal filter contained small quantities of Cr, Fe, and Ni. Results of gamma-ray spectrometric analysis indicated the presence of ^{137}Cs , ^{89}Sr , ^{103}Ru or ^{106}Ru , ^{110m}Ag , ^{95}Nb , and ^{140}La . All samples were analyzed for determination of the presence of Be, and the concentration present was below the detectable limit of 0.1%. Attempts to determine the presence of Zr were complicated by the presence of large quantities of Sr. The fraction of soluble hydrocarbons was determined for the materials present on the Yorkmesh mat and in other samples was found to range from 60 to 80%. Carbon disulfide extracts were made of the organics and were allowed to evaporate; the residues were used for infrared analysis. All samples were identical and indicated the presence of long-chain hydrocarbons. There was no evidence of any functional groups other than those involving carbon and hydrogen, nor was there any evidence suggesting double or triple bonds. There was an indication of a possible mild cross-linkage. It is likely that there is more cross-linkage of the organic in the gas stream than appeared in these samples, and the low indication could be due to the insolubility of the cross-linked organic and the high operating temperatures of the wire mesh, which would

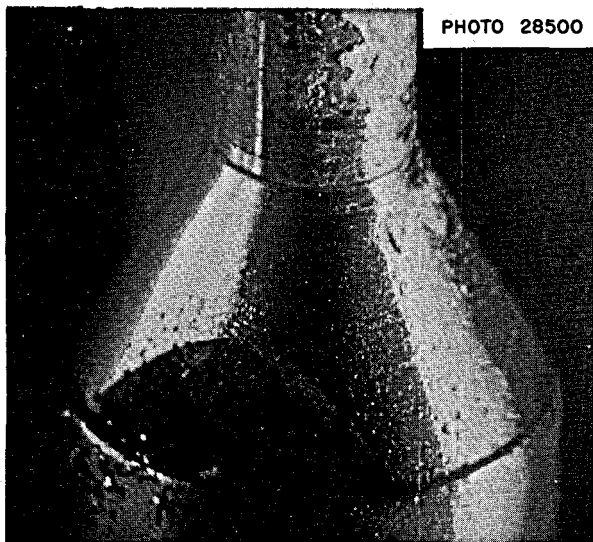


Fig. 11.1. MSRE valve HCV-621 poppet.

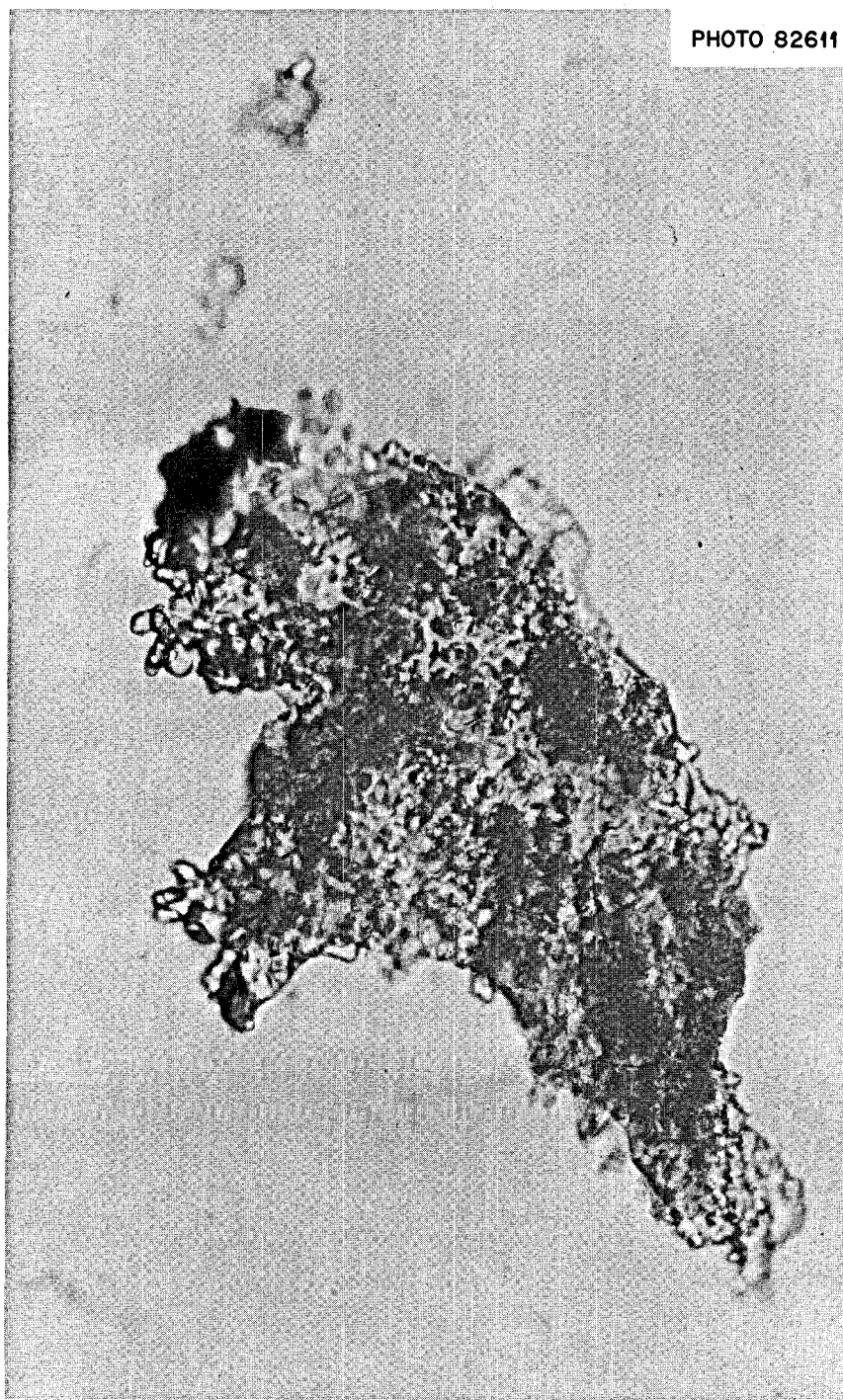


Fig. 11.2. MSRE sample 8-1. Fragment of material removed from line 521 pressure equalizing capillary. Photographed in 1.414 refractive index oil. 206X.

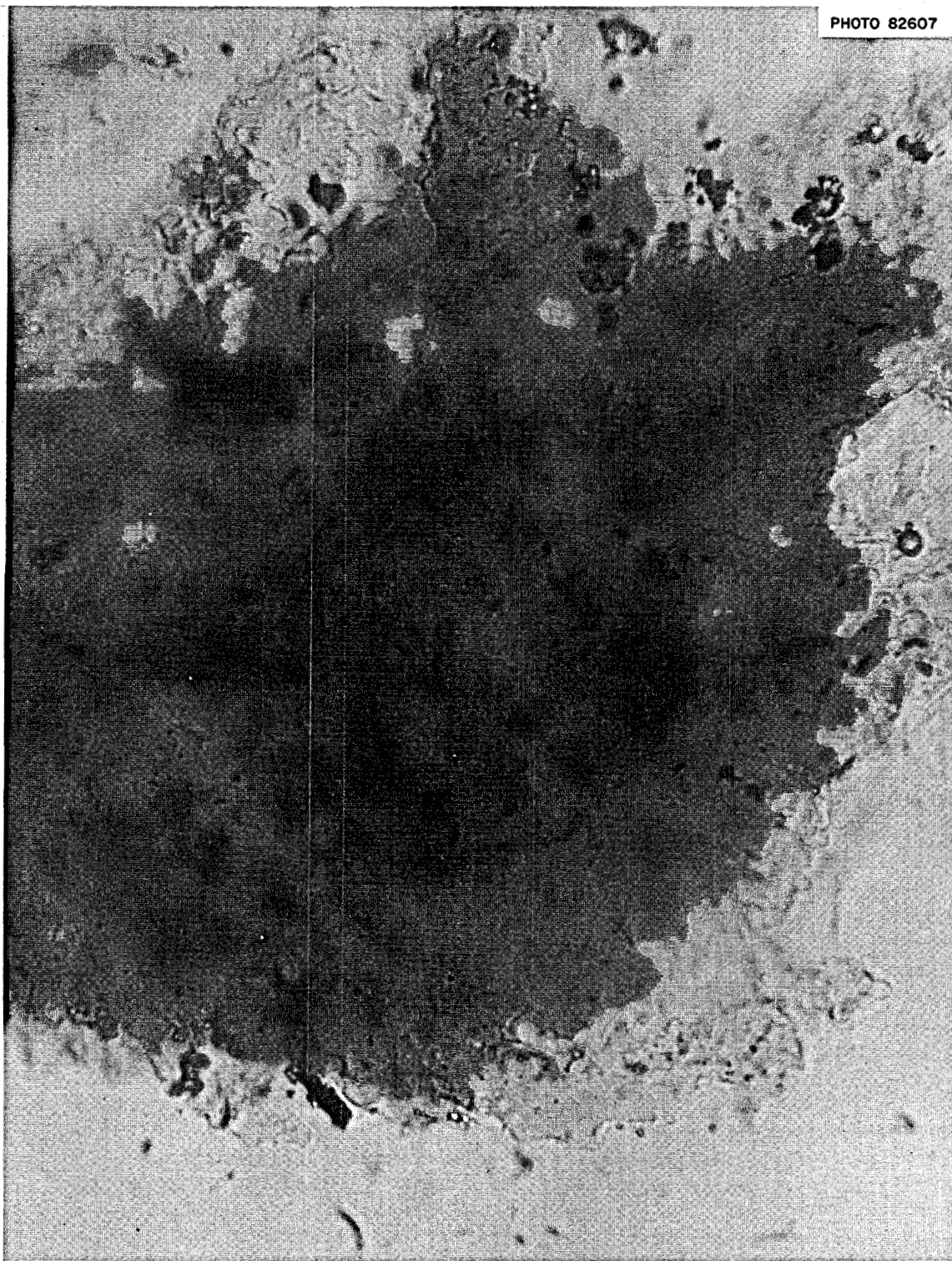


Fig. 11.3. MSRE sample 8-3. Fragment of material removed from line 521 pressure equalizing capillary. Photographed in 1.520 refraction index oil. 645X. Reduced 20.5%.

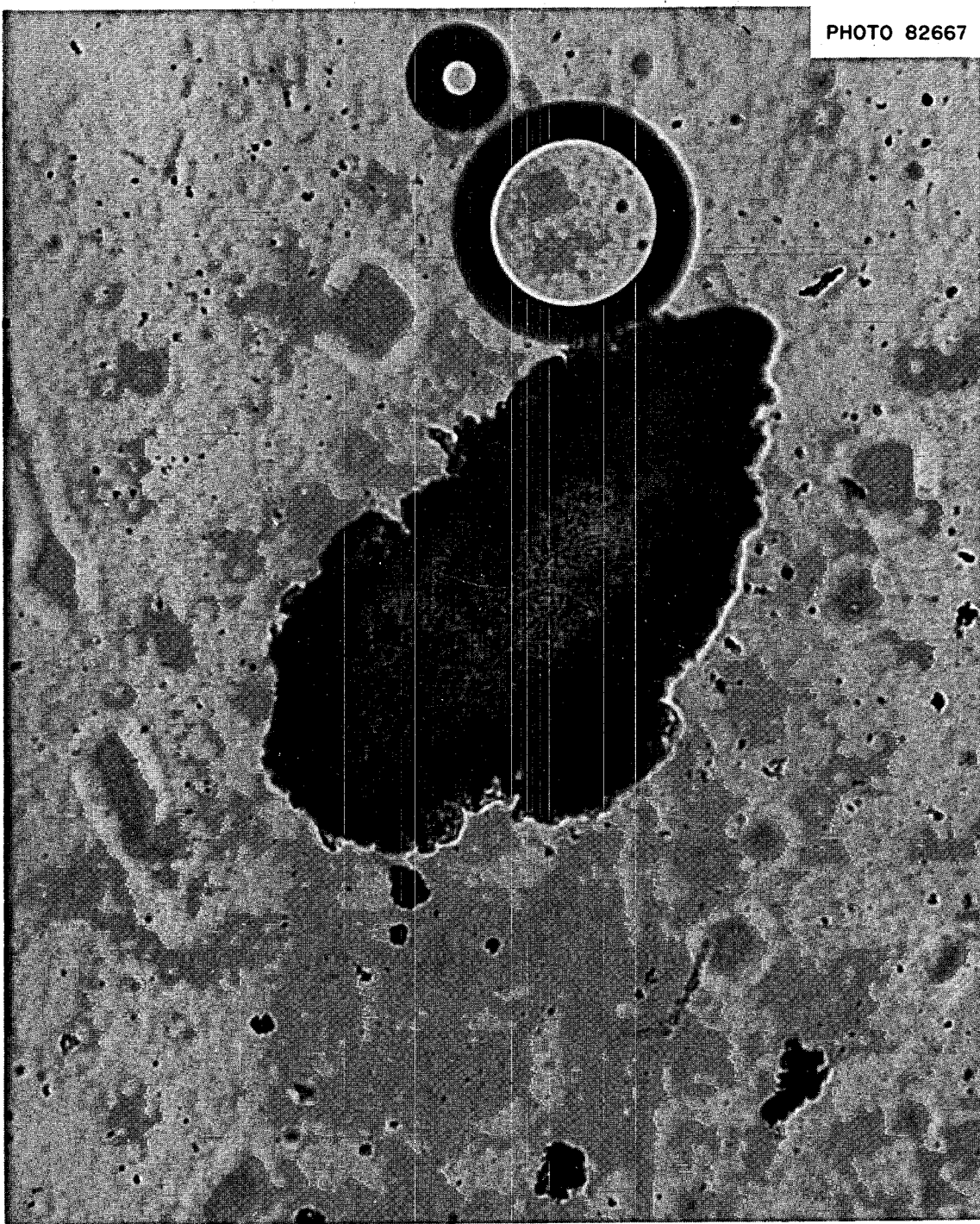


Fig. 11.4. MSRE sample 8-2c. Fragment of translucent birefringent material removed from stainless steel filter. Refractive index more than 1.468. 160X.

cause breakdown of the organic into elemental carbon and volatiles.

The following conclusions can be drawn from the results of the examination:

1. Since the spectrographic analysis indicated that the concentrations of Be and Zr were very small compared with those of the fission products Ba and Sr, the amount of entrained salt mist carried to the filter was negligible.
2. The high activity and the large amount of barium and strontium in the inlet section of the particle trap indicate that a large fraction of the solid daughters of Kr and Xe which decay in the line is carried down the line with the off-gas stream.
3. The distribution of activity indicates that entrance areas of the Yorkmesh mat were unexpectedly effective in trapping the solid fission products. Decay heat in this area resulted in temperatures above 1200°F.
4. The collection of hydrocarbon mist on the Yorkmesh mat had probably enhanced the collecting efficiency of the mesh for solid particles.

With the adoption of methods to minimize the effect of hydrocarbon transport in the off-gas streams, little further operational difficulty was encountered with the MSRE, and no additional chemical studies were made.

The chemical effects of continually passing hydrocarbon degradation products through the fuel stream are largely unknown. They were viewed as intractable to quantitative assessment with the means at hand for dynamic analysis. In attempts to gain some understanding of the possible relation of the hydrocarbons to various chemical and physical aspects of fuel salt and fission product behavior, a gas sampling facility⁷ was developed and installed at the MSRE. In use, it provided few data that were of value in appraising the effect of oil seepage and was adapted to other uses. Thermal degradation of the pump oil certainly produced a small finite concentration of hydrogen in the pump bowl atmosphere. There is no evidence in the chemical results obtained from salt analyses that indicates a recognizable effect of its presence. Possible consequences of its effects on fission product chemistry and transport were recognized some time ago. Their assessment may be found in the summary report on fission product behavior.⁸

11.3 Tritium Transport in the MSRE

Shortly before scheduled termination of operations with the MSRE, it was realized that the hot metal

containment system should be highly permeable to hydrogen and that, therefore, the tritium produced in the fuel salt could be expected to diffuse out of the fuel system. An investigation was initiated to measure the amounts of tritium in the air vented to the discharge stack, that released through the radiator tubes, and the amount of tritium in fuel salt samples. Equipment was installed by the analytical chemists in the MSRE vent-house sample station in order to measure the concentrations in the various reactor effluent gas streams. A fraction of the gas stream was passed over a bed of hot copper oxide in order to convert the tritium to water. Tests were conducted with the copper oxide beds either at 340 or 800°C. The higher temperature allows the oxidation of methane, while the lower temperature does not. The results of these tests, conducted by Dale, Apple, and Meyer,⁹ showed that the maximum amounts of tritium released from the air stack, from the radiator, and found in fuel salt, corresponded to the production of 4.6, 0.6, and 22.7 Ci/day respectively. At full power operation the MSRE produces 60 Ci of tritium per day.

In an evaluation of the results, Briggs¹⁰ concluded that the disparity in the material balance suggested that the following behavior may have occurred:

1. Either the metal walls have a much greater resistance to the diffusion of tritium than has been estimated, or most of the tritium is present in a form other than T₂ or HT. Even assuming that graphite is a sink for T₂, one cannot otherwise explain the small fraction that passes through the radiator tubes and the piping and vessel walls in the primary system.
2. When TF is taken into consideration but reactions with the graphite are neglected, the fraction of the tritium that leaves the fuel pump off-gas system increases and the amount that passes through the metal walls decreases. Assuming equilibration of liquid and gas in the pump bowl and UF₄/UF₃ = 1000, the distribution begins to look like that measured for the MSRE. One would have to further assume that much of the tritium is retained on the carbon beds as TF or organic compounds and that T₂ and TF react with materials in the off-gas system to produce the organic compounds found in the exit of the carbon beds. These calculations contain several uncertainties and simplifications that can considerably affect the results; the results are insensitive to the solubility of TF but are quite sensitive to the solubility of T₂ in the salt and to the value of the equilibrium constant, k. The presence of hydrogen and organic compounds from decomposition of oil in the pump bowl could be important

but is neglected. Agreement between calculations and measurements may be entirely accidental.

3. When retention or reaction with the graphite in the core is considered along with the presence of TF, the graphite becomes a major sink for tritium, mostly as TF. If UF_4/UF_3 increases from 100 to 1000, almost all the tritium enters the graphite as TF. Very little diffuses through the metal walls or through the fuel pump off-gas system. A distribution about like that observed for the MSRE would be calculated if one assumed partial reaction of TF with graphite to produce hydrocarbons that are released from the graphite and removed through the fuel pump off-gas line. Such reactions are believed to be highly unlikely.

Briggs' assessment thus shows that the transport mechanisms for tritium in the MSRE were not clarified from the data obtained and that inevitably their characteristics must be established because of their significance to design of and procedures for operational control of MSBRs. Termination of operations with the MSRE precluded further assessment of transport mechanisms under realistic conditions. This was not necessarily unfavorable, for the leakage of oil from the fuel pump shaft seal into the pump bowl was unquestionably a complicating factor in attempts to interpret the results of on-site analysis. The fuel pump was known to have permitted small amounts, generally believed to have been $\sim 1 \text{ g/day}$, of lubricating oil to enter the fuel pump bowl and thus become rapidly, and perhaps heterogeneously, thermally degraded. It seems very probable that radiation also must have had some role in the degradation process. Generation of a spectrum of hydrogenous degradation products in the off-gas must complicate theoretical models of transport mechanisms to a great extent and probably even accounts for the wide range of analytical values obtained at the MSRE. An initial model of tritium behavior was advanced recently by Strehlow.¹¹ As fundamental to the development of a model of tritium transport, Strehlow noted that "transport processes and chemical behavior of hydrogen isotopes are interrelated parameters in molten-salt reactor design considerations. The transport of hydrogen is determined by the solubility and diffusivity in moderator, salt, and metal. The chemical behavior is a function of the oxidation-reduction potential in the salt, radiation field, and possibly reactivity with the graphite moderator."

Additional tests were conducted at the MSRE near the end of operations in which CuO specimens and Ni rods were exposed to the gas and salt before and after

the addition of beryllium to the salt. The results of these tests have not yet been completed. After termination of the MSRE, one of the graphite stringers was removed for examinations and tests. These tests, conducted by S. S. Kirslis and F. F. Blankenship, were completed in July 1971. The results indicated that about 15% of the tritium produced in the MSRE was sorbed on the moderator graphite. The concentration of tritium in thin surface samples was as high as $10^{11} \text{ dis min}^{-1} \text{ g}^{-1}$, fell to about $10^9 \text{ dis min}^{-1} \text{ g}^{-1}$ at 60 mils depth, and then decreased slowly to about $6 \times 10^8 \text{ dis min}^{-1} \text{ g}^{-1}$ for penetrations to 800 mils. These results are of particular interest in that they suggest a means for controlling the distribution of tritium in molten-salt reactors.

References

1. J. R. Hightower, Jr., and L. E. McNeese, *MSR Program Semiannu. Progr. Rep.* Feb. 28, 1970, ORNL-4548, p. 317.
2. F. F. Blankenship, E. G. Bohlmann, S. S. Kirslis, and E. L. Compere, *Fission Product Behavior in the MSRE*, ORNL-4684 (in preparation).
3. These and other related examinations were made by T. N. McVay (consultant) and the author in the High-Radiation-Level Analytical Facility (HRLAF).
4. Performed by L. J. Brady et al., Analytical Chemistry Division, ORNL.
5. *MSR Program Semiannu. Progr. Rep.* Aug. 31, 1965, ORNL-3872, p. 26.
6. D. Scott and A. N. Smith, *MSR Program Semiannu. Progr. Rep.* Feb. 28, 1967, ORNL-4119, p. 47.
7. *MSR Program Semiannu. Progr. Rep.* Feb. 28, 1966, ORNL-3936, p. 67.
8. F. F. Blankenship, E. G. Bohlmann, S. S. Kirslis, and E. L. Compere, *Fission Product Behavior in MSRE*, ORNL-4684 (in preparation).
9. J. M. Dale, R. F. Apple, and A. S. Meyer, *MSR Program Semiannu. Progr. Rep.* Feb. 28, 1970, ORNL-4548, p. 183.
10. R. B. Briggs, *Additional Calculations for the Distribution of Tritium in the MSRE*, ORNL-CF-71-7-8 (July 1971).
11. R. A. Strehlow, *MSR Program Semiannu. Progr. Rep.* Feb. 28, 1970, ORNL-4548, p. 167.

12. IMPLICATIONS OF THE MSRE CHEMISTRY FOR FUTURE MOLTEN SALT REACTORS

The Molten-Salt Reactor Experiment was spectacularly successful as a materials demonstration: the

molten fluoride fuel and coolant-salt mixtures flowed through their containment circuitry for thousands of hours, causing little or no corrosion in these systems; the graphite moderator experienced no measurable dimensional changes in use and remained free of penetration by the fuel salt. The reactor equipment operated reliably, and the radioactive liquids and gases were contained safely. The fuel was completely stable. Xenon was removed rapidly from the salt. When necessary, radioactive equipment was repaired and replaced in reasonable time and without overexposing maintenance personnel.

That the MSRE was completed so successfully did not come about as the result of frequent adjustments in the chemical properties of the circulating fluids. A major conclusion that emerges from experience with the MSRE is that chemical surveillance, as carried out with individual samples obtained and removed from the reactor and transferred via necessarily cumbersome processes to off-site laboratories, is of value principally as a basis for attempting to control trends in behavior. Irrespective of the quality of the analytical data obtained, the information feedback process is generally too slow to afford frequent control direction. Chemical surveillance for future MSRs coupled to steam plants, therefore, must be obtained through on-line monitoring systems, and such surveillance systems must function dynamically. In addition, for safety, incorporation of the associated on-line instrumentation that is required must not add significantly to the complexity of the reactor system.

The next molten-salt reactor which is likely to be built will be constructed either exclusively as a federal enterprise, for example, the MSBE, involving both a steam generation system and on-line chemical reprocessing for the removal of rare-earth fission products, or a larger reactor developed partly under the impetus of private industry. Such a reactor would generate steam but would not include a chemical reprocessing plant for the removal of rare-earth fission products. Either of these reactors would utilize a fuel salt containing the same constituents as have been proposed for the MSBR fuel, for which the standard reference design composition is ^7LiF - BeF_2 - ThF_4 - UF_4 (72-16-11.7-0.3 mole %). Heat removal would be accomplished through a secondary salt system. Final choice of the coolant for this system has not yet been made for the reasons described below.

It is essential that the tritium produced from fuels based on ^7LiF - BeF_2 be managed so that essentially none of the tritium produced in the reactor core can find its way into the steam plant. Complete removal of

tritium from the fuel salt before it passes into the heat exchanger is highly improbable, and accordingly, management of the tritium transferred through the heat-exchanger walls is required.

Fluoroborate mixtures were proposed as suitable for molten-salt reactor coolants¹ and have been under examination for some time for that application. Consideration was given to the possibility that the NaF - NaBF_4 eutectic mixture would be substituted for the LiF - BeF_2 coolant salt in the MSRE before operations with the reactor were terminated. However, the plan was not implemented for lack of financial support.

A barrier to the selection of fluoroborates as suitable coolants for molten-salt reactors has been their seeming inability to retain hydrogenous species in melts contained in nickel-based alloys. Unless a finite but small, ~50 ppm, concentration of hydrogenous species can be retained in these melts as a reservoir for TF, their applicability seems tenuous. As an alternative, a reactor design which employs Hitec [NaNO_3 - NaNO_2 - KNO_3 (6.9-48.5-44.6 mole %)] as the coolant salt, isolated from possible contact with fuel salt by an LiF - BeF_2 buffer salt, has been proposed. It is necessary to eliminate the possibility that Hitec might come into contact with the graphite moderator. Evaluations of this alternative have begun but will require a considerable research and development effort before the potential applicability of Hitec can be judged.

It is thus evident that the next molten-salt reactor to be built, of whatever type, will employ both fuel and coolant salts unlike those which were used in the MSRE. Even so, the chemistry of molten salts, as advanced by experience with the MSRE, is sufficiently similar to be of practical value.

Until specific choice of a coolant is made, it seems unnecessary to project from MSRE experience the character of surveillance programs for the coolant system. It is most likely that the earliest indications of coolant-fuel mixing would be given by the nuclear surveillance instrumentation and that, therefore, chemical surveillance of the separate systems would be of little operational consequence. The details of coolant-system surveillance must therefore be relegated to future planning efforts.

At this point, no timetable exists for construction of follow-on reactors to the MSRE. Accordingly, as our understanding of the chemical behavior of materials in the MSRE is extended, it can serve to develop detailed surveillance programs as needed. Fuel surveillance, at a minimum, must include consideration of the following chemical factors:

1. Oxide contaminants in the fuel salt. A fuel salt which does not contain a highly polar cation component which interacts chemically with the oxide ion, as did Zr^{4+} in the ZrF_4 contained in the MSRE fuel salt, will almost certainly not tolerate relatively large concentrations of dissolved oxide ion without precipitation. In the MSRE, the oxide tolerance of the fuel salt was estimated to be ~ 680 ppm at the operating temperature of the fuel salt, $650^\circ C$ ($1200^\circ F$), whereas in the MSBR reference fuel salt the tolerance is probably not greater than ~ 40 ppm at this temperature. It has been tacitly assumed that all versions of molten-salt reactors operated in the future would include processing equipment for maintaining the concentration of oxide in the fuel salt at quite low levels through continuous processing of a bleed stream of salt.

A detailed evaluation of the consequences of contamination of fuel salt by oxides has been made, from which it was concluded that "there is no necessity for an oxygen getter, such as ZrF_4 , in the MSBR fuel," but that "swift, satisfactory, and preferably on-line, methods for determination of O^{2-} and UF_3 concentrations of the MSBR fuel after storage and during startup and operation"² must be available.

Preliminary conceptual designs of on-line oxide detection apparatus have been devised by members of the Analytical Chemistry Division.³ Increasing efforts will undoubtedly be devoted to this activity in the future.

2. Corrosion detection. The extent of generalized corrosion in the MSRE was estimated routinely from changes in the concentration of chromium found in the salt samples removed from the reactor. Results of examinations of surveillance specimens removed occasionally from the reactor core and from postoperational examinations of the alloy removed from the heat exchanger confirmed the general validity of these estimates. The use of Cr^{2+} concentration as a corrosion indicator thus continues to be uniquely attractive. To verify corrosion-free operation of a large reactor from analyses of numerous samples removed from the reactor would probably be limited by the slow feedback as mentioned above. An alternate means would be far more desirable. One generalization which emerges from MSRE experience is that during periods when the relative concentration of $[U^{3+}]/[\Sigma U]$ in the fuel salt was $\geq 0.5\%$, the system appeared to be protected against corrosion. This observation, along with a consideration of the expense, inconvenience, and irrelevance of individual results of chemical analyses, suggests that a more suitable means for establishing that corrosion-free conditions prevail would be to ensure that at all times the proper redox potential existed in the salt stream.

As part of the MSRE experiment, evidence appeared to indicate the possibility that the disposition of niobium in the fuel salt could be exploited as a means of monitoring corrosion in molten-salt reactors on a continuous basis. The lack of success we have experienced in attempting to determine the concentration of trivalent uranium in the fuel salt when the total concentration of uranium was ≤ 0.5 mole % suggests that there is a clear incentive to develop methods of detecting corrosion such as by niobium monitoring by gamma spectrometry, which can provide on-line continuous monitoring of the chemical potential of the fuel salt.

As noted in Chap. 6, several aspects of corrosion chemistry in molten-salt reactor systems were left unresolved at termination of MSRE operations. The outstanding example of these was that corrosion attack during ^{235}U operations might have been anticipated to be some threefold greater than was observed. Further, examinations of metal surveillance specimens removed from the heat exchanger indicated that mass transfer of metal from hot to cold zones was so little as to be undetectable. Temperature differences in the salt circuits were modest, $\sim 50^\circ F$, whereas in future molten-salt reactors projected differences run to about $200^\circ F$. The absence of base-line data for mass transfer that results from these examinations obviated the possibility of projecting mass-transfer coefficients for larger reactors. Generalized corrosion was deduced from chemical measurements of the chromium concentration in fuel-salt samples.

Current developments in the attempts to improve the radiation-induced loss of ductility that Hastelloy N experiences after use in high radiation fluxes include the possible inclusion of small amounts of titanium, hafnium, or zirconium in the alloy.⁴ All of these metals are more chemically active than chromium, the most chemically active constituent of the unmodified alloy; their inclusion as constituents in significant concentrations may affect the chemical methods for monitoring corrosion on a dynamic basis.

3. Oils and hydrocarbons in the fuel system. The extent of oil leakage into the fuel system must be known accurately and ascertained on a regular basis because of the operational implications of such leakage and because of the chemical effects induced by the presence of hydrocarbon degradation products in the system. Hydrogen, evolved in the thermal degradation of hydrocarbons, will unquestionably be involved in the distribution of tritium in the reactor and will control fission product chemistry, perhaps even favorably if, for example, it enhances the retention of iodine in the

system as iodide or tellurium as the element. Surveillance of the off-gas by means of a gas spectrometer seems to be very desirable; it may possibly be an important requisite for continuous operation. If the gas analysis by mass spectrometry proves to be adaptable for determination of a variety of species, it could provide the most precise source of control data for the reactor.

4. Miscellaneous. One of the most useful kinds of analysis in the MSRE was that provided by mass spectrometric measurements of the isotopic composition of uranium and plutonium. Occasional removal of salt samples from reactors built in the future, principally for mass spectrometric determination of inventory, burnup, etc., could also be used for confirmation by general analyses that the on-line instrumentation was functioning correctly.

Little advantage would accrue from any routine efforts to determine chemically whether there were any chronic leaks from fuel to coolant or in the reverse direction, for, in either event, nuclear data would provide operational control. Similarly, laboratory determination of the condition of auxiliary fluids, such as cooling tower water, oil from pump reservoirs, etc., should probably not be done at all. Experience with the MSRE has shown that there will be little difficulty in maintaining these fluids in condition so they will meet physical and chemical criteria over long periods of time. Information pertaining to their condition can be acquired simply and quickly and should be obtained at suitable predetermined intervals by in-line automated monitoring equipment.

In summary, it becomes evident that operational adjustments for future molten-salt reactors should

originate from chemical controls provided almost exclusively from on-line instrumentation. It is imperative that such instrumentation be stringently restricted to the minimum for safety, because there should be little reason to use the information derived for frequent adjustments of the salt systems. These reduce to (1) a continuous method for determining the identity of species in and composition of the gas above the fuel salt; in all likelihood this will entail the development of an automated mass spectrometer; (2) a method of establishing the redox potential of the fuel salt to ensure corrosion-free operation; for this function, further development of a niobium monitor by on-line gamma spectrometry will be required; (3) verification that bismuth does not enter the fuel stream via the incoming stream from the chemical reprocessing plant; (4) development of a highly sensitive and accurate method for continuous or frequent on-line determination of oxide concentration in the fuel salt.

References

1. R. E. Thoma and G. M. Hebert, *Coolant Salt for a Molten Salt Breeder Reactor*, U.S. patent No. 3,448,054, June 3, 1969.
2. W. R. Grimes, correspondence to Milton Shaw, "Assessment of Need for Oxygen Getter in Molten Salt Breeder Reactor Fuel," February 3, 1971.
3. A. S. Meyer and J. M. Dale, personal communication.
4. H. E. McCoy et al., *Nucl. Appl. Technol.* 8, 156 (1970).

INTERNAL DISTRIBUTION

1. J. L. Anderson
2. R. F. Apple
3. C. F. Baes
4. C. E. Bamberger
5. C. J. Barton
6. J. B. Bates
7. H. F. Bauman
8. S. E. Beall
9. M. J. Bell
10. M. Bender
11. E. S. Bettis
12. D. S. Billington
13. F. F. Blankenship
14. E. G. Bohlmann
15. G. E. Boyd
16. J. Braunstein
17. M. A. Bredig
18. R. B. Briggs
19. H. R. Bronstein
20. G. D. Brunton
21. S. Cantor
22. D. W. Cardwell
23. R. S. Carlsmith
24. W. L. Carter
25. E. L. Compere
26. W. H. Cook
27. J. W. Cooke
28. L. T. Corbin
29. J. L. Crowley
30. F. L. Culler
31. D. R. Cuneo
32. J. M. Dale
33. J. H. DeVan
34. J. R. Distefano
35. S. J. Ditto
36. F. A. Doss
37. A. S. Dworkin
38. W. P. Eatherly
39. J. R. Engel
40. R. B. Evans III
41. D. E. Ferguson
42. L. M. Ferris
43. A. P. Fraas
44. J. H. Frye, Jr.
45. W. K. Furlong
46. C. H. Gabbard
47. R. B. Gallaher
48. L. O. Gilpatrick
49. W. R. Grimes
50. A. G. Grindell
51. R. H. Guymon
52. P. H. Harley
53. P. N. Haubenreich
54. R. F. Hibbs
55. G. H. Jenks
56. E. M. King
57. A. P. Malinauskas
58. H. E. McCoy
59. H. F. McDuffie
60. H. A. McLain
61. L. E. McNeese
62. J. R. McWherter
63. A. S. Meyer
64. R. L. Moore
65. E. L. Nicholson
66. L. C. Oakes
67. R. B. Parker
68. A. M. Perry
69. H. B. Piper
70. B. E. Prince
71. A. S. Quist
72. G. L. Ragan
73. J. D. Redman
74. D. M. Richardson
75. G. D. Robbins
76. R. C. Robertson
- 77-78. M. W. Rosenthal
79. R. G. Ross
80. J. P. Sanders
81. H. C. Savage
82. Dunlap Scott
83. J. L. Scott
84. H. E. Seagren
85. J. H. Shaffer
86. M. J. Skinner
87. A. N. Smith
88. G. P. Smith
89. A. H. Snell
90. Din Sood
91. R. A. Strehlow
92. D. A. Sundberg
93. J. R. Tallackson
94. E. H. Taylor
- 95-97. R. E. Thoma
98. L. M. Toth
99. D. B. Trauger
100. G. C. Warlick
101. C. F. Weaver
102. A. M. Weinberg
103. J. R. Weir
104. M. E. Whatley
105. J. C. White
106. R. P. Wichner
107. L. V. Wilson
108. H. C. Young
109. J. P. Young
110. J. W. Cobble (consultant)
111. P. H. Emmett (consultant)
112. H. Insley (consultant)
113. E. A. Mason (consultant)
114. R. F. Newton (consultant)
115. J. E. Ricci (consultant)
116. C. H. Secoy (consultant)
117. H. Steinfink (consultant)
118. L. R. Zumwalt (consultant)
- 119-121. Central Research Library
122. ORNL - Y-12 Technical Library
Document Reference Section
- 123-157. Laboratory Records Department
158. Laboratory Records, ORNL R.C.

EXTERNAL DISTRIBUTION

- 159-160. MSBR Program Manager, AEC, Washington, D.C.
161. Merson Booth, AEC, Washington, D.C.
162. Paul Cohen, Westinghouse Elect. Corp., P.O. Box 158, Madison, Pa. 15663
163. D. F. Cope, RDT Site Office, ORNL
164. J. D. Corbett, Iowa State University, Ames, Iowa 50010
165. J. W. Crawford, AEC, Washington, D.C.
166. F. E. Dearing, RDT Site Office (ORNL)
167. D. R. deBoisblanc, Ebasco Services, Inc., 2 Rector St., New York 10006
168. C. B. Deering, Black & Veatch, P.O. Box 8405, Kansas City, Mo. 64114
169. A. R. DeGrazia, AEC, Washington, D.C.
170. S. G. English, AEC, Washington, D.C.
171. J. J. Ferritto, Poco Graphite, P.O. Box 2121, Decatur, TX 76234
172. T. A. Flynn, Jr., Ebasco Services, Inc., 2 Rector St., N.Y., N.Y. 10006
173. E. E. Fowler, AEC, Washington, D.C.
174. J. E. Fox, AEC, Washington, D.C.
175. Norton Habermann, RDT, USAEC, Washington, D.C. 20545
176. A. Houtzeel, TNO, 176 Second Ave., Waltham, MA 02154
177. G. M. Kavanagh, AEC, Washington, D.C.
178. H. H. Kellogg, Henry Krumb School of Mines, Columbia U., N.Y., N.Y. 10027
179. M. Klein, AEC, Washington, D.C.
180. S. J. Lanes, AEC, Washington, D.C.
181. Kermit Laughon, AEC, RDT Site Office (ORNL)
182. J. M. Longo, Esso Research & Eng., P.O. Box 45, Linden, N.J. 07036
183. T. W. McIntosh, AEC, Washington, D.C. 20545
184. J. Neff, AEC, Washington, D.C.
185. R. E. Pahler, AEC, Washington, D.C.
186. A. J. Pressesky, AEC, Washington, D.C.
187. M. V. Ramaniah, Bhabha Atomic Research Centre, Radiological Labs., Trombay, Bombay-85, AS, India
188. David M. Richman, AEC, Washington, D.C.
189. H. M. Roth, AEC-ORO, Oak Ridge, Tn.
190. R. M. Scroggins, AEC, Washington, D.C.
191. M. Shaw, USAEC, Washington, D.C.
192. T. G. Schlieter, AEC, Washington, D.C.
193. J. M. Simmons, AEC, Washington, D.C.
194. S. A. Szawlewicz, AEC, Washington, D.C.
195. A. R. Van Dyken, AEC, Washington, D.C.
196. N. Srinivasan, Bhabha Atomic Research Centre, Trombay, Bombay 74, India
197. R. C. Steffy, Jr., TVA, 540 Mkt. St., Chattanooga, Tn. 37401
198. A. E. Swanson, Black & Veatch, P.O. Box 8405, 1500 Meadowlake, K.C., Mo.
199. J. A. Swartout, UCC, New York, N.Y. 10017
200. B. L. Tarmy, Esso Research & Engr. Co., P.O. Box 101, Florham Pk., N.J. 07923
201. J. R. Trinko, Ebasco Services, Inc., 2 Rector St., N.Y., N.Y. 10006
202. C. E. Larson, Commissioner, AEC, Washington, D.C.
203. W. W. Grigorieff, Oak Ridge Associated Universities
204. Leo Brewer, Lawrence Radiation Laboratory
205. R. C. Vogel, Argonne National Laboratory
206. S. Spaepen, Head of Chemical Technology, SCK-CEN, MOL, Belgium
207. V. K. Moorthy, Metallurgy Div., BARC, Bombay 83, India

- 208. R. A. Penneman, Los Alamos Scientific Laboratory
- 209. R. K. Steunenberg, Argonne National Laboratory
- 210. M. K. Reser, American Ceramic Soc., 4055 N. High St., Columbus, Ohio 43214
- 211. Sidney Langer, Gulf General Atomic, San Diego, California
- 212. C. W. Keenan, Dept. of Chem., University of Tennessee, Knoxville
- 213. Gleb Mamantov, Dept. of Chem., University of Tennessee, Knoxville
- 214. Rustum Roy, Materials Res. Lab., Penn State Univ., University Park, Pa.
- 215. Minoo D. Karkhanavala, Chem. Div., BARC, Bombay, India
- 216. W. Danner, Max-Planck-Institut Fur Plasmaphysik, 8046 Garching Bei, Munchen, West Germany
- 217. David Elias, AEC, Washington, D.C.
- 218. Ronald Feit, AEC, Washington, D.C.
- 219. P. A. Halpine, AEC, Washington, D.C.
- 220. W. H. Hannum, AEC, Washington, D.C.
- 221. R. Jones, AEC, Washington, D.C.
- 222-224. Director, Division of Reactor Licensing (DRL), AEC, Washington, D.C.
- 225-226. Director, Division of Reactor Standards (DRS), AEC, Washington, D.C.
- 227-231. Executive Secretary, Advisory Committee on Reactor Safeguards, AEC, Washington, D.C.
- 232. Laboratory and University Division, AEC, ORO
- 233. Patent Office, AEC, ORO
- 234-452. Given distribution as shown in TID-4500 under Reactor Technology category (25 copies - NTIS)